High-density electroencephalography in Parkinson's disease : longitudinal tracking and disease phenotyping

Sahar Yassine

COLLEGE SCIENCES
DOCTORAL DE LA VIE
BRETAGNE ET DE LA SANTE

Université de Rennes

THESE DE DOCTORAT DE

L'UNIVERSITE DE RENNES

ECOLE DOCTORALE N° 637
Sciences de la Vie et de la Santé
Spécialité : *« Analyse et Traitement de l'Information et des Images Médicales »*

Par

Sahar YASSINE

L'Électroencéphalographie à haute résolution dans la maladie de Parkinson : Suivi longitudinal et phénotypage de la maladie

Thèse présentée et soutenue à Rennes, le 2 Juin 2023
Unité de recherche : Laboratoire de Traitement de Signal et de l'Image

Rapporteurs avant soutenance :

Alain Dagher Professeur, McGill University
Görsev Yener Professeur, Izmir University

Composition du Jury :

Président :	Dominique Guehl	Professeur, Université de Bordeaux
Examinateurs :	James Cavanagh	Professeur, University of New Mexico
	Mahmoud Hassan	Chercheur, Reykjavik University
Dir. de thèse :	Marc Vérin	Professeur, Université de Rennes

High-Density Electroencephalography in Parkinson's disease: longitudinal tracking and disease phenotyping

Sahar Yassine

Under the supervision of Professor Marc Vérin and Doctor Mahmoud Hassan

April, 2023.

RESUME EN FRANÇAIS

Le cerveau humain est reconnu comme un système hautement complexe qui repose sur l'activité collaborative de milliards de neurones (Fornito et al., 2016). Ces neurones sont interconnectés par un réseau sophistiqué de synapses possédant une structure et une connectivité méticuleusement organisées, gouvernant la dynamique collective sous-jacente du fonctionnement cérébral (Sporns et al., 2004). Des preuves émergentes suggèrent que dans les premiers stades des troubles neurodégénératifs, une dysfonction synaptique et un repliement anormal des protéines peuvent survenir dans de petites populations neuronales vulnérables dans des régions spécifiques du cerveau (Dugger et Dickson, 2017; Seeley et al., 2009; Stam, 2014). Cependant, à mesure que la maladie progresse, le processus pathologique peut se propager à travers le réseau à grande échelle (Fornito et al., 2015; Fornito et Bullmore, 2015), causant des anomalies structurelles et fonctionnelles dans le réseau cérébral (Catani et ffytche, 2005), reflétées par une dysfonction cognitive, comportementale et motrice progressive chez les personnes affectées (Dugger et Dickson, 2017). Comprendre les altérations du fonctionnement cérébral dues aux troubles neurologiques et leur progression tout au long de la maladie reste l'un des principaux défis de la neuroscience clinique.

La maladie de Parkinson (MP) est le trouble du mouvement le plus courant et le deuxième trouble neurologique le plus répandu, touchant 2 à 3 % de la population âgée de plus de 65 ans (Bloem et al., 2021 ; Poewe et al., 2017 ; Simon et al., 2020). Parmi les affections neurologiques, la MP présente le taux de croissance le plus élevé et devrait augmenter de manière spectaculaire, doublant dans les deux prochaines décennies et contribuant significativement à la charge mondiale d'incapacité (Dorsey et al., 2018 ; Feigin et al., 2017). Bien qu'elle soit principalement caractérisée par plusieurs caractéristiques motrices clés, la MP entraîne également une large gamme de symptômes non moteurs tels que les déclins cognitifs et les comorbidités neuropsychiatriques. Cliniquement, la présentation des symptômes de la MP est très hétérogène chez les personnes affectées et leur progression graduelle réduit la qualité de vie des patients (Bloem et al., 2021 ; Poewe et al., 2017). Par conséquent, la compréhension des corrélats neuronaux sous-jacents à la progression de la maladie ainsi que les profils hétérogènes des patients sont des sujets prédominants dans la recherche récente sur la MP.

Les techniques avancées d'imagerie cérébrale ont considérablement avancé notre compréhension des mécanismes cérébraux sous-jacents à ces aspects dans la MP. En utilisant la tomographie par émission de positons (TEP), l'imagerie par résonance magnétique (IRM) structurelle et fonctionnelle et la magnétoencéphalographie (MEG), les chercheurs ont identifié des anomalies dans plusieurs schémas d'activité cérébrale et de réseaux fonctionnels associés à la manifestation de symptômes moteurs et non moteurs de la MP, ainsi qu'à leur progression des stades précoces aux stades avancés de la maladie (Devignes et al., 2022; Pourzinal et al., 2022; Boonstra et al., 2021; Mitchell et al., 2021; Wolters et al., 2019; Boon et al., 2019; Barber et al., 2017; Wen et al., 2016). Bien que ces techniques aient considérablement amélioré la recherche et la pratique cliniques en fournissant des informations précieuses sur la dysfonction pathologique de ce trouble multisystémique, elles présentent également plusieurs limitations en milieu clinique, telles que leur coût élevé et leur impraticabilité. En revanche, l'électroencéphalographie (EEG) est devenue une technique d'imagerie cérébrale pratique dans les applications cliniques en raison de sa facilité d'utilisation, de sa non-invasivité, de son coût abordable et de son potentiel de mobilité (Müller-Putz, 2020). Lorsqu'elle est combinée à des méthodes de traitement de signal appropriées, l'EEG a démontré sa capacité à fournir des informations précieuses sur la dysfonction des réseaux cérébraux dans la MP (Shirahige et al., 2020; Q. Wang et al., 2020; Geraedts et al., 2018; Cozac, Gschwandtner, et al., 2016) et d'autres maladies neurodégénératives (Sánchez-Reyes et al., 2021; Al-Ezzi et al., 2020; Livint Popa et al., 2020; de Aguiar Neto & Rosa, 2019; Cassani et al., 2018; J. Wang et al., 2013; Acharya et al., 2013; Arns et al., 2013). Ainsi, l'utilisation de l'EEG à haute résolution (combinée avec des méthodes de localisation de sources) a bien amélioré la résolution spatiale de l’EEG et son exploitation dans des études longitudinales pourraient présenter un cadre prometteur pour identifier des marqueurs fiables de la maladie et suivre leur progression au fil du temps.

Dans ce contexte, l'objectif globale de cette thèse est d'étudier dans quelle mesure l'EEG à haute résolution en état de repos peut caractériser de manière précise les dysfonctionnements cérébraux anormaux associés à différents aspects cliniques de la MP et identifier des mesures basées sur l'EEG qui peuvent prédire les résultats de la maladie, dans le but de combler certaines des lacunes de la littérature. Dans ce but, nous avons mené trois études différentes en utilisant des enregistrements EEG à haute résolution en état de repos longitudinal et une batterie de tests neuropsychologiques et cliniques pour des patients atteints de la MP et des sujets sains au début de l'étude ainsi qu'aux suivis après 3 ans et 5 ans.

- Premièrement, nous avons proposé d'examiner le changement longitudinal des réseaux fonctionnels cérébraux des patients atteints de la MP sur 5 ans et d'associer différents schémas d'anomalies avec les scores cognitifs des patients et la latéralisation des symptômes moteurs. Les résultats ont révélé des schémas de connectivité décroissante progressive, principalement entre les lobes fronto-temporal de l'hémisphère droit, dans les bandes alpha2 et bêta. Ces réseaux de dysconnectivité sont propres aux patients atteints de la MP et ne sont pas observés chez les sujets sains et sont corrélés au profil cognitif global des patients. De plus, des motifs de connectivité diminuée, principalement dans l'hémisphère droit, caractérisent l'évolution de la maladie chez les patients atteints de la MP avec des symptômes du côté gauche, contre des schémas de dysconnectivité fonctionnelle, principalement dominants dans l'hémisphère gauche qui délimitent la progression de la maladie chez les patients atteints de la MP avec des symptômes du côté droit.

- Dans notre deuxième étude, nous avons cherché à identifier les sous-types de la MP en exploitant l'hétérogénéité de la maladie en fonction des caractéristiques basées sur l'EEG. Nous avons effectué une analyse de “clustering” pour identifier ces sous-types et les associer à des motifs uniques de perturbations. Nous avons montré que l'EEG en état de repos peut identifier trois sous-types distincts de patients atteints de la MP, caractérisés par différents niveaux de perturbations dans le réseau somatomoteur (bandes delta et bêta), le réseau fronto-temporal (bande alpha2) et le réseau du mode par défaut (bande alpha1). Ces sous-types sont associés à différents profils cliniques et peuvent être classés en tant que modérément-moteur ou diffus-maligne à 5 ans. Notre suivi longitudinal a révélé que les caractéristiques basées sur l'EEG, qui caractérisent les sous-types modérés uniquement moteurs des sous-types diffus-malignes à 5 ans, sont pertinentes tout au long de la trajectoire de la maladie et peuvent prédire le déclin cognitif chez les patients à partir de la ligne de base, lorsque les scores cliniques cognitifs étaient en chevauchement important.

- Enfin, notre troisième étude visait à exploiter les empreintes électrophysiologiques caractérisant l'anxiété chez les patients atteints de la MP et qui se corrèle aux résultats cliniques liés à l'anxiété tout au long de la progression de la maladie. Les résultats ont montré des schémas de puissance spectrale altérée dépendant de la fréquence, ainsi que des réseaux de fonctionnement hyper- et hypo-connectivité, distinguant le groupe de patients atteints MP-anxieux des patients MP-non-anxieux et des sujets sains. Nous

avons également constaté que les scores électrophysiologiques quantifiables correspondants étaient corrélés avec les résultats cliniques de l'anxiété tout au long de la progression de la maladie.

Nous croyons que cette thèse démontre le potentiel de l'EEG à haute résolution en état de repos pour développer des biomarqueurs fiables des symptômes et de la progression de la MP, ce qui peut éventuellement conduire à un pronostic et un diagnostic plus précis ainsi qu'à de meilleures stratégies thérapeutiques.

ABSTRACT

Understanding how neurological disorders affect brain functions from disease onset and throughout progression is a significant challenge in clinical neuroscience. Parkinson's disease (PD) is the most common movement disorder and a prevalent neurological condition that significantly contributes to the global burden of disability due to its variability in symptoms and progression. Therefore, accurately predicting PD's severity and progression is a significant step towards optimal patient counselling, symptom-specific care, and effective treatments. However, achieving this objective depends on developing reliable biomarkers that not only characterize the disease but also accurately track and predict its evolution. In recent years, electroencephalography (EEG) has emerged as a valuable tool in clinical practice for this purpose. This direct, non-invasive, inexpensive, and relatively easy-to-use neuroimaging technique allows for the extraction of key information about alterations in brain activity associated with neurological conditions such as PD. Within this context, this dissertation aims to investigate the extent to which resting-state high-density (HD)-EEG can precisely characterize the abnormal brain functions associated with different clinical aspects in PD and identify EEG-based measures that can predict disease outcomes. To this end, we conducted three different studies using longitudinal resting-state HD-EEG recordings and a battery of neuropsychological and clinical tests for PD patients and healthy controls at baseline as well as at follow-ups after 3 years and 5 years. We first examine the longitudinal changes in brain functional networks of PD patients over 5 years and associate different patterns of abnormalities with patients' cognitive scores and lateralization of motor symptoms. Second, we identify PD subtypes by deconstructing disease heterogeneity using EEG features. We conducted a clustering analysis to identify these subtypes and associated them with unique patterns of disruptions. We investigated their ability to predict cognitive decline in patients, as well as to characterize the clinical disease trajectory over the course of the disease. Third, we investigate the electrophysiological fingerprints that characterize the anxiety in PD patients and correlate with clinical disease outcomes related to anxiety throughout disease progression. Overall, our results showed different patterns of abnormalities that characterized the distinct aspects of interest and we were able to identify EEG-based markers that can correlate with the clinical outcomes of the disease and can predict its evolutions. We believe that this dissertation demonstrates the potential of resting-state HD-EEG in developing reliable biomarkers of PD

symptoms and progression, which can ultimately lead to more accurate prognosis and diagnosis as well as better therapeutics strategies.

ACKNOWLEDGMENT

I would like to begin by expressing my sincere gratitude to my supervisors, Prof. Marc Vérin and Dr. Mahmoud Hassan. Without their invaluable guidance and support, the completion of this thesis would not have been possible. Their profound understanding and insights into the subject matter as well as their valuable feedback were pivotal in guiding me throughout this research. I am truly grateful to Marc for his kind demeanor, constant support, enthusiasm for the project, and for the insightful discussions that greatly enriched my knowledge. I am particularly grateful to Mahmoud for his unwavering support, which dates back to six years ago since my master's thesis. He has been a constant source of encouragement, even during times when I lacked self-belief. I learned a lot from him throughout this journey, and his fervor for his work has always been a source of inspiration.

Besides my advisors, I would like to thank Dr. Manon Auffret and Dr. Joan Duprez from Rennes university, as well as Dr Ute Gschwandtner and Prof. Peter Fuhr from University of Basel, for their invaluable contributions and insightful discussions during our collaboration on this research project.

I would also like to thank Prof. Alain Dagher, Prof. Görsev Yener, Prof. Dominique Guehl and Prof. James Cavanagh, for generously offering their time to read my work, be part of my Ph.D. defense jury, and provide valuable comments.

I would also like to extend my sincere gratitude to my friends in Rennes who have been like a second family to me throughout this journey. I am especially grateful to Iman (and Zayn) for being more than a sister and an ultimate source of comfort and support. I am also thankful for Asma, Abdallah, Ghina, Ahmad, and their families, as well as Maria, Mariam, Sana, Sahar, Israa, Lara and Sourour.

My deepest gratitude goes to my parents Ibrahim and Khouloud and my brothers Abdelkader and Walid, for their unconditional and endless love, care and support. I would not have reached this stage without their sacrifices. Last but not least, a very special and heartfelt thanks goes to my husband Saad. His constant love, care, help and support have been my guiding light throughout this journey, and accomplishing this thesis would have been much more difficult without his motivation and encouragement.

TABLE OF CONTENT

LIST OF FIGURES

LIST OF TABLES

LIST OF ABBREVIATIONS

AEC:	Amplitude envelope correlation
BOLD:	Blood-oxygenation-level-dependent
DBS:	Deep Brain Stimulation
DMN:	Default mode network
EEG:	Electroencephalography
EOG:	Electrooculography
FC:	Functional connectivity
FPN:	Frontoparietal network
FTN:	Fronto-temporal network
fMRI:	functional magnetic resonance imaging
LPD:	Left-sided Parkinson's disease
MCI:	Mild cognitive impairment
MEG:	Magnetoencephalography
MMSE:	Mini-mental state examination
MNE:	Minimum norm estimate
MoCA:	Montreal cognitive assessment
MRI:	Magnetic resonance imaging
PD:	Parkinson's disease
PDD:	Parkinson's disease dementia
PET:	Positron emission tomography
PPMI:	Parkinson progression marker initiative

PLV:	Phased-locked value
RBD:	Rapid eye movement sleep behaviour disorder
ROI:	Region of interest
RPD:	Right-sided Parkinson's disease
SAN:	Salience network
SMN:	Somatomotor network
SNF:	Similarity Network Fusion
SPECT:	Single-photon emission computed tomography
STN:	Subthalamic nucleus
UPDRS:	Unified Parkinson's disease rating scale
VBM:	Voxel-based morphometry
wMNE:	weighted minimum norm estimate

CHAPTER 1: GENERAL INTRODUCTION

1.1. Context

The human brain is increasingly recognized as a highly complex and self-regulating system that relies on the collaborative activity of billions of neurons (Fornito et al., 2016). These neurons are interconnected through a sophisticated network of synapses possessing a meticulously organized structure and connectivity, governing the collective dynamics underlying brain functions (Sporns et al., 2004). Compelling evidence suggests that in the early stages of neurodegenerative disorders, synaptic dysfunction and aberrant protein misfolding may occur in small vulnerable neuronal populations within specific brain regions (Dugger & Dickson, 2017; Seeley et al., 2009; Stam, 2014). However, as the disease progresses, the pathological process may propagate through the large-scale network (Fornito et al., 2015; Fornito & Bullmore, 2015), causing structural and functional abnormalities in the brain (Catani & ffytche, 2005), reflected by progressive cognitive, behavioural and motor dysfunction in the affected individuals (Dugger & Dickson, 2017). Understanding alterations in brain function due to neurological disorders and their progression throughout the disease remains one of the foremost challenges facing modern clinical neuroscience.

Parkinson's disease (PD) is the most common movement disorder and the second most prevalent neurological disorder, affecting 2 to 3% of the population above 65 years of age (Bloem et al., 2021; Poewe et al., 2017; Simon et al., 2020). Among neurological conditions, PD has the highest growth rate and is expected to double in prevalence by 2040, contributing significantly to the worldwide burden of disability (Dorsey et al., 2018; Feigin et al., 2017). Despite being primarily characterized by several key motor features, PD also leads to a wide range of non-motor symptoms such as cognitive impairment and neuropsychiatric comorbidities. Clinically, the presentation of PD symptoms is very heterogeneous among affected individuals and their gradual progression reduces patients' quality of life (Bloem et al., 2021; Poewe et al., 2017). Therefore, understanding the neural correlates underlying disease progression as well as the heterogeneous profiles of the patients have been prominent subjects in recent PD research.

Neuroimaging techniques have made significant strides in enhancing our comprehension of the physiopathological mechanisms of PD. By using positron emission tomography (PET), structural and functional magnetic resonance imaging (MRI), and magnetoencephalography (MEG), researchers have identified abnormalities in multiple patterns of brain activity and structural/functional networks associated with the manifestation of motor and non-motor PD symptoms, as well as their progression from the early to advanced stages of the disease (Devignes et al., 2022; Pourzinal et al., 2022; Boonstra et al., 2021; Mitchell et al., 2021; Wolters et al., 2019; Boon et al., 2019; Barber et al., 2017; Wen et al., 2016). While these techniques have greatly enhanced clinical research and practice by providing valuable insights into the pathological dysfunction of this multisystem disorder, they also have several limitations in clinical settings, such as their high cost and impracticality. On the other hand, electroencephalography (EEG) has emerged as a convenient neuroimaging technique in clinical applications due to its ease of use, non-invasiveness, affordability, and potential for mobility (Müller-Putz, 2020). When combined with appropriate signal processing methods, EEG has demonstrated its ability to provide valuable information about brain network dysfunction in PD (Shirahige et al., 2020; Q. Wang et al., 2020; Geraedts et al., 2018; Cozac, Gschwandtner, et al., 2016) and other neurodegenerative diseases (Sánchez-Reyes et al., 2021; Al-Ezzi et al., 2020; Livint Popa et al., 2020; de Aguiar Neto & Rosa, 2019; Cassani et al., 2018; J. Wang et al., 2013; Acharya et al., 2013; Arns et al., 2013). Thus, we hypothesised that the use of high-density (HD)-EEG in longitudinal studies may present a promising framework to identify reliable markers of the disease and track their progression over time.

1.2. Objectives, contributions and overview

The general objective of this thesis is to investigate to what extent longitudinal resting-state HD-EEG can accurately characterize the abnormal brain functions associated with different clinical aspects of PD and identify EEG-based measures that can predict disease outcomes, with the aim of addressing some of the gaps in the literature.

- First, investigates the longitudinal progression in functional brain networks of PD patients over 5 years.
    - To this end we conducted the first study published in Movement Disorders journal (Yassine et al., 2022).

- Second, explores the potential of resting-state EEG-based features in identifying clinically relevant PD subphenotypes with distinct electrophysiological profiles.
    - To this end, we carried out the second study under revision for publication in the Movement Disorder journal as a full paper and in the American Academy of Neurology (AAN-2023) annual meeting as well as in the Organization for Human Brain Mapping (OHBM-2023) annual meeting as a poster presentation for scientific abstract.
- Third, investigates the electrophysiological signatures that characterize the anxiety in PD.
    - To this end, we conducted the third study to be submitted soon for revision in a journal, and accepted for oral presentation in AAN-2023 and for poster presentation in OHBM-2023.

This manuscript is organized as follow:

- Chapter 2 cover the background of the work performed in this thesis:
    - The first section introduces PD history, epidemiology and risk factors, symptomatology, pathophysiology, and treatments.
    - The second section outlines the background work of neuroimaging research in PD and introduces thesis objectives.
- Chapter 3 outlines the materials and methods used in this thesis: we introduce EEG and the longitudinal study cohort and we detail the different analyses conducted in the studies presented in this thesis.
- Chapter 4 presents the results of the thesis in the form of articles that have been published, submitted for publication, or are in preparation. For each article, we provide details on the corresponding objectives, methodology, results, and discussion.
- Chapter 5 concludes the thesis by summarizing the general conclusions. This includes an overall discussion that covers several clinical and methodological considerations, as well as suggestions for future directions.

CHAPTER 2: BACKGROUND

This thesis investigates the electrophysiological markers of progression, heterogeneity and anxiety in PD using resting state HD-EEG. This research topic encompasses various background knowledge that should be presented. Therefore, in this chapter, we introduce PD from a clinical point of view, as well as the current outcomes of neuroimaging studies addressing our three aspects of interests in PD. We conclude with the thesis objectives.

2.1. Parkinson's disease - Clinical overview

2.1.1. History of PD

James Parkinson's essay on the "Shaking Palsy", published in 1817, marked the first comprehensive clinical description of what is now widely known as Parkinson's disease. Parkinson wrote the monograph prior to his retirement from medical practice with the intention of raising awareness among the medical community about a condition that had not yet been formally defined. In the essay, Parkinson reported six cases he had seen as a physician or observed in his neighborhood, he defined the disorder as "*Involuntary tremulous motion with lessened muscular power, in parts in action and even when supported; with a propensity to bend the trunk forwards and to pass from a walking to a running pace: the senses and intellects being uninjured*". He referred to the condition as "*paralysis agitans*" (Lees, 2007; Parkinson, 2002).

Few decades later in the mid-1800s, Jean Martin Charot, the father of modern neurology, made significant contributions in understanding and disseminating information about this disorder (Gomes & Engelhardt, 2013). He refined and expanded upon Parkinson's early description, separating it from multiple sclerosis and other tremor-inducing disorders and recognized cases that would be later classified as Parkinsonism-plus syndromes. With his students, Charcot has described the full clinical spectrum of the disease, including two prototypes, the tremorous and the rigid/akinetic form, as well as introducing several typical non-motor symptoms such as muscle pain and fatigue. Charcot also distinguished bradykinesia as a separate cardinal feature of PD (Goetz, 2011; Jm Charcot, 1861; Lees, 2007).

In the late 19th and early 20th centuries, both Gowers and Oppenheim wrote extensively on PD (Garcia-Ruiz et al., 2014; Goetz, 2011). Gowers described PD's motor and non-motor symptoms, including pain, sensory changes, autonomic dysfunction, cognitive decline, and neuropsychiatric disturbances (Gowers William R., 1899). While Oppenheim, summarized the known clinical characteristics of the disorder, and included hyperhidrosis, salivation, anxiety, and depression as common late-stage symptoms (Oppenheim, 1905). Both authors recognized the heterogeneity of PD symptoms with Gowers considering cognitive decline as a potential feature. Moreover, throughout this period, tremendous progress has been made by neurologists to understand PD progression and its underlying mechanisms. In 1953, Greenfield and Bosanquet performed the most in-depth analysis of PD including a clear definition of brain stem lesions (Greenfield & Bosanquet, 1953). Later, Hoehn and Yahr introduced the widely accepted staging system for PD based on the distinction between unilateral and bilateral disease and the onset of postural reflex impairment (Hoehn M.M. & Yahr M.D., 1976). All these early works emphasized the importance of considering the diverse symptoms of PD and its progressive aspect in diagnosis and management.

2.1.2. Epidemiology and risk factors of PD

PD is a neurodegenerative disorder that becomes increasingly prevalent with age (Twelves et al., 2003). The worldwide incidence of PD ranges from 5 to over 35 cases per 100,000 people annually with higher rates in male population (Simon et al., 2020; Twelves et al., 2003; Wooten et al., 2004). PD is rare before the age of 50, but the incidence rises 5 to 10 fold from the 6th to the 9th decade of life, and its estimated prevalence of 0.3% in the overall population increases to over 3% in individuals over 80 years of age (Poewe et al., 2017; Savica et al., 2013; Simon et al., 2020). Although mortality rates are unchanged in the first decade after diagnosis, they increase later on with the progression of the disease (Pinter et al., 2015). Current estimates suggest that PD prevalence is expected to dramatically escalate, doubling in the next two decades, as the global population ages (Dorsey et al., 2018; Feigin et al., 2017). This rise in prevalence will heighten the social and economic burden of PD unless more effective treatment, cures or means of prevention are found.

Moreover, PD has a multifactorial aetiology from a combination of environmental and genetic factors (Simon et al., 2020). Environmental exposures such as toxicant chemicals, viral infections and head injury increase the risk of PD (S. M. Goldman, 2014; Kenborg et al., 2015;

Olsen et al., 2018; Tanner et al., 2014), while certain lifestyle factors, such as caffeine consumption, smoking and physical activity, may have a protective effect (Ascherio & Schwarzschild, 2016; Ritz et al., 2007). Nonetheless, environmental exposures may be influenced by genetic susceptibility factors. Genome-wide association studies have linked PD with 90 genetic loci and these genetic variants account for 16-36% of PD's heritability (Nalls et al., 2019). Gene mutations, specifically those in *LRRK2* and *SNCA*, are known to cause inherited forms of PD. *LRRK2* mutations are responsible for a significant proportion (3-41%) of cases with familial inheritance and are also found in a smaller number of sporadic cases (Corti et al., 2011; Trinh et al., 2018). Additionally, mutations in the Glucocerebrosidase *GBA* gene have been linked to 5-10% of cases of sporadic PD (Beavan & Schapira, 2013; S. M. Goldman et al., 2019). Nevertheless, these mutations are not present in most PD patients and have incomplete penetrance suggesting the complex interaction of multiple contributing factors in the manifestation of PD (Bloem et al., 2021).

2.1.3. Clinical presentation of PD

2.1.3.1. Motor Symptoms

The three cardinal motor symptoms of PD are bradykinesia, rigidity, and rest tremor (R. Xia & Mao, 2012). Bradykinesia (slowness of movement) may be associated with akinesia (difficulty initiating movement) and hypokinesia (reduced movement amplitude) and are all characteristics of basal ganglia disorders, which affect movement planning and execution (Moustafa et al., 2016). Their initial manifestation usually includes slow performances in daily activities and difficulties with tasks requiring precise motor control such as handwriting (Jankovic, 2008; Kalia & Lang, 2015). Rigidity in PD is characterized by increased muscle resistance during limb movements, often accompanied by a "cogwheel'' phenomenon at different joints of the body such as neck, shoulder, wrists, ankles… (Jankovic, 2008). While tremor at rest, the most recognizable symptom of PD, is characterized by unilateral tremors occurring at frequency between 4 to 6 Hz and is prominent in distal part of extremities, particularly the hands. It can also affect the lips, chin, jaw and legs and is likely to disappear during action or sleep (Dovzhenok & Rubchinsky, 2012; Jankovic, 2008). Postural instability and gait freezing are also common gait abnormalities in PD that typically appear after the onset of other symptoms. They can lead to falls and flexed postures in later stages of the disease (Jankovic, 2008; Lees et al., 2009).

Clinical studies have shown varying rates of progression for the hallmark motor symptoms of PD, with patients displaying heterogeneity in progression (Poewe & Mahlknecht, 2009). Those with rigidity, bradykinesia and postural instability tend to experience faster progression compared to those with tremor-dominant PD, who have slower progression (Lees et al., 2009; R. Xia & Mao, 2012). In addition, PD typically starts as a unilateral-disorder with motor symptoms appearing on one side of the body and later spreading to the other (Djaldetti et al., 2006; Riederer & Sian-Hülsmann, 2012). Interestingly, rates of progression of PD were also linked with the initially affected-side of the disease. More rapid worsening was associated with right-dominant symptoms profiles whereas longer disease durations correlated with left-dominant symptomatology (Baumann et al., 2014; Heinrichs-Graham et al., 2017; Munhoz et al., 2013).

2.1.3.2. Non-Motor Symptoms

Although the diagnosis of PD traditionally occur with the onset of motor symptoms, evidence shows that this disease is a heterogeneous multisystem disorder comprising various non-motor symptoms that may predate the emergence of motor features by years or even decades (Figure 1), and impact the quality of life of patients (Gonzalez-Latapi et al., 2021; Hiseman & Fackrell, 2017; Pfeiffer, 2016; Poewe, 2008). These non-motor symptoms are often overlooked and undertreated due to under-recognition in clinical practice and lack of awareness or embarrassment from the patients (Chaudhuri & Schapira, 2009). Among the most common non-motor symptoms of PD are pain, fatigue, olfactory dysfunction (hyposmia), rapid eye movement sleep behaviour disorder (RBD) and those related to autonomic dysfunction such as constipation, erectile dysfunction and urinary urgency (Chaudhuri et al., 2006; A. Park & Stacy, 2009; Pfeiffer, 2016).

Additionally, cognitive declines and neuropsychiatric symptoms are particularly common during the course of PD. Mild cognitive impairment (MCI) can occur in up to 40% of PD patients with high prevalence estimated at about 31% for the multiple-domain subtype (Baiano et al., 2020) and with executive and visuo-spatial abilities being the most affected (J. Goldman & Litvan, 2011). Cognitive declines can occur at any stage of the disease, even prior to diagnosis, and PD-MCI patients are at higher risk to develop dementia (PDD) with the disease progression (Aarsland et al., 2021). The estimated cumulative prevalence of PDD for patients who have lived with the disease for over 10 years is around 80% (Gonzalez-Latapi et al., 2021),

and these patients commonly experience visual hallucinations, visuo-spatial difficulties, delusions and fluctuations in alertness (Emre et al., 2007).

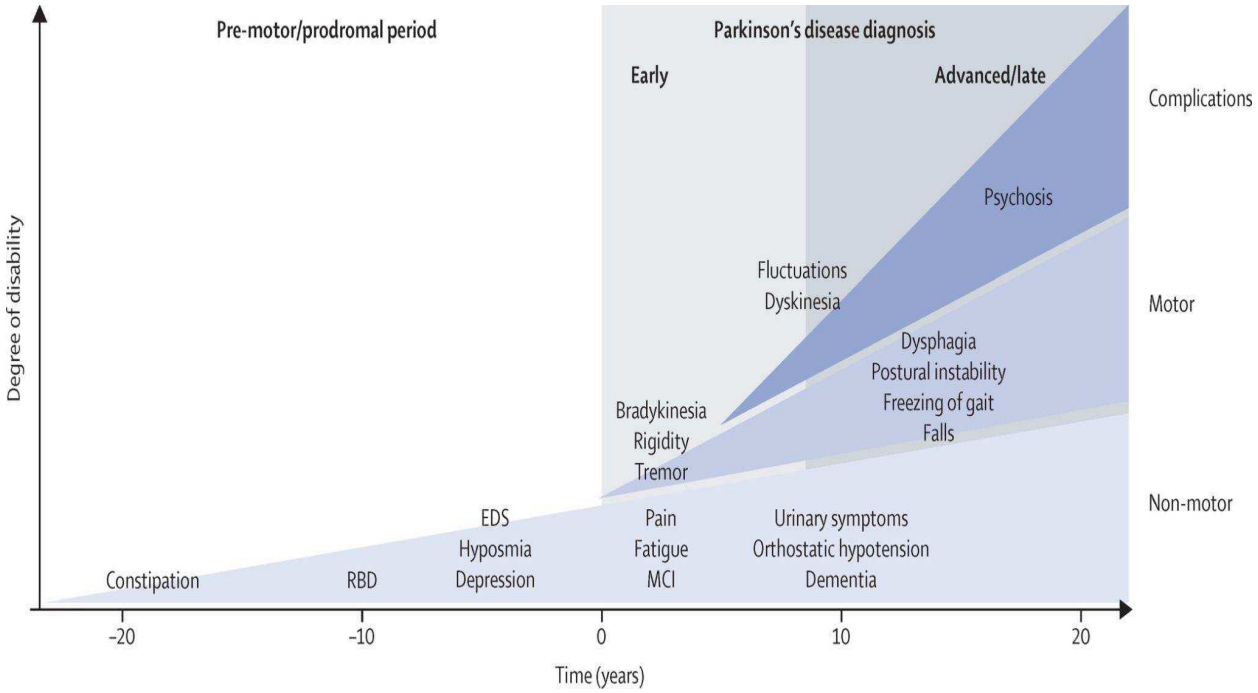

Figure 1. ***Clinical symptoms and time course of Parkinson's disease progression. Adapted from (Kalia & Lang, 2015).*** *The diagnosis of PD is established when motor symptoms begin (0 years) but can be preceded by a prodromal phase, characterized by several non-motor symptoms, that can last for 20 years or more. Further non-motor symptoms emerge after diagnosis and as the disease progresses, they lead to significant disability. Advanced stages to disease tend to involve axial motor symptoms, such as postural instability with frequent falls and freezing of gait. Long-term consequences of dopaminergic treatment, such as fluctuations, dyskinesia and psychosis also contribute to disability. RBD: Rapid Eye Movement Sleep Behaviour Disorder. EDS: Excessive Daytime Sleepiness. MCI: Mild Cognitive Impairment.*

Furthermore, common neuropsychiatric symptoms in PD including depression, anxiety, apathy and psychosis, often comorbid with the existing symptoms and increase disease burden (Aarsland et al., 2009; Eichel et al., 2022). In particular, anxiety is among the highly prevalent neuropsychiatric symptoms occurring in 31% of PD patients (Broen et al., 2016), a frequency greater than that found in age-matched control of the general population (N. N. W. Dissanayaka et al., 2010; Pontone et al., 2011). It can arise at any stage of the disease, worsening the existing motor (Coakeley et al., 2014; Pirogovsky-Turk et al., 2017; Siemers et al., 1993) and cognitive symptoms (Toloraia et al., 2022; Ehgoetz Martens et al., 2018; N. N. W. Dissanayaka et al., 2017; Reynolds et al., 2017) and exacerbating the challenges for patients and caregivers over the course of the disease (Eichel et al., 2022; S. Jones et al., 2020; Balestrino & Martinez-Martin, 2017; Sagna et al., 2014; Aarsland et al., 2009). Anxiety can present with a range of subtypes including general anxiety disorder, non-episodic and episodic anxiety, panic attacks,

and social phobia (N. N. N. W. Dissanayaka et al., 2014; Ishihara & Brayne, 2006; Shiba et al., 2000). However, Anxiety in PD can also co-occur with depression and apathy and the substantial overlap in their features often hampers their clinical dissociation (Rutten et al., 2015; Wen et al., 2016), thus this comorbidity is often under-diagnosed and undertreated and little is known about its underlying PD-related mechanisms.

Considering the widespread heterogeneity in the clinical spectrum of PD, it is important to acknowledge the existence of different subtypes with distinct clusters of symptoms and diverse disease trajectories. Recognizing these subtypes is important in understanding the disease process and in providing insights into prognosis and personalized treatments (Bloem et al., 2021; A. J. Espay et al., 2017, 2020).

2.1.4. Pathophysiology of PD

The pathophysiological hallmark of idiopathic PD is the loss of dopaminergic neurons in the pars-compacta of the substantia nigra, accompanied by the accumulation of intracellular α-synuclein in the form of Lewy bodies (Bloem et al., 2021; Kalia & Lang, 2015). Although these two major neuropathologies are not specific to PD, when combined they form its definitive diagnosis (Poewe et al., 2017).

Clinical-pathological studies of PD have revealed that the loss of pigmented dopaminergic neurons in the ventrolateral area of the substantia nigra creates a gradient of dopamine depletion in the region (Dickson, 2018; Dickson et al., 2009). This leads to an imbalance between the direct and indirect pathways in the basal ganglia, resulting in motor features, in particular bradykinesia and rigidity (Bloem et al., 2021; Calabresi et al., 2014) (Figure 2-A). The dramatic loss of nigral neurons, even in the early stages of the disease, suggests that degeneration in this region begins prior to the onset of motor symptoms and becomes more widespread as the disease progresses (Dijkstra et al., 2014; Kordower et al., 2013).

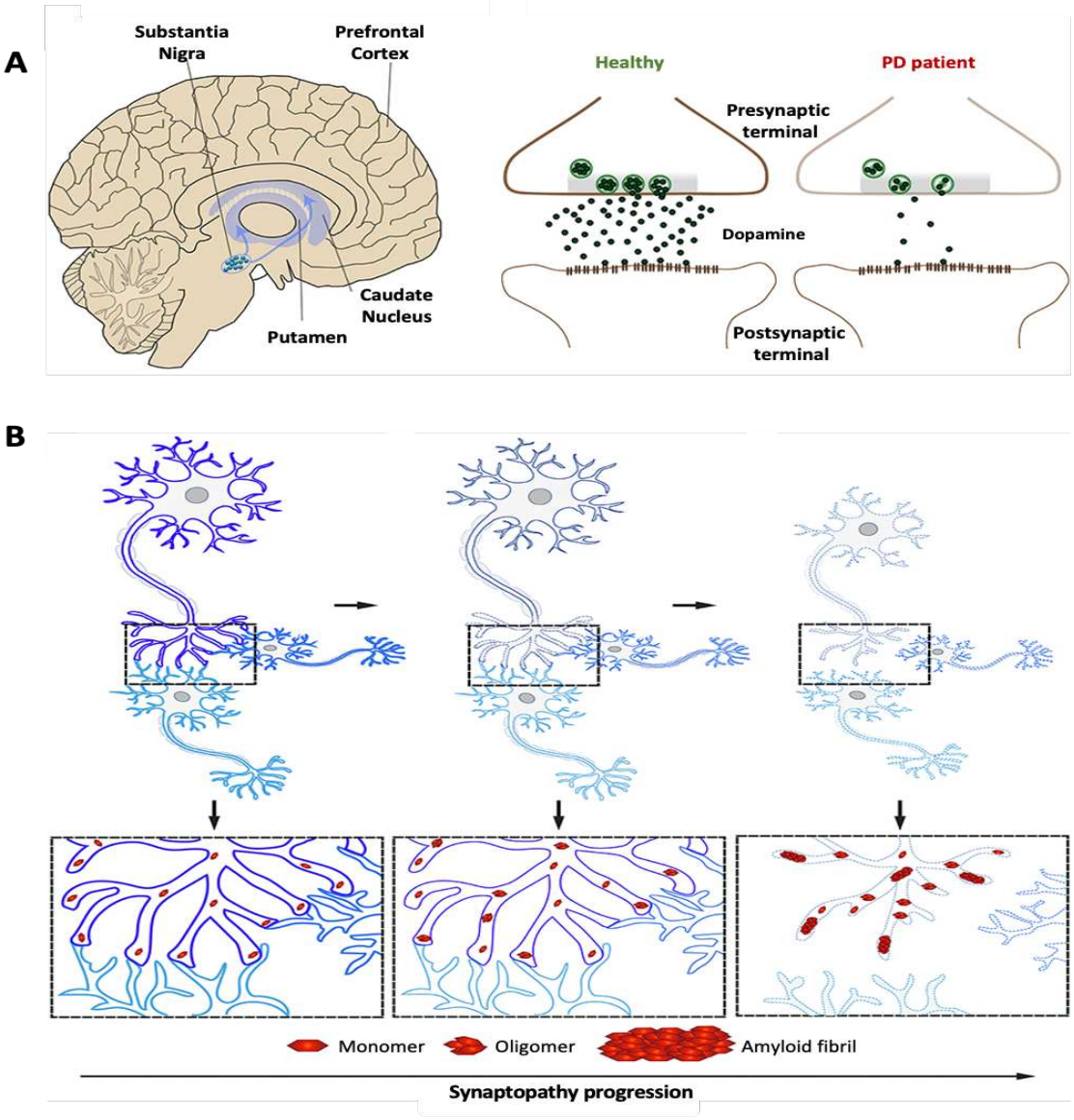

Figure 2. ***The pathological hallmarks of Parkinson's disease, adapted from (Bridi & Hirth, 2018).*** ***A)*** *The loss of dopaminergic neurons in the striatal system: the degeneration of the dopaminergic neurons in the substantia nigra (SN) is preceded by dysfunction and subsequent degeneration of the nigrostriatal pathway. This pathway connects the SN to the caudate nucleus and the putamen, which together form the striatum. As a result of nigrostriatal degeneration, the neurotransmitter dopamine is depleted and ultimately lost on the synaptic terminals of striatal neurons. This stands in contrast to healthy controls, whose striatal neurons have normal dopamine levels.* ***B)*** *The progressive accumulation of intracellular α-synuclein in presynaptic terminals: under normal conditions, α-synuclein functions as monomers in synaptic transmission (left). Toxic species like oligomers and fibrils start to accumulate at presynaptic terminals implicating the pathogenesis of PD (middle). These toxic species alter protein involved in synaptic transmission, causing synaptic dysfunction, loss of neuronal connections and ultimately death of neuronal cells (right).*

Furthermore, the loss of dopaminergic neurons in PD is accompanied by the formation of Lewy bodies, which are intracellular inclusions in the cytoplasm of affected neurons. Lewy bodies have a complex composition of α-synuclein and ubiquitin, and when α-synuclein misfolds, it becomes insoluble and aggregates to form Lewy bodies and Lewy neurites (Goedert et al.,

2013) (Figure 2-B). Their propagation in the central nervous system is proposed to be associated with the disease progression (Brás & Outeiro, 2021; Recasens & Dehay, 2014).

Braak and colleagues have proposed a 6-stage model for the progression of Lewy pathology in PD. The model outlines a stereotypical pattern that corresponds with the clinical course of the disease, with stages 1-2 associated with the onset of premotor symptoms, stage 3 with motor symptoms due to dopamine deficiency, and stages 4-6 with non-motor symptoms of advanced PD (Braak et al., 2003). The complex mechanisms underpinning the pathology of PD are thought to begin in the peripheral nervous system and to spread, with the disease progression, to the mesocortex and neocortex in a caudal-to-rostral direction, leading to structural and functional changes (Bove & Travagli, 2019; Michely et al., 2015).

2.1.5. Treatments of PD

Given that the cardinal motor features of PD result from the loss of dopaminergic neurons and the depletion of dopamine in the nigrostriatal system, the dopamine replacement therapies have been established for over 5 decades as the simplest and most effective treatments in alleviating these symptoms (Poewe et al., 2017). In particular, Levodopa is widely regarded as the most effective treatment for the motor symptoms of PD and is eventually required by the majority of patients with the disease (LeWitt & Fahn, 2016; Nemade et al., 2021). It is administered in low doses and adjusted based on the patient's response and side effects. Despite its efficacy, long-term use can result in motor complications such as motor response oscillations and drug-induced dyskinesias caused by discontinuous drug delivery due to its short half-life and variability in absorption and transport across the blood-brain barrier (Cenci, 2014; Poewe & Antonini, 2015; Zahoor et al., 2018). Additionally, levodopa is not effective in treating various motor (such as gait and speech) and non-motor (such as cognitive, sensory, and vegetative) symptoms of PD (You et al., 2018).

Other introduced therapies include non-ergot derived dopamine receptor agonists, which have been associated with a lower risk of dyskinesias compared to levodopa (Nemade et al., 2021; Zahoor et al., 2018). However, they are less potent and less well-tolerated, as they have been reported to cause higher rates of adverse effects such as nausea, vomiting, insomnia, sleepiness, and hallucinations, particularly in the elderly population (Goldenberg, 2008). Another class of drugs in PD includes the inhibitors of levodopa metabolism which aim to block the activity of enzymes involving in the breakdown of dopamine, such as the monoamine oxidase B (MAO-

B) and the Catechol-O-methyltransferase (COMT). These inhibitors could be used as a first-line treatment for mild motor symptoms or in combination with levodopa and dopamine receptor agonists, however they also have several side effects such as dyskinesia, headache and diarrhea (Nemade et al., 2021; Goldenberg, 2008; National Collaborating Centre for Chronic Conditions (UK), 2006).

Other than pharmacological treatments, Deep Brain Stimulation (DBS) is a highly effective surgical treatment of PD that uses high-frequency electrical stimulation to improve motor symptoms (Limousin et al., 1995). The complex procedure involves implanting electrodes into specific targets within the basal ganglia and connecting them to a stimulator in the chest wall (Foltynie & Hariz, 2010). The subthalamic nucleus (STN) is the preferred target for DBS in PD due to the extensive documentation of its efficacy in reducing motor symptoms (Nemade et al., 2021; Hartmann et al., 2019; S. H. Fox et al., 2011; Follett et al., 2010; Benabid et al., 2009). Studies have shown that DBS can result in reductions in dopaminergic medications in the order of 40-60% and improvement in motor function of 30-50% with enhanced quality of life for the patients (Mahlknecht et al., 2022; Aquino et al., 2019; Deuschl & Agid, 2013; Schuepbach et al., 2013). However, there are many potential side effects of DBS affecting its long-term efficacy, including intracranial bleeding, device complications like infections and misplacements and neuro-psychiatric sequelae (apathy, depression, impulsiveness, mania, and increased risk of suicide) that result from a complex interplay between disease-related psychiatric symptoms, dopaminergic imbalance, and stimulation-induced effects on limbic basal ganglia circuits (Limousin & Foltynie, 2019; Bronstein et al., 2011; Volkmann et al., 2010; Voges et al., 2007). Cognitive decline is also a major adverse event of DBS that occurs in 15-20% of operated PD patients and can be caused by surgical neuronal damage or stimulation (Witt et al., 2013). Although the risks can be managed by adjusting DBS settings, there is currently no effective way to predict or avoid stimulation-induced cognitive decline in PD patients (Limousin & Foltynie, 2019; Witt et al., 2013; Frankemolle et al., 2010).

The non-motor symptoms of PD, which can be just as or even more debilitating than the motor symptoms, do not respond well to dopamine replacement therapies and may even be exacerbated by it (Nemade et al., 2021; Seppi et al., 2019; Storch et al., 2013). Cholinesterase inhibitors, however, can have significant positive effects on cognitive disturbances in PD patients with dementia (Seppi et al., 2019, 2011). Concerning the neuropsychiatric symptoms such as depression and anxiety, their underlying mechanisms in PD patients are uncertain and may differ from those in the general population. This raises questions about the effectiveness

of antidepressant and anxiolytic medications in treating these symptoms in PD patients (Connolly & Fox, 2014; Seppi et al., 2011, 2019).

Currently, PD therapies only alleviate symptoms and over time, as the disease progresses, most patients end up taking a combination of drugs that must be carefully balanced for optimal symptom improvement and minimal side effects (Bloem et al., 2021; Lees et al., 2009). Indeed, this explains the elusive and highest priority in current PD research to develop convergent biomarkers in order to improve disease modifying and neuroprotective interventions.

2.1.6. Objectives of the thesis

The heterogeneous profile of patients with PD in terms of symptoms and progression is due to various underlying causes originating from multiple neurodegenerative processes in the brain. As such, there is a need to explore markers that reflect the pathophysiology of disease progression, while also acknowledging the heterogeneity among patients and the neural correlates of distinct symptoms. These efforts may lead to better biomarkers and improved disease management strategies. Therefore, in this thesis, we focused on addressing three clinical problems in PD:

1. The electrophysiological mechanisms underlying the progression of PD
2. The heterogeneity in PD patients and disease phenotyping
3. The neural correlates associated with the anxiety in PD

2.2. Neuroimaging research in Parkinson's disease

2.2.1. Progression of PD

The neurodegeneration process in PD begins prior to the onset of motor signs and the progression of the neuropathology typically corresponds to the evolution of the clinical symptomatology (Braak et al., 2004, 2005). Over the past decades, neuroimaging studies have been trying to understand the progressive nature of PD and its underlying brain mechanisms. Using advanced techniques such as dopaminergic positron emission tomography (PET), single-photon emission computed tomography (SPECT), structural and functional magnetic resonance imaging (MRI and fMRI), magnetoencephalography (MEG), and

electroencephalography (EEG), there are great efforts to identify biomarkers of progression from early to advance stages of the disease.

2.2.1.1. PET / SPECT

PET and SPECT can monitor the dopaminergic damage in the nigrostriatal system of PD patients (Shen et al., 2012; Thobois et al., 2001). In preclinical and prodromal stages of PD, researchers have focused mainly on individuals with idiopathic RBD, which is considered a promising clinical prodromal marker (Boeve, 2013; Howell & Schenck, 2015; Iranzo et al., 2014). PET/SPECT scans have revealed that individuals with RBD experienced progressive dopaminergic deficits in striatal regions compared to healthy controls (Heller et al., 2017; Iranzo et al., 2011). Further, during early stages of PD, declines in striatal dopamine transporter's binding and fluorodopa uptake were reported to be more rapid in the first two years after diagnosis compared to the following three years (Brück et al., 2009; Simuni, Siderowf, et al., 2018). The progression of striatal dopaminergic markers showed an exponential decline and mostly plateaued after five years of diagnosis suggesting the propagation of the pathology towards midbrain and cortical regions (Mitchell et al., 2021; Nandhagopal et al., 2011). Indeed, the cortical dopaminergic activity becomes more impaired with the disease progression as cognitive impairment in PD has been associated with reductions in dopaminergic receptors and diminished glucose metabolism in the insular, cingulate, temporal and frontal cortices (Christopher et al., 2015; González-Redondo et al., 2014; Pappatà et al., 2011; Sasikumar & Strafella, 2020). Despite these findings, a major drawback of both PET and SPECT is that they require the exposure of subjects to ionizing radiation. This presents a particular challenge for younger individuals and for serial longitudinal studies where the cumulative risk of repeated scans may not be acceptable.

2.2.1.2. Structural and functional MRI

T1-based structural MRI methods, such as cortical thickness and voxel-based morphometry (VBM), provide a sensitive measure of the pathophysiology progression in different stages of the disease. In the prodromal stage, a VBM study revealed reduction in the volume of the hippocampal in RBD patients without dementia (Scherfler et al., 2011), whereas more widespread reductions in cortical thickness within several cortices (temporal, frontal, occipital and cingulate) were reported in RBM patients with pronounced cognitive impairments (Rahayel et al., 2018). Further, several studies on early stage PD patients have reported thinning in subcortical and cortical regions, mainly in the parietal and premotor cortices, and this

thinning has been linked to poorer cognitive performance in the patients (Ibarretxe-Bilbao et al., 2012; Mak et al., 2015; Pereira et al., 2014; Zarei et al., 2013; Zeighami et al., 2015). Another recent longitudinal study on de novo PD patients from the Parkinson's disease Progression Marker Initiative (PPMI) cohort have shown that MRI-derived patterns of brain atrophy can predict subsequent disease progression over 4.5 years in terms of motor, cognitive and global functioning (Zeighami et al., 2019). Moreover, structural changes in the brain are more prominent with the advanced stages of the disease. PD patient with mild cognitive impairment (PD-MCI) and PD patients with dementia (PDD) showed consistent gray matter atrophy associated with the cognitive functioning, mainly in the frontal, temporal, and parietal cortices as well as in the hippocampus (Delgado-Alvarado et al., 2016; Mak et al., 2014; Segura et al., 2014; Zarei et al., 2013). Also, the increased cortical thinning and the transition from unilateral to bilateral loss in gray matter were shown to be predictors for the progression from PD-MCI to PDD (Gasca-Salas et al., 2019; Xu et al., 2016).

Regarding fMRI, this technique provides indirect insight into the regional activation of the brain and the functional connectivity between different anatomic locations through the blood-oxygen-level dependent (BOLD) response (M. D. Fox & Raichle, 2007; Hall et al., 2016). In pre-symptomatic PD gene carriers' individuals, resting state fMRI studies have shown altered connectivity in subcortical and cortical regions of motor networks preceding the manifestation of PD (Helmich et al., 2015; Meles et al., 2021; Vilas et al., 2016). Decreased functional connectivity within basal ganglia networks have been also shown in RBD patients with much lower connectivity observed in diagnosed PD patients, suggesting a gradual decline along a continuous spectrum (Dayan & Browner, 2017; Ellmore et al., 2013; Rolinski et al., 2016). Moreover, fMRI studies of de novo PD patients have reported varying patterns of alterations in the cortico-subcortical functional connectivities that correlate with the clinical outcome of the patients, suggesting the propagation of the pathology throughout the brain (Prodoehl et al., 2014; Tessitore et al., 2019; Tuovinen et al., 2018). In moderate and late stages of the disease, cognitive impairment in PD patients was associated with reduced functional connectivity in the default mode network (DMN) as well as in fronto-parietal, parieto-temporal and fronto-occcipital (long-range) networks (Wolters et al., 2019; Díez-Cirarda et al., 2018; Zhan et al., 2018; Amboni et al., 2015; Baggio et al., 2015; Borroni et al., 2015). Consistent alterations in the functional connectivity of sensorimotor network (SMN) have been also reported across various stages of the disease (Strafella et al., 2018; Tessitore et al., 2014). The deterioration in

functional connectivity associated with the disease progression was also shown in several longitudinal fMRI studies (Olde Dubbelink et al., 2014; Burciu et al., 2016; Filippi et al., 2020).

Both structural and functional MRI studies have shown significant advancement in tracking the progression of PD. However, these tools are expensive and cumbersome, which poses a significant challenge in low-resource environments (McMackin et al., 2019).

2.2.1.3. MEG

MEG is a noninvasive technique that records the weak magnetic fields induced by electrical activity in the brain. With its high temporal resolution, it allows for in-depth analysis of neuronal activity and functional connections between brain regions (Cohen, 1972). At early disease stages, Stoffers and colleagues have shown widespread slowing of background MEG activity in de novo PD patients relative to controls while investigating the cortical resting state oscillations. They have also linked higher alpha1 power in central and parietal regions with early cognitive deficits in newly diagnosed patients (Stoffers et al., 2007). With the disease progression, longitudinal examinations of the power spectrum revealed an increase of the power of slower frequencies (theta and alpha) in contrast to a decrease in the power of faster frequencies (beta and gamma) , that correlate with the clinical course of both motor and cognitive symptomatology (Olde Dubbelink, Stoffers, Deijen, Twisk, Stam, & Berendse, 2013). The diffuse slowing of spectral power was also shown to characterize the progression toward late stages of the disease where patients develop dementia (Dubbelink et al., 2014; Ponsen et al., 2013). Regarding assessments of functional connectivity, a cross-sectional MEG study has shown that increased connectivity between cortical regions in the alpha1 frequency band is a characteristic of PD from early stages of the disease onward (Stoffers et al., 2008), while other studies have reported reductions in the functional connectivity in alpha and beta bands, mainly in the fronto-temporal networks, to characterize the progression into late stages of the disease (Bosboom et al., 2008; Ponsen et al., 2013). Longitudinally, Olde Dubbelink and colleagues have shown that global decreases in the source-space functional connectivity of alpha1 and alpha2 in several seed regions can characterize the progression of the disease over 4 years and correlate with motor and cognitive deteriorations of the patients (Olde Dubbelink, Stoffers, Deijen, Twisk, Stam, Hillebrand, et al., 2013). Despite these promising insights, the use of current MEG systems in clinical settings is limited due to the requirement for costly superconductive heavy systems, which hinders biomarkers development efforts.

2.2.1.4. EEG

EEG is a non-invasive method of measuring brain activity through the recording of scalp-level electric potentials. It provides a direct measure of the cortical neural activity and the functional interaction between brain regions on a millisecond timescale (Biasiucci et al., 2019). Like MEG, global spectral analysis of resting-state EEG data in PD patients showed a general slowing of cortical activity, characterized by an increase in slower band waves and a decrease in faster band waves compared to healthy controls (Caviness et al., 2016; Geraedts et al., 2018; Shirahige et al., 2020). These spectral patterns were reported to be present from early disease stages and were found to correlate with cognitive functioning and to predict cognitive decline in advanced disease stages, not only in cross-sectional cohorts but also in longitudinal studies (Caviness et al., 2007, 2015; Cozac, Gschwandtner, et al., 2016; Fonseca et al., 2009; Han et al., 2013; Klassen et al., 2011; Latreille et al., 2016; Zimmermann et al., 2015). Further, when assessing the functional connectivity in PD patients with the disease progression, most researchers have addressed the manifestation of cognitive impairments at advanced stages. In fact, several studies have reported functional dysconnectivity, mainly in alpha and beta bands, that characterize the cognitive decline in PD patients and correlate with their global or domain specific cognitive scores (Carmona Arroyave et al., 2019; Chaturvedi et al., 2019; Hassan, Chaton, et al., 2017; Peláez Suárez et al., 2021). Nevertheless, these EEG-based functional connectivity studies were all conducted at a single point in time rather than longitudinally, a key point for the development of biomarkers of progression in PD.

To facilitate the comparison between the aforementioned studies on different stages of the disease, we have summerized their major findings in Table 1, reporting the most pertinent information.

Finally, all of these neuroimaging studies have approached the progression of PD as a group average, considering PD as a single entity and grouping patients regardless of their heterogeneous phenotypes. They have focused on their pathological commonalities rather than targeting smaller groups and investigating their individualized disease trajectories. Therefore, prior distinction of patients' phenotypes, on the clinical and neurophysiological levels, is a step toward stratified medicine and may certainly enhance biomarker development strategies and disease modification therapies (A. J. Espay et al., 2017, 2020).

Table 1. Summary of the main findings of different neuroimaging techniques addressing the progression of PD through different stages of the disease. *MCI: mild cognitive impairment, PDD: PD dementia, RBD: rapid eye movement sleep behaviour disorder, FC: functional connectivity, DMN: default mode network, FTN: fronto-temporal network, FP: fronto-parietal network, FON: fronto-occipital network*

	Prodromal stage	**Early stage**	**MCI/PDD**	**Progression remarks**
PET/ SPECT	Striatal dopaminergic deficits in RBD patients	Exponential declines dopamine transporter's binding and fluorodopa uptake in the striatal system	Reductions in dopaminergic receptors and diminished glucose metabolism in the insular, cingulate, temporal and frontal cortices	Dopaminergic deficits start in the striatal system and propagate toward cortical regions with disease progression
Structural MRI	Reduced volume of the hippocampal and reductions in cortical thickness of several cortices in RBM patients	Thinning in subcortical and cortical regions, mainly in the parietal and premotor cortices.	Consistent grey matter atrophy mainly in the frontal, temporal, and parietal cortices as well as in the hippocampus	Gray matter atrophy and reductions in cortical thickness over the course of the disease
Functional MRI	Altered FC in subcortical and cortical regions of motor networks in PD gene carriers' individuals and RBD patients	Alterations in the cortico-subcortical FC	Reduced functional connectivity in the DMN, FPN, FTN and FON	Deterioration in FC associated with the disease progression
MEG	-	Slowing of background activity and increased FC in alpha1	Diffuse slowing of spectral power and reductions in the FC in alpha and beta bands, mainly in the FTN	Increase of the cortical power of slower frequencies and decrease in the power of faster frequencies. Decreased FC in alpha band
EEG	-	General slowing of cortical activity	Diffuse slowing of spectral power and reduced FC mainly in alpha and beta bands	Increase power of slower band waves and decrease power in faster band waves

2.2.2. Heterogeneity in PD and disease phenotyping

There is emerging evidence suggesting that PD is not a single entity, but rather a group of diverse, clinically, genetically and epidemiologically heterogeneous diseases (A. J. Espay et al., 2020; Farrow et al., 2022). Individuals with PD may experience a wide range of symptoms, and the substantial phenotypic heterogeneity is further complicated by differences in age of onset and progression rate (Bloem et al., 2021; Kalia & Lang, 2015; Poewe et al., 2017). This variability in PD can be better understood by identifying subtypes and defining groups of patients with unique features not only at the clinical level, but also in terms of biological and pathological mechanisms (A. Espay et al., 2017; A. J. Espay et al., 2017; Mestre et al., 2021).

The earliest attempts to address the heterogeneity of PD were carried out through hypothesis-free, data-driven subtyping studies based on clinical and behavioural assessments (van Rooden et al., 2010, 2011; Erro et al., 2013; Mu et al., 2017). Most of these studies relied on cross-sectional analysis and there was limited longitudinal assessment to evaluate the prognosis of subtypes. Although they uncovered clinically relevant PD subtypes, the depth of phenotypic information was inconsistent and their limited scope prevented a full understanding of the underlying pathophysiology (A. J. Espay & Marras, 2019; Fereshtehnejad et al., 2015; Landau et al., 2016; Lawton et al., 2018; Mestre et al., 2021; Rodriguez-Sanchez et al., 2021). In contrast, the integration of genetic, biochemical and neuroimaging data in PD studies has significantly enhanced our understanding of the biological basis of the disease (Farrow et al., 2022). Through genome wide association studies, researchers have linked various genetic variants with the onset of PD (Nalls et al., 2019), varying rates of cognitive decline (Szwedo et al., 2022) and different progression patterns of the disease (G. Liu et al., 2021; Tan et al., 2021). Other studies using levels of cerebrospinal fluid markers have associated different PD phenotypes with the severity of both motor (Kang et al., 2013, 2016; Majbour et al., 2021) and cognitive signs (Leaver & Poston, 2015; Montine et al., 2010). Neuroimaging studies have also shown correlations between specific neurophysiological processes and different forms of PD, including its clinical features (Boon et al., 2019; Boonstra et al., 2021; Geraedts et al., 2018; Hassan, Chaton, et al., 2017; Ma et al., 2018; W. Song et al., 2021; Wen et al., 2016; Wolters et al., 2019), treatment responsiveness (Ballarini et al., 2019; Yang et al., 2021) and progression rates (Filippi et al., 2020; Majbour et al., 2016; Olde Dubbelink, Stoffers, Deijen, Twisk, Stam, Hillebrand, et al., 2013). Indeed, by integrating information from such data modalities in clustering techniques, a more accurate identification of PD subtypes could be achieved. The

obtained subtypes would share common pathological processes and well-defined disease trajectories, which are major elements in supporting the discovery of biomarkers and promoting the development of stratified medicine strategies (A. Espay et al., 2017; A. J. Espay et al., 2017, 2020).

In this context, several PD studies, mainly on the PPMI cohort, have integrated clinical and biological data into supervised and unsupervised learning techniques to define different PD subtypes and assess their longitudinal progression. Fereshtehnejad and colleagues have used clinical, genetic and neuroimaging data in agglomerative hierarchical clustering to define three clinically relevant PD subtypes (mild motor predominant, intermediate and diffuse malignant) and associate them with significantly different rates of dopaminergic deficits and brain atrophy (Fereshtehnejad et al., 2017). Other studies have shown that applying machine learning and deep learning methods on a combination of comprehensive clinical and neuroimaging data can yield to identifying three PD subtypes and to categorize patients not only based on their baseline severity, but also according to their progression rates (Dadu et al., 2022; X. Zhang et al., 2019). Another study conducted by Markello and colleagues have shown that using Similarity Network Fusion (SNF) method combined with spectral clustering on multimodal clinical and neuroimaging data can lead to identifying three biotypes of PD patients with distinct underlying pathological dissimilarities. They have also demonstrated the preponderance of the neuroimaging data in such clustering approaches for yielding meaningful clusters with distinct biological profiles (Markello et al., 2021). Although the integration of EEG in clustering techniques has been previously employed to identify subtypes of different neurodegenerative disorders (Byeon et al., 2020; Dukic et al., 2021; Y. Zhang et al., 2021), the use of EEG-based features in a longitudinal framework to establish PD phenotyping is still missing.

Although clustering approaches in PD can effectively reduce the dimensionality of this heterogeneous disorder and lead to better biomarkers discoveries and stratified medicine, understanding the neural basis of each clinical symptom separately is still a crucial step in this process. Anxiety, in particular, is among the poorly understood non-motor symptoms of PD.

2.2.3. Anxiety in PD

PD is not just a movement disorder, but a multidimensional disease reflecting multiple pathologies including psychiatric comorbidities (Aarsland et al., 2009; Bloem et al., 2021;

Farrow et al., 2022; S. Jones et al., 2020). Anxiety is among the highest prevalent psychiatric symptoms occurring in at least one-third of PD patients (Broen et al., 2016). In the general population, studies have shown that the human brain process fear and anxiety through two main circuits: the fear circuit involving the amygdala, the anterior cingulate cortex (ACC), the medial prefrontal cortex (mPFC), the insular cortex, the hippocampus and the striatum, as well as the limbic cortico-striato-thalamocortical circuit involving the PFC, basal ganglia and thalamus (Daffre et al., 2020; Hartley & Phelps, 2010; Shin & Liberzon, 2010; Volkmann et al., 2010). In PD patients, the abnormalities in several regions within these circuits due to PD pathology may explain the high prevalence of anxiety in this population (Thobois et al., 2017). Still, the neural correlates of the PD-related anxiety have not been sufficiently addressed by previous PD research.

Neuroimaging studies have investigated the brain mechanisms underlying anxiety in PD through various techniques (Carey et al., 2021; Perepezko et al., 2021). PET/SPECT studies have shown that increased anxiety in PD patients is linked to decreased binding of dopamine, norepinephrine and serotonin transporters in various subcortical regions, including the bilateral amygdala (Bayram et al., 2020; Carey et al., 2021; Joling et al., 2018; Picillo et al., 2017) as well as reduced metabolism in the prefrontal and cingulate cortices (X. Wang, Zhang, et al., 2017). Anatomical MRI studies using VBM have also associated higher levels of anxiety with reduced volumes in several brain regions including the bilateral ACC, the bilateral precuneus and the left amygdala (Carey et al., 2020; Vriend et al., 2016; Wee et al., 2016). Resting state fMRI studies have reported increased functional connectivity (hyperconnectivity) between the amygdala and various brain regions including the striatum, the PFC, temporal and parietal cortices, characterizing the anxiety in PD patients (Dan et al., 2017; X. Wang, Li, et al., 2017; X. Wang et al., 2018; H. Zhang et al., 2019). Carey and colleagues have also shown hyperactivity between the fear circuit and the salience network in anxious PD patients compared to non-anxious PD patients (Carey et al., 2020). Patterns of decreased functional connectivity between the amygdala and PFC and between the orbitofrontal cortex and PFC were also associated with the severity of anxiety in PD patients (Dan et al., 2017; X. Wang et al., 2018). Further, only one study, conducted by Betrouni and colleagues, has utilized EEG to examine the electrophysiological characteristics of anxiety in PD patients (Betrouni et al., 2022). They found that the anxious PD group exhibited generally increased delta power and decreased alpha power, primarily in the frontal cortex, compared to the non-anxious PD group. Additionally, their functional connectivity analysis showed hyperconnectivity between the left

insula and various regions of the right prefrontal cortex, associated with the PD-related anxiety. However, a drawback of this study is the lack of a control group. Although neuroimaging studies have provided valuable insights in understanding the PD-related anxiety, the use of EEG in case-control longitudinal studies to investigate the neural correlate of anxiety in PD is still missing.

2.2.3. Thesis objectives

Taken together, the aforementioned findings from various neuroimaging techniques have shown promising insights into understanding the pathophysiology underlying the progression of PD and its heterogeneous clinical presentation. However, when it comes to developing reliable imaging biomarkers, EEG can be considered as a very advantageous neuroimaging tool due to its ease of use, non-insaviness, cost-effectiveness, availability (even in underprivileged countries) and potential to be a mobile technology. Additionally, the literature has largely highlighted that EEG with its high temporal resolution and when combined with adequate signal processing techniques, can provide valuable information on both normal and impaired brain networks. Therefore, the use of EEG in longitudinal studies of PD patients may provide a promising framework to identify markers of the disease and track their progression over time.

This thesis focuses on extracting, selecting and analyzing pertinent resting-state EEG markers of PD in a longitudinal perspective, aiming to address some of the literature's gaps and provide new insights into biomarkers development strategies. Mainly, this thesis focuses on addressing three clinical aspects of PD using longitudinal resting-state HD-EEG data. This was achieved by conducting three studies:

1. The first study focuses on the progression of PD. We investigated the longitudinal evolution in the functional brain networks of PD patients over 5 years and associate markers of progression with cognitive outcomes and lateralization of motor symptoms.

2. The second study aims to characterize the heterogeneity in PD by subtyping patients based on their EEG-based features. We sought to identify different PD subgroups with distinct electrophysiological profiles and appraise their clinical significance and their neurophysiological/clinical progression longitudinally.

3. The third study investigates the electrophysiological processes underlying PD-related anxiety. We aimed to identify the electrophysiological fingerprints characterizing

anxious PD patients compared to non-anxious patients and healthy control and to assess their capacity in predicting the clinical scores of anxiety over the course of the disease.

CHAPTER 3: MATERIALS AND METHODS

3.1. Electroencephalography

EEG is a neuroimaging technique that records the brain's electrical activity by measuring rhythmic fluctuations in neurons, also known as brainwaves (Biasiucci et al., 2019; Borck, 2018). Although Richard Caton was the first to record the neurophysiological activity of animals in 1875, it was the German psychiatrist Hans Berger who introduced EEG on humans in 1924 by developing a recording technique that involved connecting electrodes to the scalp (Borck, 2018). After almost 100 years, EEG has been growingly used in evaluating the dynamic functioning of the brain, particularly in medical applications (Acharya et al., 2013; Arns et al., 2013; de Aguiar Neto & Rosa, 2019; Geraedts et al., 2018; Jeong, 2004; Müller-Putz, 2020; J. Wang et al., 2013).

3.1.1. Electric source of EEG signals

The human brain forms a vast and electrically active neuronal network. Synaptic activity in these networks generates a subtle electrical impulse called the postsynaptic potential. If a large population of neurons is spatially aligned and has synchronous activity, a superimposed electrical field may be produced. Cortical pyramidal neurons are usually aligned perpendicularly to the cortical surface, and when firing in synchrony, the summation of their extracellular ionic currents is powerful enough to flow through the brain tissue, bone, and skull to the electrodes on the scalp where EEG signals are recorded (Figure 3). Due to the low magnitude of the electrical activity measured at the scalp electrodes, which is typically in the microvolt range, the recorded data is amplified and converted into a digital format (Bear et al., 2020; Buzsáki et al., 2012; Müller-Putz, 2020).

Of note, the measurement of brain activity with EEG can be complicated by the presence of various biological and instrumental noises, which can interfere with the neural signals of interest. Biological noise, such as ocular, muscular, and cardiac activity, is caused by non-neuronal ionic currents or potentials. Meanwhile, instrumental noise is due to the recording system and environmental electromagnetic sources. These artifacts must be accounted for during preprocessing of the raw EEG signals to extract the clean EEG data (Müller-Putz, 2020).

obtained subtypes would share common pathological processes and well-defined disease trajectories, which are major elements in supporting the discovery of biomarkers and promoting the development of stratified medicine strategies (A. Espay et al., 2017; A. J. Espay et al., 2017, 2020).

In this context, several PD studies, mainly on the PPMI cohort, have integrated clinical and biological data into supervised and unsupervised learning techniques to define different PD subtypes and assess their longitudinal progression. Fereshtehnejad and colleagues have used clinical, genetic and neuroimaging data in agglomerative hierarchical clustering to define three clinically relevant PD subtypes (mild motor predominant, intermediate and diffuse malignant) and associate them with significantly different rates of dopaminergic deficits and brain atrophy (Fereshtehnejad et al., 2017). Other studies have shown that applying machine learning and deep learning methods on a combination of comprehensive clinical and neuroimaging data can yield to identifying three PD subtypes and to categorize patients not only based on their baseline severity, but also according to their progression rates (Dadu et al., 2022; X. Zhang et al., 2019). Another study conducted by Markello and colleagues have shown that using Similarity Network Fusion (SNF) method combined with spectral clustering on multimodal clinical and neuroimaging data can lead to identifying three biotypes of PD patients with distinct underlying pathological dissimilarities. They have also demonstrated the preponderance of the neuroimaging data in such clustering approaches for yielding meaningful clusters with distinct biological profiles (Markello et al., 2021). Although the integration of EEG in clustering techniques has been previously employed to identify subtypes of different neurodegenerative disorders (Byeon et al., 2020; Dukic et al., 2021; Y. Zhang et al., 2021), the use of EEG-based features in a longitudinal framework to establish PD phenotyping is still missing.

Although clustering approaches in PD can effectively reduce the dimensionality of this heterogeneous disorder and lead to better biomarkers discoveries and stratified medicine, understanding the neural basis of each clinical symptom separately is still a crucial step in this process. Anxiety, in particular, is among the poorly understood non-motor symptoms of PD.

2.2.3. Anxiety in PD

PD is not just a movement disorder, but a multidimensional disease reflecting multiple pathologies including psychiatric comorbidities (Aarsland et al., 2009; Bloem et al., 2021;

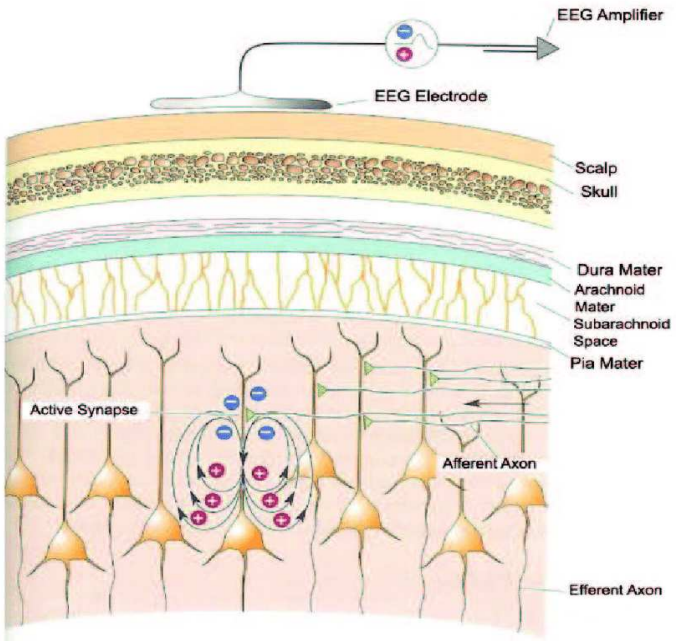

Figure 3. ***EEG principle: Electric field generated by aligned pyramidal cells.*** *Adapted from (Bear et al., 2020).*

Finally, the distance between the electrodes and the actual source of neuronal activity is a significant limitation of EEG measurements, resulting in lower spatial resolution compared to other neuroimaging techniques such as functional MRI and PET (Binnie & Prior, 1994; Buzsáki et al., 2012). Despite this drawback, EEG offers a major advantage in providing neuronal information with high temporal resolution, allowing for a better understanding of neuronal dynamics in a millisecond timescale. Additionally, EEG is relatively simple to use, inexpensive, and a mobile neuroimaging technology. While MEG shares the high temporal resolution of EEG, EEG surpasses MEG in terms of practicality and cost-effectiveness. Figure 4 shows the classification of some neuroimaging techniques in terms of temporal and spatial resolution.

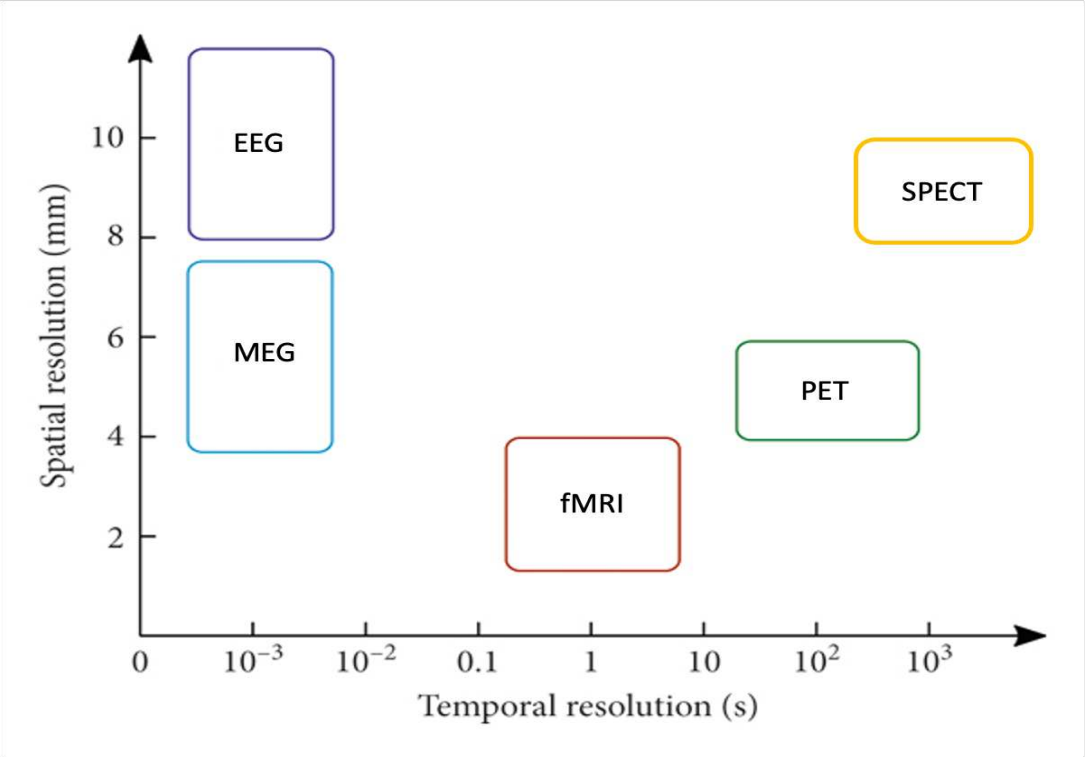

Figure 4. ***Temporal and spatial resolution of the most commonly used neuroimaging techniques.*** *Adapted from (Pfister et al., 2014; Wein et al., 2021).*

3.1.2. EEG systems

EEG signals are recorded by placing electrodes (sensors) on the scalp, either with the use of gel substance (wet electrodes) or directly on the scalp (dry electrodes). Gel electrodes, made of silver with a coating of silver chloride, are the most commonly used sensors in clinical practice and EEG research. They require applying a chloride ion-containing gel between the skin and the electrode prior to recordings, to improve the conductivity and reduce the impedance at the skin-electrode interface, which results in a better-quality signal. The placement of scalp electrodes follows the international 10-20 system, which relies on four stable skull landmarks: nasion, inion, and two pre-auricular points (Figure 5) (Müller-Putz, 2020). Standard EEG systems usually consist of arrays with 19, 32, 64, 128 or 256 electrodes. Several studies have shown that a higher number of channels is necessary for more precise characterization of spatial electrophysiological information, and as such, high-density configurations (HD-EEG) such as 128 and 256 electrodes are the most suitable for achieving decent reconstruction of cortical activity (Allouch et al., 2023; Q. Liu et al., 2017; Sohrabpour et al., 2015; J. Song et al., 2015).

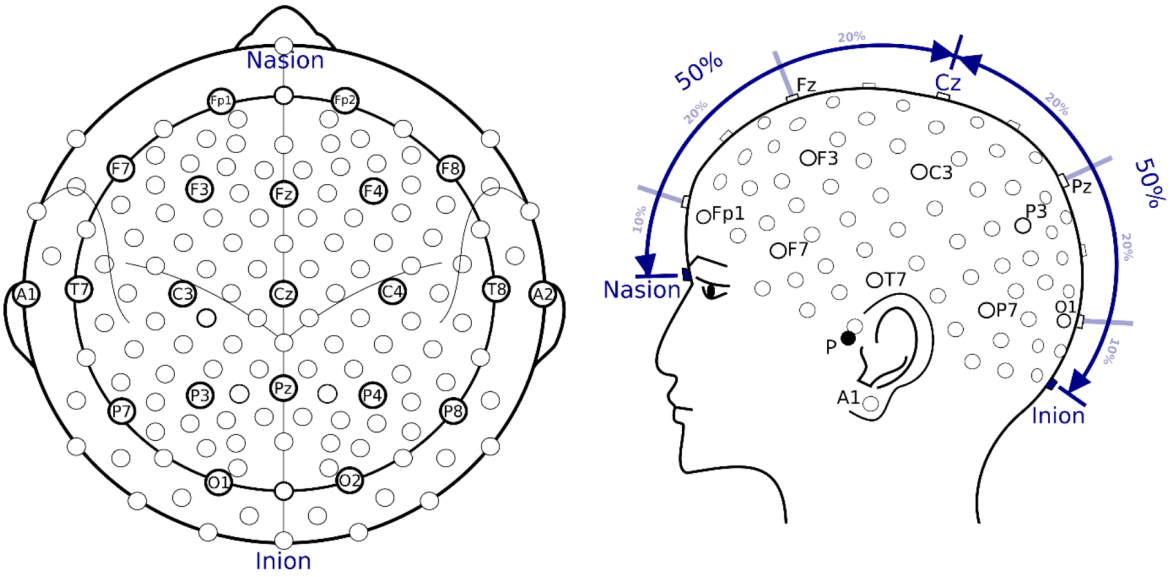

Figure 5. ***Scheme of a 10-5 electrode system.*** *Based on (Oostenveld & Praamstra, 2001) and adapted from (Müller-Putz, 2020). Selected electrode positions are shown. A1 is the earlobe, P shows the preauricular point.*

3.2. Longitudinal cohort of PD patients

3.2.1. Study population

As previously stated in the thesis objectives, our aim was to investigate three distinct clinical questions in PD through the use of EEG in a longitudinal cohort. To accomplish this, all experimental studies conducted in this thesis exploit a longitudinal database of resting state HD-EEG recording obtained from PD patients and age-matched healthy controls (HC) recruited from the Movement Disorder Clinic of University Hospitals of Basel (City of Basel, Switzerland). The patients cohort was selected based on specific criteria including a diagnosis of PD according to the UK Parkinson's Disease Brain Bank criteria (Movement Disorder Society Task Force on Rating Scales for Parkinson's Disease, 2003), a Mini-Mental State Examination (MMSE) score of 24 or above, no previous history of vascular or demyelinating brain disease, and adequate proficiency in the German language. All participants provided written informed consent and the study was approved by the local ethics committees (Ethikkommission beider Basel, Basel; Switzerland; EK 74/09). Specialists who performed the assessment of the patients were unaware of the details of the study. Recruited participants underwent resting-state HD-EEG recordings and a battery of neuropsychological and neuropsychiatric assessments at baseline (BL) and at follow-up visits after a mean interval of three years (3Y) and five years (5Y). The main cohort included 77 PD patients and 32 HC at

BL, 45 PD patients and 21 HC at 3Y, and 44 PD patients and 3 HC at 5Y. Due to the specific research objectives in each of the three conducted studies, it was necessary to exclude several subjects in each study accordingly. The flowchart of the main and sub-cohorts are presented in Figure 6 and complete details are provided in the materials and methods section of the studies in Chapter 4.

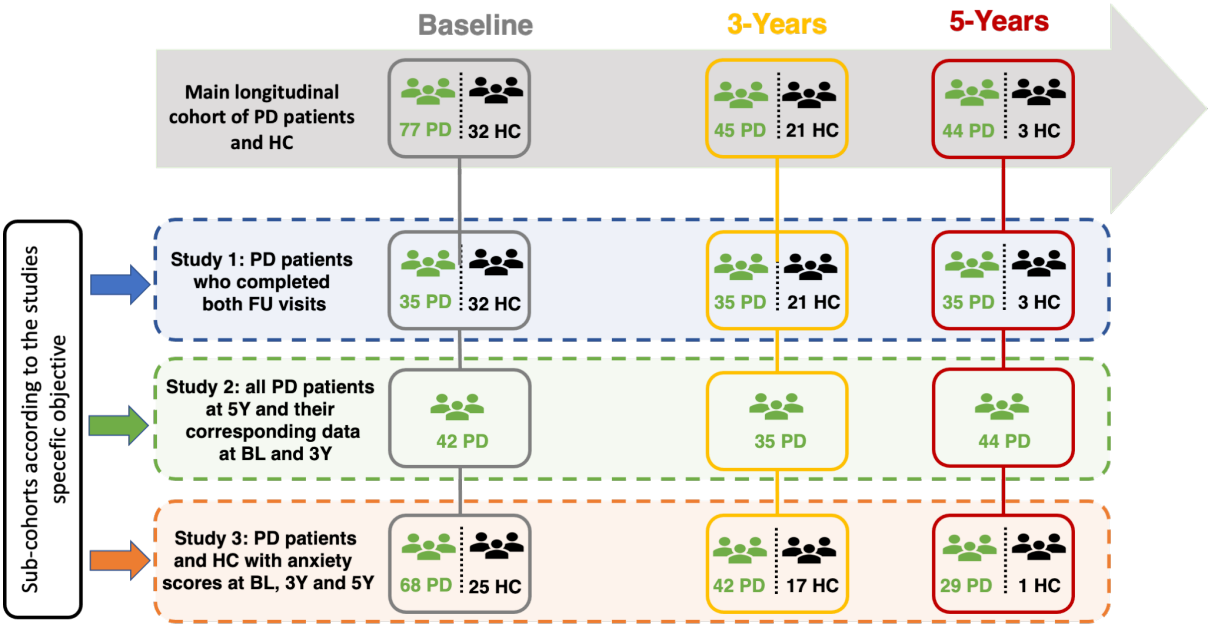

Figure 6. ***Flowcharts of the main longitudinal cohort and sub-cohorts employed in each of the three studies conducted in this thesis.***

3.2.2. Clinical, neuropsychological and neuropsychiatric evaluations

All participants underwent basic neurological and comprehensive neuropsychological examinations. Patients were evaluated while on their regular dopaminergic medication, in the 'ON' state, with reporting of antidepressant and anxiolytics treatments. Global cognitive scores were assessed using the Montreal Cognitive Assessment score (MoCA) (Nasreddine et al., 2005), and patients were classified as having or not having mild cognitive impairment (MCI), using the criteria described by the Movement Society Task Force Level II, as reported by (Litvan et al., 2012). The Unified Parkinson's Disease Rating Scale for motor experiences of daily living (UPDRS-II) and for motor examinations (UPDRS-III) were assessed by a trained physician. The lateralized items of the UPDRS-III score (item 20-26) were used in our first study to assess the patient's lateralization of motor symptoms. A comprehensive battery of neuropsychological tests was conducted to assess the following cognitive domains: attention and working memory, executive functions, verbal memory, semantic memory, language, and visuospatial functions. Anxiety symptoms were assessed in the PD patients using the German

version of the Beck Anxiety Inventory (BAI), a 21-item self-rating scale. The BAI items are evaluated on a four-point Likert scale ranging from 0 to 3 (e.g., not at all; a little; moderate; or many), and the total score ranges from 0 to 63, with higher scores indicating more severe symptoms. The use of BAI in PD has been validated by (Leentjens et al., 2011), with a score greater than 13 indicating clinically significant anxiety. As such, this threshold was considered in our third study to classify PD patients into two groups based on the presence or the absence of anxiety. Table 2 reports information about demographic, clinical and main neuropsychological characteristics of the initial cohort.

Table 2. Demographic, clinical and main neuropsychological characteristics of the main cohorts longitudinally expressed as: mean (standard deviation). *y: years, M/F: Male/Female, MoCA: Montreal Cognitive Assessment, MCI (Y/N): Mild Cognitive Impairment (yes/no), MMSE: Mini Mental State Examination, UPDRS: Unified Parkinson's Disease Rating Scale, LEDD: Levodopa Equivalent Daily Dose, WM: working memory, BAI: Beck Anxiety Inventory score, BDI-II: Beck Depression Inventory, second edition score, AES: Apathy Evaluation Scale.*

	Baseline		**3 years**		**5 years**	
	PD (N=77)	**HC (N=32)**	**PD (N=45)**	**HC (N=21)**	**PD (N=44)**	**HC (N=3)**
Demographic						
Age (y)	66.2 (8.2)	65.3 (5.6)	70.9 (7.9)	68.7 (4.9)	71.7 (7.8)	65.6 (4.1)
Sex (M/F)	51/26	18/14	31/14	9/12	28/14	2/1
Education (y)	14.6 (3.2)	13.8 (2.9)	14.8 (3.1)	13.6 (3.1)	15.1 (3.1)	11 (2)
Clinical						
Disease duration (y)	5.4 (5.2)	-	8 (5.2)	-	10.4 (4.9)	-
MoCA (/30)	26 (2.4)	26.8 (2.5)	25.2 (3.5)	27.4 (2.2)	25.1 (5.1)	
MCI (Y/N)	25/52	-	16/29	-	16/28	-
MMSE (/30)	28.7 (1.2)	29.4 (1)	28.2 (2.3)	29 (1.5)	28.3 (1.9)	
UPDRS-II	6.6 (4.7)	-	10.8 (5.7)	-	9.6 (6.6)	-
UPDRS-III	15.5 (11)	-	20.5 (12.1)	-	19.5 (13.1)	-
Medication						
LEDD (mg/day)	676 (466)	-	707 (445)	-	633 (386)	-
Neuropsychological tests z-scores by domain						
Attention + WM	-0.29 (0.5)	0.05 (0.6)	-0.29 (0.6)	0.4 (2.4)	-0.42 (0.5)	-0.12 (0.8)
Executive function	-0.22 (0.6)	0.07 (0.6)	-0.14 (0.7)	0.57 (0.4)	-0.18 (0.9)	0.24 (0.5)
Verbal memory	-0.93 (1)	-0.9 (1)	-1.38 (1.6)	-0.8 (1.2)	-0.77 (1.3)	-1.22 (1.1)
Semantic memory	-0.46 (0.8)	0.36 (1.2)	-0.47 (1.3)	0.88 (1.1)	-0.49 (1.2)	-0.2 (0.3)
Language	-0.23 (0.6)	0.35 (0.7)	-0.19 (1)	0.74 (0.9)	-0.09 (1.1)	0.14 (0.6)
Visuo-spatial abilities	-0.46 (0.9)	0.04 (0.8)	-0.14 (1.1)	0.71 (1)	0.09 (1)	0.46 (1)
Neuropsychiatric tests						
BAI (/63)	9.7 (8)	2.9 (4)	11.5 (7.5)	2.3 (2.6)	9.6 (6.9)	3.3 (4.9)
BDI-II (/63)	7.9 (4.9)	2.6 (2.4)	7.8 (4.7)	1.8 (1.7)	6.7 (6.1)	4 (3.6)
AES (/63)	32.9 (8.4)	24.1 (5.1)	31.2 (7.1)	25.1 (5.7)	31.7 (8.6)	27.7 (9)

3.2.3. EEG recording and preprocessing

The resting state EEG data were recorded in the afternoons using a 256-channel EEG system (Netstation 300, EGI, Eugene, OR) during continuous sessions of 12 minutes. The sampling rate was set to 1000 Hz. Participants were comfortably seated in a relaxing chair and instructed to close their eyes, relax, and minimize eye and body movements while remaining awake. To ensure patient vigilance, an EEG technician was present in the recording room. The HD-EEG signals were segmented into 40-second epochs and the first epoch from each recording was discarded from the analysis. Segmented epochs were preprocessed automatically using the open-source toolbox Automagic (https://github.com/methlabUZH/automagic) (Pedroni et al., 2019). In summary, the toolbox is utilized with several preconfigured steps. Firstly, signals are band-pass filtered between 1 and 45 Hz, and the electrooculography (EOG) regression is performed on 17 frontal electrodes to remove ocular artifacts. This reduces the number of channels to 239 (Figure 7-A). Next, bad channels with high variance (above 20 μV) or amplitude exceeding ±80 μV are detected and then interpolated. Further remaining artifacts were removed by the independent component analysis implemented in the toolbox. Epochs with a Ratio of Bad Channels (RBC) metric exceeding 0.15 (equivalent to 15% of the total number of electrodes) are excluded, and the remaining epochs are sorted based on the Overall High Amplitude (OHA) metric. For the remainder of the analysis, we decided to keep only the first six epochs with the best quality metrics. We also visually inspected the epochs to confirm the removal of artifacts and ensured their quality. Any remaining epochs with artifacts were either substituted with clean ones or excluded entirely from the study.

3.4. Functional connectivity analysis

3.4.1. EEG source connectivity

Previously, EEG/MEG functional connectivity studies primarily focused on scalp-level analysis, which involved evaluating the statistical interdependence among the recorded scalp potentials (Ahirwal et al., 2016; Fraga González et al., 2016; Huang et al., 2018; Sargolzaei et al., 2015). However, due to the electromagnetic volume conduction properties of the head and the fact that each scalp electrode can captures approximately 10 cm^2 of synchronous cortical activity, EEG can be viewed as a complex amalgamation of overlapping electrical signals generated simultaneously across multiple regions of the brain and detected by multiple sensors

(Figure 7-B) (Buzsáki et al., 2012; Schoffelen & Gross, 2009). As a result, the so-called scalp-connectivity may not accurately reflect the actual interaction between underlying brain regions (Lai et al., 2018). Therefore, estimating intracranial activity from scalp EEG presents a significant challenge in neuronal data processing (Brunner et al., 2016; Hassan & Wendling, 2018; Schoffelen & Gross, 2009; Van de Steen et al., 2019).

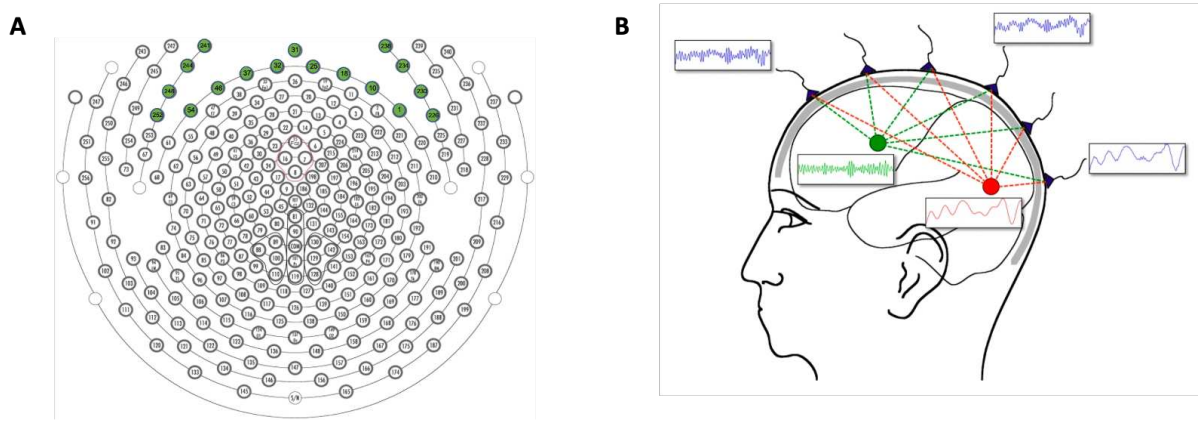

Figure 7. ***EEG sensor layout and volume conduction problem. A)*** *EGI 256-channels sensor layout adapted from (Luu et al., 2011). The 17 frontal channels used for electrooculography (EOG) regression are marked in green.* ***B)*** *Illustration of the volume conduction problem. Brain sources contribute to signals recorded at different electrodes. The statistical dependencies measured in the electrode space do not provide a direct interpretation of the functional connectivity between the cortical regions generating the signals.* A*dapted from (https://ikuz.eu/supervision/eeg-source-localization-a-machine-learning-approach-by-gagandeep-singh/)*

In recent years, the "EEG source connectivity" method has been proposed to reduce the aforementioned limitations (Hassan & Wendling, 2018; Hassan et al., 2014; Mehrkanoon et al., 2014). Rather than assessing connectivity between recorded EEG signals, this method involves analyzing connectivity between cortical sources which reduces source-leakage effects and provides higher spatial resolution (Lai et al., 2018). The EEG source connectivity method is a two-step process, the first step involves solving the EEG inverse problem to estimate the cortical sources and reconstruct their temporal dynamics, while the second step involves measuring the functional connectivity between the reconstructed sources (Hassan et al., 2014; Hassan & Wendling, 2018). The full analysis pipeline is illustrated in Figure 8.

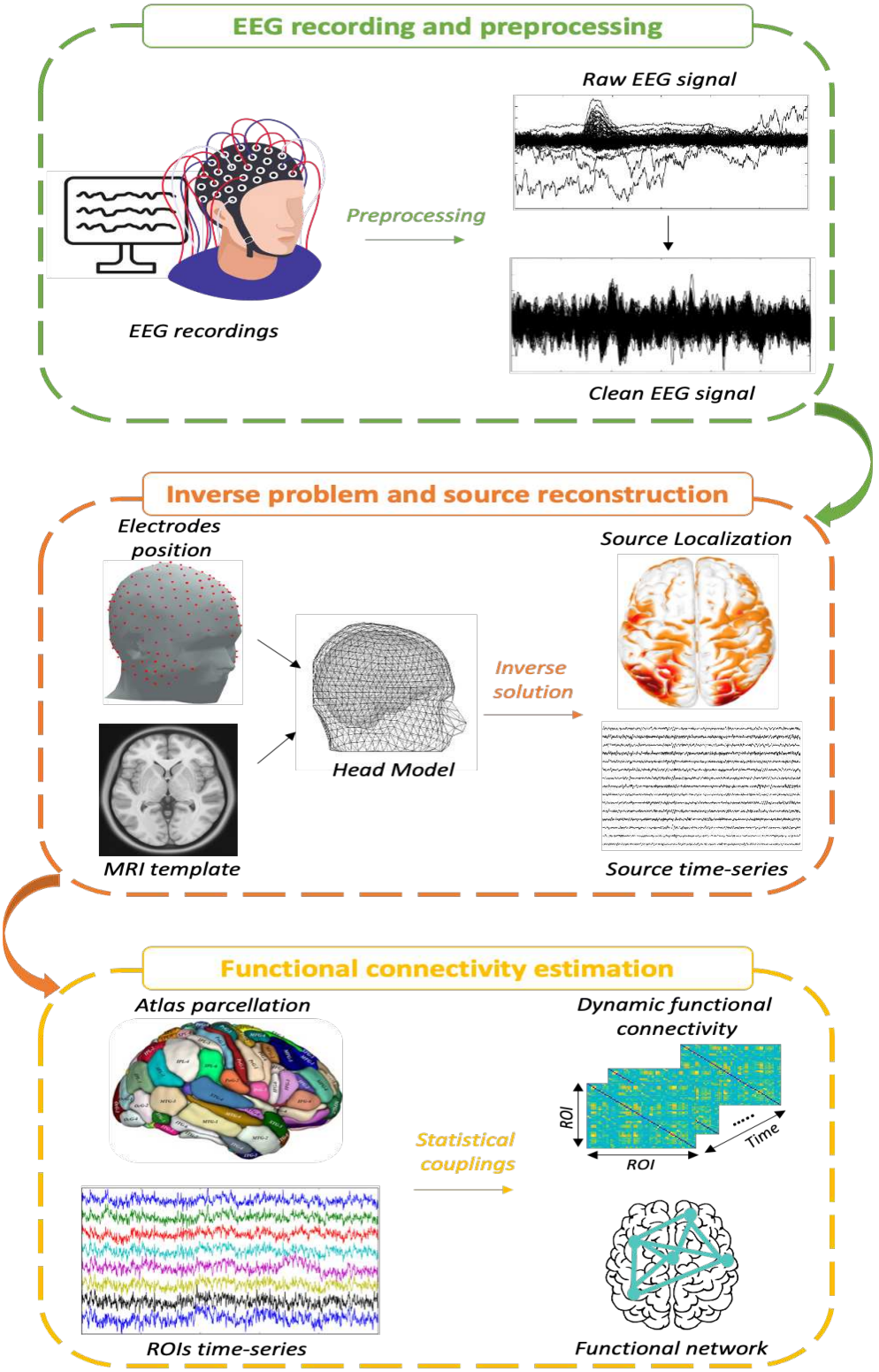

Figure 8. ***Schematic diagram illustrating the fundamental processing steps of the EEG source connectivity pipeline.*** *The process includes recording of EEG signals at the scalp level, preprocessing the signals, computing the lead field (gain) matrix, solving the inverse problem and reconstruct the source time series, clustering source signals into predefined ROIs and compute their time series, estimate the statistical couplings between ROIs and obtain both dynamic and static functional networks.*

3.4.2. Inverse problem and source reconstruction

To estimate the intracranial neural activity that generates a scalp potential map, an inverse problem needs to be solved (Baillet et al., 2001; Grech et al., 2008; Hassan & Wendling, 2018; He et al., 2018; Michel et al., 2004; Michel & Brunet, 2019). The dipole theory states that recorded EEG signals $X(t)$ from M sensors can be expressed as a linear combination of P dynamic dipolar sources $S(t)$:

$$X(t) = G.S(t) + N(t)$$

where $G(M \times P)$ is the lead field matrix (gain) that indicates the contribution of each cortical source to the sensors and $N(t)$ represents the additive noise. The lead field matrix can be computed using the positions of the M electrodes and a realistic multiple-layer head model that accounts for the flow of electric activity from sources to sensors through the head tissues (brain, skull, and skin). A commonly used numerical approach for building realistic head models is the Boundary Element Method (BEM), which takes into account detailed head anatomy characteristics (Gramfort et al., 2010).

Due to the ill-posed nature of the inverse problem (where $P>>M$), additional mathematical and physical constraints are necessary to obtain an approximate solution. One common approach is to assume that sources (mainly the pyramidal cells) are homogeneously distributed over the cortex and are normally constrained to the cortical surface (Dale & Sereno, 1993; Grech et al., 2008; He et al., 2018). This reduces the problem to estimating the magnitude of the dipolar sources using the equation:

$$S(t) = W.X(t)$$

Where W is the inverse matrix, also known as spatial filters or weights. To estimate W, several algorithms have been proposed (Baillet et al., 2001), including beamforming family methods (Van Veen et al., 1997) and two commonly used least-squares minimum-norm type estimates: the weighted minimum norm estimate (wMNE) (Fuchs et al., 1999; Lin et al., 2006; Hämäläinen & Ilmoniemi, 1994) and the standardized/exact low-resolution brain electromagnetic tomography (s/eLORETA) (Pascual-Marqui et al., 1999). These methods are typically applied to a high-resolution surface mesh with approximately 15000 vertices. The selection of the appropriate inverse method to achieve more accurate source estimation has been the subject of numerous studies (Allouch et al., 2022, 2023; Anzolin et al., 2019; Halder

et al., 2019; Hassan et al., 2014; Hedrich et al., 2017; Tait et al., 2021). Despite these efforts, no consistent conclusions have been reached regarding a single method that outperforms the others in terms of performance. In the studies presented in this thesis, we chose to adopt the weighted minimum norm estimate (wMNE) to estimate the inverse matrix, as it was shown to perform better than other methods in (Hassan et al., 2014) as well as in (Allouch et al., 2022, 2023; Hassan, Merlet, et al., 2017) in the context of resting-state real and simulated epileptiform activity.

wMNE, which has been described in (Fuchs et al., 1999; Lin et al., 2006), is based on the minimum norm estimate (MNE) (Hämäläinen & Ilmoniemi, 1994). MNE offers a solution that minimizes the square error to fit the measurements. However, wMNE goes beyond MNE by compensating for MNE's tendency to prioritize surface and weak sources:

$$W_{WMNE} = BG^T(GBG^T + \lambda \mathrm{C})^{-1}$$

Where λ is the regularization parameter (set to default value of 1/SNR; SNR=3 as recommended by the brainstorm toolbox (Tadel et al., 2011)) and C is the noise covariance matrix obtained from a noisy epoch in the recordings. Matrix B is diagonal matrix built from the lead field (gain) matrix G. The non-zero terms of B are inversely proportional to the norm of the lead field vectors. This matrix is used to adjust the solution by reducing the bias that is typically found in the standard MNE solution:

$$B_{ij} = \begin{cases} \left(G_i{}^T G_i\right)^{\frac{1}{2}}, & if\ i = j; \\ 0, & if\ i \neq j; \end{cases}$$

Once the temporal dynamics at the cortical source level have been estimated, it is crucial to define a source space comprising precise regions of interest (ROIs) to accurately calculate the corresponding regional time series. Typically, brain sources are clustered into ROIs, which can be defined based on anatomical brain parcellations such as the Desikan-Killiany atlas (68 ROIs) (Desikan et al., 2006) or Destrieux atlas (148 ROIs) (Destrieux et al., 2010), or based on functional parcellations such as the Brainnetome functional atlas (246 ROIs) (Fan et al., 2016; Yu et al., 2011). To obtain a single representative time series for each ROI, there are several approaches available, with signal averaging being the most common. Therefore, the regional time series can be calculated by averaging the source time series across the corresponding ROIs. In our studies, we aimed to obtain the dynamics of the brain regions with high spatial

resolution. Thus, we chose the Brainnetome atlas, which includes 210 cortical ROIs, to define our source space (Fan et al., 2016).

3.4.3. Functional connectivity estimation

After reconstructing the cortical dynamics, the next step is to assess functional connectivity, which refers to the statistical coupling between distinct brain regions (ROIs). The literature proposes various methods to characterize and quantify the large-scale functional organization of the human brain, including linear or nonlinear approaches, phase and/or amplitude-based synchronization, temporal and/or spectral measures, with or without correction for source leakage, see (Cao et al., 2022; Friston, 2011; Pereda et al., 2005) for reviews. However, similar to the inverse solutions, these methods have shown considerable variation in performance and interpretation (Allouch et al., 2022, 2023; Colclough et al., 2016; Hassan et al., 2014; Hassan, Merlet, et al., 2017; H. E. Wang et al., 2014; Wendling et al., 2009), making it difficult to determine the ideal approach that outperforms others. In the context of detecting epileptic spikes, (Hassan et al., 2014) and (Hassan, Merlet, et al., 2017) found that the Phase-locking Value (PLV) connectivity method (Lachaux et al., 1999) combined with wMNE inverse method have higher accuracy compared to other algorithms. This approach also performed well in the context of simulated epileptic activity (Allouch et al., 2022). Additionally, methods that correct for source leakage, such as orthogonalized Amplitude Envelope Correlation (AEC) (Brookes et al., 2011; Colclough et al., 2015), have been shown to perform well when combined with wMNE for reconstructing resting-state networks (Allouch et al., 2023). Thus, in this thesis, we chose to use PLV and AEC as functional connectivity metrics.

The PLV (Lachaux et al., 2000) for two brain signals $x(t)$ and $y(t)$ is defined as follows:

$$PLV = x(t)\left|E\left\{e^{i(\phi_x(t)-\phi_y(t))}\right\}\right|$$

where $E\{.\}$ is the expected value operator and $\phi(t)$ is the instantaneous phase derived from the Hilbert transform. To compute PLV, we used consecutive non-overlapping sliding windows with a length of $\frac{6}{central\ frequency}$ as recommended in (Lachaux et al., 1999), with 6 being the number of cycles in a given frequency band.

As for the AEC with source leakage correction, zero-lag signal overlaps caused by spatial leakage were removed using a multivariate symmetric orthogonalization approach (Colclough et al., 2015). Briefly, the approach involves computing the closest orthonormal matrix to the

uncorrected regional time courses, and then iteratively adjusting the magnitudes of the orthogonalized vectors to minimize the least-squares distances between corrected and uncorrected signals. Orthogonalization is applied to the entire data segment. Following the orthogonalization procedure, AEC is computed as the Pearson correlation between signals' envelopes derived from the Hilbert transform (Brookes et al., 2011). Here, we used the brainstorm implementation of the method with windows of 5 seconds each without overlap.

At the end of this step, the human brain is depicted as a network consisting of a set of nodes (brain regions) and a set of edges that represent the functional interaction between these nodes. Mathematically, a $N_r \; x \; N_r$ connectivity matrix is obtained, where N_r is the number of ROIs and each element $a_{i\;j}$ in the matrix represents the strength of the connection between region i and region j.

In our studies, we calculated the dynamic functional connectivity matrices in the six different EEG frequency bands: delta (1-4 Hz), theta (4-8 Hz), alpha1 (8-10 Hz), alpha2 (10-13 Hz), beta (13-30 Hz) and gamma (30-45 Hz). The dynamic matrices were computed for each epoch and subsequently averaged across time and trials to obtain a single static connectivity matrix that represents the functional brain networks of the participants.

3.3. Power spectral analysis

Power spectral analysis is a widely used technique in EEG signal analysis. It involves decomposing the complex EEG signal into its component frequencies using the Fourier transform (Kim & Im, 2018), which allows for the quantification of the amount of rhythmic or oscillatory activity (power) across different frequency bands. Spectral power can be assessed at the scalp level from preprocessed EEG signals or at the cortical level from the temporal dynamics of the reconstructed sources. In our studies, the Welch method was used to estimate the power spectrum of signals (Welch, 1967). The periodogram was computed using the Hamming window and averaged across segments with 50% overlap to obtain the final spectral estimate. The relative power was used to assess the relative contribution of a specific frequency to the EEG signal (Heisz & McIntosh, 2013) and was calculated by dividing the absolute power in a given frequency band by the total power of the broadband (1-45 Hz). Here, we investigated the relative power in the six different EEG frequency bands: delta (1-4 Hz), theta (4-8 Hz), alpha1 (8-10 Hz), alpha2 (10-13 Hz), beta (13-30 Hz) and gamma (30- 45 Hz).

3.5. Clustering analysis

In our second study, the main objective was to cluster PD patients based exclusively on their EEG-based features. To achieve this, we used a data-driven unsupervised clustering approach that relied on the Similarity Network Fusion (SNF) method (B. Wang et al., 2014). SNF is a novel technique that allows the combination of features from multiple data sources into a single fused similarity network or graph. This graph captures both mutual and complementary information between features. SNF constructs similarity networks for each data source using a K-nearest neighbours weighted kernel and iteratively combines them using a non-linear message passing protocol (Pearl, 1988). The final fused network contains sample relationships representing information from all data sources and can be subjected to clustering or other types of graph analysis. We opted to use SNF because it has been shown to be effective in disentangling heterogeneity in PD, amyotrophic lateral sclerosis and psychiatric disorders (Dukic et al., 2021; Jacobs et al., 2021; Markello et al., 2021; Stefanik et al., 2018).

In our study, we used SNF to extract and combine similarity networks corresponding to the power spectral and/or functional connectivity features from different frequency bands (Figure 9-A). To summarize, the initial step involved normalizing the features, followed by constructing distance matrices using the squared Euclidean distance. Subsequently, a scaled exponential kernel was applied to transform the distance matrices into unique similarity matrices:

$$W(i,j) = \frac{1}{\sqrt{2\pi\sigma^2}}\, e^{-\frac{\rho^2(x_i, x_j)}{2\sigma^2}}$$

where $\rho(x_i - x_j)$ is the Euclidean distance between patients x_i and x_j and σ is defined as:

$$\sigma = \mu \frac{\underline{\rho}^2(x_i, N_i) + \underline{\rho}^2(x_j, N_j) + \underline{\rho}^2(x_i, x_j)}{3}$$

where $\underline{\rho}(x_i, N_i)$ represents the average value of distances between x_i and each of its neighbors $N_{1..k}$. Both k and μ are hyperparameters that need to be chosen beforehand. The value of k should be selected from the range [1, j], where j is an integer to control the number of k-nearest neighbors. The parameter μ, on the other hand, should be chosen from the range of [0.3, 1] in order to scale the exponential kernel. Once the similarity matrices are constructed, they are fused together using a nonlinear message-passing method. This involves iteratively updating

each similarity network with complementary information from the other networks to maximize their similarity until convergence or a pre-specified number of iterations is reached. Lastly, the resulting fused similarity network undergoes spectral clustering, which necessitates a pre-selection of the number of clusters. The entire process was conducted using the MATLAB implementation of the SNF method (http://compbio.cs.toronto.edu/SNF/SNF/Software.html).

To prevent bias in our results due to the choice of hyperparameters and the number of clusters, we adopted an approach proposed by (Markello et al., 2021), which involved an exhaustive parameter search combined with a consensus analysis. We performed SNF with various combinations of k (k = 1, 2, 3, ..., N-1) and (μ = 0.3, 0.35, 0.4, ..., 1), resulting in a set of fused networks. Using spectral clustering (Yu & Shi, 2003), these networks were then partitioned into two, three, and four clusters, as these were the most reasonable choices reported in previous studies on PD subtyping (Figure 9-B) (Dadu et al., 2022; Fereshtehnejad et al., 2017; Markello et al., 2021; X. Zhang et al., 2019). To ensure the stability of the clustering solutions, we retained only the combinations of hyperparameters where slight changes in either k or did not significantly affect the clustering outcome. For each number of clusters, we calculated a pairwise z-Rand similarity index (Traud et al., 2016) between the clustering solutions of each combination of hyperparameters (k, μ) and their four closest combinations (k-1, μ), (k+1, μ), (k, μ-0.05), and (k, μ+0.05). We retained the clustering solutions corresponding to the highest 5% of z-Rand similarity indexes, which were then used in a consensus analysis inspired by community detection studies (Bassett et al., 2012; Lancichinetti & Fortunato, 2012). The resulting NxN co-assignment matrix contained normalized probabilities of two patients belonging to the same cluster across assignments. This matrix was thresholded by comparing it with another matrix generated from a permuted null model (Bassett et al., 2012), and the resulting matrix was then clustered using a modularity maximization procedure (Blondel et al., 2008) to obtain the final clustering partition representing PD subtypes (Figure 9-C).

To evaluate the stability of the identified clusters against data perturbations, we conducted a sensitivity analysis by repeating the entire clustering process 100 times, each time randomly removing 10% of the patients. To estimate the robustness of the clusters, we calculated a robustness coefficient at each iteration by comparing the resulting cluster assignments with those obtained in the original analysis. We corrected for chance agreement between the cluster assignments using the Rand index (Hubert & Arabie, 1985). All codes used in this analysis are available at: https://github.com/yassinesahar/ClusteringPD.

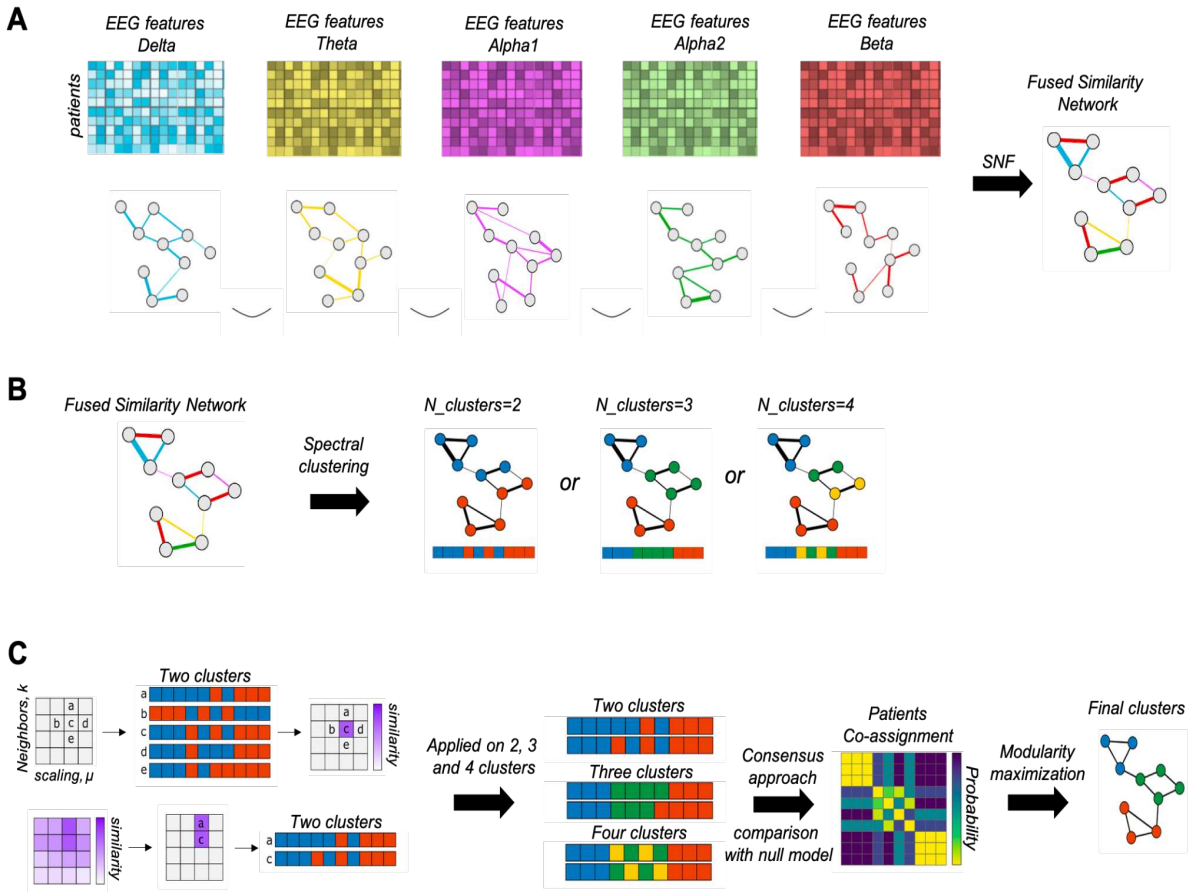

Figure 9. ***Clustering analysis pipeline adapted and modified from (Markello et al., 2021). A)*** *The process of Similarity Network Fusion involves creating separate similarity networks for each data type (frequency bands), which are then combined through iterative fusion. The patients' nodes, depicted as circles, are connected by edges that reflect the similarity of their disease phenotype.* ***B)*** *The obtained fused similarity network can be subjected to spectral clustering to produce two, three or four clusters' solutions.* ***C)*** *Exhaustive parameter search and consensus analysis to generate the final patient clusters.*

3.6. Statistical analysis

3.6.1. Network Based Statistic (NBS)

In our first study on PD progression, we aimed to uncover the functional brain networks that underwent significant changes in connectivity weight over the course of the disease. To achieve this, we utilized the Network Based Statistic toolbox (NBS) to compare the brain networks of PD patients at baseline (BL) and at the five-year follow-up (5Y). This method assumes that subnetworks of disrupted connections are more indicative of real alterations than isolated disconnections and provides a more powerful statistical analysis than generic methods (Zalesky et al., 2010). To identify the significant networks, NBS conducts a t-test to assess the significant differences in connectivity values along the $(N^2-N)/2$ edges of the [N x N] connectivity matrices

of the PD patients between the BL and 5Y. A primary component-forming threshold of $p<0.05$ is then applied to identify supra-threshold connections, from which all possible connected components and their sizes were determined. Next, a corrected p-value is evaluated for each component with respect to the null distribution of maximal connected component size obtained using a nonparametric permutation approach (2000 permutations). We performed this analysis with different thresholds for the t-test (ranging from 2.6 to 3.7) to assess the consistency of the results. Age, gender, education, levodopa equivalent daily dose (LEDD), and dominant side of motor symptoms were considered as confounding factors in this analysis.

3.6.2. Permutation-based statistical analysis

In our third study, our primary objective was to identify the electrophysiological signature of anxiety in PD. We aimed to compare EEG-based features of the anxious PD group (PD-A) with those of non-anxious PD patients (PD-NA) and healthy controls (HC). To perform this three-group comparison, we used a two-step process involving a permutation-based non-parametric analysis of covariance (Perm-ANCOVA), followed by a two-tailed between-groups Wilcoxon test. The Perm-ANCOVA was applied to the relative power spectrum and functional connectivity networks of the three groups at BL, with 1000 permutations used to determine a first set of significant power/connectivity features ($p<0.05$). We then defined two conditions: the PD-A_{high} condition, where the power/connectivity values of the PD-A group were significantly higher than those of both the PD-NA and HC groups (PD-A > PD-NA & PD-A > HC), and the PD-A_{low} condition, where the power/connectivity features had significantly lower values in the PD-A group compared to both other groups (PD-A < PD-NA & PD-A < HC). Next, we applied a two-tailed between-groups Wilcoxon test (corrected for multiple comparisons, $p<0.0167$) on the previous set of statistically significant features to identify those that primarily represent the PD-A group. Thus, features meeting one of the above conditions were retained and considered as electrophysiological signatures of anxiety in PD.

CHAPTER 4: RESULTS

4.1. Study I- Functional brain dysconnectivity in Parkinson's disease: A 5-years longitudinal study

Sahar Yassine, Ute Gschwandtner, Manon Auffret, Sophie Achard, Marc Verin, Peter Fuhr, Mahmoud Hassan.

***Published in: Movement Disorders* 37.7 (2022): 1444-1453.**
https://movementdisorders.onlinelibrary.wiley.com/doi/full/10.1002/mds.29026

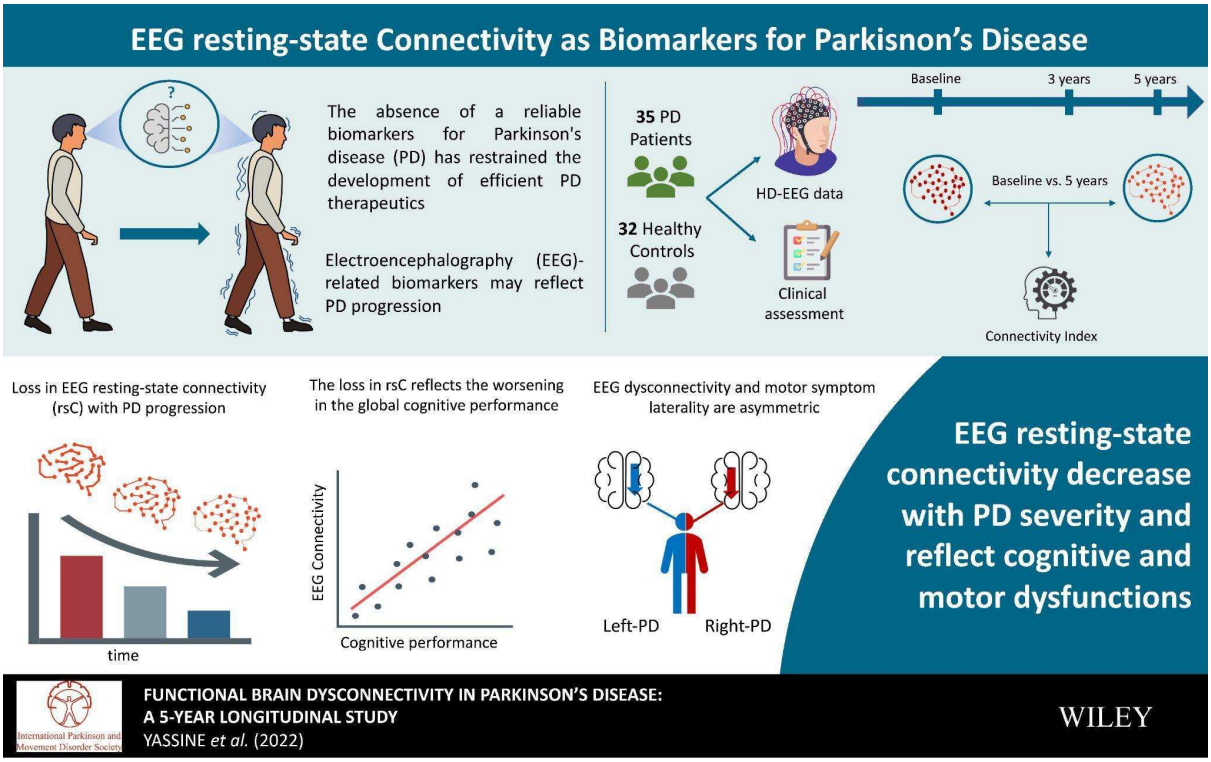

Figure 10. ***Graphical abstract of the first study published in Movement Disorders journal.***

RESEARCH ARTICLE

Functional Brain Dysconnectivity in Parkinson's Disease: A 5-Year Longitudinal Study

Sahar Yassine, MSc,[1,2] Ute Gschwandtner, MD,[3] Manon Auffret, PharmD, PhD,[4] Sophie Achard, PhD,[5] Marc Verin, MD, PhD,[1,4,6,7*] Peter Fuhr, MD,[3#] and Mahmoud Hassan, PhD[8,9#*]

[1]*Univ Rennes, Inserm, LTSI - U1099, Rennes, F-35000, France*
[2]*NeuroKyma, Rennes, F-35000, France*
[3]*Department of Neurology, Hospitals of the University of Basel, Basel, Switzerland*
[4]*Comportement et noyaux gris centraux, EA 4712, CHU Rennes, Rennes, France*
[5]*University Grenoble Alpes, CNRS, Inria, Grenoble INP, LJK, 38000 Grenoble, France*
[6]*Movement Disorders Unit, Neurology Department, Pontchaillou University Hospital, Rennes, France*
[7]*Institut des Neurosciences Cliniques de Rennes (INCR), Rennes, France*
[8]*MINDig, Rennes, F-35000, France*
[9]*School of Science and Engineering, Reykjavik University, Reykjavik, Iceland*

ABSTRACT: Background: Tracking longitudinal functional brain dysconnectivity in Parkinson's disease (PD) is a key element to decoding the underlying physiopathology and understanding PD progression.

Objectives: The objectives of this follow-up study were to explore, for the first time, the longitudinal changes in the functional brain networks of PD patients over 5 years and to associate them with their cognitive performance and the lateralization of motor symptoms.

Methods: We used a 5-year longitudinal cohort of PD patients (n = 35) who completed motor and non-motor assessments and sequent resting state (RS) high-density electroencephalography (HD-EEG) recordings at three timepoints: baseline (BL), 3 years follow-up (3YFU) and 5 years follow-up (5YFU). We assessed disruptions in frequency-dependent functional networks over the course of the disease and explored their relation to clinical symptomatology.

Results: In contrast with HC (n = 32), PD patients showed a gradual connectivity impairment in $\alpha 2$ (10-13 Hz) and β (13–30 Hz) frequency bands. The deterioration in the global cognitive assessment was strongly correlated with the disconnected networks. These disconnected networks were also associated with the lateralization of motor symptoms, revealing a dominance of the right hemisphere in terms of impaired connections in the left-affected PD patients in contrast to dominance of the left hemisphere in the right-affected PD patients.

Conclusions: Taken together, our findings suggest that with disease progression, dysconnectivity in the brain networks in PD can reflect the deterioration of global cognitive deficits and the lateralization of motor symptoms. RS HD-EEG may be an early biomarker of PD motor and non-motor progression. © 2022 The Authors. *Movement Disorders* published by Wiley Periodicals LLC on behalf of International Parkinson and Movement Disorder Society

Key Words: Parkinson's disease; functional brain networks; electroencephalography; follow-up study; movement disorders

*__Correspondence to:__ Marc Verin, Neurology Departement Pontchaillou University Hospital, Rue Henri Le Guilloux 35033 Rennes Cedex 9, France; E-mail: marc.verin@chu-rennes.fr
Mahmoud Hassan, Reykjavik University, Menntavegur 1, 101 Reykjavik, Iceland; E-mail: mahmoud.hassan.work@gmail.com

[Corrections added on 27 May 2022, after first online publication: The degrees for Ute Gschwandtner and Peter Fuhr have been corrected. The affiliation for Sophie Achard has been corrected.]

Relevant conflicts of interest: There are no financial conflicts of interest to disclose.

#These authors have contributed equally to this work.

Received: 31 January 2022; **Revised:** 19 March 2022; **Accepted:** 24 March 2022

Published online 14 April 2022 in Wiley Online Library (wileyonlinelibrary.com). DOI: 10.1002/mds.29026

Introduction

Parkinson's disease (PD) is one of the most frequent neurodegenerative disorders in the elderly population.[1] Along with its well-known prominent motor symptoms (resting tremor, bradykinesia, rigidity, and postural imbalance), a broad spectrum of non-motor disturbances (cognitive impairment up to dementia, neuropsychiatric disturbances, autonomic or sleep disorders, etc.) can manifest from early (even prodromal) disease stages onward diminishing the quality of life of the patients.[2-4] Pathologically, the most prevalent hypotheses suggest that the degeneration of dopaminergic neurons in the nigrostriatal system associated with Lewy body inclusions are the leading features in most forms of PD at early stages.[5,6] However, with the disease progression, the neuropathological process may propagate across interconnected networks reaching the cortex and causing functional alterations within and between brain regions.[7] Still, these neuropathological insights do not sufficiently expound the heterogeneous phenotype[8,9] of the patients and the progression-related changes in their brain activity.

Functional disruptions related to both motor and cognitive deficits at early and advanced PD stages were reported using mainly functional magnetic resonance imaging techniques (fMRI).[10-13] Moreover, electro/magneto-encephalography (EEG/MEG) are increasingly shown as powerful, cost-effective, and non-invasive electrophysiological techniques, to explore functional brain networks in neurodegenerative disorders.[14-18] In PD, MEG/EEG studies uncovered an increase in the cortico-cortical connectivity, characterizing PD patients from earliest disease clinical stages onward,[19,20] whereas decreases in the functional connectivity, mainly in the frontotemporal networks, were proclaimed to reflect the development of mild cognitive impairment and dementia conditions in advanced stages.[17,21,22] Reductions in the weight of the functional connections associated with the cognitive phenotype of PD patients were also revealed in several EEG studies.[23,24] However, an important limitation in these findings lies in the fact that these studies were all achieved in a single time point rather than longitudinally, a key point to ultimately develop biomarkers in PD.

Here, we used resting state high density (HD)-EEG recordings of 77 PD patients that underwent a follow-up study at baseline (BL), 3-year follow-up (3YFU) and 5-yearfollow-up (5YFU) at the Basel university hospital. Our primary goal was to explore the disruptions in the functional brain networks of those PD patients between the BL, 3YFU, and the 5YFU. We examined their progressive evolution and compared it to that of age-matched healthy control subjects. In addition, we correlated the patient-specific altered network with the change in the clinical scores. Finally, to link the disrupted networks with the lateralized motor symptoms of the patients, we revealed different altered networks between BL and 5YFU characterizing the progression of the disease in the left-affected (LPD) and right-affected (RPD) patients.

Materials and Methods

Participants

Patients were selected from a longitudinal study cohort of patients with idiopathic PD and healthy controls (HC). Patients were recruited from the outpatient clinic of the Department of Neurology and Neurophysiology of the Hospital of the University of Basel (City of Basel, Switzerland) in the period from 2011 to 2015 based on the following selection criteria: PD according to United Kingdom Parkinson's Disease Society Brain Bank criteria,[25] Mini-Mental State Examination (MMSE) above 24/30, no history of vascular and/or demyelinating brain pathology, and sufficient knowledge of the German language. HC were matched in age and education. Included patients underwent neurological, cognitive, and EEG examinations at BL and follow-ups after a mean interval of 3 years and 5 years. The study was approved by the local ethics committees (Ethikkommission beider Basel, Basel; Switzerland; EK 74/09) and all patients gave written informed consent before the study inclusion. Specialists who performed the assessment of the patients were unaware of the details of this study. The main cohort included 77 patients at BL, from which 42 did not complete all the follow-ups examinations (see Table S1 for the detailed demographic and clinical measures of the main cohort). All patients were under dopaminergic medications during the examinations. To be noted, 10 patients used cholinesterase inhibitors. We first analyzed the subgroup of 35 PD patients who underwent all the examinations at BL, 3YFU, and 5YFU, and we then cross-validated the results on the remaining patients. The HC group included 32 participants at BL, from which 21 completed the 3YFU and 3 the 5YFU (see Fig. S1 for details of the subject's study flow). The 35 PD patients were also classified into two subgroups by a specialist based on the dominant side of their motor symptoms in all the three visits: LPD patients (n = 23) and RPD patients (n = 10). The division was done using the lateralized items of the Unified Parkinson's Disease Rating Scale III (UPDRS-III) score (items 20–26). Patients with symmetric symptoms in all visits (n = 2) were excluded from this subgroup division.

Data Acquisition and Preprocessing

Resting state EEG data were recorded in the afternoons using a 256-channel EEG System (Netstation 300, EGI, Eugene, OR) during continuous 12 minutes. Patients were seated comfortably in a relaxing chair, instructed to close their eyes and relax while staying awake with minimum eye and body movements. An EEG technician present in the recording room controlled for vigilance of the patients. The sampling rate of the signals was set to 1000 Hz. The high density (HD-EEG) signals were segmented into epochs of 40 seconds each and the first epoch from each recording was discarded from the study. They were preprocessed automatically using the open-source toolbox Automagic[26] and the first six epochs with best quality metrics were retained for the rest of the analysis. See Appendix S1, method section, for more technical details about the preprocessing.

Brain Networks Reconstruction

After preprocessing, the functional brain networks were estimated using the EEG source-connectivity method.[27] First the dynamics of cortical brain sources were reconstructed by solving the inverse problem. To do so, EEG channels and magnetic resonance imaging (MRI) template (ICBM152) were co-registered, and using the OpenMEEG toolbox,[28] a realistic head model was built. The weighted minimum norm estimate (wMNE)[29] was used to calculate the regional time series of the 210 cortical regions of interest (ROIs) of the Brainnetome atlas.[30] Afterward, the regional time series were filtered in different EEG frequency bands: θ (4–8 Hz), α1 (8–10 Hz), α2 (10–13 Hz), and β (13–30 Hz). For each frequency band, functional connectivity was computed between the reconstructed sources using the phase locking value (PLV).[31] We obtained for each participant six dynamic connectivity matrices in each frequency band. Those matrices were ultimately averaged across time and epochs to obtain a single static functional connectivity matrix per frequency band, used in the further analysis.

Statistical Analysis

The network-based statistic (NBS)[32] was used to identify the brain networks of PD patients that are significantly different between BL and 5YFU visits. This approach assumes that subnetworks of disrupted connections are more likely to indicate real alterations than isolated disconnections and has been shown to provide considerably greater statistical power than generic methods. Age, gender, education, levodopa equivalent daily dose (LEDD), and dominant side of motor symptoms were considered as confounding factors in this analysis. More details about the statistical analysis are provided in the Appendix S1, methods section.

Network Index and Correlation Analysis

We defined a metric called network index (NI), inspired from previous work of Hassan et al,[23] as the average weight (connectivity) of the output significant networks issued from NBS:

$$NI = \frac{\sum_i^N W_i}{N},$$

where W_i represents the connectivity value of the edge i of the significant network from NBS and N represents the total number of edges in this network. This NI was computed for each patient in each of the three visits to quantify the longitudinal disruptions in the networks as

TABLE 1 *Demographic and clinical characteristics of the participants at BL, 3YFU, and 5YFU visits*

	Baseline			3YFU			5YFU	
	PD (n = 35)	HC (n = 32)	*P* value	PD (n = 35)	HC (n = 21)	*P* value	PD (n = 35)	HC (n = 3)
Sex (M/F)	26/9	18/14	0.13	—	10/11	—	—	2/1
Age (y)	67.4 (8.2)	65.3 (5.6)	0.24	70.4 (8.2)	68.7 (5.5)	0.37	72.5 (8.2)	65.7 (4.2)
Education (y)	15.2 (3.2)	13.8 (2.9)	0.07	—	13.6 (3)	—	—	11 (2)
Disease dur. (y)	4.1 (3.7)	NA	—	7.1 (3.7)	NA	—	9.2 (3.8)	NA
LEDD (mg/day)	555 (430)	NA	—	660 (449)	NA	—	647 (396)	NA
UPDRS-III	13.9 (10.2)	NA	—	18.4 (9.7)	NA	—	18 (12.4)	NA
MoCA	26.2 (2.4)	26.8 (2.5)	0.26	25.1 (3.8)	27.3 (2.1)	0.016*	24.5 (5.5)	23.3 (4.6)

Values are expressed as mean (standard deviation). *Indicates results are significant.
BL, baseline; 3YFU, 3 year follow-up; 5YFU, 5 year follow-up; PD, Parkinson's disease patients; HC, healthy controls; M/F, male/female; y, years; LEDD, Levodopa equivalent daily dose; UPDRS-III, Unified Parkinson's Disease Rating Scales motor ratings; MoCA, Montreal Cognitive Assessment, NA, Not Applicable.

the disease progressed in time. For the correlation analysis, the Pearson's correlation was computed to evaluate the relationship between the NI and the clinical scores of PD patients at and between different timepoints. All parameters are described in the shared GitHub containing the codes necessary to reproduce the results (https://github.com/yassinesahar/FuncDysconnectivityPD).

Results

Participant Characteristics

Table 1 summarized the demographic and clinical characteristics of the PD patients and HC subjects included in this study. Their complete neuropsychological and neuropsychiatric assessments are shown in Table S2. There was no significance difference in age, sex, or duration of formal education between the PD patients and the HC at BL.

Longitudinal Alterations in Functional Connectivity Networks of PD Patients

The overall pipeline of the study is summarized in Figure 1. We followed a data-driven approach supposing that the networks at BL are different from those at 5YFU. The longitudinal change in the NI for both PD patients and HC was explored for the three timepoints. This includes the intermediate timepoint 3YFU whose networks were not used in the comparisons to confirm the overall tendency in the networks and to evaluate the potential correlations with the clinical scores.

Decreasing Networks of PD Patients (BL > 5YFU)

At the α2 band (10–13 Hz), results revealed a statistically significant network ($t = 3.2$, $P = 0.021$, corrected using permutation), where the connectivity at 5YFU was significantly lower than BL. This network included 125 connections and 72 regions located principally within the right hemisphere (88.8% of the edges and 88.9% of the regions). Regions with the highest number of connections (highest degree) were mainly part of the right superior and inferior frontal gyrus, right precentral gyrus and the right precuneus, with a dominance of the frontotemporal (12%), the frontofrontal (11.2%), and frontocentral (11.2%) connections (Fig. 2A). These results are in line with previous studies that linked the decrease in frontotemporal connectivity at the α band with the severity of disease progression.[17,23] The remarkable dominance of the right hemisphere will be explored later when conducting the analysis on the lateralized subgroups. Furthermore, to better understand the longitudinal changes in the network, the NI was computed for the three visits: BL, 3YFU, and 5YFU. Results showed that the NI undergoes a significant decrease between BL and 5YFU ($P < 0.001$). This decrease was progressive and significant between BL and 3YFU ($P < 0.01$) and likewise between 3YFU and 5YFU ($P < 0.05$). All P values were corrected using Bonferroni for multiple comparisons. This NI applied on the functional connectivity networks of the HC showed no significant longitudinal changes between BL and 3YFU (Fig. 2B).

Regarding the β band (13–30 Hz), the obtained network ($t = 3.7$, $P = 0.009$, corrected using permutation) comprised 103 connections issued from 58 regions. The

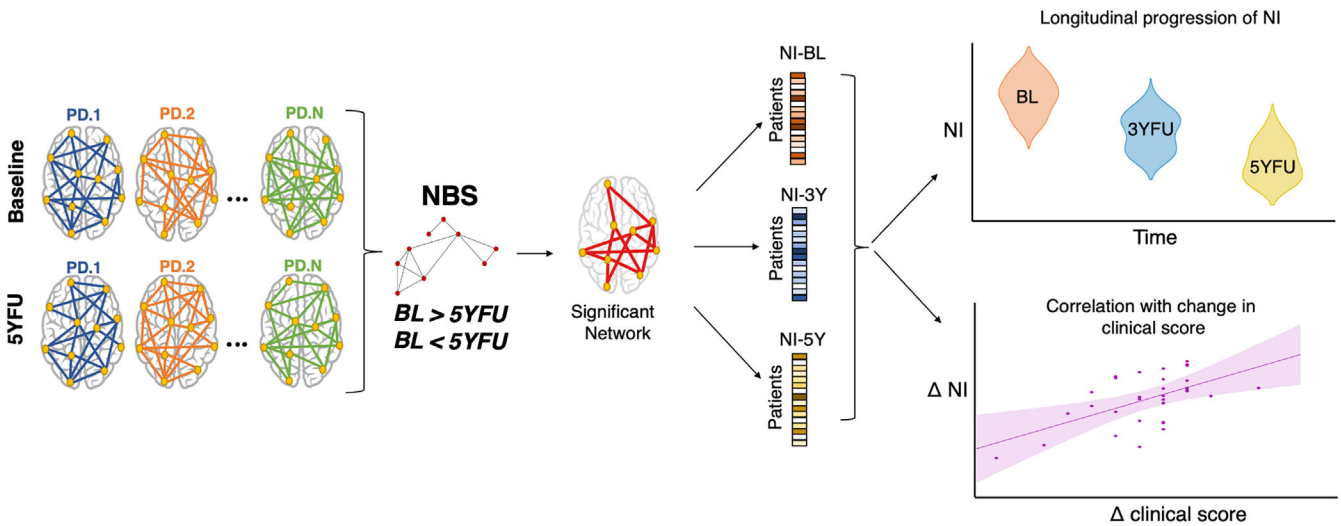

FIG. 1. General description of the analysis. The connectivity networks of the PD patients at BL and 5YFU were compared using the Network-Based Statistics (NBS) to retrieve a subnetwork of significantly hypo (BL > 5Y)/hyper (BL < 5Y) connectivity. From this significant network, A network index (NI) was attributed to each PD patient in each of the three visits to evaluate their progression in time and to correlate their longitudinal change with the change in clinical scores. [Color figure can be viewed at wileyonlinelibrary.com]

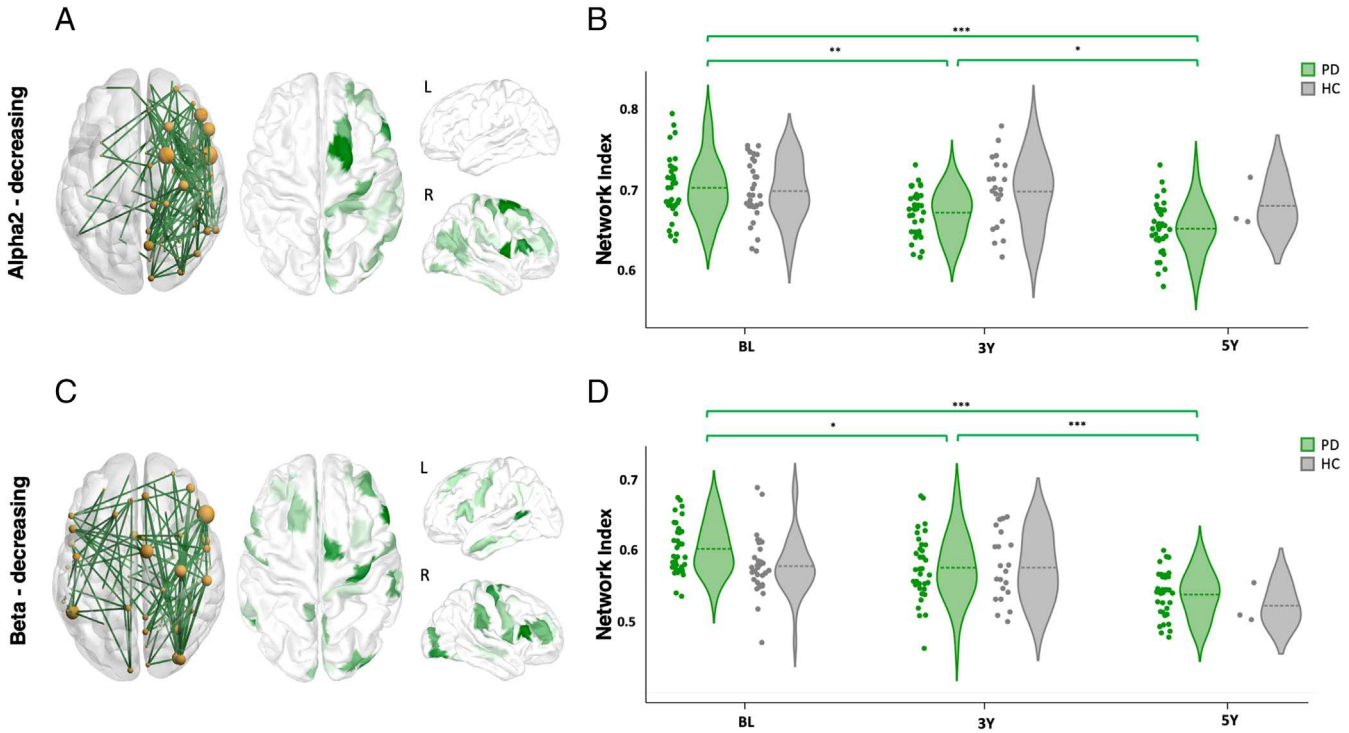

FIG. 2. Dysconnectivity networks between BL and 5YFU and their corresponding highest degree regions in (**A**) α2, (**C**) β. Violin plot representing the longitudinal change of the network index of the PD patients and HC in (**B**) α2, (**D**) β. ***$P < 0.001$, **$P < 0.01$, *$P < 0.05$ (corrected for multiple comparisons using Bonferroni). [Color figure can be viewed at wileyonlinelibrary.com]

right hemisphere was also dominant in terms of number of local edges (56.3%) and regions (58.6%). Highest degree regions were largely located in the right superior and inferior frontal, precentral and occipital cortex with a dominance of the frontotemporal (12.6%), fronto-occipital (9.7%), and frontofrontal (8.7%) connections (Fig. 2C). A significant decrease in the NI was observed between BL and 5YFU ($P < 0.001$). This decrease was more severe in terms of linear slope between 3YFU and 5YFU ($P < 0.001$) than between BL and 3YFU ($P < 0.05$). As for the HC, they showed no significant change in their NI between BL and 3YFU, and because of their small sample size at 5YFU, we were not able to statistically test the decrease observed between 3YFU and 5YFU (Fig. 2D). Results of the other frequency bands, the increasing networks and the cross validation on the entire cohort are provided in the Appendix S1.

Relationship between the NI and the Global Cognitive and Motor Scores

Results showed a global positive correlation between the NI of PD patients and their global cognitive score represented by the Montreal Cognitive Assessment score (MoCA) at both follow-up timepoints with a statistical significance at the intermediate timepoint 3YFU ($r = 0.36$, $P < 0.05$) (Fig. 3A,B). In addition, we uncovered a subnetwork issued from the previously found dysconnectivity networks, in which the longitudinal changes in the connectivity of its edges correlates with the longitudinal changes in the MoCA scores between BL and 5YFU. In α2, a subnetwork was revealed comprising 16 connections located mostly in the right hemisphere and its corresponding NI was computed (Fig. 3C). A positive significant correlation was observed between the change in both NI and MoCA between BL and 5YFU ($r = 0.64$, $P < 0.001$). This positive correlation persists also when introducing the NI of the intermediate timepoint (3YFU) reaching a significant level mainly between 3YFU and 5YFU ($r = 0.40$, $P < 0.05$). Concerning the subnetwork of the β band, it involved 40 connections distributed between both hemispheres (Fig. 3E). The longitudinal change of its corresponding NI was highly correlated with the change in MoCA score between BL and 5YFU ($r = 0.72$, $P < 0.001$) as well as between 3YFU and 5YFU ($r = 0.55$, $P < 0.01$). To ensure that the significant correlation observed in the change between BL and 5Y in both bands was not driven by the 2 patients that showed a sharp decrease in their MoCA scores (as it might be shown in the Fig. S4), we computed the correlation after excluding these patients. Results show that the correlation remains significant in α2 ($r = 0.38$, $P < 0.05$) (Fig. 3D) and β ($r = 0.49$, $P < 0.01$) (Fig. 3F). We also found significant correlation between the

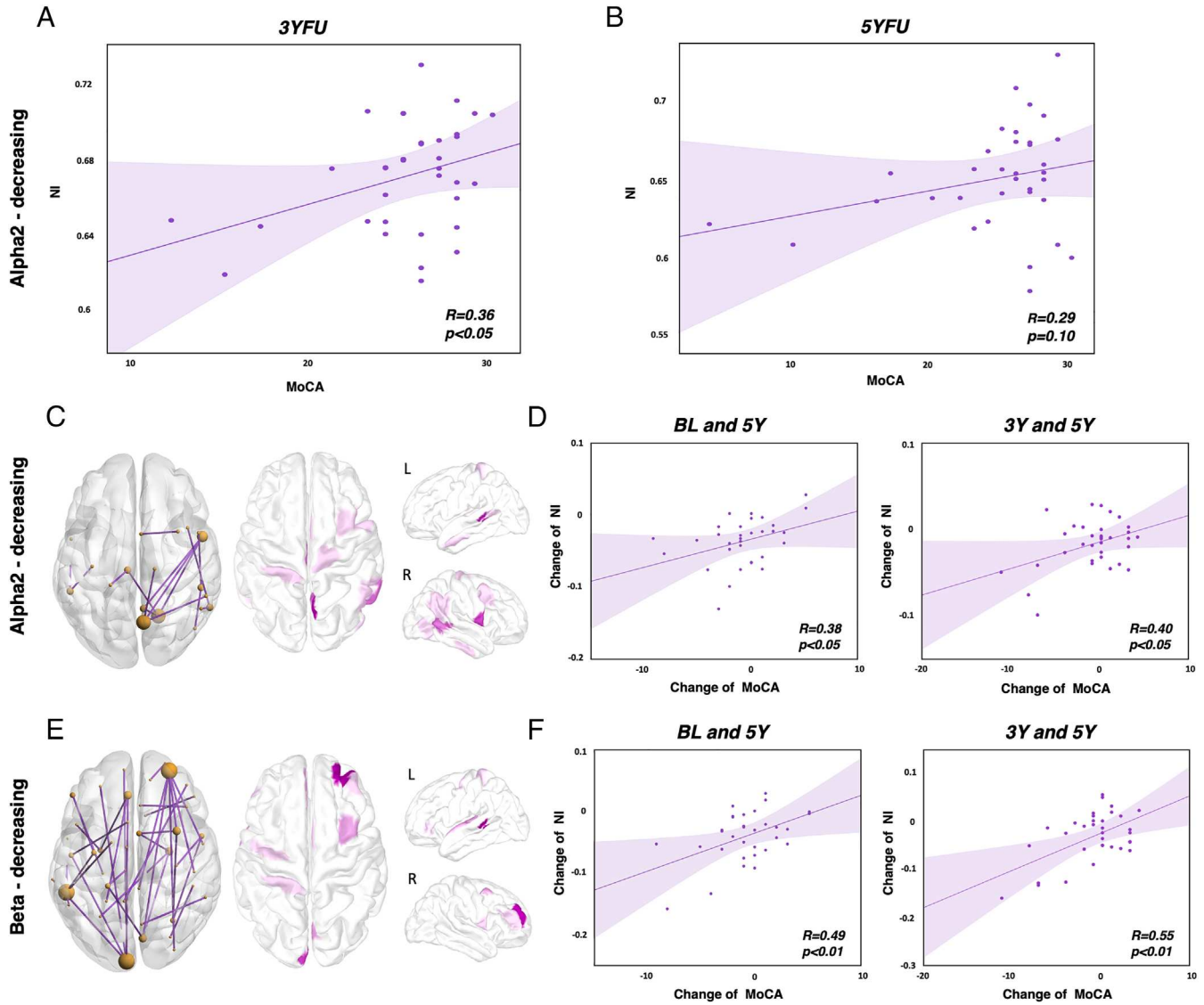

FIG. 3. Longitudinal change in the NI and in the MoCA score of PD patients. Correlation between the NI (issued from the hypo-connectivity networks reported above) and the MoCA score of PD patients at (**A**) 3YFU and (**B**) 5YFU. Dysconnectivity subnetworks and corresponding highest degree regions where the longitudinal change in the value of connectivity correlates with the longitudinal change in MoCA score of PD patients in (**C**) α2 and (**E**) β. Correlation between the change in NI and the change in MoCA observed between BL and 5YFU (left), 3YFU, and 5YFU (right) in (**D**) α2 and (**F**) β. [Color figure can be viewed at wileyonlinelibrary.com]

changes in NI and the changes in motor score (the UPDRS-III) at α2 ($r = -0.38$, $P < 0.05$) and β ($r = -0.41$, $P < 0.05$) between 3YFU and 5YFU. Figure and more details are provided in the Appendix S1.

Disrupted Networks of PD Patients with Lateralized Motor Symptoms

The above obtained networks showed a majority of disrupted connections located in the right hemisphere in α2 and β bands. To investigate this asymmetry, we divided the PD patients into two subgroups according to the dominance of their lateralized motor symptoms: LPD and RPD. No significant difference in demographic and clinical tests was observed between both subgroups at baseline or within the same subgroup across the different visits (Table S3). To retrieve the specific dysconnectivity networks associated with the affected side of motor symptoms, we conducted the same previous analysis using NBS on the two lateralized subgroups of PD patients independently.

For the LPD patients, the α2 band revealed a disrupted network ($t = 3$, $P = 0.039$, corrected) between BL and 5YFU comprising predominantly regions (71%) and connections (63%) within the right hemisphere. Highest degree regions were located principally in the frontal, occipital, and central lobes of the right hemisphere. The corresponding NI of those LPD patients showed a significant decrease between BL and 3YFU ($P < 0.05$), 3YFU and 5YFU ($P < 0.05$), BL and

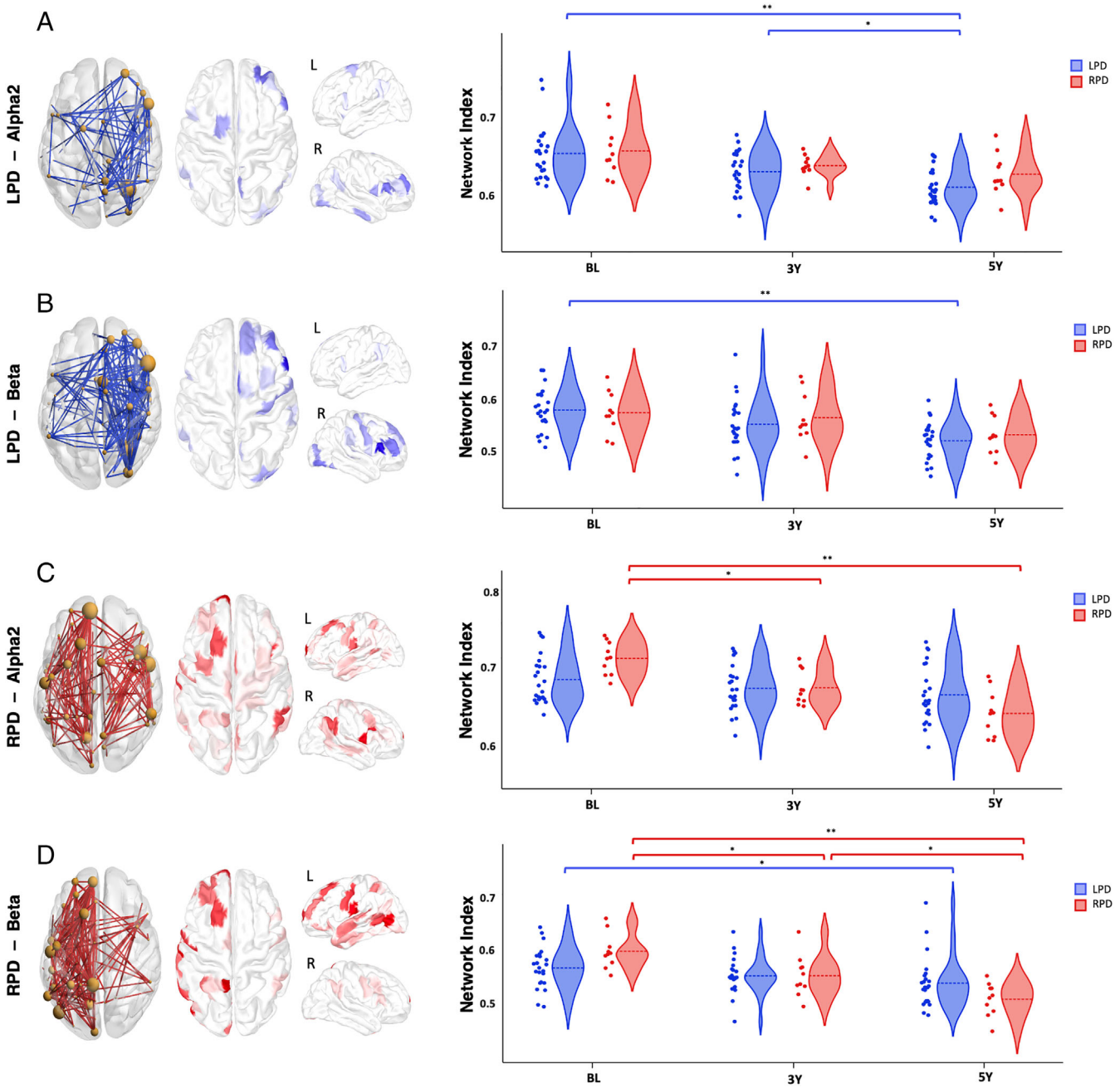

FIG. 4. Dysconnectivity networks with their corresponding highest degree regions (left) and the longitudinal change of the NI in both LPD and RPD patients (right). (**A**) Network of the LPD patients in α2, (**B**) network of the LPD patients in β, (**C**) network of the RPD patients in α2, (**D**) network of the RPD patients in β. $^{**}P < 0.001$, $^{*}P < 0.05$ (corrected for multiple comparisons using Bonferroni). [Color figure can be viewed at wileyonlinelibrary.com]

5YFU ($P < 0.001$). However, this same NI does not reveal any significant differences between the three timepoints when applied on the RPD patients (Fig. 4A) and between BL and 3YFU when applied on the HC ($P = 0.65$). In contrast, dysconnectivity networks of the RPD patients between BL and 5YFU revealed a dominance of the left hemisphere in terms of altered connections. In α2 ($t = 3.2$, $P = 0.044$, corrected using permutation), the disrupted network encompassed a total of 167 connections and 83 regions. Although the majority of the edges (52.7%) were located within the left hemisphere with the highest degree regions among the left-frontal and left-central lobes, the right hemisphere comprises 40.1% of the disrupted edges mainly issued from regions in right-central, right-frontal, and right-parietal lobes. The corresponding NI presented a significant decrease between BL and 3YFU ($P < 0.05$) and between BL and 5YFU ($P < 0.001$) in RPD patients. Yet, it did not mark any significant change between timepoints in LPD patients (Fig. 4C) and

between BL and 3YFU in HC ($P = 0.08$). More details about these results in the βband are described in the Appendix S1.

Discussion

In this longitudinal study, we investigated the evolution of the functional brain networks over a 5-year period in PD patients using resting state HD-EEG recordings. We unveiled disrupted networks in both α2 and β frequency bands where the functional connectivity decreases progressively between BL, 3YFU, and 5YFU, only in PD patients and not in HC. We also showed a positive correlation between the loss of functional connectivity in time and the deterioration in the MoCA score that is used largely to examine the global cognitive performance of PD patients. Furthermore, we noticed a dominance of the right hemisphere in terms of altered connections that led us to inspect more in depth the relationship between the motor symptoms lateralization of PD patients and the disruptions in their functional brain networks.

Our main findings revealed disrupted networks in α2 and β bands where the functional connectivity drops in function of time. Several previous cross-sectional and longitudinal studies reported a decrease in the power of both alpha and beta bands in PD patients at early and advanced stages of the disease.[33-36] Likewise, these frequency bands were relevant in highlighting reductions in the functional connectivity associated with the motor and cognitive deteriorations over the course of the disease.[17,22,23,37] Our results are in line with these previous findings. In addition, our network index (computed at the patient-level) derived from these networks has encountered a progressive decrease only in PD patients and not in healthy subjects in both bands, which could express the progression of the disease rather than the progression in age. Note that we obtained no significant differences when we performed the NBS analysis on PD patients between consecutive timepoints.

Regarding the spatial distribution of the disrupted connections and regions in α2 and β, the right hemisphere was predominant. In particular, the dominance of the right-frontal and right-central lobes was clear in both bands because they included most of the highest degree regions (involving most of the altered connections). A recent meta-analysis showed that both right-superior-frontal and right-central gyrus presented a reduced functional connectivity in cognitively impaired PD patients compared to HC.[38] Besides, reductions in the functional connectivity of the right frontal and right somatomotor-sensory cortex were previously reported to reflect reductions in cortical thinning in PD patients.[39,40] Moreover, we unfold here, that the frontotemporal connections were dominant in terms of altered connections in α2 and β. Indeed, functional disturbances between the frontal and temporal lobes in the α band were observed when comparing non-demented to demented PD patients in several MEG study.[17,22] In EEG, these patterns of connections were relevant in α2 when comparing cognitively intact to cognitively impaired PD patients.[23]

We have also investigated the potential relationships between the lateralization of motor symptoms and the longitudinal change of the functional brain networks in PD patients. Although previous studies have reported changes in the cortical and subcortical areas related to the asymmetry of the motor symptoms[41,42] and linked them with the progression of both motor and cognitive symptoms of the disease,[43-45] to date, no functional connectivity study has tackled their relationship longitudinally. When we conducted the same analysis based on NBS on the two subgroups separately, we found hypo-connectivity networks in both α2 and β bands predominantly located in the right hemisphere and characterizing the longitudinal progression of the disease in the LPD patients in contrast to a dominance of the left hemisphere in the RPD patients. This contralaterality observed between the altered hemisphere and the side of the symptoms may be in line with previous studies that showed the correspondence between the side of the motor symptoms and the dopaminergic neuronal loss in the contralateral substantia nigra.[46,47] Furthermore, we found that the α2 frequency band revealed disturbances in the right hemisphere in RPD patients. Notably, when we first compared the evolution of the original NI over time in LPD and RPD patients, both subgroups showed significant decrease between different timepoints (Fig. S6). Therefore, alterations in the right hemisphere could be associated with the progression of the disease in both subgroups. Moreover, the previous results revealing the dominance of the right hemisphere in PD patients of the initial group could be related not only to the outnumber of the LPD patients over the RPD patients, (N=23 vs. N=10, respectively) but also to a pertinent pattern of disturbances within the right hemisphere that could reflect a common clinical deterioration in all patients. Another interpretation for these patterns of disturbances could be the fact that after more than 5 years of evolution, and despite the worsening of motor symptoms on the predominant side, the disease may become bilateral.[47] This may also explain why the loss of connectivity in the left hemisphere characterizing the RPD patients in β band appears to be significant also in LPD patients (Fig. 4D).

In this study, we used the data of the PD patients that complete both follow-up examinations to retrieve the disrupted networks in time, which relatively reduced the sample size from 77 to 35. However, we cross-validated our results on the initial cohort to confirm the

hypoconnectivity found between timepoints (Fig. S3 in Appendix S1). Unfortunately, having only three healthy subjects at 5YFU is not representative and prevents us from validating the longitudinal change in the network statistically in HC. We, therefore, only took into consideration the corresponding evolution occurring between BL and 3YFU. The relatively small sample size of RPD patients (n = 10) might also affect the statistical power of this comparison. As for the correlation analysis, we chose the global cognitive score MoCA (that covers several cognitive domains) rather than domain specific tests because our dysconnectivity analysis is more likely to reveal a large-scale network rather than a domain-specific one. For instance, the NI showed no correlation with tests that assessed only the visuospatial abilities. Finally, all patients were under dopaminergic treatments (*on* state) during both the EEG recordings and the neuropsychological assessments, which may mask the magnitude of their motor symptoms as well as their global cognitive performance and may, ultimately, affect our analysis. To overcome this issue, the affected side of PD patients was computed based on the lateralized items of the UPDRS-III in the three timepoints, whereas the LEDD was considered as confounding in the correlation analysis. Despite these considerations, the effect of the dopaminergic medications could still be present in the measures of functional connectivity as shown by several studies.[48,49]

In conclusion, the current study is the first to date to assess longitudinal changes in the functional brain networks of PD patients with the disease progression using HD-EEG. Our findings suggest that disruptions in the networks may characterize not only the evolution of the disease, but also the evolution in the cognitive performance of the patients and the lateralization of their motor symptoms. Further investigations may lead to the identification of potential neuromarkers assisting in subtyping PD patients and predicting the evolution of their motor and cognitive symptoms in time. ●

Acknowledgments: We thank all patients, their families, and caregivers for their participation in the study. We would like to thank also Beltrani Selina Maria for her help in EEG data management and data sharing.

Data Availability Statement

The data that support the findings of this study are available on request from the corresponding author. The data are not publicly available due to privacy or ethical restrictions.

References

1. Bloem BR, Okun MS, Klein C. Parkinson's disease. The Lancet 2021;397:2284–2303.
2. Poewe W, Seppi K, Tanner CM, et al. Parkinson disease. Nat Rev Dis Primer 2017;3:17013
3. Martinez-Martin P, Rodriguez-Blazquez C, Kurtis MM, Chaudhuri KR, Group, on B. of the N. V. The impact of non-motor symptoms on health-related quality of life of patients with Parkinson's disease. Mov Disord 2011;26:399–406.
4. Chaudhuri KR, Healy DG, Schapira AH. Non-motor symptoms of Parkinson's disease: diagnosis and management. Lancet Neurol 2006;5:235–245.
5. Horsager J, Andersen KB, Knudsen K, et al. Brain-first versus body-first Parkinson's disease: a multimodal imaging case-control study. Brain 2020;143:3077–3088.
6. Dickson DW, Braak H, Duda JE, et al. Neuropathological assessment of Parkinson's disease: refining the diagnostic criteria. Lancet Neurol 2009;8:1150–1157.
7. Prodoehl J, Burciu RG, Vaillancourt DE. Resting state functional magnetic resonance imaging in Parkinson's disease. Curr Neurol Neurosci Rep 2014;14:448
8. Rodriguez-Sanchez F, Rodriguez-Blazquez C, Bielza C, et al. Identifying Parkinson's disease subtypes with motor and non-motor symptoms via model-based multi-partition clustering. Sci Rep 2021;11:23645
9. Mestre TA, Eberly S, Tanner C, Grimes D, Lang AE, Oakes D, Marras C. Reproducibility of data-driven Parkinson's disease subtypes for clinical research. Parkinsonism Relat Disord 2018;56:102–106.
10. Luo C, Qiu C, Guo Z, et al. Disrupted functional brain connectivity in partial epilepsy: a resting-state fMRI study. PLOS ONE 2012;7:e28196
11. Baggio H-C, Segura B, Sala-Llonch R, et al. Cognitive impairment and resting-state network connectivity in Parkinson's disease. Hum Brain Mapp 2015;36:199–212.
12. Tuovinen N, Seppi K, de Pasquale F, et al. The reorganization of functional architecture in the early-stages of Parkinson's disease. Parkinsonism Relat Disord 2018;50:61–68.
13. Fiorenzato E, Strafella AP, Kim J, Schifano R, Weis L, Antonini A, Biundo R. Dynamic functional connectivity changes associated with dementia in Parkinson's disease. Brain 2019;142:2860–2872.
14. Stam CJ. Use of magnetoencephalography (MEG) to study functional brain networks in neurodegenerative disorders. J Neurol Sci 2010;289:128–134.
15. Stam C, Jones B, Nolte G, Breakspear M, Scheltens P. Small-world networks and functional connectivity in Alzheimer's disease. Cereb Cortex 2007;17:92–99.
16. Hata M, Kazui H, Tanaka T, et al. Functional connectivity assessed by resting state EEG correlates with cognitive decline of Alzheimer's disease – an eLORETA study. Clin Neurophysiol 2016;127:1269–1278.
17. Bosboom JLW, Stoffers D, Wolters EC, Stam CJ, Berendse HW. MEG resting state functional connectivity in Parkinson's disease related dementia. J Neural Transm 2008;116:193
18. Fingelkurts AA, Fingelkurts AA, Rytsälä H, Suominen K, Isometsä E, Kähkönen S. Impaired functional connectivity at EEG alpha and theta frequency bands in major depression. Hum Brain Mapp 2007;28:247–261.
19. Stoffers D, Bosboom JLW, Deijen JB, Wolters EC, Stam CJ, Berendse HW. Increased cortico-cortical functional connectivity in early-stage Parkinson's disease: an MEG study. Neuroimage 2008;41:212–222.
20. Sánchez-Dinorín G, Rodríguez-Violante M, Cervantes-Arriaga A, Navarro-Roa C, Ricardo-Garcell J, Rodríguez-Camacho M, Solís-Vivanco R. Frontal functional connectivity and disease duration interactively predict cognitive decline in Parkinson's disease. Clin Neurophysiol 2021;132:510–519.
21. Rucco R, Lardone A, Liparoti M, Lopez ET. Brain networks and cognitive impairment in Parkinson's disease. Brain Connect 2021. https://doi.org/10.1089/brain.2020.0985
22. Ponsen MM, Stam CJ, Bosboom JLW, Berendse HW, Hillebrand A. A three dimensional anatomical view of oscillatory resting-state activity and functional connectivity in Parkinson's disease related dementia: an MEG study using atlas-based beamforming. NeuroImage Clin. 2013;2:95–102. https://pubmed.ncbi.nlm.nih.gov/24179762/

23. Hassan M, Chaton L, Benquet P, et al. Functional connectivity disruptions correlate with cognitive phenotypes in Parkinson's disease. NeuroImage Clin 2017;14:591–601.
24. Utianski RL, Caviness JN, van Straaten ECW, et al. Graph theory network function in Parkinson's disease assessed with electroencephalography. Clin Neurophysiol 2016;127:2228–2236.
25. Gibb WR, Lees AJ. The relevance of the Lewy body to the pathogenesis of idiopathic Parkinson's disease. J Neurol Neurosurg Psychiatry 1988;51:745–752.
26. Pedroni A, Bahreini A, Langer N. Automagic: standardized preprocessing of big EEG data. Neuroimage 2019;200:460–473.
27. Hassan M, Wendling F. Electroencephalography source connectivity: aiming for high resolution of brain networks in time and space. IEEE Signal Process Mag 2018;35:81–96. https://ieeexplore.ieee.org/document/8351910
28. Gramfort A, Papadopoulo T, Olivi E, Clerc M. OpenMEEG: opensource software for quasistatic bioelectromagnetics. Biomed Eng Online 2010;9:45
29. Hämäläinen MS, Ilmoniemi RJ. Interpreting magnetic fields of the brain: minimum norm estimates. Med Biol Eng Comput 1994;32:35–42.
30. Fan L, Li H, Zhuo J, et al. The human Brainnetome atlas: a new brain atlas based on connectional architecture. Cereb Cortex N Y NY 2016;26:3508–3526.
31. Lachaux J-P, Rodriguez E, Martinerie J, Varela FJ. Measuring phase synchrony in brain signals. Hum Brain Mapp 1999;8:194–208.
32. Zalesky A, Fornito A, Bullmore ET. Network-based statistic: identifying differences in brain networks. Neuroimage 2010;53:1197–1207.
33. Han C-X, Wang J, Yi G-S, Che Y-Q. Investigation of EEG abnormalities in the early stage of Parkinson's disease. Cogn Neurodyn 2013;7:351–359.
34. Caviness JN, Hentz JG, Evidente VG, et al. Both early and late cognitive dysfunction affects the electroencephalogram in Parkinson's disease. Parkinsonism Relat Disord 2007;13:348–354.
35. Bosboom JLW, Stoffers D, Stam CJ, van Dijk BW, Verbunt J, Berendse HW, Wolters EC. Resting state oscillatory brain dynamics in Parkinson's disease: an MEG study. Clin Neurophysiol 2006;117:2521–2531.
36. Olde Dubbelink KTE, Stoffers D, Deijen JB, Twisk JWR, Stam CJ, Berendse HW. Cognitive decline in Parkinson's disease is associated with slowing of resting-state brain activity: a longitudinal study. Neurobiol Aging 2013;34:408–418.
37. Olde Dubbelink KTE, Stoffers D, Deijen JB, Twisk JWR, Stam CJ, Hillebrand A, Berendse HW. Resting-state functional connectivity as a marker of disease progression in Parkinson's disease: a longitudinal MEG study. NeuroImage Clin 2013;2:612–619.
38. Wolters AF, van de Weijer SCF, Leentjens AFG, Duits AA, Jacobs HIL, Kuijf ML. Resting-state fMRI in Parkinson's disease patients with cognitive impairment: a meta-analysis. Parkinsonism Relat Disord 2019;62:16–27.
39. Yau Y, Zeighami Y, Baker TE, et al. Network connectivity determines cortical thinning in early Parkinson's disease progression. Nat Commun 2018;9:12
40. Mak E, Su L, Williams GB, et al. Baseline and longitudinal grey matter changes in newly diagnosed Parkinson's disease: ICICLE-PD study. Brain 2015;138:2974–2986.
41. Heinrichs-Graham E, Santamaria PM, Gendelman HE, Wilson TW. The cortical signature of symptom laterality in Parkinson's disease. NeuroImage Clin 2017;14:433–440.
42. Wu T, Hou Y, Hallett M, Zhang J, Chan P. Lateralization of brain activity pattern during unilateral movement in Parkinson's disease. Hum Brain Mapp 2015;36:1878–1891.
43. Haaxma CA, Helmich RCG, Borm GF, Kappelle AC, Horstink MWIM, Bloem BR. Side of symptom onset affects motor dysfunction in Parkinson's disease. Neuroscience 2010;170:1282–1285.
44. Verreyt N, Nys GMS, Santens P, Vingerhoets G. Cognitive differences between patients with left-sided and right-sided Parkinson's disease. A review. Neuropsychol Rev 2011;21:405–424.
45. Fiorenzato E, Antonini A, Bisiacchi P, Weis L, Biundo R. Asymmetric dopamine transporter loss affects cognitive and motor progression in Parkinson's disease. Mov Disord 2021;36:2303–2313.
46. Kempster PA, Gibb WR, Stern GM, Lees AJ. Asymmetry of substantia nigra neuronal loss in Parkinson's disease and its relevance to the mechanism of levodopa related motor fluctuations. J Neurol Neurosurg Psychiatry 1989;52:72–76.
47. Djaldetti R, Ziv I, Melamed E. The mystery of motor asymmetry in Parkinson's disease. Lancet Neurol 2006;5:796–802.
48. Esposito F, Tessitore A, Giordano A, et al. Rhythm-specific modulation of the sensorimotor network in drug-naive patients with Parkinson's disease by levodopa. Brain J Neurol 2013;136:710–725.
49. Silberstein P, Pogosyan A, Kühn AA, et al. Cortico-cortical coupling in Parkinson's disease and its modulation by therapy. Brain J Neurol 2005;128:1277–1291.

Supporting Data

Additional Supporting Information may be found in the online version of this article at the publisher's web-site.

Supplementary materials

Functional brain dysconnectivity in Parkinson's disease: A 5-year longitudinal study

Sahar Yassine[1,2] MSc, Ute Gschwandtner[3] MD, PhD, Manon Auffret[4] PharmD, PhD, Sophie Achard[5] PhD, Marc Verin[1,4,6,7] MD, PhD, Peter Fuhr[3] MD, PhD, Mahmoud Hassan[8,9] PhD

[1] Univ Rennes 1, LTSI - U1099, F-35000 Rennes, France

[2] NeuroKyma, F-35000 Rennes, France

[3] Dept. of Neurology, Hospitals of the University of Basel, Switzerland

[4] Comportement et noyaux gris centraux, EA 4712, CHU Rennes, Univ Rennes 1, F-35000 Rennes, France

[5] CNRS, Grenoble INP, GIPSA-Lab, University of Grenoble Alpes, Grenoble, France

[6] Movement Disorders Unit, Neurology Department, Pontchaillou University Hospital, Rennes, France

[7] Institut des Neurosciences Cliniques de Rennes (INCR), Rennes, France

[8] MINDig, F-35000 Rennes, France

[9] School of Science and Engineering, Reykjavik University, Reykjavik, Iceland

Methods

Data acquisition and preprocessing

Briefly, the Automagic toolbox is configured to filter the signals between 1 and 45 Hz, perform the electroencephalography (EOG) regression to eliminate the ocular artifacts (therefore the final number of channels is reduced to 239), and to detect and interpolate bad channels with high variance (higher than 20 µV) or whose amplitude exceeds the ±80 µV at any temporal point of the signal. The independent component analysis was also chosen in the configuration to remove further artefacts. Epochs whose Ratio of Bad Channels (RBC), one of Automagic quality metrics, exceeds the 0.15 threshold (representing 15% of the total number of electrodes) were excluded and the rest were sorted according the Overall High Amplitude (OHA) metric and only the first six epochs were chosen for the rest of the study. This step was confirmed manually by a visual inspection of the epochs and those with remaining artefacts were modified or removed totally from the study. All these parameters are described in the shared GitHub containing the codes necessary to reproduce the results (https://github.com/yassinesahar/FuncDysconnectivityPD) .

Statistical Analysis

In brief, to identify the significant networks in NBS, a t-test was performed to evaluate the significant difference in the value of connectivity along the $(N^2-N)/2 = 21945$ edges of the [210 x 210] connectivity matrices of the PD patients between the BL and 5YFU visits. A primary component-forming threshold ($p<0.05$) was then applied to identify a set of supra-threshold connections, within which all the possible connected components and their size could be determined. A corrected *p*-value was then evaluated for each component with respect to the null distribution of maximal connected component size obtained using a nonparametric permutation approach (2000 permutations). The analysis was performed with different thresholds for the t-test (range from 2.6 to 3.7) which affect the final size of the resulting significant networks. The statistical differences in demographic and clinical characteristics between PD patients and HC as well as between PD patients at different timepoints were computed using the t-test and the fisher's test. The Wilcoxon test (two-tailed) corrected for multiple comparisons (Bonferroni) was used to examine the difference in the network between different visits.

Correlation analysis

The Pearson's correlation was computed to evaluate the relationship between the Network Index (NI) and the global clinical score of PD patients represented by the Montreal Cognitive Assessment score (MoCA)[1] at

different timepoints. Further, in order to emphasize the disrupted connections that reflect the fluctuations in the MoCA score over time, we sought also to identify a subnetwork from the significant network already uncovered in NBS, in which the change in the connectivity values of its edges correlates significantly with the change in the MoCA. For this purpose and inspired by the edges selection approach used in the Connectome-based Predictive modeling (CPM) studies[2], the Pearson's correlation was computed between the difference in the weight of the connections (W_i^{BL} - W_i^{5YFU}) and the difference in the MoCA score ($MoCA_i^{BL}$ - $MoCA_i^{5YFU}$) in both BL and 5YFU visits. Connections that show significant correlation (p<0.05) were considered as part of this subnetwork and their corresponding NI was computed.

We estimated also the correlation between the longitudinal change of NI and the longitudinal change in the UPDRS-III to assess the relationship between the loss of connectivity in PD patients and their motor impairments. The dose of antiparkinsonian medications (LEDD) was considered as a confounding factor when estimating the Pearson's correlation at each timepoint (and its average between timepoints when correlating the longitudinal changes).

Results

Decreasing networks of PD patients in alpha1 and theta bands (BL>5YFU)

The alpha1 band (8-10 Hz) showed similar results to those observed in alpha2 concerning the predominance of connections in the right hemisphere as well as the significant progressive decreasing trend of NI between different visits in PD patients and not in HC (figure S2 A, B).

Another decreasing network was observed in the theta band (*t=3.2, p=0.036,* corrected using permutation) involving 83 connections and 65 regions distributed quasi-equally between both hemispheres. The highest degree regions were parts of the left-temporal, left-central and right-parietal lobes (figure S2 C). The NI in this band decreases significantly between BL and 5YFU (*p<0.001*) notably between 3YFU and 5YFU (*p<0.05*). However, this decreasing trend was also observed in HC with a significant difference between BL and 3YFU (*p<0.05*) (figure S2 D). We should note that results were consistent across different thresholds of the t-test in NBS, in all frequency bands (see table S2).

Increasing networks of PD patients (BL<5YFU)

Concerning the network where the connectivity in 5YFU was significantly higher than in BL (a hyper-connectivity), the alpha2 was the only frequency band to reveal significant components in NBS. The network

(*t=3.1, p=0.025,* corrected using permutation) comprises 93 connections and 64 regions. Highest degree regions were among the right-parietal, right-frontal, right-occipital and left-parietal lobes and a predominance in the interhemispheric connections was observed (73.1%) (figure S2 E). These results are in line with the findings of Stoffers et al. that reported a positive association between the connectivity of the interhemispheric connections and the duration of the disease in alpha2[3]. However, we found that the associated NI goes through a progressive increase between BL and 5YFU (*p<0.001*) not only in PD patients, but also in HC between BL and 3YFU (*p<0.05*) (figure S2 F). This increase may be interpreted as age-related and not pathology- specific. However, this was not confirmed statistically as the correlation between the NI and the age was unsignificant (*p=0.62*).

Cross-validating the results on the entire cohort

In order to cross-validate the hypoconnectivity associated with the disrupted networks shown previously, we computed the corresponding NI on the initial cohort that includes in addition to the 35 PD patients of the analysis, the PD patients who did not complete the follow up-visits (total of 77 PD patients at BL, 45 PD at 3YFU and 42 PD at 5YFU).We chose to apply this validation on the decreasing networks of the alpha2 and beta bands as their corresponding NI showed a significant decrease in PD and not in HC. Results revealed that in alpha2, the significant progressive decreasing trend of NI persists on this larger dataset between BL and 3YFU (*p<0.05*) and BL and 5YFU (*p<0.001*). The same decreasing trend was also observed in beta mainly between BL and 5YFU (*p<0.001*) and 3YFU and 5YFU (*p<0.05*). Results are represented in the figure S3.

Relationship between the longitudinal change in the network and in the UPDRS-III score

In order to assess the relationship between the loss of the connectivity and the motor impairment in PD patients, we evaluated the correlation between the change in their NI and the change in their UPDRS-III score between different timepoints. A significant negative correlation was found in both frequency bands alpha2 (*r=-0.38, p<0.05*) and beta (*r=-0.41, p<0.05*) only between 3YFU and 5YFU (figure S5). This negative correlation reflects a worsening of motor symptoms associated with the loss of connectivity when the disease progress in time.

Disrupted networks of PD patients with lateralized motor symptoms in beta band.

The dominance of the right hemisphere was observed in the detected dysconnectivity network of the beta band in LPD patients (*t=3.2, p=0.045*, *corrected*) that included 69.4% of the detected connections and 67.2% of the detected regions. The regions with the highest number of connections were part of the right-frontal, right-

occipital and right-central lobes. The fronto-temporal and fronto-frontal were among the highest altered connections. the decrease in the NI was significant between BL and 5YFU ($p<0.001$) in LPD patients and not in RPD patients (figure 4 B) nor in HC between BL and 3YFU ($p=0.26$).

As for the RPD patients, the beta band revealed a network ($t=3.5$, $p=0.035$, corrected using permutation) with a confirmed dominance of the left hemisphere which comprises 86.1% of the total connections and 81.8% of the involved regions. The fronto-temporal and the fronto-parietal were the prominent altered interactions and the highest degree regions were among the frontal, central and occipital lobes of the left hemisphere. A progressive significant decrease in the corresponding NI was perceived in RPD patients between different visits: BL and 5YFU visits ($p<0.001$), BL and 3YFU ($p<0.05$), 3YFU and 5YFU ($p<0.05$). However, we observed this decrease also in the NI of the LPD patients between BL and 5YFU ($p<0.05$) (figure 4 D) while the change in HC between BL and 3YFU was not significant ($p=0.07$). All of these results were consistent independently from the chosen t-threshold for the t-test in NBS (see table S5).

Supplementary figures

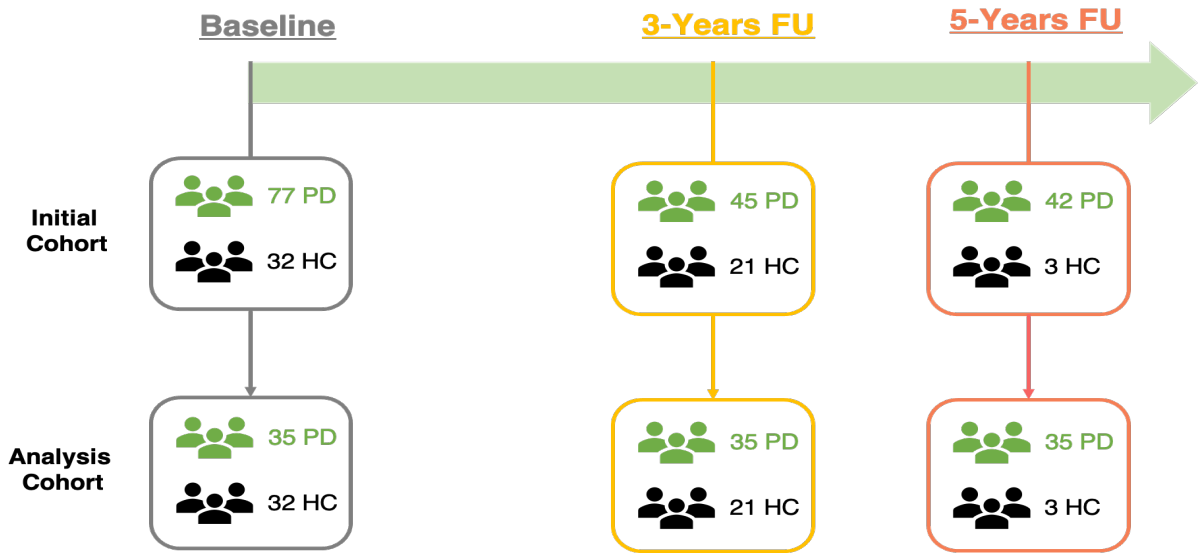

Figure S1*-Flowchart of the enrolled and followed subjects with Parkinson's disease (PD) and healthy controls (HC) during the three timepoints of the study. The analysis cohort included only the 35 patients that underwent all three visits and all the HC. Seven patients from the 5YFU dataset were discarded from the analysis cohort as they were DBS patients at BL or at 3YFU (or at both timepoints) with no EEG recordings at that time.*

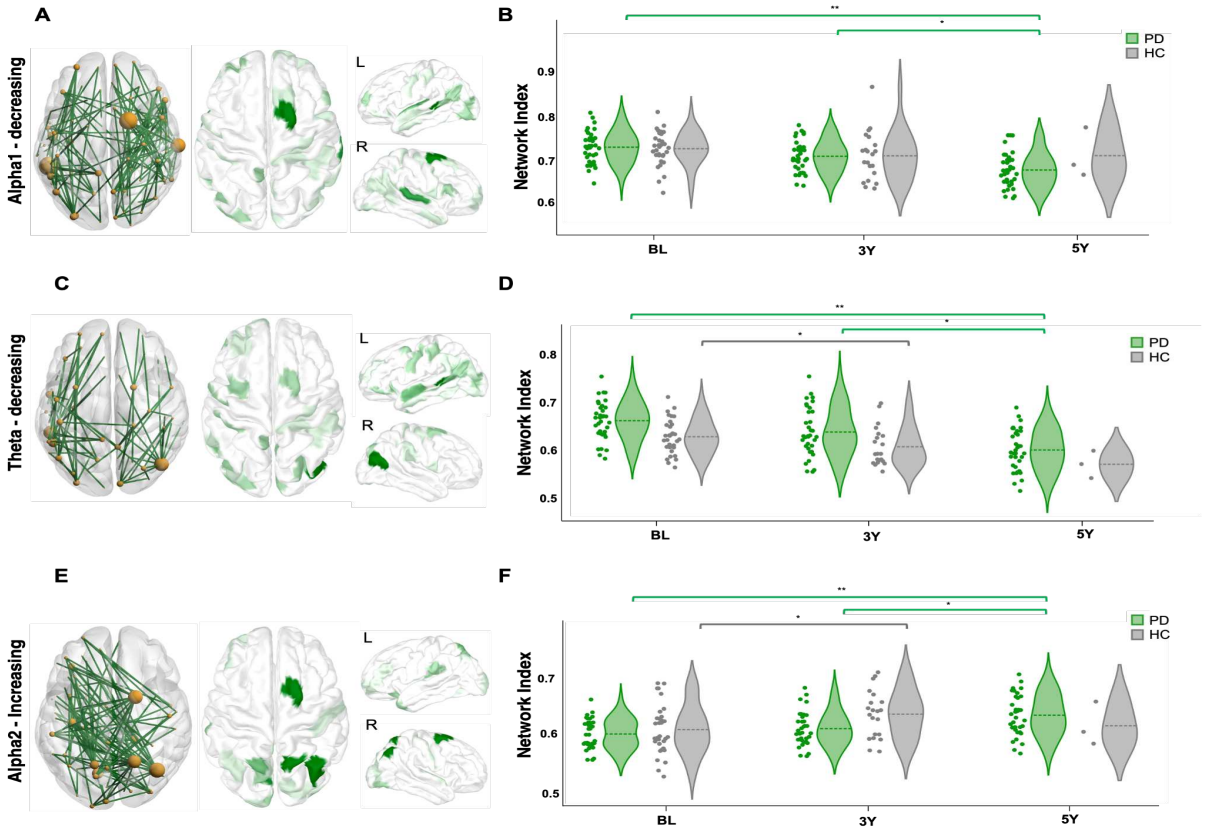

Figure S2- *Disrupted networks with corresponding highest degree regions in **A)** alpha1-decreasing **C)** theta-decreasing **E)** alpha2-increasing. The longitudinal change of the network index of the PD patients and HC in **B)** alpha1-decreasing **D)** theta-decreasing **F)** alpha2-increasing.*
*** p<0.001, * p<0.05 (corrected for multiple comparisons using Bonferroni).*

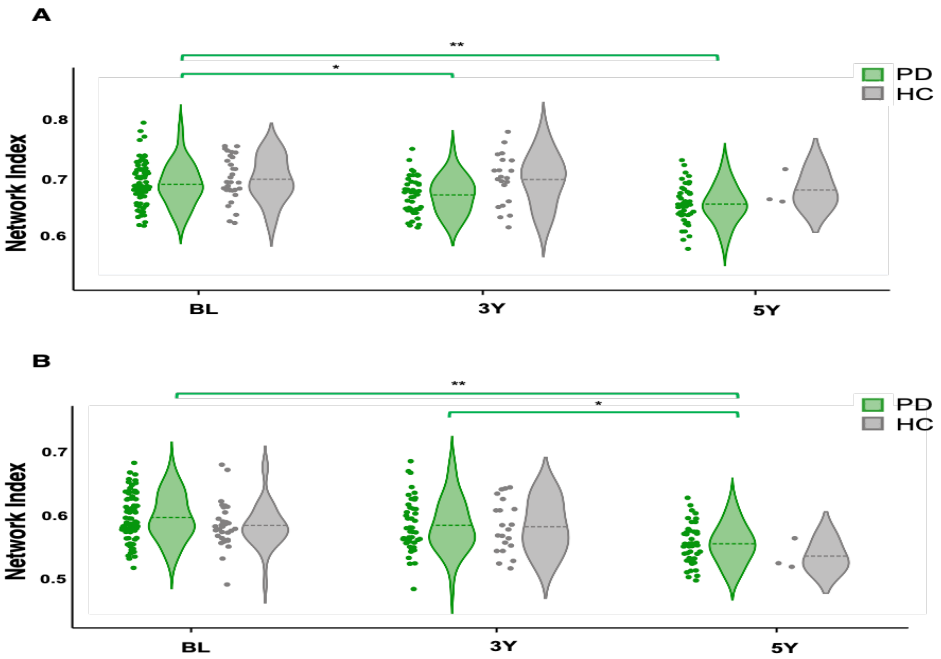

Figure S3-Cross validation on the main cohort: the longitudinal change in the NI of PD patients and HC corresponding to the decreasing network of alpha2 (up) and the decreasing network of beta (down).
*** p<0.001, * p<0.05 (corrected for multiple comparisons using Bonferroni)*

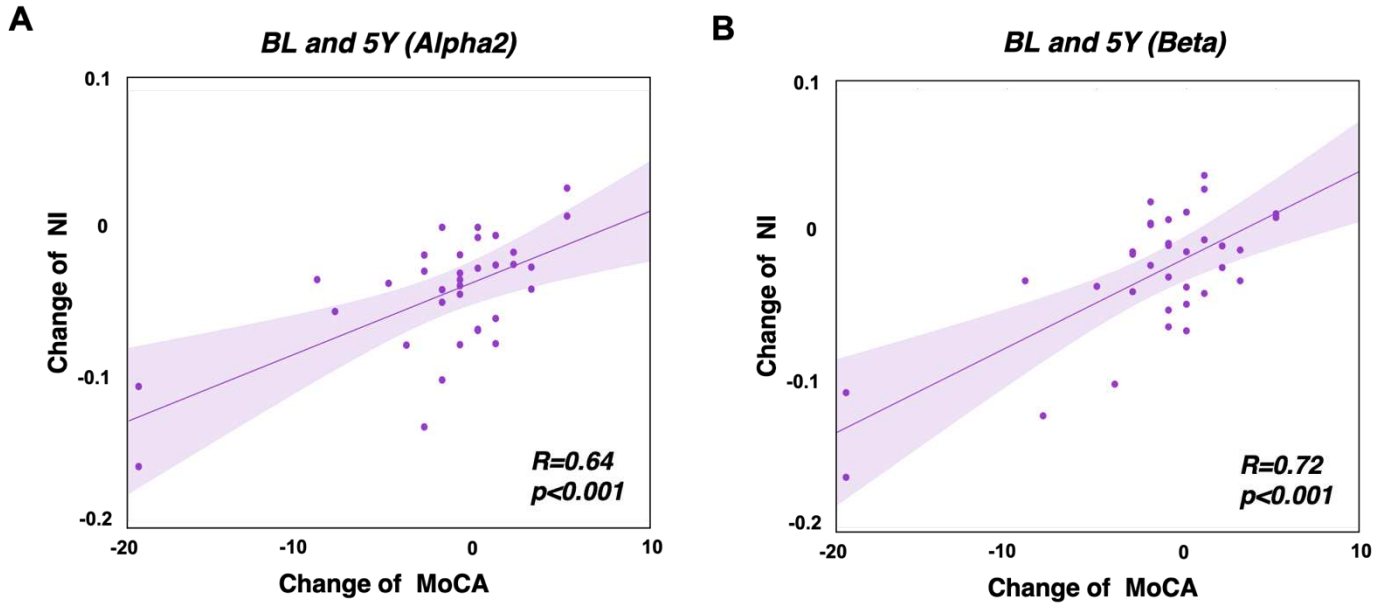

Figure S4- *Correlation between the change in Network Index (NI) and the change in MoCA observed between BL and 5YFU in A) Alpha2 and B) Beta*

.

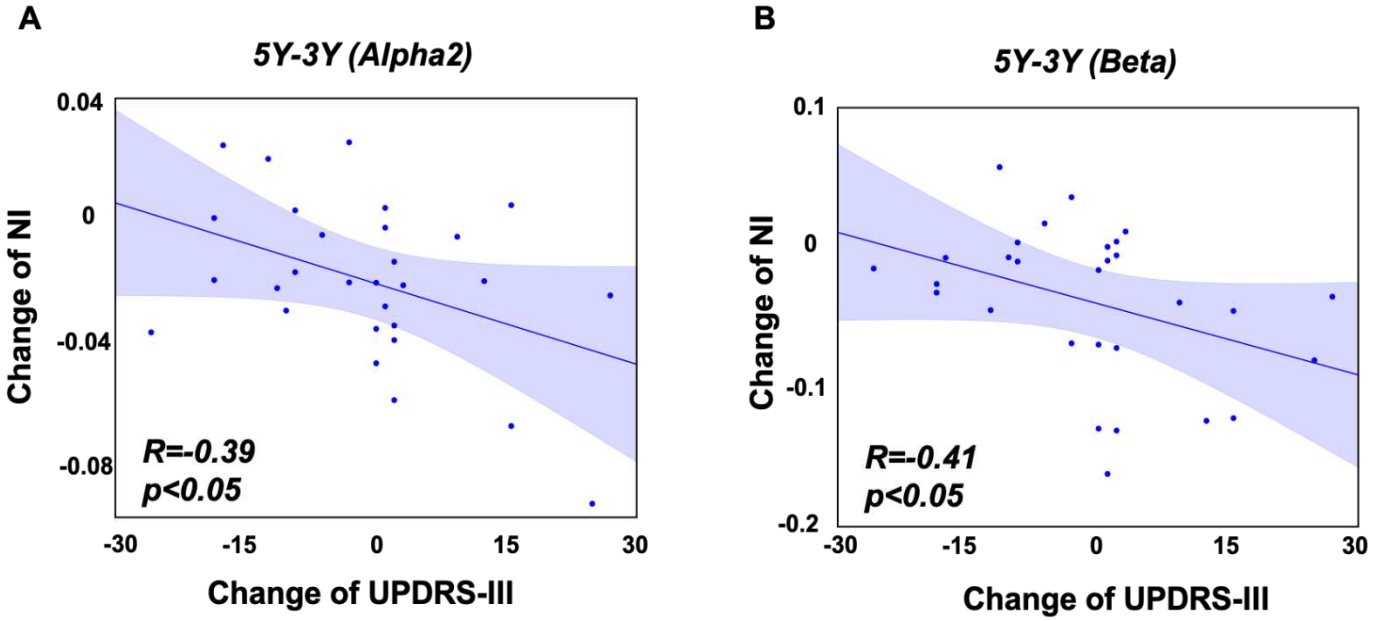

Figure S5- *Correlation between the change in Network Index (NI) and the change in UPDRS-III score observed between 3YFU and 5YFU in* ***A)*** *Alpha2 and* ***B)*** *Beta.*

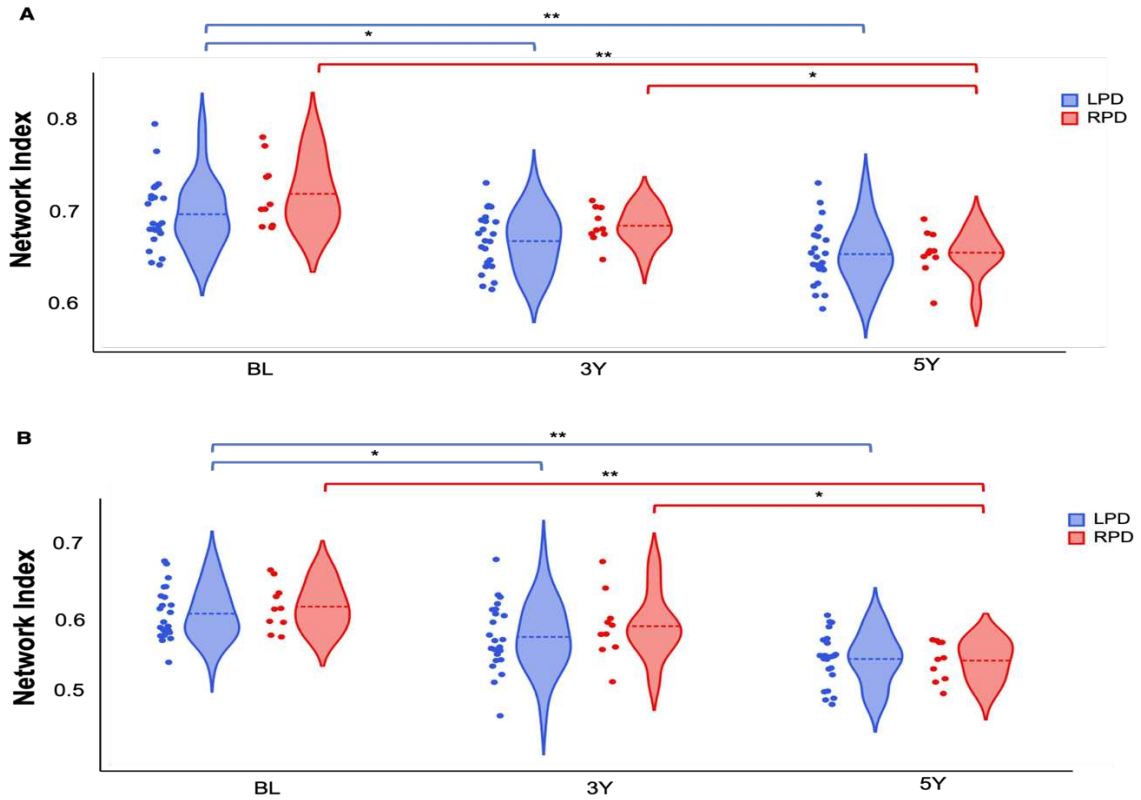

Figure S6- *The longitudinal change of the Network Index (NI) (derived from the dysconnectivity networks of all PD patients (N=35)) of the left-affected PD patients (LPD, N=23) and the right-affected PD patients (RPD, N=10) separately in **A)** alpha2 and **B)** beta frequency bands.*
*** p<0.01, * p<0.05 (corrected for multiple comparisons using Bonferroni).*

Supplementary tables

Table S1- *Demographic and clinical data of the initial cohort in Baseline, 3YFU and 5YFU expressed as mean (standard deviation). PD: Parkinson's disease patients; HC: Healthy Controls; M/F: Male/Female; y: years; LEDD: Levodopa equivalent daily dose; UPDRS-III: Unified Parkinson's Disease Rating Scales motor ratings; MoCA: Montreal Cognitive Assessment, MMSE: Mini-Mental State Examinations.*

	Baseline	3 Years Follow UP	5 Years Follow UP
	PD (N=77)	PD (N=45)	PD (N=42)
Sex (M/F)	51/26	31/14	28/14
Age (y)	66.2 (8.2)	70.9 (7.9)	71.9 (7.9)
Education (y)	14.6 (3.2)	14.8 (3.1)	15.0 (3.1)
Disease Duration (y)	5.4 (5.2)	8.0 (5.2)	10.5 (5.0)
LEDD (mg/day)	676 (466)	707 (447)	642 (386)
UPDRS-III	15.5 (11.0)	20.5 (12.1)	20.1 (13.1)
MoCA	26 (2.4)	25.2 (3.5)	24.9 (5.2)

Table S2- *Performance at the neuropsychological and neuropsychiatric tests of the 35 PD patient in the three visits: Baseline (BL), 3 years follow-up (3YFU) and 5 years follow-up (5YFU), expressed as mean (standard deviation).*

Domain	Name of the test	BL	3YFU	5YFU
Attention and working memory	TAP-Alertness, reaction time without alerting sound (ms)	295 (61)	312 (69)	318 (64)
	TAP-Alertness, reaction time with alerting sound (ms)	281 (47)	300 (67)	304 (55)
	Trail Making Test, time for Part A	47.9 (15.4)	52.8 (28.9)	59.7 (36.4)
	Digit Span, correct forward	7.3 (2.1)	7.8 (2.1)	7.5 (1.7)
	Digit span, correct backward	5.9 (2.1)	6.1 (1.7)	5.7 (1.7)
	Corsi block, correct forward	7.9 (1.4)	7.9 (1.7)	7.5 (1.9)
	Corsi block, correct backward	7.5 (1.3)	7.1 (1.7)	5.9 (1.7)
Episodic Memory	California Verbal Learning Test, trial 1	5.5 (2)	4.7 (2.4)	4.9 (1.7)
	California Verbal Learning Test, trial 5	10.9 (3)	11 (3.4)	10.4 (3.4)
	California Verbal Learning Test, saving	94.8 (21.2)	82.4 (24.3)	88.4 (24.8)
	California Verbal Learning Test, discriminability	98.8 (5.5)	90.6 (8.7)	90.8 (11.3)
	Rey-Osterrieth Complex Figure, savings	66.9 (15.5)	70.6 (19.8)	70 (20.2)
Executive Function	Five-Point test, correct answers	24.7 (7.7)	24.8 (7.1)	25.6 (7)
	Semantic verbal fluency test, correct answers	20.2 (4.8)	19.8 (6.5)	19.3 (5.8)
	Phonemic verbal fluency, correct answers	13.2 (4.1)	13 (4.9)	13.7 (4.9)
	Trail Making Test,time for Part B / time for Part A	2.5 (0.8)	2.6 (1.6)	3 (1.6)
	Stroop, interference index	1.9 (0.6)	1.8 (0.5)	1.9 (0.7)
Visuo-spatial function	Rey-Osterrieth Complex Figure, copy	29.9 (4)	29.3 (5.6)	30 (5.4)
	Block design test, sum score	26.4 (8.6)	26.4 (8.8)	24.5 (7.7)
Language	Boston Naming Test, correct answers	14.1 (1)	13.9 (1.7)	13.8 (2.6)
Neuropsychiatry	Beck Depression Inventory, total	7.6 (5)	8.2 (5)	7.5 (6.8)
	Beck Anxiety Inventory, total	10.5 (7.1)	11.9 (8)	10.2 (7.4)
	Perceived deficits questionnaire - depression, total	32.7 (21.1)	37.4 (22.2)	36 (20)

Table S3- *Demographic and clinical characteristics of the Left-affected (LPD) and right-affected (RPD) patients in BL, 3YFU and 5YFU* e*xpressed as Median [min, max]. M/F: Male/Female; y: years; LEDD: Levodopa equivalent daily dose; UPDRS-III: Unified Parkinson's Disease Rating Scales motor ratings; MoCA: Montreal Cognitive Assessment (score between 0 and 30). P-values between groups are calculated using the Wilcoxon's statistical test.*

	Baseline		
	LPD (N=23)	**RPD (N=10)**	***p-value***
Sex (M/F)	19M/4F	5M/5F	*0.09*
Age (y)	69 [47-82]	65.5 [55-84]	*0.46*
Education (y)	16 [9-20]	13.5 [9-20]	*0.19*
Disease Duration (y)	2.8 [0-15.3]	4.2 [0.1-8.2]	*0.54*
LEDD (mg/day)	460 [0-1425]	575 [150-1148]	*0.31*
UPDRS-III	16 [0-34]	11.5 [1-35]	*0.37*
MoCA	27 [22-29]	25 [19-29]	*0.1*

	3 Years Follow Up		
	LPD (N=23)	**RPD (N=10)**	***p-value***
Sex (M/F)	-	-	-
Age (y)	72 [50-85]	68.5 [58-87]	*0.43*
Education (y)	-	-	-
Disease Duration (y)	5.9 [3.1-18.5]	7.25 [3.5-11.8]	*0.57*
LEDD (mg/day)	512.5 [0-2028]	585 [114-1480]	*0.85*
UPDRS-III	17 [1-34]	18.5 [10-38]	*0.48*
MoCA	26 [15-29]	26 [12-30]	*0.96*

	5 Years Follow Up		
	LPD (N=23)	**RPD (N=10)**	***p-value***
Sex (M/F)	-	-	-
Age (y)	74 [52-87]	70.5 [60-89]	0.44
Education (y)	-	-	-
Disease Duration (y)	8.1 [5.2-20.5]	9.3 [5.5-13.3]	0.57
LEDD (mg/day)	574.5 [0-1330]	537 [94-1629]	0.96
UPDRS-III	15 [1-52]	11 [0-37]	0.38
MoCA	27 [4-29]	26 [17-30]	0.94

Table S4- *Results using different t-test thresholds in NBS when finding the hypo/hyperconnectivity networks between BL and 5YFU of the PD patients in different frequency bands. t-thresh: the t-test threshold used in NBS, p-value: the corrected p-value using NBS, N° Edges: the number of edges in the significant network, N° Regions: the number of regions in significant network, Edges within RH: the percentage of edges within the right hemisphere, NI-PD/HC (p-value): the significance of the Wilcoxon test (corrected for multiple comparison using Bonferroni) computed to evaluate the difference between the network index of PD patients between different timepoints and of Healthy controls between BL and 3YFU. Significant p-values are corrected for multiple comparisons using Bonferroni. * p-value<0.05 without correction for multiple comparison.*

						NI-PD (p-value)			NI-HC (p-value)
	t-thresh	p-value	N° Edges	N° Regions	Edges in RH	BL - 5Y	BL - 3Y	3Y - 5Y	BL - 3Y
Alpha 2 hypo-Con	2.6	0.050	466	151	69%	<0.001	<0.01	<0.05	0.86
	2.9	0.034	275	128	73%	<0.001	<0.01	<0.05	0.87
	3.0	0.033	209	109	78%	<0.001	<0.01	<0.05	0.89
	3.1	0.033	182	104	78%	<0.001	<0.01	<0.05	0.86
	3.2	0.021	125	72	89%	<0.001	<0.01	<0.05	0.86
	3.5	0.028	29	27	93%	<0.001	<0.01	<0.05	0.69
	3.7	0.023	20	18	90%	<0.001	<0.01	<0.05	0.24
Beta hypo-Con	2.6	0.038	817	158	39%	<0.001	0.031*	<0.001	0.69
	2.9	0.025	500	139	41%	<0.001	0.017*	<0.001	0.67
	3.0	0.022	420	130	43%	<0.001	<0.05	<0.001	0.64
	3.1	0.019	359	123	45%	<0.001	<0.05	<0.001	0.61
	3.2	0.018	302	118	46%	<0.001	<0.05	<0.001	0.61
	3.5	0.011	158	76	55%	<0.001	<0.05	<0.001	0.92
	3.7	0.009	103	58	56%	<0.001	<0.05	<0.001	0.75
Theta hypo-Con	2.6	-	-	-	-	-	-	-	-
	2.9	-	-	-	-	-	-	-	-
	3.0	-	-	-	-	-	-	-	-
	3.1	0.045	104	73	-	<0.001	0.034*	<0.05	0.05
	3.2	0.036	83	65	-	<0.001	0.028*	<0.05	0.037
	3.5	0.041	17	18	-	<0.001	0.135	<0.01	0.035
	3.7	-	-	-	-	-	-	-	-
Alpha1 hypo-Con	2.6	0.044	488	161	51%	<0.001	0.038*	<0.05	0.21
	2.9	0.038	248	118	51%	<0.001	0.024*	<0.01	0.13
	3.0	0.035	195	105	53%	<0.001	0.022*	<0.01	0.13
	3.1	0.033	149	93	51%	<0.001	0.02*	<0.01	0.14
	3.2	0.031	121	81	47%	<0.001	0.019*	<0.01	0.09
	3.5	0.020	52	49	50%	<0.001	0.018*	<0.01	0.06
	3.7	0.023	18	19	55%	<0.001	<0.05	<0.001	0.26
Alpha2 hyper-Con	2.6	0.049	334	105	-	<0.01	0.23	<0.05	0.025
	2.9	0.035	168	79	-	<0.01	0.12	<0.05	0.023
	3.0	0.028	139	75	-	<0.01	0.14	<0.05	0.023
	3.1	0.026	106	66	-	<0.01	0.13	<0.05	0.023
	3.2	0.023	75	55	-	<0.01	0.18	<0.05	0.016
	3.5	0.015	20	21	-	<0.01	0.32	<0.05	0.015
	3.7	-	-	-	-	-	-	-	-

Table S5- *Results using different t-test thresholds in NBS when finding the hypo-connectivity networks between BL and 5YFU of the PD patients in different frequency bands. t-thresh: the t-test threshold used in NBS, p-value: the corrected p-value using NBS, N° Edges: the number of edges in the significant network, N° Regions: the number of regions in significant network, Edges within LH/RH: the percentage of edges within the left/right hemisphere, NI (p-value): the significance of the Wilcoxon test computed to evaluate the difference between the network index of LPD or RPD patients between different timepoints. Significant p-values are corrected for multiple comparisons using Bonferroni. * p-value<0.05 without correction for multiple comparison.*

							NI (p-value)		
	t-thresh	p-value	N° Edges	N° Regions	Edges in LH	Edges in RH	BL - 5Y	BL - 3Y	3Y - 5Y
LPD Alpha2	2.7	-	-	-	-	-	-	-	-
	2.9	0.045	103	71	9%	60%	<0.001	0.027*	<0.05
	3.0	0.039	81	62	6%	63%	<0.001	0.033*	<0.05
	3.1	0.038	53	46	8%	66%	<0.001	0.028*	<0.05
	3.2	0.038	28	24	0%	89%	<0.001	0.023*	<0.05
	3.5	0.039	5	6	0%	100%	<0.05	0.048*	0.071
	3.7	-	-	-	-	-	-	-	-
LPD Beta	2.7	-	-	-	-	-	-	-	-
	2.9	-	-	-	-	-	-	-	-
	3.0	0.046	217	57	6%	67%	<0.001	0.061	<0.05
	3.1	0.049	181	67	6%	70%	<0.001	0.058	0.022*
	3.2	0.045	147	61	5%	69%	<0.001	0.048*	0.025*
	3.5	0.025	88	44	1%	80%	<0.001	0.031*	0.028*
	3.7	0.017	59	32	2%	83%	<0.001	0.029*	0.026*
RPD Alpha2	2.7	0.046	501	164	47%	42%	<0.001	<0.05	<0.05
	2.9	0.042	301	114	54%	36%	<0.01	<0.05	0.017*
	3.0	0.049	262	107	55%	37%	<0.001	<0.05	<0.05
	3.1	0.035	215	100	53%	38%	<0.01	<0.05	0.017*
	3.2	0.044	167	83	53%	40%	<0.001	<0.01	0.017*
	3.5	0.029	94	56	52%	44%	<0.01	<0.05	<0.05
	3.7	0.022	-	-	51%	45%	<0.001	<0.05	<0.05
RPD Beta	2.7	0.045	686	174	66%	16%	<0.001	<0.05	<0.05
	2.9	0.040	520	159	70%	14%	<0.001	<0.05	<0.05
	3.0	0.048	445	149	73%	13%	<0.001	<0.05	<0.05
	3.1	0.037	387	141	75%	11%	<0.001	<0.05	<0.05
	3.2	0.035	323	131	75%	11%	<0.001	<0.05	<0.05
	3.5	0.035	194	88	86%	5%	<0.001	<0.05	<0.05
	3.7	0.028	113	48	97%	0%	<0.001	<0.05	0.037*

References

1. Nasreddine ZS, Phillips NA, Bédirian V, et al. The Montreal Cognitive Assessment, MoCA: A Brief Screening Tool For Mild Cognitive Impairment. *J Am Geriatr Soc*. 2005;53(4):695-699. doi:10.1111/j.1532-5415.2005.53221.x

2. Shen X, Finn ES, Scheinost D, et al. Using connectome-based predictive modeling to predict individual behavior from brain connectivity. *Nat Protoc*. 2017;12(3):506-518. doi:10.1038/nprot.2016.178

3. Stoffers D, Bosboom JLW, Deijen JB, Wolters ECh, Stam CJ, Berendse HW. Increased cortico-cortical functional connectivity in early-stage Parkinson's disease: An MEG study. *NeuroImage*. 2008;41(2):212-222. doi:10.1016/j.neuroimage.2008.02.027

4.2. Study II- Identification of Parkinson's disease subtypes from resting state electroencephalography

Sahar Yassine, Ute Gschwandtner, Manon Auffret, Joan Duprez, Marc Verin, Peter Fuhr, Mahmoud Hassan.

Under review in Movement Disorders.

Identification of Parkinson disease subtypes from resting-state electroencephalography

Sahar Yassine[1,2,3] MSc, Ute Gschwandtner[4] MD, Manon Auffret[1,3,6,7,] PharmD, PhD, Joan Duprez[1] PhD, Marc Verin[1,3,5,6,†] MD, PhD, Peter Fuhr[4,†] MD, Mahmoud Hassan[3,8,*,†] PhD

[1] University of Rennes 1, LTSI - U1099, F-35000 Rennes, France

[2] NeuroKyma, F-35000 Rennes, France

[3] Behavior & Basal Ganglia, CIC1414, CIC-IT, CHU Rennes, Rennes, France

[4] Dept. of Neurology, Hospitals of the University of Basel, Basel, Switzerland

[5] Movement Disorders Unit, Neurology Department, Pontchaillou University Hospital, Rennes, France

[6] Institut des Neurosciences Cliniques de Rennes (INCR), Rennes, France

[7] France Développement Electronique, Monswiller, France

[8] School of Science and Engineering, Reykjavik University, Reykjavik, Iceland

[†]**These authors contributed equally to this work.**

Corresponding author: Marc Vérin, marc.verin@chu-rennes.fr

Professor, Neurology department Pontchaillou University Hospital, Rennes, France.

Abstract

Background: Parkinson's Disease (PD) patients present with a heterogeneous clinical phenotype, including motor, cognitive, sleep, and affective disruptions. However, this heterogeneity is often either ignored or assessed using only clinical assessments.

Objectives: We aimed to identify different PD sub-phenotypes in a longitudinal follow-up analysis and their electrophysiological profile based on resting-state electroencephalography (RS-EEG) and to assess their clinical significance over the course of the disease.

Methods: Using electrophysiological features obtained from RS-EEG recordings and data-driven methods (similarity network fusion and source-space spectral analysis), we have performed a clustering analysis to identify disease sub-phenotypes and we examined whether their different patterns of disruption are predictive of disease outcome.

Results: We showed that PD patients (N = 44) can be sub-grouped into three phenotypes with distinct electrophysiological profiles. These clusters are characterized by different levels of disruptions in the somatomotor network (delta and beta band), the frontotemporal network (alpha2 band) and the default mode network (alpha1 band), which consistently correlate with clinical profiles and disease courses. We demonstrated that these clusters are statistically robust, and can be classified into either moderate (only-motor) or mild-to-severe (diffuse) disease. Using follow-up data, we showed that EEG-based features characterzing these subtypes remain relevant throughout the disease trajectory and can predict the cognitive evolution of PD patients from baseline, when the cognitive clinical scores were overlapped.

Conclusions: The identification of novel PD subtypes based on electrical brain activity signatures may provide a more accurate prognosis in individual patients in clinical practice and help to stratify subgroups in clinical trials. Innovative profiling in PD can also support new therapeutic strategies that are brain-based and designed to modulate brain activity disruption.

1. Introduction

Parkinson's disease (PD) is a neurodegenerative disorder characterised by significant clinical (presentation and prognosis) and pathological heterogeneity[1–4]. This heterogeneity is delineated by a constellation of motor and non-motor symptoms (sleep disturbance, cognitive decline, emotional and vegetative disorders…) and associated with multiple genetic, environmental and comorbidity factors. It has therefore largely endorsed the emerging concept of approaching PD as the final common pathway of multiple disease mechanisms rather than a single entity[5–7]. Considering PD as a single disorder has been indeed ineffective when attempting disease modification[6]. To take this heterogeneity in PD into account, efforts are currently focused on what is known as 'precision (or stratified) medicine', that requires a prior identification of distinct prodromal PD subtypes[7–10] probably based on differing primary disease processes.

Most previous PD subtyping studies are based only on clinical/behavioural assessments[11–14]. Despite revealing clinically relevant PD subtypes, uncovering the extent of the underlying physiopathology remained very limited. In contrast, genome-wide association studies, cerebrospinal fluid analysis and neuroimaging studies have led to better understanding of the biological underpinnings of the disease by associating common genetic variants, proteins or neurophysiological processes with different forms of PD in terms of clinical features[15–17], treatment's responsiveness[18,19] and rates of progression[20,21]. Indeed, integrating features from such data modalities in the clustering approaches would result in better identification of PD subtypes that share latent pathological mechanisms[22–25].

Moreover, stratifying PD patients according to their individual disease trajectories is fundamental to improve biomarkers development strategies[9]. This can not be done without an adequate methodological framework that includes sufficient longitudinal assessments. In recent years, electroencephalography (EEG) has shown its worthiness as a promising low-cost technique for biomarkers discoveries providing non-invasive access to the electrophysiological activity of the whole brain at the millisecond[26,27]. Several studies used EEG features and clustering techniques to identify subphenotypes of different brain disorders[28–30]. In parallel, the advent of longitudinal studies assessing the evolution of clinical and biological features of different PD subtypes has afforded reliable tracking of the clinical trajectory and disease progression by attributing a well-defined biological/clinical profile for each subphenotype[13,22–

[25,31]. Yet, the use of EEG in a longitudinal framework to establish PD phenotyping based on neurophysiological brain activity is still missing.

In this study, we used resting-state high-density (HD)-EEG recordings of 44 PD patients from their 5-year follow-up examinations to perform a clustering analysis based on an unsupervised learning technique called Similarity Network Fusion (SNF)[32]. We aimed to identify different PD subgroups with distinct electrophysiological profiles and appraise their clinical significance and neurophysiological progression longitudinally. We also investigated the ability of the relevant electrophysiological features to distinguish between PD subtypes from early disease stages at baseline and associate them with the global cognitive state of patients. Finally, we validated the categorical subtyping by applying a dimensionality reduction analysis on the input features of the clustering analysis and associating the low-dimensional representations with the significant EEG measures.

2. Materials and Methods

2.1. Participants

Patients with idiopathic Parkinson's disease (PD) were prospectively recruited from the Movement Disorders Clinic of University Hospital of Basel (City of Basel, Switzerland) as part of a 5-year longitudinal cohort described in our previous study[33]. HD-EEG examinations along with neurological and cognitive assessments were performed for the included patients at Baseline (BL) and at follow-up visits after a mean interval of three years (3Y) and five years (5Y). All patients gave written informed consent to the research protocol, which was approved by the local ethics committees (Ethikkommission beider Basel, Basel; Switzerland; EK 74/09). Out of the 77 PD patients recruited for the main cohort BL, only 45 who participated in the 5Y examinations were selected for this study. One patient was subsequently excluded due to significant artifacts in their corresponding EEG recordings. Therefore, the final sample size for the clustering analysis at 5Y is N=44 PD patients. Among these patients, nine did not complete the 3Y follow-up examinations and were excluded due to missing EEG recordings, and two patients had significant artifacts in their corresponding EEG recordings at baseline and were excluded from the study cohort. As a result, the sample size was subsequently reduced to 35 PD patients at 3Y and 42 PD patients at BL. Patients were evaluated while taking their regular

dopaminergic medication. The demographic and clinical characteristics of this longitudinal study cohort are presented in the supplementary materials and methods section.

2.2. Data acquisition, preprocessing and source reconstruction

The experimental paradigm consisted of 12 minutes of continuous resting state with closed eyes. Patients were seated in a comfortable chair and asked to relax while staying awake with minimum body movements. HD-EEG data were collected using a 256-channel system (Netstation 300, EGI, Inc, Eugene, OR) and sampled at 1000 Hz. Segmentation and preprocessing procedures are detailed in the supplementary material, methods section. Further, to estimate brain activity at the cortical level rather than at the scalp level, we applied the first step of the EEG source connectivity method[34]. This involved reconstructing the dynamics of the brain at the cortical-source level from the artifact-free data segments by solving the inverse problem. The procedure included co-registering EEG channels with an MRI template (ICBM152), building a realistic head model (using the OpenMEEG toolbox[35]), and applying the weighted minimum norm estimate method[36]. The outputs were the time-varying signals of the 210 cortical regions of interest (ROIs) from the Brainnetome atlas[37].

2.3. Power spectral and functional connectivity features

The 210 source-reconstructed signals were used to estimate the power spectrum at the cortical level using the Welch method[38]. Relative band power features were then estimated in five different EEG frequency bands: delta (1-4 Hz), theta (4-8 Hz), alpha1 (8-10 Hz), alpha2 (10-13 Hz) and beta (13-30 Hz) and a total of 210 x 5 power spectral features were obtained for each patient for further analysis. Regarding functional connectivity features, in each frequency band, statistical couplings were estimated between the 210 regional time series using the "Amplitude Envelope Correlation (AEC)" method[39] with leakage correction to reduce the volume conduction effect and a total of 21945*5 unique connectivity features were attributed to each patient for further analysis. More details about these approaches are provided in the supplementary materials, methods section.

2.4. Clustering analysis and dimensionality reduction

In order to retrieve clusters of patients with distinct neurophysiological profiles, we followed a data-driven unsupervised clustering approach based on the Similarity Network Fusion (SNF) method[32]. SNF is a novel approach for combining features from different data sources into a single fused similarity network that captures both mutual and complementary information between features offering insights into the strength of relationship between patients. Here, we used SNF to extract and combine similarity networks corresponding to the power spectral (or/and functional connectivity) features from the different frequency bands. More details about the method and the clustering pipeline can be found in the supplementary materials, method section.

Further, to validate the categorical representation derived from the clustering analysis, we conducted a dimensionality reduction analysis using diffusion map embedding as described in[23]. This approach produced a continuous low-dimensional representation that contained the most meaningful properties of the original data (i.e., the underlying pathology). See supplementary materials, method section, for more technical details about the process.

2.5. Neurophysiological profiles of the clusters and correlation analysis

In order to attribute a specific neurophysiological profile for each of the identified clusters, we defined four spectral power/connectivity measures corresponding to the average relative power/connectivity of regions within four brain networks (SMN: somatomotor network, DMN: default mode network, FTN: fronto-temporal network and FPN: fronto-parietal network). Those networks are recognized to be activated at rest[40] and to be disrupted in PD[41,42]. The affiliation of brain regions to each of these networks are presented in the Supplementary Table S3. More in depth details about the statistical and correlation analysis are provided in the method section of the supplementary materials.

3. Results

3.1. EEG reveals three PD clusters with distinct electrophysiological profiles

The clustering analysis applied to the EEG power spectral features at the five different frequency bands yielded the identification of three PD subgroups: G1(N=9), G2 (N=22) and G3 (N=13) (Fig. 1A). The clusters were stable under perturbations in the data with an average robustness coefficient of 91% over 100 iterations. The overall changes in their relative spectral power over all brain regions are illustrated in Fig. 1B. Higher relative power appears to characterise the neural activity of G3 compared to G1 and G2 at low frequency bands (delta, theta), in contrast a shift toward slower neural activity for G3 compared to G1 and G2 was observed for both alpha and beta frequency bands.

Concerning the most relevant brain networks in maximally dissociating the identified clusters in terms of relative spectral power, results showed that the somatomotor network (SMN) was the most significant in both delta ($F=20.2$, $p<0.001$) and beta ($F=30.6$, $p<0.001$), the Default Mode Network (DMN) in alpha1 ($F=11.5$, $p<0.05$) and the fronto-temporal network (FTN) in alpha2 ($F=18.6$, $p<0.001$). No network appeared to significantly distinguish between groups in the theta band. This approach allowed us to attribute a distinctive neurophysiological profile to each subgroup (Fig. 1C). For example, G1 is characterized with low SMN power in delta and high SMN power in beta, whereas G2 shows a high power within the DMN in alpha1. Moreover, high power within the FTN in alpha2 appeared to represent both G1 and G2. Finally, high delta power for the SMN in contrast with low powers for the DMN in alpha1, the FTN in alpha2 and the SMN in beta were characteristic of the neurophysiological profile of G3.

Furthermore, by associating a relevant brain network for each frequency band, we computed a quantifiable power measure at the patient level to investigate their distributions across subtypes. At 5Y, results revealed significantly higher values for G3 compared to G1 ($p<0.01$) and G2 in terms of SMN-delta power ($p<0.001$). Conversely, this metric presented significantly lower values for G3 when computed for the DMN in alpha1 (G3<G2, $p<0.01$), the FTN in alpha2 (G3<G1, $p<0.01$; G3<G2, $p<0.001$) and the SMN in beta (G3<G1, $p<0.01$). Differences between G1 and G2 were only significant for the SMN-beta power (G1>G2, $p<0.001$) (Fig. 1D). All reported p-values were corrected using Bonferroni for multiple comparisons.

We then investigated the longitudinal evolution of the EEG-based clusters between BL, 3Y and 5Y. Post-hoc analysis revealed that both G1 and G2 showed a relatively constant power spectrum over time compared to G3 where an increase in EEG power between BL and 5Y was clearly observed mainly at lower frequency bands delta and theta (Supplementary Fig.S1). A broad examination on the longitudinal progression of the significant EEG-based features that characterize the three groups was also assessed for the different frequency bands. We also validated the categorical representation over continuous severity dimension showing that the three groups are dissociable along the first two dimensions of the embedding. Detailed results are provided in the supplementary materials.

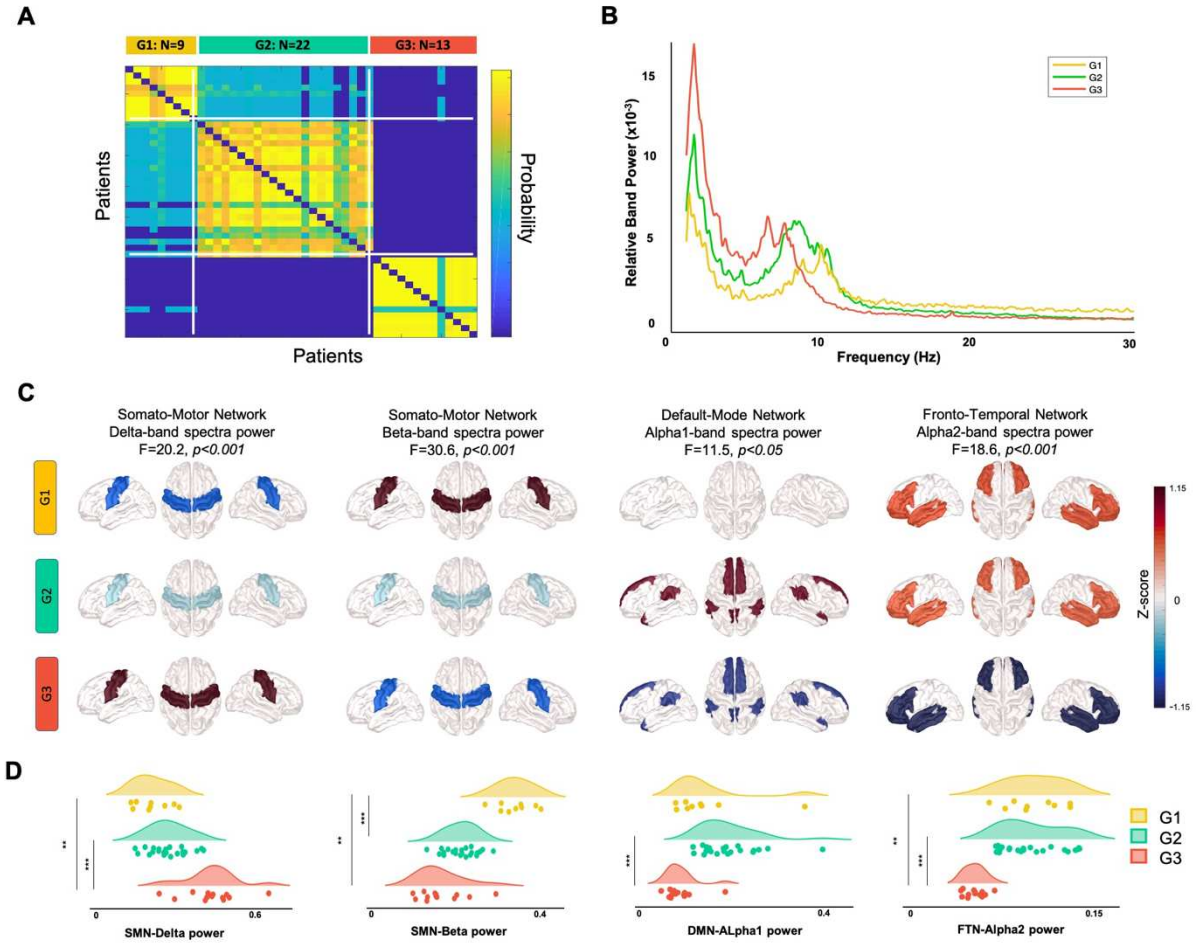

Figure 1- ***PD subtypes and their electrophysiological profiles.*** ***(A)*** *Patient co-assignment matrix representing the three identified subgroups and indicating the probability of two patients being assigned to the same cluster across clustering solutions.* ***(B)*** *Changes in the relative power spectra for the three PD subtypes.* ***(C)*** *Distinct neurophysiological profiles characterizing PD patients in each subgroup across frequency bands. For representation purposes, the average power in each brain network was converted to z-score.* ***(D)*** *Distribution of the quantifiable power measures between the three PD subgroups: average power of somatomotor network (SMN) in delta and beta, default mode network (DMN) in alpha1, fronto-temporal network (FTN) in alpha2. Significant differences between subgroups are marked as ** for p<0.01 and *** for p<0.001. P-values were corrected for multiple comparisons using Bonferroni.*

3.2. Clinical profiles of EEG clusters

The demographic and clinical characteristics of the identified clusters are represented in Table 1. Significant inter-group differences were observed only for age (p=0.021) between G1 and G3, with the latter group being older, and for the Montreal Cognitive Assessment score (MoCA) (p=0.001) with G3 having significantly lower scores compared to G1 and G2. To assess the clinical relevance of each subgroup, we conducted a series of one-way ANOVAs on the different neuropsychological tests. Performances of each PD subgroup in those tests are represented in the Supplementary Table S4. Significant inter-groups differences were found mainly in tests assessing the executive function with G3 having significantly lower scores than G1 and G2. Overall, G3 showed lower scores in all cognitive domains (Fig. 2A, C) with significantly lower global cognitive score MoCA which express a more severe cognitive state compared to G1 and G2, in contrast it showed higher UPDRS-II and UPDRS-III scores which reflects more severe motor deficits (Fig. 2B). We also investigated for the three subtypes, the longitudinal patterns of progression of the MoCA scores (Fig. 2D), the UPDRS-III scores (Fig. 2F) and the mean Z-score of the tests assessing the executive function (as several tests assessing this domain were discriminable between subgroups at 5Y; Fig. 2E). Results showed that at BL, these scores overlapped with no significant differences between subgroups, however longitudinally, G3 had the most prominent decline in general cognitive ability and executive function in contrast to relatively unchanged patterns in G1 and G2. When considering the different scores collectively (Fig. 2), G3 can be categorized as a mild-to-severe (diffuse) PD group with progressive decline in cognitive function, whereas both G1 and G2 can be viewed as moderate (motor only) groups, with G1 exhibiting a more rapid motor progression.

Finally, to further investigate the plausibility of the spectral power features in identifying clinically relevant PD subtypes with distinct neurophysiological profiles, we conducted the same previous analysis using source-space functional connectivity solely and on the combination of both functional connectivity and spectral power features. Detailed results are available in the supplementary materials.

Table 1- ***Demographic and clinical characteristics of the three identified subgroups of PD patients expressed as mean (standard deviation).*** *M/F: Male/Female, y: years, LPD: Left-affected PD, RPD: Right-affected PD, both: bilateral PD, UPDRS-II: Unified Parkinson's Disease Rating Scale motor experiences of daily living, UPDRS-III: Unified Parkinson's Disease Rating Scale motor examinations, LEDD: Levodopa Equivalent Daily Dose, MoCA: Montreal Cognitive Assessment, MMSE: Mini Mental State Examinations*

		G1 (N=9)	**G2 (N=22)**	**G3 (N=13)**	**p-value**	
Demographic	**Age (y)**	65.6 (6.4)	72.6 (7.8)	74.4 (6.7)	0.021	G1<G3
	Sex (M/F)	6/3	15/7	9/4	0.992	-
	Education (y)	14.8 (2.9)	14.9 (3.4)	15.6 (2.8)	0.785	-
Clinical	**Disease duration (y)**	12.25 (5.8)	9.3 (5.2)	10.9 (3.5)	0.301	-
	Disease side (LPD/RPD/both)	7/2/0	14/8/0	7/4/2	-	-
	UPDRS-II	10.4 (7.1)	8.3 (6.6)	11.6 (6.5)	0.420	-
	UPDRS-III	21.5(12.7)	15.9 (12.8)	25.3 (13)	0.209	-
Medication	**LEDD (mg/day)**	839 (399)	613 (411)	524 (292)	0.160	-
Global cognition	**MoCA**	27.7 (1.6)	26.3 (1.9)	21 (8)	0.001	G1,G2>G3
	MMSE	28.9 (1.7)	28.6 (1.3)	27.2 (2.6)	0.051	-

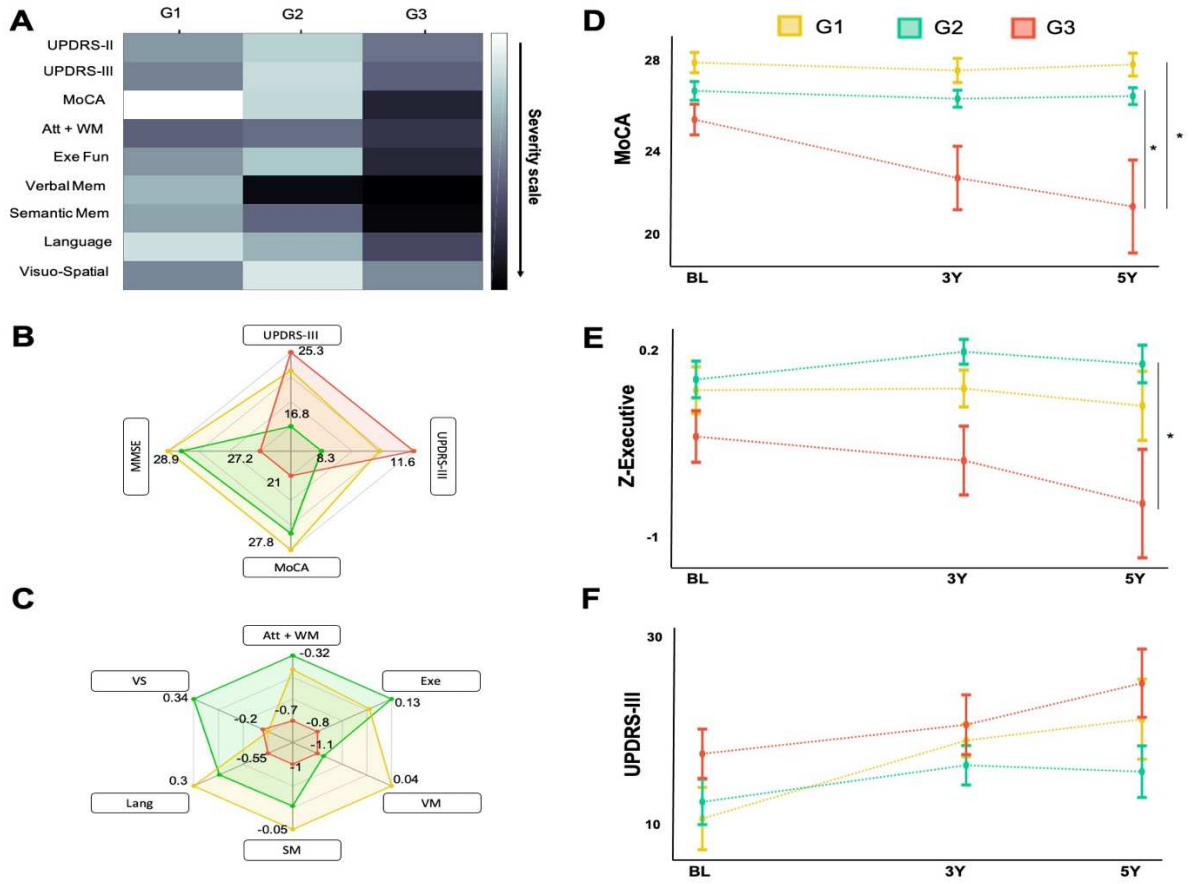

*Figure 2- **PD subtypes and their clinical significance. (A)** Heatmap illustration of the main global clinical scores (UPDRS-II, UPDRS-III and MoCA) and the average of the neuropsychological scores per domain (attention + working memory (att + WM), executive function (Exe), verbal memory (VM), semantic memory (SM), language (Lang) and visuo-spatial abilities (VS)) across the three identified PD subtypes. Darker colours represent more severe deficits for the variable. Spider plots of **(B)** the main global clinical scores and **(C)** the average of the neuropsychological z-scores per cognitive domain. Longitudinal progression in time of each of the **(D)** MoCA, **(E)** average Z-score of the tests assessing the executive function and **(F)** UPDRS-III score. Error bars represent the standard error and significant differences between subgroups are marked as * for $p<0.05$.*

3.3. EEG distinguish mild-to-severe PD from moderate PD longitudinally

Here, we investigate further the effectiveness of the EEG-based features that characterize these subtypes at 5Y in discriminating between the mild-to-severe PD group and the moderate PD groups from early disease stages at BL, where the clinical scores were not discriminative yet. To do so, we aggregated both G1 and G2 into one moderate only-motor group (G1+G2) and we compared their corresponding discriminative measures with those of the mild-to-severe group G3 longitudinally. Results showed that the DMN power in alpha1 and the FTN power in alpha2 were the most prominent in significantly distinguishing both PD groups

longitudinally. In particular, the power of the FTN in alpha2 was the most relevant in terms of statistical differences between PD subgroups throughout the disease trajectory. The statistical differences were significant from BL even after eliminating the outliers (Cohen's d = 1.9, p<0.001) toward the follow-up examinations at 3Y (Cohen's d = 1.5, p<0.01) and at 5Y (Cohen's d = 2.2, p<0.001) (Fig. 3A). The power of the FTN in alpha2 could thus be considered predictive of the disease's evolution towards either only-motor or diffuse disease.

We also computed Spearman correlation (with covariate control) between EEG measures and the MoCA scores. Results revealed a significant positive correlation between the DMN-alpha1 power and the Moca Score at 3Y (R=0.39, *p=0.027)* and not at 5Y. As for the FTN-alpha2 power measures, they were positively correlated with the MoCA scores at 3Y (R=0.34, *p=0.054*) and at 5Y (R=0.31, *p=0.051*) but without reaching the significance level (Fig. 3B).

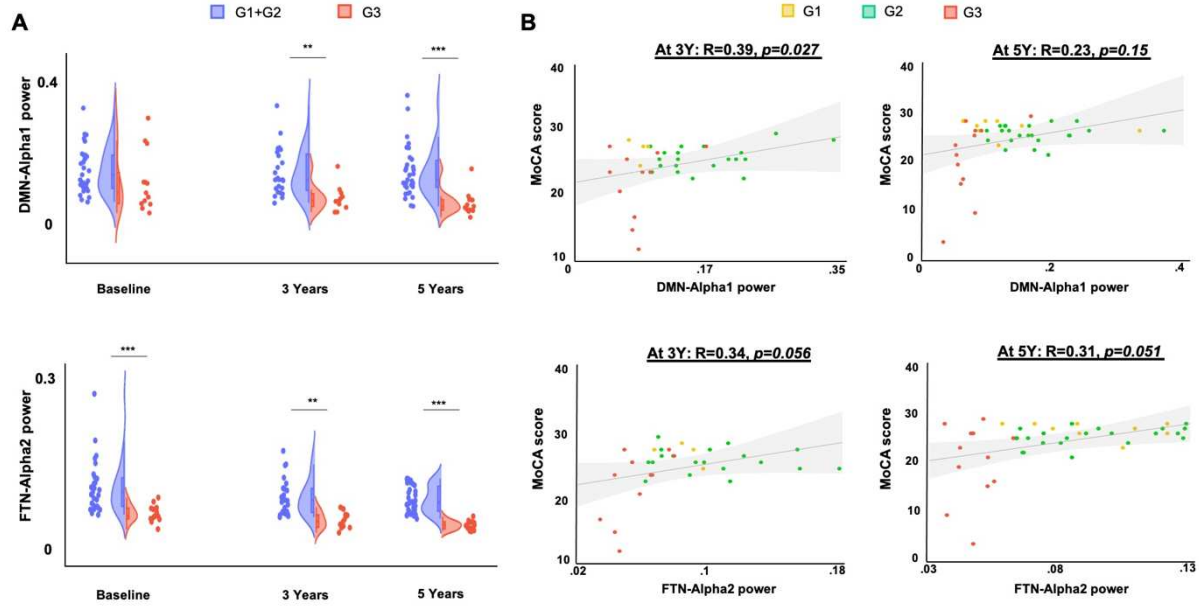

Figure 3- ***Longitudinal dissociation between the severe and the moderate groups.*** ***(A)*** *Longitudinal progression of the default mode network (DMN) power in alpha1 and the fronto-temporal network (FTN) power in alpha2 for the moderate group G1+G2 against the severe group G3. Significant differences between both groups are marked as ** for p<0.01 and *** for p<0.001.* ***(B)*** *Correlation between DMN-alpha1/FTN-alpha2 power measures and the global cognitive score MoCA at 3Y and 5Y.*

4. Discussion

As the wide spectrum of motor and non-motor symptoms in PD advocates for an undoubtable heterogeneity between patients, there is a need for disease subtyping frameworks to deal with this heterogeneity and empower disease-modification strategies[6,7,9]. Until recently, defining PD subtypes was based mainly on clinical features, lacking a characterisation of the underlying pathobiology of the identified phenotypes[2,13]. In the present study, we used resting state HD-EEG to reveal subtypes of PD patients using an unsupervised data-driven clustering approach. The analysis led to identifying three different clinically relevant PD subtypes with distinct electrophysiological profiles.

4.1. Resting state EEG-based PD clusters

Several studies have used quantitative EEG to characterize PD electrophysiological abnormalities[43–45]. Higher spectral power in the low frequency bands (delta and theta) and lower power in the high frequency bands (alpha and beta) were associated with cognitive deterioration of PD patients in several electrophysiological cross-sectional[46,47] and longitudinal studies[48–50]. Interestingly, those spectral patterns appeared to characterize our identified subgroup G3 compared to G1 and G2. Moreover, the electrophysiological profile attributed to this cluster is characterized by prominent low powers within the default mode network and the fronto-temporal networks. Intrinsic metabolic[51], oscillatory brain activity[52] and functional connectivity[17,50,53–55] abnormalities within those networks were strongly associated with PD-related cognitive decline and dementias. This may suggest that patients of G3 are more cognitively impaired than those of G1 and G2 which was confirmed by the high proportion of patients classified clinically with Mild Cognitive Impairment (MCI) within G3 (9/13 = 69%) and by their clinical assessments with stronger deficits in both their motor and non-motor scores.

Concerning the electrophysiological differences between G1 and G2, both groups had relatively similar EEG characteristics in all frequency bands except for beta where G1 showed significantly higher power than G2, mainly within the somatomotor network. Accordingly, the clinical profile of those clusters overlapped in almost all assessments. However, only the motor functionalities of G1 have decayed more rapidly over time than G2, suggesting a motor predominant profile for this cluster. These observations correlated with previous EEG findings

that associated the increase in beta power with low non-dopaminergic disease severity[56] and impairments in motor symptoms[57].

Furthermore, disruptions in functional connectivity have been broadly associated with clinical phenotyping of PD using EEG[54,58], MEG[55,59] or fMRI[31] studies. Here, investigating the prospect of HD-EEG functional connectivity features in dissociating multiple phenotypes of PD was also promising and has led to identify three subgroups different from those issued using the spectral power features. Despite presenting inter-group statistical differences, some eccentric values of connectivity for few patients have weakened the relevance of the corresponding electrophysiological profiles of the clusters (Supplementary Fig. S3). This was confirmed later by the lack of pronounced clinical differences between subtypes and the major overlap endorsed by the low-dimensional projections of the input connectivity features. Additionally, integrating both spectral power and functional connectivity features has also generated three clusters but with more similar affiliations to those yielded when using only the spectral power features. One possible interpretation of these findings could be the preponderance of information derived from power features over those of connectivity. It is worth mentioning that handling the same analysis by using spectral power features computed at the scalp level rather than at source level yielded to the identification of two subtypes rather than three, the first combining G1 and G2 and the second involving the same patients of G3. Although this approach has separated the moderate group from the mild-to-severe group clinically, features computed at source level were more effective in splitting the moderate group into two subtypes with different clinical and electrophysiological profiles.

Finally, several longitudinal studies on PD subtyping, mainly on the PPMI cohort, have used clustering, machine learning and deep learning techniques. Inline with our study, they also identified three PD subgroups with different disease severity and progression rates[22–25]. In particular, Fereshtehnejad et al.[22] and Markello et al.[23] have demonstrated that integrating functional data into clustering approaches is relevant in identifying clinically meaningful clusters attributed with several patterns of functional disruptions, in terms of brain atrophy and dopamine binding.

4.2. Clinical prominence of EEG clusters

Our longitudinal assessment has enabled an accurate clinical/electrophysiological tracking of the disease progression in each subphenotype. The most clinically distinct identified subtype was the mild-to-severe group G3 that showed longitudinal deteriorations in both motor and

non-motor scores. Patients of this cluster were older with relatively shorter disease durations than those of the moderate groups, endorsing thus the association of older age at onset with the severity of motor and non-motor features[60]. In addition, a rapid motor progression has differentiated the moderate subtype G1 from the moderate subtype G2 despite the 'ON' dopaminergic medication state of the patients and the heterogeneity of their LEDD intakes. Indeed, those findings would suggest that the unique neurophysiological patterns of the EEG-based subphenotypes presumably reflect their distinction in terms of non-dopaminergic disease severity, in accordance with a previous quantitative EEG study[56].

Furthermore, the longitudinal assessment has also shown an extensive overlap between the cognitive scores of the mild-to-severe subgroup and the moderate subgroups at baseline. However, their distinct electrophysiological profiles, mainly in the alpha band, remained separable not only at the 5Y examinations but at earlier stages of the disease. The presented work has therefore emphasised a potential predictive ability for the resting state EEG in distinguishing between patients according to their future clinical deterioration trajectories. This is in line with several longitudinal subtyping studies that showed that identifying biological-based subphenotypes of PD[22–25] or other neurodegenerative disorders[28,29] provides a link toward causative pathological mechanisms with a confirmed clinical relevance contrary to exclusively clinical-based subtyping studies. In this context, insights provided by the EEG are promising for what is known as "stratified medicine" since prior biologically and clinically relevant subtyping would ultimately yield to improve disease modifying/ interventions strategies in well-defined targeted patients[6,7,9].

4.3. Limitations

Despite the 5-year longitudinal assessments provided for this work, the number of patients who participated in the 5Y examinations and included in the clustering analysis was relatively low due to the complexity in upholding long-term follow-up studies. It's important to acknowledge the limitations of the study and the exploratory nature of the results, particularly when dealing with small sample sizes and a large number of features and statistical tests. In our study, this issue specifically impacted the statistical comparisons for G2, which consisted of only four patients at the 3Y assessment. On another note, although the 'ON' dopaminergic medication state of the patients appraised the non-dopaminergic severity of the disease in the identified subphenotypes, nevertheless it may also conceal the magnitude of the motor signs in patients, hindering thus the clinical interpretation of the inter-group motor dissimilarities. Lastly, a

more-in-depth analysis that explores the consistency of the presented results to be replicated on independent longitudinal cohorts is much needed for further validation. Such endeavours will verify the capacity of spectral power and connectivity features in predicting patient's stratification without prior knowledge of their disease severity.

4.4. Conclusion

To sum up, we showed for the first time that EEG spectral and connectivity features can be used to cluster PD patients into subphenotypes with distinct clinical/electrophysiological profiles and disease trajectories. This electrophysiological profiling showed potential stratification capabilities at early disease stages before the clear manifestation of the clinical symptoms. Further investigations would enhance biomarkers discovery efforts addressing the heterogeneity of PD and improve the development of neuroprotective therapies.

Acknowledgment

The authors thank all the patients, their families and caregivers for their participation in this study. The authors would like to also thank Beltrani Selina Maria for her help in EEG data management and data sharing. There are no financial conflicts of interest to disclose.

Author Roles

1 Research project: A. Conception, B. Organization, C. Execution; 2 Statistical Analysis: A. Design, B. Execution, C. Review and Critique; 3 Manuscript: A. Writing of first draft, B. Review and critique

S. Y. contributed in: 1B, 1C, 2A, 2B, 3A

U. G. contributed in: 1A, 1B, 2C, 3B

M. A. contributed in: 3B

J. D. contributed in: 2C, 3B

M. V. contributed in: 1A, 2C, 3B

P. F. contributed in: 1A, 1B, 2C, 3B

M.H. contributed in: 1B, 1C, 2A, 2B, 3A.

There are no financial conflicts of interest to disclose

Funding information

This study is based on work that has been supported by the Camelia Botnar Foundation, Parkinson Schweiz Foundation, Gottfried und Julia Bangerter-Rhyner Foundation, Jacques and Gloria Gossweiler Foundation, Freiwillige Akademische, the Institute of Clinical Neurosciences of Rennes (INCR), and university of Rennes.

Competing interests

The authors report no competing interests.

Data and code availability statement

The data that supports the findings of this study are available on request from the corresponding author. The data are not publicly available due to privacy or ethical restrictions. All codes necessary to reproduce the results are available at: https://github.com/yassinesahar/ClusteringPD.

References

1. Bloem, B. R., Okun, M. S. & Klein, C. Parkinson's disease. *The Lancet* **397**, 2284–2303 (2021).

2. Mestre, T. A. *et al.* Parkinson's Disease Subtypes: Critical Appraisal and Recommendations. *J. Park. Dis.* **11**, 395–404 (2021).

3. Surmeier, D. J., Obeso, J. A. & Halliday, G. M. Selective neuronal vulnerability in Parkinson disease. *Nat. Rev. Neurosci.* **18**, 101–113 (2017).

4. Horsager, J. *et al.* Brain-first versus body-first Parkinson's disease: a multimodal imaging case-control study. *Brain* **143**, 3077–3088 (2020).

5. Farrow, S. L., Cooper, A. A. & O'Sullivan, J. M. Redefining the hypotheses driving Parkinson's diseases research. *Npj Park. Dis.* **8**, 1–7 (2022).

6. Espay, A. J. *et al.* Disease modification and biomarker development in Parkinson disease: Revision or reconstruction? *Neurology* **94**, 481–494 (2020).

7. Espay, A., Brundin, P. & Lang, A. Precision medicine for disease modification in Parkinson disease. *Nat. Rev. Neurol.* **13**, (2017).

8. Vijiaratnam, N., Simuni, T., Bandmann, O., Morris, H. R. & Foltynie, T. Progress towards therapies for disease modification in Parkinson's disease. *Lancet Neurol.* **20**, 559–572 (2021).

9. Espay, A. J. *et al.* Biomarker-driven phenotyping in Parkinson disease: a translational missing link in disease-modifying clinical trials. *Mov. Disord. Off. J. Mov. Disord. Soc.* **32**, 319–324 (2017).

10. Poewe, W., Seppi, K., Marini, K. & Mahlknecht, P. New hopes for disease modification in Parkinson's Disease. *Neuropharmacology* **171**, 108085 (2020).

11. van Rooden, S. M. *et al.* The identification of Parkinson's disease subtypes using cluster analysis: A systematic review. *Mov. Disord.* **25**, 969–978 (2010).

12. van Rooden, S. M. *et al.* Clinical subtypes of Parkinson's disease. *Mov. Disord.* **26**, 51–58 (2011).

13. Lawton, M. *et al.* Developing and validating Parkinson's disease subtypes and their motor and cognitive progression. *J. Neurol. Neurosurg. Psychiatry* **89**, 1279–1287 (2018).

14. Rodriguez-Sanchez, F. *et al.* Identifying Parkinson's disease subtypes with motor and non-motor symptoms via model-based multi-partition clustering. *Sci. Rep.* **11**, 23645 (2021).

15. Nalls, M. A. *et al.* Identification of novel risk loci, causal insights, and heritable risk for Parkinson's disease: a meta-analysis of genome-wide association studies. *Lancet Neurol.* **18**, 1091–1102 (2019).

16. Wolters, A. F. *et al.* Resting-state fMRI in Parkinson's disease patients with cognitive impairment: A meta-analysis. *Parkinsonism Relat. Disord.* **62**, 16–27 (2019).

17. Majbour, N. K. *et al.* Cerebrospinal α-Synuclein Oligomers Reflect Disease Motor Severity in DeNoPa Longitudinal Cohort. *Mov. Disord. Off. J. Mov. Disord. Soc.* **36**, 2048–2056 (2021).

18. Over, L., Brüggemann, N. & Lohmann, K. Therapies for Genetic Forms of Parkinson's Disease: Systematic Literature Review. *J. Neuromuscul. Dis.* **8**, 341–356 (2021).

19. Mueller, K. *et al.* Brain connectivity changes when comparing effects of subthalamic deep brain stimulation with levodopa treatment in Parkinson's disease. *NeuroImage Clin.* **19**, 1025–1035 (2018).

20. Tan, M. M. X. *et al.* Genome-Wide Association Studies of Cognitive and Motor Progression in Parkinson's Disease. *Mov. Disord.* **36**, 424–433 (2021).

21. Majbour, N. K. *et al.* Longitudinal changes in CSF alpha-synuclein species reflect Parkinson's disease progression. *Mov. Disord.* **31**, 1535–1542 (2016).

22. Fereshtehnejad, S.-M., Zeighami, Y., Dagher, A. & Postuma, R. B. Clinical criteria for subtyping Parkinson's disease: biomarkers and longitudinal progression. *Brain J. Neurol.* **140**, 1959–1976 (2017).

23. Markello, R. D. *et al.* Multimodal phenotypic axes of Parkinson's disease. *Npj Park. Dis.* **7**, 1–12 (2021).

24. Zhang, X. *et al.* Data-Driven Subtyping of Parkinson's Disease Using Longitudinal Clinical Records: A Cohort Study. *Sci. Rep.* **9**, 797 (2019).

25. Dadu, A. *et al.* Identification and prediction of Parkinson's disease subtypes and progression using machine learning in two cohorts. *Npj Park. Dis.* **8**, 1–12 (2022).

26. Biasiucci, A., Franceschiello, B. & Murray, M. M. Electroencephalography. *Curr. Biol.* **29**, R80–R85 (2019).

27. Müller-Putz, G. R. Chapter 18 - Electroencephalography. in *Handbook of Clinical Neurology* (eds. Ramsey, N. F. & Millán, J. del R.) vol. 168 249–262 (Elsevier, 2020).

28. Zhang, Y. *et al.* Identification of psychiatric disorder subtypes from functional connectivity patterns in resting-state electroencephalography. *Nat. Biomed. Eng.* **5**, 309–323 (2021).

29. Dukic, S. *et al.* Resting-state EEG reveals four subphenotypes of amyotrophic lateral sclerosis. *Brain* awab322 (2021) doi:10.1093/brain/awab322.

30. Byeon, J., Choi, T. Y., Won, G. H., Lee, J. & Kim, J. W. A novel quantitative electroencephalography subtype with high alpha power in ADHD: ADHD or misdiagnosed ADHD? *PLOS ONE* **15**, e0242566 (2020).

31. Filippi, M. *et al.* Longitudinal brain connectivity changes and clinical evolution in Parkinson's disease. *Mol. Psychiatry* (2020) doi:10.1038/s41380-020-0770-0.

32. Wang, B. *et al.* Similarity network fusion for aggregating data types on a genomic scale. *Nat. Methods* **11**, 333–337 (2014).

33. Yassine, S. *et al.* Functional Brain Dysconnectivity in Parkinson's Disease: A 5-Year Longitudinal Study. *Mov. Disord. Off. J. Mov. Disord. Soc.* (2022) doi:10.1002/mds.29026.

34. Hassan, M. & Wendling, F. Electroencephalography Source Connectivity: Aiming for High Resolution of Brain Networks in Time and Space. *IEEE Signal Process. Mag.* **35**, 81–96 (2018).

35. Gramfort, A., Papadopoulo, T., Olivi, E. & Clerc, M. OpenMEEG: opensource software for quasistatic bioelectromagnetics. *Biomed. Eng. OnLine* **9**, 45 (2010).

36. Hämäläinen, M. S. & Ilmoniemi, R. J. Interpreting magnetic fields of the brain: minimum norm estimates. *Med. Biol. Eng. Comput.* **32**, 35–42 (1994).

37. Fan, L. *et al.* The Human Brainnetome Atlas: A New Brain Atlas Based on Connectional Architecture. *Cereb. Cortex N. Y. NY* **26**, 3508–3526 (2016).

38. Welch, P. The use of fast Fourier transform for the estimation of power spectra: A method based on time averaging over short, modified periodograms. *IEEE Trans. Audio Electroacoustics* **15**, 70–73 (1967).

39. Brookes, M. J. *et al.* Measuring functional connectivity using MEG: Methodology and comparison with fcMRI. *NeuroImage* **56**, 1082–1104 (2011).

40. Thomas Yeo, B. T. *et al.* The organization of the human cerebral cortex estimated by intrinsic functional connectivity. *J. Neurophysiol.* **106**, 1125–1165 (2011).

41. Baggio, H.-C. *et al.* Functional brain networks and cognitive deficits in Parkinson's disease. *Hum. Brain Mapp.* **35**, 4620–4634 (2014).

42. Tinaz, S. Functional Connectome in Parkinson's Disease and Parkinsonism. *Curr. Neurol. Neurosci. Rep.* **21**, 24 (2021).

43. Wang, Q., Meng, L., Pang, J., Zhu, X. & Ming, D. Characterization of EEG Data Revealing Relationships With Cognitive and Motor Symptoms in Parkinson's Disease: A Systematic Review. *Front. Aging Neurosci.* **12**, (2020).

44. Geraedts, V. J. *et al.* Clinical correlates of quantitative EEG in Parkinson disease: A systematic review. *Neurology* **91**, 871–883 (2018).

45. Pourzinal, D. *et al.* Systematic review of data-driven cognitive subtypes in Parkinson disease. *Eur. J. Neurol.* (2022) doi:10.1111/ene.15481.

46. Caviness, J. N. *et al.* Differential spectral quantitative electroencephalography patterns between control and Parkinson's disease cohorts. *Eur. J. Neurol.* **23**, 387–392 (2016).

47. Bosboom, J. L. W. *et al.* Resting state oscillatory brain dynamics in Parkinson's disease: An MEG study. *Clin. Neurophysiol.* **117**, 2521–2531 (2006).

48. Caviness, J. N. *et al.* Longitudinal EEG Changes Correlate with Cognitive Measure Deterioration in Parkinson's Disease. *J. Park. Dis.* **5**, 117–124 (2015).

49. Arnaldi, D. *et al.* Prediction of cognitive worsening in de novo Parkinson's disease: Clinical use of biomarkers. *Mov. Disord.* **32**, 1738–1747 (2017).

50. Olde Dubbelink, K. T. E. *et al.* Cognitive decline in Parkinson's disease is associated with slowing of resting-state brain activity: a longitudinal study. *Neurobiol. Aging* **34**, 408–418 (2013).

51. Ruppert, M. C. *et al.* The default mode network and cognition in Parkinson's disease: A multimodal resting-state network approach. *Hum. Brain Mapp.* **42**, 2623–2641 (2021).

52. Ponsen, M. M., Stam, C. J., Bosboom, J. L. W., Berendse, H. W. & Hillebrand, A. A three dimensional anatomical view of oscillatory resting-state activity and functional connectivity in Parkinson's disease related dementia: An MEG study using atlas-based beamforming. *NeuroImage Clin.* **2**, 95–102 (2013).

53. Hou, Y. *et al.* Primary disruption of the default mode network subsystems in drug-naïve Parkinson's disease with mild cognitive impairments. *Neuroradiology* **62**, 685–692 (2020).

54. Hassan, M. *et al.* Functional connectivity disruptions correlate with cognitive phenotypes in Parkinson's disease. *NeuroImage Clin.* **14**, 591–601 (2017).

55. Olde Dubbelink, K. T. E. *et al.* Resting-state functional connectivity as a marker of disease progression in Parkinson's disease: A longitudinal MEG study. *NeuroImage Clin.* **2**, 612–619 (2013).

56. Geraedts, V. J. *et al.* Quantitative EEG reflects non-dopaminergic disease severity in Parkinson's disease. *Clin. Neurophysiol.* **129**, 1748–1755 (2018).

57. Singh, A. *et al.* Frontal theta and beta oscillations during lower-limb movement in Parkinson's disease. *Clin. Neurophysiol.* **131**, 694–702 (2020).

58. Utianski, R. L. *et al.* Graph theory network function in Parkinson's disease assessed with electroencephalography. *Clin. Neurophysiol.* **127**, 2228–2236 (2016).

59. Dubbelink, K. T. E. O. *et al.* Functional connectivity and cognitive decline over 3 years in Parkinson disease. *Neurology* **83**, 2046–2053 (2014).
60. Pagano, G., Ferrara, N., Brooks, D. J. & Pavese, N. Age at onset and Parkinson disease phenotype. *Neurology* **86**, 1400–1407 (2016).

Supplementary materials

Identification of Parkinson disease subtypes from resting-state electroencephalography

Sahar Yassine[1,2,3] MSc, Ute Gschwandtner[4] MD, Manon Auffret[1,3,6,7,] PharmD, PhD, Joan Duprez[1] PhD, Marc Verin[1,3,5,6,†] MD, PhD, Peter Fuhr[4,†] MD, Mahmoud Hassan[3,8,*,†] PhD

[1] University of Rennes 1, LTSI - U1099, F-35000 Rennes, France

[2] NeuroKyma, F-35000 Rennes, France

[3] Behavior & Basal Ganglia, CIC1414, CIC-IT, CHU Rennes, Rennes, France

[4] Dept. of Neurology, Hospitals of the University of Basel, Basel, Switzerland

[5] Movement Disorders Unit, Neurology Department, Pontchaillou University Hospital, Rennes, France

[6] Institut des Neurosciences Cliniques de Rennes (INCR), Rennes, France

[7] France Développement Electronique, Monswiller, France

[8] School of Science and Engineering, Reykjavik University, Reykjavik, Iceland

[†]**These authors contributed equally to this work.**

Corresponding author: Marc Vérin, marc.verin@chu-rennes.fr

Professor, Neurology department Pontchaillou University Hospital, Rennes, France.

Methods

Data characteristics and clinical neurological/neuropsychological assessments

The demographic and clinical characteristics of the Patients are presented in Table S1. All patients underwent basic neurological examinations. Unified Parkinson's Disease Rating Scale (motor experiences of daily living: UPDRS-II and motor examinations: UPDRS-III) were obtained in the 'ON' medication state by a trained physician. A comprehensive battery of neuropsychological tests was carried out to test for the following cognitive domains: attention and working memory, executive functions, verbal memory, semantic memory, language and visuo-spatial functions. The individual tests grouped into domains are shown in Table S2.

Data segmentation and preprocessing

Among the 12 minutes of the continuous eyes-closed RS-EEG recordings, only the first 10 minutes of the signals were considered for the analysis. They were segmented into epochs of 40 seconds each and the first epoch was excluded from the study. Epochs were then preprocessed automatically using the open-source toolbox Automagic[1]. The preprocessing steps are similar to those described in our previous study[2] and only six epochs with the best quality metrics were considered for the rest of the analysis.

Power spectral and functional connectivity analysis

The Welch method was used to estimate the power spectrum at the cortical level from the 210 source reconstructed signals. For each time-series epoch, a periodogram is computed using the Hamming window and averaged across 8 segments with 50% overlap to compute the spectral estimate. Then, the average power was calculated in five different EEG frequency bands: delta (1-4 Hz), theta (4-8 Hz), alpha1 (8-10 Hz), alpha2 (10-13 Hz) and beta (13-30 Hz). Spectral activity within the gamma band (30-45 Hz) was excluded from this study due to abnormal noise during the recordings in most of the patients. For each patient, the oscillatory power at each of the five frequency bands was averaged across the six time-series epochs. To assess the relative contribution of each particular frequency to the EEG signal, the relative band power was

calculated by dividing the absolute power of the band by the total power. Thus, we obtained for each patient a total of 210 x 5 power spectral features.

Regarding functional connectivity estimations, the "Amplitude Envelope Correlation (AEC)" method[34] with leakage correction was used. It consists of estimating and orthogonalizing the pairwise correlation (Pearson's correlation) between the power envelope of two oscillatory time series obtained by computing the Hilbert transform. Connectivity measures were computed using the brainstorm implementation of the method[3] on 8 windows of 5 seconds each without overlap. They were ultimately averaged across the six time-series epochs and time in each frequency band. This resulted for each patient, a 210 x 210 symmetrical connectivity matrix from which 210 x 209/2 = 21945 features were unique in each frequency band. Thus, we obtained for each patient a total of 21945*5 connectivity features.

Similarity Network Fusion and clustering analysis

Power spectral and/or functional connectivity features (from different frequency bands) were first normalised and distance matrices were constructed using the squared Euclidean distance. Then, a scaled exponential kernel is used to convert distance matrices into unique similarity matrices:

$$W(i,j) = \frac{1}{\sqrt{2\pi\sigma^2}}\, e^{-\frac{\rho^2(x_i,x_j)}{2\sigma^2}} \quad (1)$$

where $\rho(x_i - x_j)$ is the Euclidean distance between patients x_i and x_j and σ is defined as:

$$\sigma = \mu\, \frac{\underline{\rho}^2(x_i,N_i) + \underline{\rho}^2(x_j,N_j) + \underline{\rho}^2(x_i,x_j)}{3} \quad (2)$$

where $\underline{\rho}(x_i, N_i)$ represents the average value of distances between x_i and each of its neighbors $N_{1..k}$. Both k and μ are hyperparameters that should be pre-selected with $k \in (1,2,..,j), j \in Z$, controlling for the number of k-nearest neighbours and μ, a scaling factor in the range of [0.3, 1]$\epsilon\, R^+$. Afterwards, the separate similarity matrices issued from different data sources are fused via a nonlinear method based on message-passing theory. This step consists in iteratively updating every similarity network with the complementary information from the other networks, owing to maximising the similarity between them until convergence or after a pre-specified number of iterations. Finally, the obtained fused similarity network is subjected to spectral clustering[4] which requires an a priori choice of the number of clusters. Those steps were performed using the MATLAB implementation of the SNF package (http://compbio.cs.toronto.edu/SNF/SNF/Software.html).

To avoid biasing our results by the choice of the two hyperparameters k and μ and the number of clusters, we followed an approach proposed by Markello et al.[5] based on an exhaustive parameter search combined with a consensus analysis. To do so, SNF was performed with different possible combination of k *(k = 1,2, 3, .. ,N-1)* where N is the number of patients, and μ (μ = 0.3,0.35,0.4,...,1) resulting in a set of 645 fused networks. Subsequently, these networks were subjected to a spectral clustering for two, three and four cluster's solutions selected for being the most reasonable choices reported in previous PD subtyping studies[6,7]. Among the clustering solutions, only those generated from a stable combination of hyperparameters were retained for the further analysis. This includes the combinations where slight changes in either k or μ do not impact the final clustering solutions remarkably. For this purpose, and for each number of clusters separately, a pairwise z-Rand similarity index[8] was calculated and averaged between the clustering solutions of each combination of hyperparameters (k,μ) and their four closest combinations (k-*1*,μ), (k+*1*,μ), (k,μ-0.05) and (k,μ+0.05). Clustering solutions corresponding to the highest 5% of z-Rand similarity indexes (32 x 3= 96 assignments) were retained and injected in the consensus analysis inspired from community detection studies[9,10]. A NxN co-assignment matrix was consequently generated from these solutions with each element representing the normalised probability of two patients belonging to the same cluster across assignments. This matrix was ultimately thresholded by comparing it with another generated from a permuted null model[10]. Finally, the thresholded matrix is clustered by applying a modularity maximization procedure[11] in order to obtain a final clustering partition representing PD subtypes.

We also wanted to assess the robustness of the identified clusters under small perturbations in the data. For this purpose, we repeated the clustering pipeline 100 times after randomly removing 10% of the subjects (i.e., 4 patients) at each iteration. A robustness coefficient was estimated at each iteration by comparing the obtained assignments with those of the same patients issued from the main analysis with correction to chance using the Rand index[12]. All codes necessary to reproduce the results are available at: https://github.com/yassinesahar/ClusteringPD.

Dimensionality reduction using diffusion maps embedding

Different from linear dimensionality reduction methods such as Principal Component Analysis (PCA), diffusion map embedding is relatively robust to noise perturbations and relies on non-

linear approximations using the Fokker-Planck diffusion equation to provide a low-dimensional representation of graph structures[13,14]. The diffusion process involves specifying a time-parameter *t*, which serves also as a scaling parameter for the geometry of the input data. Here, the fused similarity networks corresponding to the stable combinations of hyperparameters for the three different clustering solutions (32 x 3 = 96 similarity networks) were the inputs of our analysis. We set the diffusion time to zero (*t=0*) in order to obtain the most global representation of the stable fused networks. The obtained embeddings were aligned via rotations and reflections using a generalised orthogonal Procrustes analysis and then averaged to obtain a final set of low-dimensional representation (composed of 5 final components/embeddings) used in further analysis. MATLAB codes used for the diffusion procedure were obtained from the Brainspace toolbox (https://brainspace.readthedocs.io/en/latest/index.html).

Neurophysiological profiles of the clusters and correlation analysis

To retrieve the most discriminable networks between subgroups, we performed a series of separate one-way ANOVA across groups for each network in each frequency band. Age, sex, education and the levodopa equivalent daily dose (LEDD) were considered as confounding factors and the reported results were corrected for multiple comparisons using Bonferroni (number of comparisons= 4 networks x 5 bands = 20, $p<0.05/20$, $p<0.0025$). Within each frequency band, the network with the lowest *p*-value was considered as the most discriminable between subtypes and characterizing their dissimilarities in the corresponding frequency band. The average power/connectivity within each of these networks were later used as a single electrophysiological quantifiable measure computed at the patient level in each frequency band. Statistical differences between groups were assessed using the Wilcoxon test (two-tailed) and results were corrected for multiple comparisons using Bonferroni (number of comparisons = 3 groups x 5 bands=15, $p<0.05/15$, $p<0.0033$). Spearman correlation, with covariate control, was computed to evaluate the relationships between the EEG-based metrics, the clinical scores and the components of the embeddings.

Results

Longitudinal progression of the EEG clusters

Results on the longitudinal progression of the quantifiable power measures of the three groups showed that the SMN power in delta was not discriminable between PD subtypes defined by the HD-EEG at BL nor at 3Y (Fig. S2-A). As for the DMN power in alpha1 (Fig. S2-B), differences between G2 and G3 started to be significant at the follow-up examinations 3Y ($p<0.01$) and 5Y ($p<0.001$). Furthermore, the FTN power in alpha2 significantly distinguish between G3 and both G1 and G2 not only at 5Y, but earlier at 3Y (G3 vs G2, $p<0.01$) and at BL (G3 vs G1, $p<0.05$; G3 vs G2, $p<0.01$) (Fig. S2-C). In addition, the SMN power in beta of G1 showed statistically higher values compared to G2 ($p<0.01$) and G3 ($p<0.01$) at BL and at 5Y (Fig. S2-D). Finally, we were not able to test statistical differences between G1 and other groups at 3Y due to low sample size (N=4) after eliminating the missing data. All reported p-values were corrected using Bonferroni for multiple comparisons.

Patient clusters distinct over continuous severity dimensions

To validate the categorical representation issued from the clustering approach, we used diffusion maps embeddings to generate a continuous low-dimensional space of components that highlight the most prevalent features of the data. Results showed that the three PD subtypes were dissociable along the first two dimensions of the embedding with limited overlap between the moderate groups G1 and G2 (Fig. S3-A). Further, we wanted to examine the relationships between the primary components encoding the most prominent features and general clinical scores reflecting both cognitive and motor deficiencies. Indeed, the first dimension of the embedded space positively correlated with the general cognitive score MoCA (R=0.27, $p=0.09$) whereas the second dimension negatively correlated with the motor score UPDRS-III (R=-0.44, $p<0.01$) (Fig. S3-B). Moreover, exploring the extent to which the quantifiable power measures issued from the clustering approach are likely to correlate with the first dimension of the embedding space revealed a robust significant correlation for the SMN-delta power (R=-0.81, $p<0.001$), the DMN-alpha1 power (R=0.66, $p<0.001$), the FTN-alpha2 power (R=0.84, $p<0.001$) and the SMN-beta power (R=0.72, $p<0.001$) (Fig. 4C).

Clustering using functional connectivity features

Applying the clustering pipeline on the orthogonalized AEC features from the five different frequency bands, we obtained three different subtypes g1 (N=10), g2 (N=13) and g3 (N=21). When assessing the clinical relevance of the subgroups, the largest group g3 was clinically different from g1 and g2 with lower scores in all cognitive domains and a longitudinal decreasing trend in MoCA between BL and 3Y. g1 and g2 were not dissociable along any of the clinical features. However, the clustering was not robust as for the dimensionality reduction analysis, a major overlap was perceived between the three clusters along the first two dimensions of the embeddings (Supplementary Fig. S4).

Moreover, combining both functional connectivity and spectral power features yielded to identify also three groups of n=15, 16 and 13 PD patients. Interestingly, comparing these groups (g1, g2, g3) with the ones issued when using only spectral power features (G1, G2, G3), we found that the latter group comprised the same 13 PD patients as the mild-to-severe group G3 defined previously, while 15 out of the 16 PD patients of the second group were also part of the moderate group G2 and 8 out of 15 were also attributed previously to the moderate group G1. Nevertheless, no significant differences were found between the first two groups in terms of clinical tests. Concerning the electrophysiological features, differences between groups were found only for power spectral features and not for connectivity features and the three groups were separable along the first two dimensions of the embeddings (Fig. S5).

References

1. Pedroni, A., Bahreini, A. & Langer, N. Automagic: Standardized preprocessing of big EEG data. *NeuroImage* **200**, 460–473 (2019).
2. Yassine, S. *et al.* Functional Brain Dysconnectivity in Parkinson's Disease: A 5-Year Longitudinal Study. *Mov. Disord. Off. J. Mov. Disord. Soc.* (2022) doi:10.1002/mds.29026.
3. Tadel, F., Baillet, S., Mosher, J. C., Pantazis, D. & Leahy, R. M. Brainstorm: a user-friendly application for MEG/EEG analysis. *Comput. Intell. Neurosci.* **2011**, 879716 (2011).
4. Yu & Shi. Multiclass spectral clustering. in *Proceedings Ninth IEEE International Conference on Computer Vision* 313–319 vol.1 (2003). doi:10.1109/ICCV.2003.1238361.
5. Markello, R. D. *et al.* Multimodal phenotypic axes of Parkinson's disease. *Npj Park. Dis.* **7**, 1–12 (2021).
6. Dadu, A. *et al.* Identification and prediction of Parkinson's disease subtypes and progression using machine learning in two cohorts. *Npj Park. Dis.* **8**, 1–12 (2022).
7. Fereshtehnejad, S.-M., Zeighami, Y., Dagher, A. & Postuma, R. B. Clinical criteria for subtyping Parkinson's disease: biomarkers and longitudinal progression. *Brain* **140**, 1959–1976 (2017).
8. Traud, A., Kelsic, E., Mucha, P. & Porter, M. Comparing Community Structure to Characteristics in Online Collegiate Social Networks. *SIAM Rev.* **53**, (2016).
9. Lancichinetti, A. & Fortunato, S. Consensus clustering in complex networks. *Sci. Rep.* **2**, 336 (2012).
10. Bassett, D. S. *et al.* Robust detection of dynamic community structure in networks. *Chaos Interdiscip. J. Nonlinear Sci.* **23**, 013142 (2013).
11. Blondel, V. D., Guillaume, J.-L., Lambiotte, R. & Lefebvre, E. Fast unfolding of communities in large networks. *J. Stat. Mech. Theory Exp.* **2008**, P10008 (2008).
12. Hubert, L. & Arabie, P. Comparing partitions. *J. Classif.* **2**, 193–218 (1985).
13. Coifman, R. R. *et al.* Geometric diffusions as a tool for harmonic analysis and structure definition of data: diffusion maps. *Proc. Natl. Acad. Sci. U. S. A.* **102**, 7426–7431 (2005).
14. Lafon, S. & Lee, A. B. Diffusion maps and coarse-graining: a unified framework for dimensionality reduction, graph partitioning, and data set parameterization. *IEEE Trans. Pattern Anal. Mach. Intell.* **28**, 1393–1403 (2006).

Supplementary figures

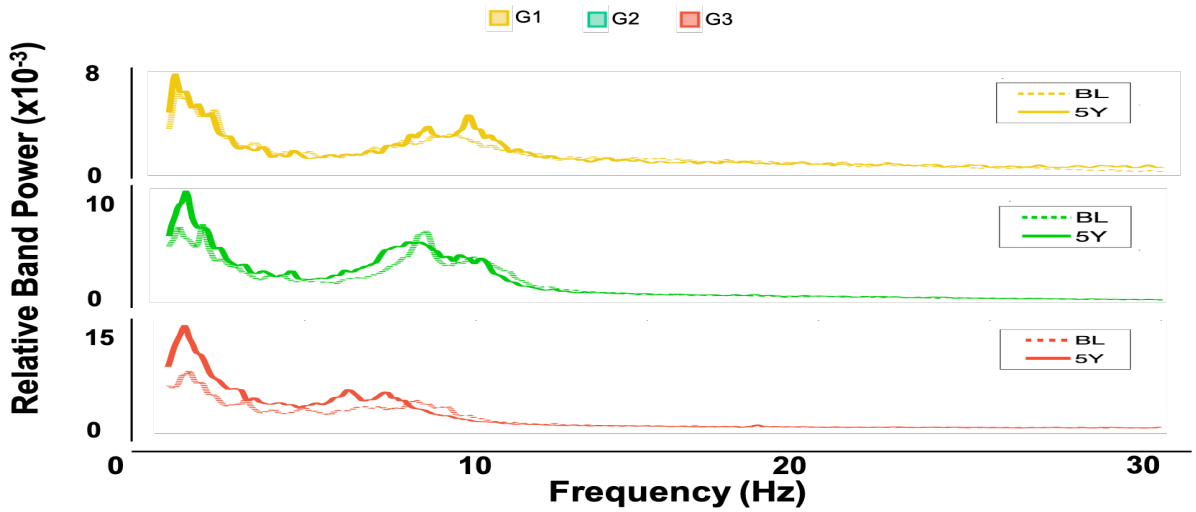

Figure S1- Longitudinal evolution of the relative power spectrum between BL and 5Y for the three PD subtypes.

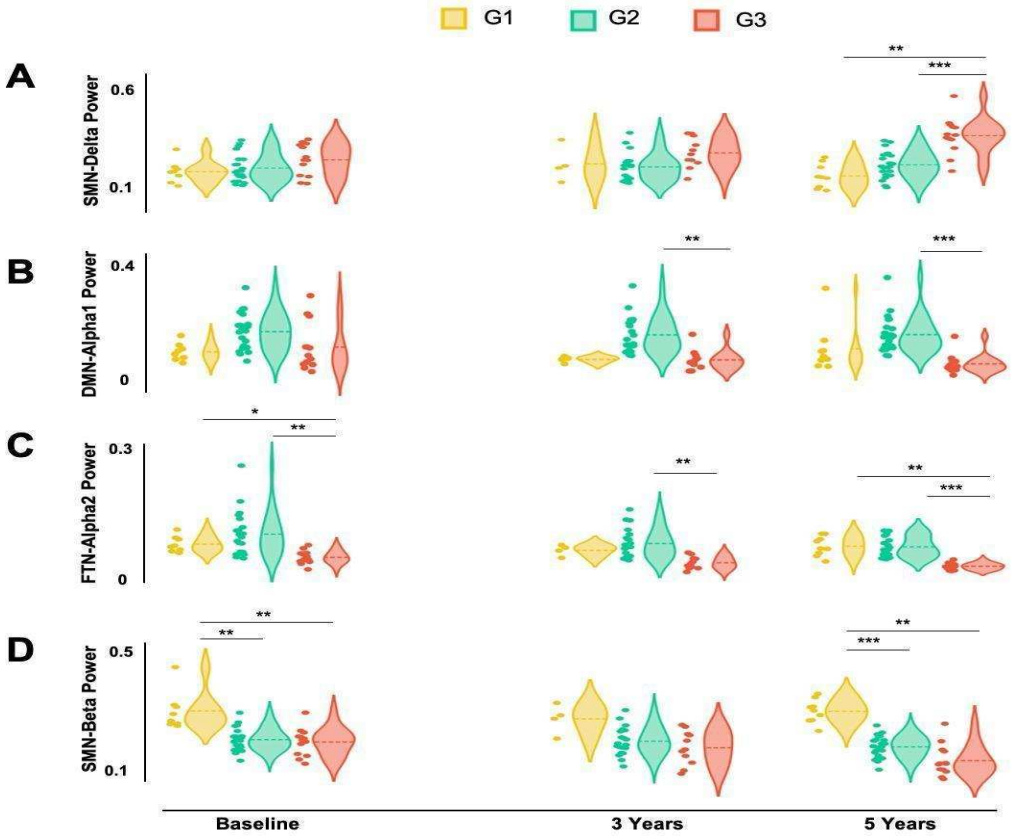

Figure S2- Longitudinal progression in time of the quantifiable power measures for the three PD subgroups. (A) Somatomotor network (SMN) power in delta power, **(B)** Default mode network (DMN) power in alpha1, **(C)** Fronto-temporal network (FTN) power in alpha2 and **(D)** SMN power in beta. Significant differences between subgroups are marked as * for $p<0.05$, ** for $p<0.01$ and *** for $p<0.001$. P-values were corrected for multiple comparisons using Bonferroni.

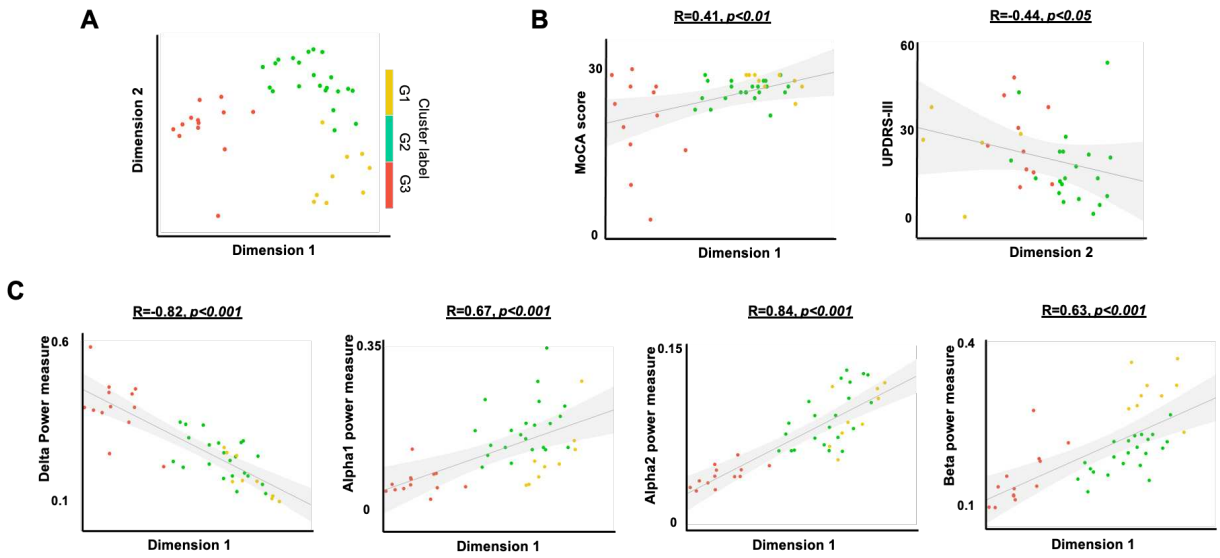

Figure S3- Low-dimensional representation of the three PD subtypes. (A) Representation of the patients from each subtype along the first two dimensions of the embedding space. **(B)** Correlation between MoCA score/UPDRS-III score and first/second dimensions of the embedding space. **(C)** Correlation between the first component of the embedding space and the SMN-delta, DMN-alpha1, FTN-alpha2 and SMN-beta powers.

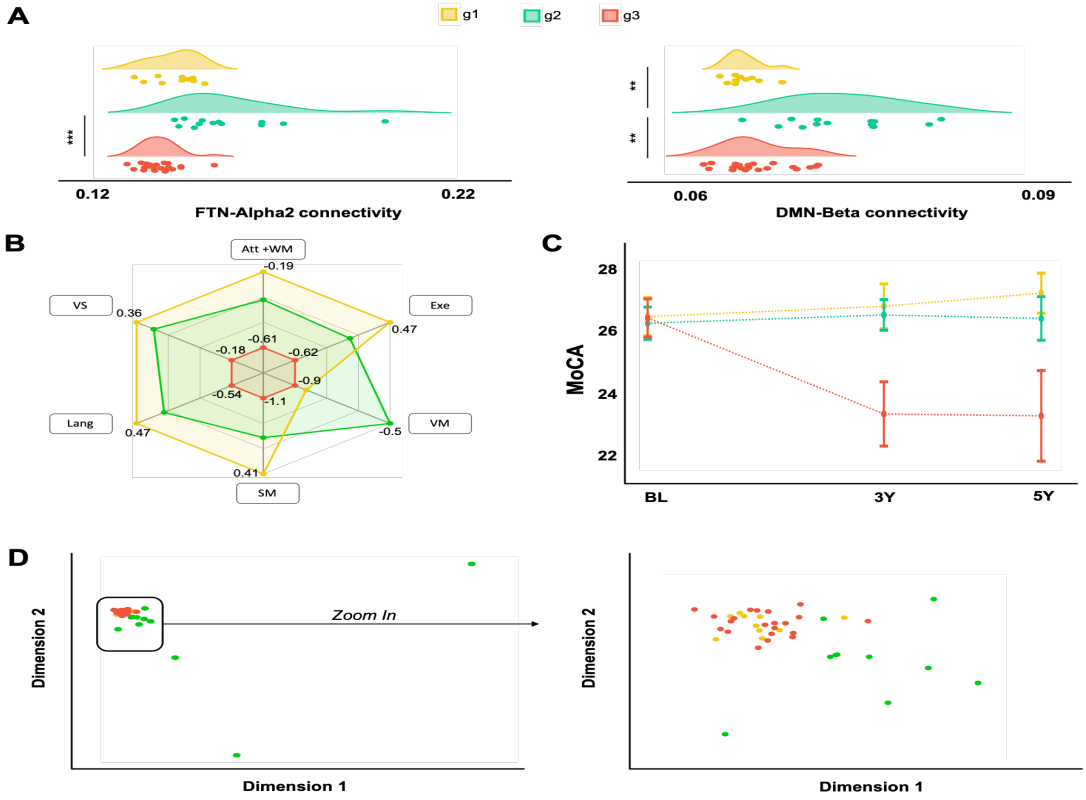

Figure S4- PD clustering using functional connectivity features. (A) Distribution of the average functional connectivity of the relevant brain networks (fronto-temporal network (FTN in alpha2 and the default mode network (DMN) in beta) between the three PD subtypes. **(B)** Spider plot of the average of the neuropsychological z-scores per cognitive domain (attention + working memory (att + WM), executive function (Exe), verbal memory (VM), semantic memory (SM), language (Lang) and visuo-spatial abilities (VS)) for the three subtypes. **(C)** Longitudinal progression in time of the global cognitive score MoCA. **(D)** Representation of the patients from each subtype along the first two

dimensions of the embedding space. Error bars represent the standard error and significant differences between subgroups are marked as * for $p<0.05$.

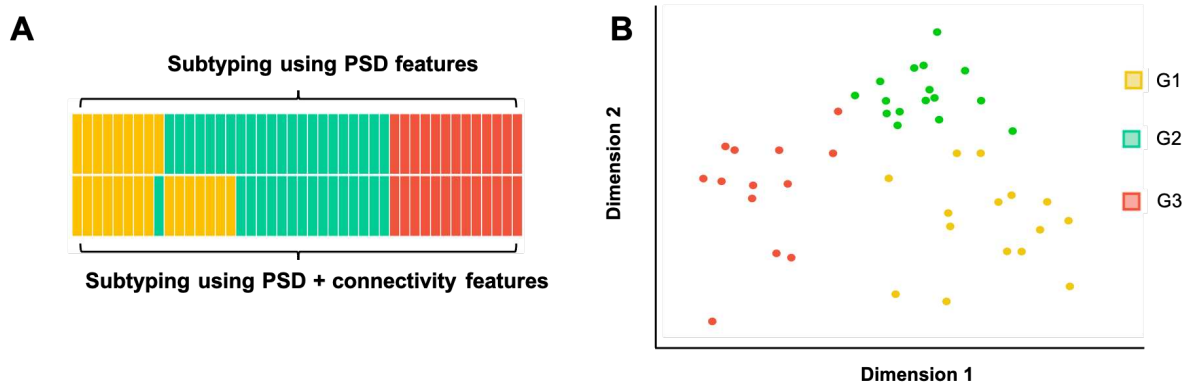

Figure S5- PD clustering using spectral power and functional connectivity features combined. (A) Common PD patients between subtypes issued from using only power spectral density (PSD) features and those issues of combining both PSD and connectivity features. **(B)** Representation of the patients from each subtype along the first two dimensions of the embedding space, PD subtypes are issued from applying clustering on both PSD and connectivity features.

Supplementary tables

Table S1- Demographic and clinical characteristics of the study cohort of PD patients at Baseline (BL) and at both follow-up examinations after 3-years (3Y) and 5-years (5Y) expressed as Mean (standard deviation). M/F: Male/Female, y: years, LPD: Left-affected PD, RPD: Right-affected PD, both: bilateral PD, UPDRS-III: Unified Parkinson's Disease Rating Scale motor experiences of daily living, UPDRS-III: Unified Parkinson's Disease Rating Scale motor examinations, LEDD: Levodopa Equivalent Daily Dose, MoCA: Montreal Cognitive Assessment, MMSE: Mini Mental State Examinations

		BL (N=42)	3Y (N=35)	5Y (N=44)
Study design	**Time between visits (y)**	-	3.1 (0.3)	5.2 (0.1)
Demographic	**Age (y)**	66.7 (8)	70.5 (8.2)	71.7 (7.8)
	Sex (M/F)	28/14	26/9	30/14
	Education (y)	15 (3)	15.2 (3.2)	15.1 (3.1)
Clinical	**Disease duration (y)**	4.5 (3.8)	7.1 (3.7)	10.4 (4.9)
	Disease side (LPD/RPD/both)	27/13/2	23/10/2	28/14/2
	UPDRS-II	5.9 (4.2)	10.5 (5.9)	9.6 (6.6)
	UPDRS-III	14 (10.5)	18.3 (9.9)	20.1 (13.1)
Medication	**LEDD (mg/day)**	646 (505)	692 (442)	633 (386)
Global cognition	**MoCA**	26.4 (2.3)	25.1 (3.8)	25.1 (5.1)
	MMSE	28.7 (1.4)	28.3 (2.6)	28.3 (1.9)

Table S2- Individual neuropsychological tests grouped into six different domains

Domain	Neuropsychological Tests
Attention and working memory	Test of Attentional Performance (TAP)-Alertness, reaction time without alerting sound
	Test of Attentional Performance (TAP)-Alertness, reaction time with alerting sound
	Corsi block correct forward
	Corsi block correct backward
	Digit span correct forward
	Digit span correct backward
Executive Function	Constructive Praxis test
	Trail Making test: time for part B/ time for part A
	Stroop test: interference index
	Wisconsin Card Sorting test: categories and errors
	Five Point test: correct, strategic and repeated answers
	Mosaik test
	Rey-Osterrieth Complex figure: copy, immediate recall, delayed recall
	Fluency test: Semantic and phonemic
Verbal and episodic memory	Basel Verbal Learning Test (BVLT): correct answers trial 1 to 5
	BVLT - SDCR: Short Delay Cued Recall
	BVLT - SDFR: Short Delay Free Recall
	BVLT - LDCR: Long Delay Cued Recall
	BVLT - LDFR: Long Delay Free Recall
Semantic Memory	Semantic fluency test: correct answers
Language	Boston Naming test: correct answers
	Fluency test: Semantic and phonemic
Visuo-Spatial abilities	Rey-Osterrieth Complex figure: copy, immediate recall, delayed recall
	Benton judgement of line Orientation test

Table S3- Affiliation of brain regions to the four brain networks activated at rest and mostly affected in Parkinson's disease

Brain networks	Brain regions
Somatomotor network (SMN)	Precentral gyrus (L/R)
	Paracentral lobule (L/R)
	Postcentral gyrus (L/R)
Default mode network (DMN)	Superior frontal gyrus (L/R)
	Cingulate gyrus (L/R)
	Precuneus (L/R)
	Inferior parietal lobule (L/R)
	Superior temporal gyrus, temporal pole (L/R)
Fronto-temporal network (FTN)	Orbito-frontal gyrus (L/R)
	Middle frontal gyrus (L/R)
	Inferior frontal gyrus (L/R)
	Superior temporal gyrus (L/R)
	Middle temporal gyrus (L/R)
	Posterior superior temporal sulcus (L/R)
Fronto-parietal network (FPN)	Middle frontal gyrus (L/R)
	Inferior frontal gyrus (L/R)
	Inferior parietal lobule (L/R)
	Insular lobule (L/R)

Table S4- Performances at the main neuropsychological tests in each domain for three identified subgroups of PD patients expressed as mean (standard deviation).

		G1 (N=9)	G2 (N=22)	G3 (N=13)	p-value	
Attention and working memory (Att_WM)	**Test of Attentional Performance - reaction time (ms)**	621 (172)	618 (110)	645 (68)	0.829	-
	Corsi Block forward	7.4 (1.7)	8.1 (1.5)	6.3 (2.1)	0.023	G2>G3
	Corsi Block backward	7.4 (1.6)	6.9 (1.2)	7.1 (2.3)	0.704	-
	Digit Span forward	7 (1.4)	7.8 (1.8)	6.9 (1.4)	0.289	-
	Digit Span backward	5.9 (1.9)	5.7 (1.9)	5.4 (1)	0.783	-
	Z-score Att_WM	-0.39 (0.73)	-0.32 (0.47)	-0.67 (0.45)	0.211	-
Executive Function (Exe_Fun)	**Constructive Praxis test**	7.9 (2.9)	9 (2.1)	6.7 (2.6)	0.051	-
	Trail Making Test B/A	3.1 (2.4)	2.5 (0.9)	3.5 (1.6)	0.196	-
	Stroop Test interference	2 (0.6)	1.8 (0.4)	2.4 (0.9)	0.033	G2>G3
	Wisconsin card sorting test	5.6 (1)	5.8 (0.5)	5.3 (1.2)	0.331	-
	Five Point Test-correct	27.3 (5.9)	26.4 (8.2)	20 (4.7)	0.043	G1, G2>G3
	Phonemic fluency-correct	15.4 (5.5)	13.1 (4.2)	13.8 (4.4)	0.431	-
	Mosaik test	25.2 (9.7)	25.9 (5.9)	18.6 (9.1)	0.048	G2>G3
	Z-score Exe_Fun	-0.14 (0.67)	0.13 (0.57)	-0.77 (1.3)	0.017	G2>G3
Verbal Memory (VM)	**BVLT-trial 1 to 5**	53.6 (14)	42.1 (10.3)	43.9 (19)	0.114	-
	BVLT-SDCR	12.7 (3.8)	10.5 (2.5)	9.3 (5.3)	0.133	-
	BVLT-SDFR	12.1 (3.6)	8.3 (3.8)	8.7 (7.4)	0.078	-
	BVLT-LDCR	13.2 (3.5)	10 (3)	9.9 (4.6)	0.062	-
	BVLT-LDFR	12.6 (4.4)	9.5 (3)	9.4 (5.1)	0.128	-
	Z-score VM	0.04 (1.2)	-0.97 (1.1)	-1.1 (1.7)	0.108	-
Semantic Memory (SM)	**Semantic Fluency**	22.9 (4.7)	19.5 (4.6)	17 (7.2)	0.061	-
	Z-score SM	-0.04 (1)	-0.39 (1)	-1 (1.5)	0.163	-
Language (Lang)	**Boston Naming Test**	14.7 (0.7)	14.4 (0.8)	12.7 (4.2)	0.081	-
	Z-score Lang	0.3 (0.8)	0 (0.77)	-0.55 (1.5)	0.169	-
Visuo-Spatial abilities (VS)	**BJLO Test**	27.1 (2.5)	27.9 (1.6)	28 (2.1)	0.533	-
	Rey Osterrieth Test	27.9 (6.2)	31 (4.7)	28.6 (4.7)	0.212	-
	Z-score VS	-0.22 (1.3)	0.34 (0.84)	-0.17 (1.1)	0.254	-

4.3. Study III- Electrophysiological signatures of anxiety in Parkinson's disease

Sahar Yassine, Sourour Almarouk, Ute Gschwandtner, Manon Auffret, Mahmoud Hassan, Marc Verin, Peter Fuhr.

To be submitted soon.

Electrophysiological signatures of anxiety in Parkinson's disease

Sahar Yassine[1,2,3,*] MSc, Sourour Almarouk[1,3,9,*] MSc, Ute Gschwandtner[4] MD, Manon Auffret[1,3,6,7,] PharmD, PhD, Mahmoud Hassan[3,8,10†] PhD, Marc Verin[1,3,5,6,†] MD, PhD, Peter Fuhr[4,†] MD

[1] Univ Rennes 1, LTSI - U1099, F-35000 Rennes, France

[2] NeuroKyma, F-35000 Rennes, France

[3] Behavior & Basal Ganglia, CIC1414, CIC-IT, CHU Rennes, Rennes, France

[4] Dept. of Neurology, Hospitals of the University of Basel, Basel, Switzerland

[5] Movement Disorders Unit, Neurology Department, Pontchaillou University Hospital, Rennes, France

[6] Institut des Neurosciences Cliniques de Rennes (INCR), Rennes, France

[7] France Développement Electronique, Monswiller, France

[8] School of Science and Engineering, Reykjavik University, Reykjavik, Iceland

[9] Neuroscience Research Centre, Lebanese University, Faculty of Medicine, Beirut, Lebanon

[10] MINDIG, F-35000, Rennes, France

[*,†] **These authors contributed equally to this work.**

Abstract

Anxiety is a common non-motor symptom in Parkinson's disease (PD) occurring in up to 31% of the patients and affecting their quality of life. Despite the high prevalence, anxiety symptoms in PD are often underdiagnosed and, therefore, undertreated. To date, functional and structural neuroimaging studies have contributed to our understanding of the motor and cognitive symptomatology of PD. Yet, the underlying pathophysiology of anxiety symptoms in PD remains largely unknown and studies on their neural correlates are missing. Here, we used resting state electroencephalography (RS-EEG) of 68 non-demented PD patients with or without clinically-defined anxiety and 25 healthy controls (HC) to assess spectral and functional connectivity fingerprints characterizing the PD-related anxiety. When comparing the brain activity of the PD anxious group (PD-A, N=18) to both PD non-anxious (PD-NA, N=50) and HC groups (N=25) at baseline, our results showed increased fronto-parietal delta power and decreased frontal beta power depicting the PD-A group. Results also revealed hyper-connectivity networks predominating in delta, theta and gamma bands against prominent hypo-connectivity networks in alpha and beta bands as network signatures of anxiety in PD where the frontal, temporal, limbic and insular lobes exhibited the majority of significant connections. Moreover, the revealed EEG-based electrophysiological signatures were strongly associated with the clinical scores of anxiety over the course of the disease. We believe that the identification of the electrophysiological correlates of anxiety in PD using EEG is conducive toward more accurate prognosis and diagnosis and can ultimately support the development of new therapeutics strategies.

Introduction

Anxiety is a highly prevalent psychiatric comorbidity in Parkinson's Disease (PD), affecting up to 31% of the patients[1], which is three times more prevalent than the general elderly population[2]. It can emerge at any stage of the disease, and be present even during the prodromal stage[3,4]. The clinical presentation of this disorder can include various subtypes [1,5,6] such as General Anxiety Disorder, non-episodic and episodic anxiety, panic attacks, social phobia, which can worsen motor symptoms [7–9] and cognitive functioning [10–13] and decrease the quality of life of patients[14,15]. Moreover, anxiety in PD comorbid often with other psychiatric symptoms such as depression and apathy [16,17], and the extensive overlap in their relevant features has hindered their clinical dissociation[18]. As a result, anxiety in PD is often underdiagnosed[1,19] and undertreated[20] yet limited scientific attention has been given to understand its underlying pathophysiology.

Non-invasive neuroimaging techniques are increasingly used to investigate the neural mechanisms of anxiety in PD[17,21]. Positron emission tomography (PET) and anatomical magnetic resonance imaging (MRI) studies have associated the anxiety in PD with reduced metabolism and cortical thickness in several subcortical regions including the amygdala, as well as in the bilateral anterior cingulate and prefrontal cortex[21–25]. Using fMRI resting state studies, functional disruptions in emotional-related cortical and subcortical regions were reported to correlate with anxiety symptoms[21,26–28].

Electroencephalography (EEG) has been growingly employed to uncover the neural correlates of complex neuropathologies, such as neuropsychiatric disorders[29,30]. Providing direct measures of the neural activity, EEG has proven to be a valuable, non-invasive and cost-effective tool for biomarkers development. To date, only one study has compared anxious and non-anxious PD patients using EEG, revealing frequency-related spectral and functional disruptions, mainly in the frontal cortex, that characterize the anxiety in PD[31]. Yet, the use of EEG in case-control longitudinal studies to assess the neural correlates of anxiety in PD is still missing.

Here, we used High-Density (HD)-EEG recordings to excerpt the electrophysiological signature of anxiety in PD by comparing the spectral patterns and functional networks of anxious PD patients (PD-A) to non-anxious PD patients (PD-NA) and healthy controls (HC). We quantified the spectral signature in terms of network signature in terms of lobes-interactions

and highest degree regions. We also explored the relationship between the EEG signatures at baseline and the clinical scores assessing anxiety at three and five years.

Materials and Methods

Participants

The study population, described in our previous studies[32,33], was composed of PD patients and healthy controls (HC) enrolled from the Movement Disorders Clinic of University Hospital of Basel (city of Basel, Switzerland) as a part of a longitudinal study approved by the local ethics committees (Ethikkommission beider Basel, Basel; Switzerland; EK 74/09). The diagnosis of PD was based on the United Kingdom Brain Bank criteria for idiopathic Parkinson's disease[34]. To be included in the study, patients had to meet specific criteria including a Mini-Mental State Examination (MMSE) score of 24 or above, no previous history of vascular or demyelinating brain disease, and sufficient proficiency in the German language. All participants provided written informed consent and were fully informed of the nature of the study. Included patients underwent neurological, neuropsychological, neuropsychiatric and EEG examinations at baseline (BL) and follow-up after a mean interval of 3 years (3Y) and 5 years (5Y).

As we focused on anxiety in PD, only participants that presented anxiety assessments were included in this study. Accordingly, 68 non-demented PD patients (22 females, age : 66.4 $\pm$ 8.3) and 25 HC (10 females, age: 66.4 $\pm$ 4) were selected at BL. As for the 3Y follow-up, the sample size was set to 42 PD patients (14 females, age: 70.5 $\pm$ 7.9) and 17 HC (9 females, age: 68.9 $\pm$ 6). Finally at 5Y, only 29 PD patients (12 females, age: 71 $\pm$ 7) and one healthy control presented anxiety assessments and were included only for the correlation analysis. A flowchart of the study (Figure S1) as well as the main demographic, clinical and neuropsychological characteristics of the main cohort (Tables S1) and analysis cohort (Table S2) are presented in the supplementary materials.

Neurological, neuropsychological and neuropsychiatric evaluations

Basic neurological and comprehensive neuropsychological examinations were carried out in all the participants. Patients were evaluated on their regular dopaminergic medication ("ON" state) and the use of antidepressant and anxiolytics treatments was reported. The global cognitive score was assessed using the Montreal cognitive assessment score[35] (MoCA), and patients were classified as with or without mild cognitive impairment (MCI) according to the Movement Society Task Force Level II criterias described in Litvan et al.[36]. Depression was

measured using the Beck Depressive Inventory, second edition[37] (BDI-II, German version) and apathy was assessed based on the Apathy Evaluation Scale[38] (AES, German version).
Anxiety symptoms were evaluated using the German version of the Beck Anxiety Inventory[39] (BAI), a 21 items self-rating scale. Each item is evaluated on a four-point Likert scale ranging from 0 to 3 (e.g., not at all; a little; moderate; or many). The total score ranges from 0 to 63 with higher scores representing increased symptoms severity. Leentjens et al.[40] have validated the use of BAI in PD. As a score higher than 13 has been identified to show clinically significant anxiety, this cut-off was considered to divide the PD patients into two groups: PD patients with clinically relevant anxiety PD-A (N=18) and PD patients without anxiety PD-NA (N=50).

EEG acquisition and preprocessing

Resting state EEG data were recorded for all participants using a HD-EEG system with 256 channels (Netstation 300, EGI, Inc., Eugene, OR). Participants were asked to relax, close their eyes and stay awake while seated in a comfortable chair for 12 minutes. The sampling rate was set to 1000 Hz. The raw EEG data were segmented into epochs of 40 seconds each and the first epoch of each recording was discarded from the analysis. As described in our previous study[32], epochs were preprocessed automatically using the open-source toolbox Automagic[41]. Briefly, signals are subjected to band-pass filtering between 1 and 45 Hz, followed by the electrooculography (EOG) regression on 17 frontal electrodes to eliminate ocular artifacts. This step reduces the final number of channels to 239 which are mapped to four lobes of interest: frontal, parietal, temporal and occipital (see Table S3 and Figure S2 of the supplementary materials). Subsequently, bad channels exhibiting high variance (higher than 20 μV) or amplitude exceeding ± 80 μV are identified and interpolated. Finally, the artefact-free epochs were sorted according to their quality metrics[32] and only the best six were retained for the rest of the analysis.

Power spectral analysis

The Welch method [42] was used to estimate the power spectrum of signals at the scalp level. It consisted of computing a modified periodogram using the Hamming window with 20 seconds duration and 50% overlap to obtain the absolute power spectral density (PSD). The relative power spectrum was then computed by normalising each value of the absolute power spectrum by the total sum of the powers at each frequency of the EEG broadband (1-45 Hz). A [239 x 45] relative power features at the scalp level were thus obtained and used for further analysis.

Functional connectivity analysis

The functional brain networks were estimated using the source-connectivity method[43]. First, the inverse problem was solved to reconstruct the dynamics of the cortical brain sources: the EEG channels and the MRI template (ICBM152) were co-registered, a realistic head-model was built using the OpenMEEG[44] toolbox, and the weighted Minimum Norm Estimate (wMNE) method[45] was applied on the cortical signals. The obtained source signals were then averaged into the 210 regions of interest (ROIs) of the brainnetome atlas[46], which are mapped into seven cortical lobes of interest: Prefrontal (PFC), Motor (Mot), Parietal (Par), Temporal (Tmp), Occipital (Occ), Limbic (Lmb) and insular (Ins). Their affiliation is presented in Table S4 of the supplementary materials. Afterwards, the phase synchrony between different ROIs was computed using the Phase Locking Value (PLV) method[47] and the dynamic functional connectivity matrices were estimated for six different EEG frequency bands: delta (1-4 Hz), theta (4-8 Hz), alpha1 (8-10 Hz), alpha2 (10-13 Hz), beta (13-30 Hz) and gamma (30-45 Hz). Those matrices were ultimately averaged across time and trials and their 21945 unique connections [=210 x 209/2] in each frequency band were used for further analysis.

Statistical analysis

The statistical differences in demographic and clinical characteristics between the PD-A, PD-NA and HC groups were examined using the one-way analysis of variance (ANOVA). The chi-square test (for the categorical variables) and the independent samples t-test (for the continuous variables) were applied to examine the difference between the PD-A and PD-NA groups. Covariates such as age, sex, education levels and variables that showed significant differences between groups were included in the subsequent analysis.

Our main objective was to compare EEG-based features of the PD-A group to both PD-NA and HC groups. To accomplish this three-group comparison, we employed a two-step statistical process. First, we used a permutation-based non-parametric analysis of covariance (Perm-ANCOVA) to examine statistical differences in the relative power spectrum [239 channels x 45 frequencies] and functional connectivity networks [21945 connections x 6 bands] of the three groups at BL. We used 1000 permutations to identify the first set of significant power/connectivity features ($p<0.05$). As we were interested in identifying the features that predominantly represent the PD-A group, we defined two conditions: the PD-A_{high} condition, where the power/connectivity values of the PD-A group were significantly higher than both the PD-NA and HC groups (PD-A > PD-NA & PD-A > HC), and the PD-A_{low} condition, where

the power/connectivity values of the PD-A groups were significantly lower than both other groups (PD-A < PD-NA & PD-NA < HC). Next, the second step of the process involved applying a two-tailed between-groups Wilcoxon test (corrected for multiple comparisons, $p<0.0167$) on the previous set of statistically significant features. Significant features that meet one of the above conditions were subsequently retained and considered as electrophysiological signatures of anxiety in PD.

Anxiety signature scores and correlation analysis

In order to quantify the electrophysiological signature of anxiety in PD, two separate signature scores were defined: the spectral signature score (SSS) and the network signature score (NSS). The SSS is delineated as the ratio between the power indexes (PI) of the two previously defined conditions: PD-A $_{\text{high}} \rightarrow PI_{\ high}$ and PD-A $_{\text{low}} \rightarrow PI_{\ low}$:

$$SSS = \frac{PI_{\ high}}{PI_{\ low}} \quad (1)$$

where PI is the mean relative power of the significant channels in the significant frequency slices and defined as:

$$PI = \frac{1}{Nslices} \sum_{i=1}^{chan} \sum_{j=1}^{freq} SigPower(i,j) * PSD_{rel}(i,j) \quad (2)$$

Where $SigPower$ is a [239 x 45] binary matrix obtained from the statistical analysis representing the significant channels and their corresponding frequency slices, PSD_{rel} is the [239 x 45] matrix of the relative power features, $chan$ is the total number of channels, $freq$ is the total number of examined frequencies and $Nslices$ is the total number of significant slices in $SigPower$.

Similarly, the NSS is defined as the ratio between the network indexes (NI) obtained from the significant edges of both conditions: PD-A $_{\text{high}} \rightarrow NI_{\ high}$ and PD-A $_{\text{low}} \rightarrow NI_{\ low}$:

$$NSS = \frac{NI_{\ high}}{NI_{\ low}} \quad (3)$$

where NI is the mean connectivity of the significant edges (connections) in all frequency bands:

$$NI = \frac{1}{Nconnections} \sum_{i=1}^{con} \sum_{j=1}^{band} SigNetwork(i,j) * W(i,j) \quad (4)$$

Where $SigNetwork$ is a [21945 x 6] binary matrix obtained from the statistical analysis representing the significant connectivity features in each frequency band, W is the [21945 x 6] matrix containing the functional connectivity features, con is the total number of unique

connections, $band$ is the total number of EEG frequency bands and $Nconnections$ is the total number of significant connections in $SigNetwork$.

A general mixed signature score (MSS) was also computed as the sum of the normalized SSS and NSS, representing thus both spectral and network signatures of anxiety in PD. Pearson's correlation was used to examine the relationship between the electrophysiological signature scores (SSS/ NSS/ MSS) and the clinical anxiety score (BAI) not only at BL but also at 3Y and 5Y to assess their prediction capacity.

Results

Participant's characteristics

Table 1 shows the demographic and clinical characteristics of the participants. No significant differences were found neither in the demographic features (age, sex and education) between all groups nor in the clinical assessments and the antiparkinsonian medication doses between the PD groups. Evidently, the BAI score was significantly discriminable between the three groups ($p<0.0001$). Also, both depression score (BDI-II) and apathy score (AES) presented a significant difference between groups ($p<0.001$) and significantly correlated with the BAI score. Therefore, they were both considered as covariates in the statistical analysis.

Table 1- Demographic and clinical characteristics of the three groups expressed as: mean (standard deviation). *PD-A: PD patients with anxiety, PD-NA: PD patients without anxiety, HC: healthy controls, y: years, M/F: Male/Female, MoCA: Montreal Cognitive Assessment, MCI (Y/N): Mild Cognitive Impairment (yes/no), LEDD: Levodopa Equivalent Daily Dose, BAI: Beck Anxiety Inventory score, BDI-II: Beck Depression Inventory, second edition score, AES: Apathy Evaluation Scale. Significant p-values are marked in bold.*

	PD-A (N=18)	**PD-NA (N=50)**	**HC (N=25)**	**P-value of ANOVA**	**P-value of t-test PD-A vs PD-NA**
Demographic					
Age (y)	65.7 (8)	66.6 (8.4)	66.6 (4)	0.89	0.68
Sex (M/F)	12/6	34/16	15/10	0.79	0.92
Education (y)	14.9 (3.7)	14.7 (3.1)	14.2 (2.9)	0.74	0.78
Clinical					
Disease duration (y)	4.9 (5.6)	5.3 (5.1)	-	-	0.79
MoCA (/30)	26 (2.8)	26 (2.3)	26.6 (2.7)	0.63	0.99
MCI (Y/N)	5/13	17/33	-	-	0.73
Medication					

LEDD[48] (mg/day)	616 (461)	664 (470)	-	-	0.71
Antidepressant (Y/N)	5/13	8/42	-	-	0.28
Anxiolytics (Y/N)	4/14	8/42	-	-	0.20
Neuropsychiatric tests					
BAI (/63)	20.3 (7.2)	6.2 (3.9)	2.4 (3.2)	**<0.0001**	**<0.0001**
BDI-II (/63)	11.2 (5.1)	6.4 (4.1)	2.6 (2.5)	**<0.0001**	**<0.001**
AES (/63)	17.5 (10)	6 (7)	1(4)	**<0.001**	0.29

Spectral signature of anxiety in PD

The average relative spectral power over all EEG channels for the three groups is illustrated in Figure 1-A. Our statistical analysis on the overall [239 x 45] spectral features at BL allowed us to identify the spectral signature of anxiety in PD. This includes the EEG channels with their corresponding frequency slices where the PD-A group has either significantly higher or significantly lower spectral power than both the PD-NA and HC groups (PD-A_{high} and PD-A_{low} conditions). For the PD-A_{high} condition, results showed 20 significant channels with corresponding frequency slices mainly within the delta band (between 1 and 4 Hz). Those channels were presented notably in the parietal and frontal lobes. As for the PD-A_{low} condition, 11 channels mainly located within the frontal lobe and presenting significant frequency slices between 13 and 25 Hz (within the beta band) were revealed (Figure 1-B). The cortical topography of the relative spectral power observed in each group for the relevant frequency slices (delta and beta bands) of both conditions, along with the spatial distribution of the corresponding significant channels are illustrated in Figure 1-C.

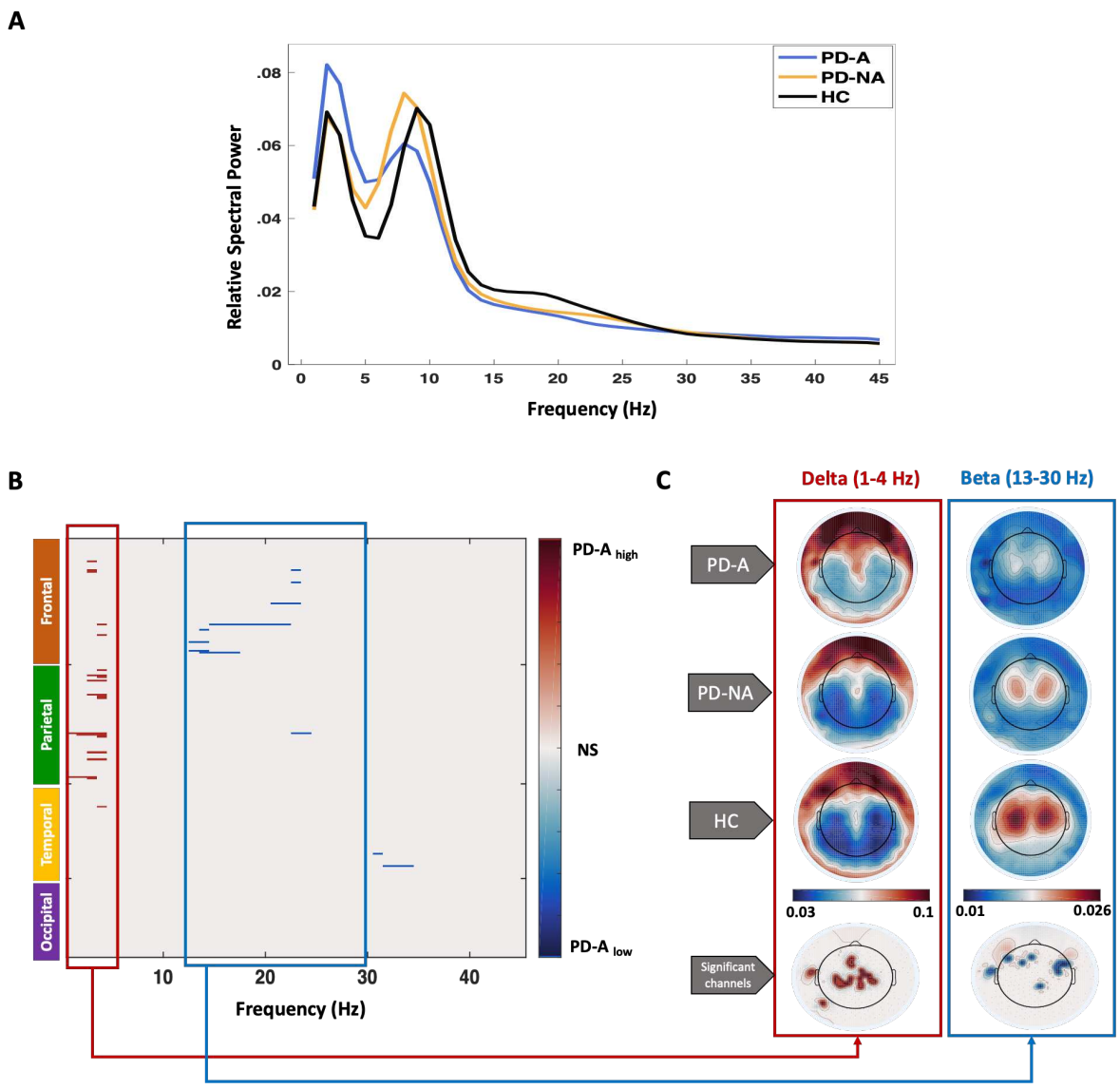

Figure 1- Spectral signature of anxiety in PD. A) *the relative power spectra of the three groups: PD patients with anxiety (PD-A) and without anxiety (PD-NA) and healthy controls (HC).* ***B)*** *Significant channels and frequency slices of the PD-A$_{high}$ (PD-A > PD-NA, HC) condition in red and PD-A$_{low}$ (PD-A< PD-NA, HC) condition in blue.* ***C)*** *Cortical topography of the relative spectral power of the relevant frequency bands (delta in PD-A$_{high}$ and beta in PD-A$_{low}$) for the three groups and the corresponding spatial distribution of the significant channels (significant channels are marked in red for delta band and in blue for beta band). NS: no-significance.*

Spectral signature score

In order to appraise the spectral signature of anxiety in PD and associate it with clinical scores, we computed the SSS as the ratio between the average power of the significant channels/slices of the PD-A$_{high}$ condition over the PD-A$_{low}$ condition. Consequently, this resulted in investigating the spectral ratio between delta and beta bands. Results showed that the SSS of the PD-A group was significantly higher than both the PD-NA and HC groups ($p<0.001$,

Bonferroni corrected, Figure 2-A). This SSS was significantly correlated with the BAI score (R=0.39, p<0.001) of the participants at BL (Figure 2-B). Additionally, when assessing the capacity of the SSS at BL in predicting the clinical scores of anxiety, results showed that the correlation remained significant with the BAI score at 3Y (R=0.41, p=0.011, Figure 2-C). A positive trend toward significance was also shown at 5Y (R=0.33, p=0.07, Figure 2-D).

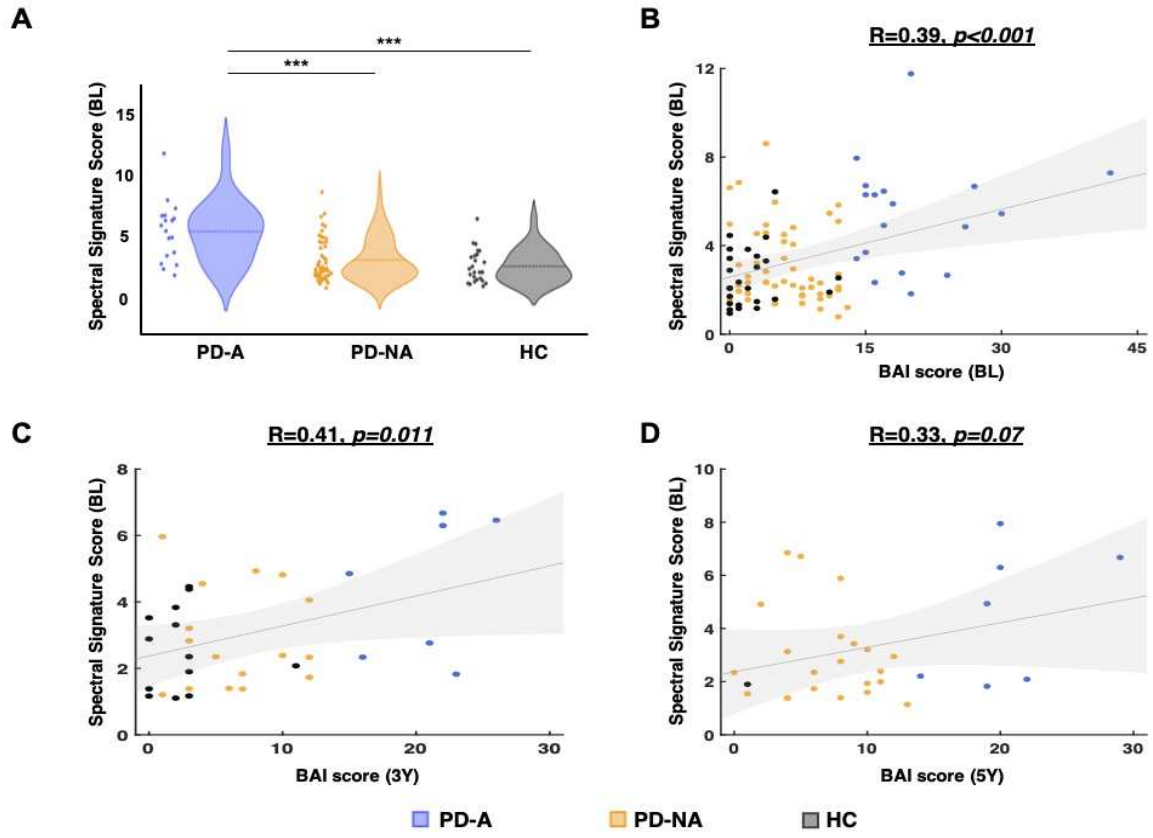

Figure 2- Spectral signature score (SSS) of anxiety in PD and its relationship with the BAI score. ***A)*** *Distribution of the SSS between the three groups: PD patients with anxiety (PD-A), without anxiety (PD-NA) and healthy controls (HC). Relationship between the SSS at BL and the BAI score:* ***B)*** *at BL,* ***C)*** *at 3Y,* ***D)*** *at 5Y. *** p<0.001 (Bonferroni corrected for multiple comparisons).*

Network signature of anxiety in PD

Owing to uncovering the network signature of anxiety in PD, we repeated the same statistical analysis described above on the 21945 unique functional connectivity features of the six examined frequency bands. This resulted in identifying for each frequency band, a significant network of both hyper-connectivity edges (PD-A_{high} condition: where the connectivity in PD-A is significantly higher than in PD-NA and HC) and hypo-connectivity edges (PD-A_{low} condition: where the connectivity in PD-A is significantly lower than in PD-NA and HC).

Results showed that hyper-connectivity networks characterizing the PD-A group were dominant in delta, theta and gamma bands, while hypo-connectivity networks were more prevalent in alpha and beta bands (Figure 3-A). Further investigation of brian regions with the most number of connections (highest degree regions) in these significant networks revealed that regions within the temporal lobes were present in almost all bands. In particular the middle temporal gyrus (MTG) appeared in theta, alpha2 and beta bands. Additionally, the inferior frontal gyrus (IFG) was featured in networks of higher frequencies (alpha2, beta and gamma). Regions within the salience network (SAN) were among the most prevalent in theta (the caudodorsal region of the anterior cingulate gyrus (CG-cd)), alpha1 and gamma (the insula (INS)) (Figure 3-B).

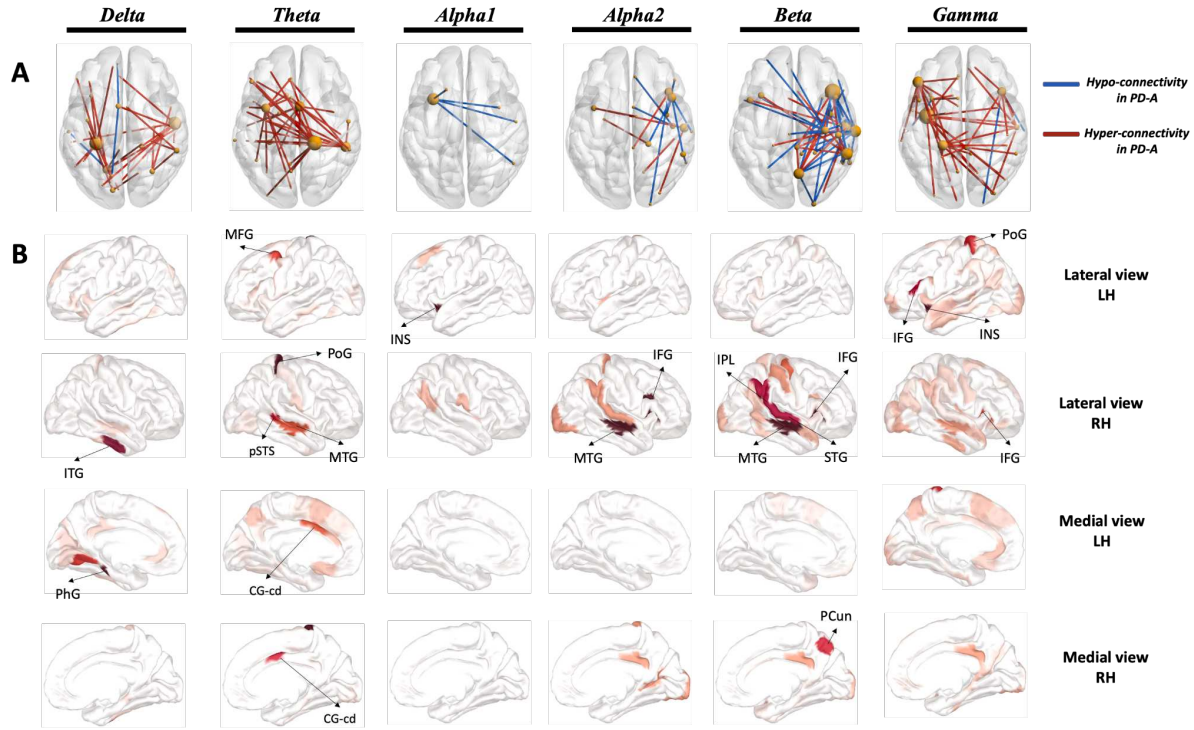

Figure 3- Network signature of anxiety in patients with PD. A) *Significant networks of the different investigated frequency bands. The networks were thresholded for visualisation purposes. Edges presenting hyper-connectivity in PD-A are illustrated in red (PD-A_{high}) and those presenting hypo-connectivity in PD-A are illustrated in blue (PD-A_{low}).* ***B)*** *Highest degree regions (thresholded for visualisation purposes) represented with different views (lateral and medial) of the left hemisphere (LH) and right hemisphere (RH). ITG: Inferior Temporal Gyrus, PhG: Parahippocampal Gyrus, MFG: Middle Frontal Gyrus, PoG: Postcentral Gyrus, pSTS: posterior Superior Temporal Sulcus, MTG: Medial Temporal Gyrus, CG-cd: Cingulate Gyrus caudodorsal region, INS: Insula, IFG: Inferior Frontal Gyrus, IPL: Inferior Parietal Lobule, STG: Superior Temporal Gyrus, PCun: Precuneus.*

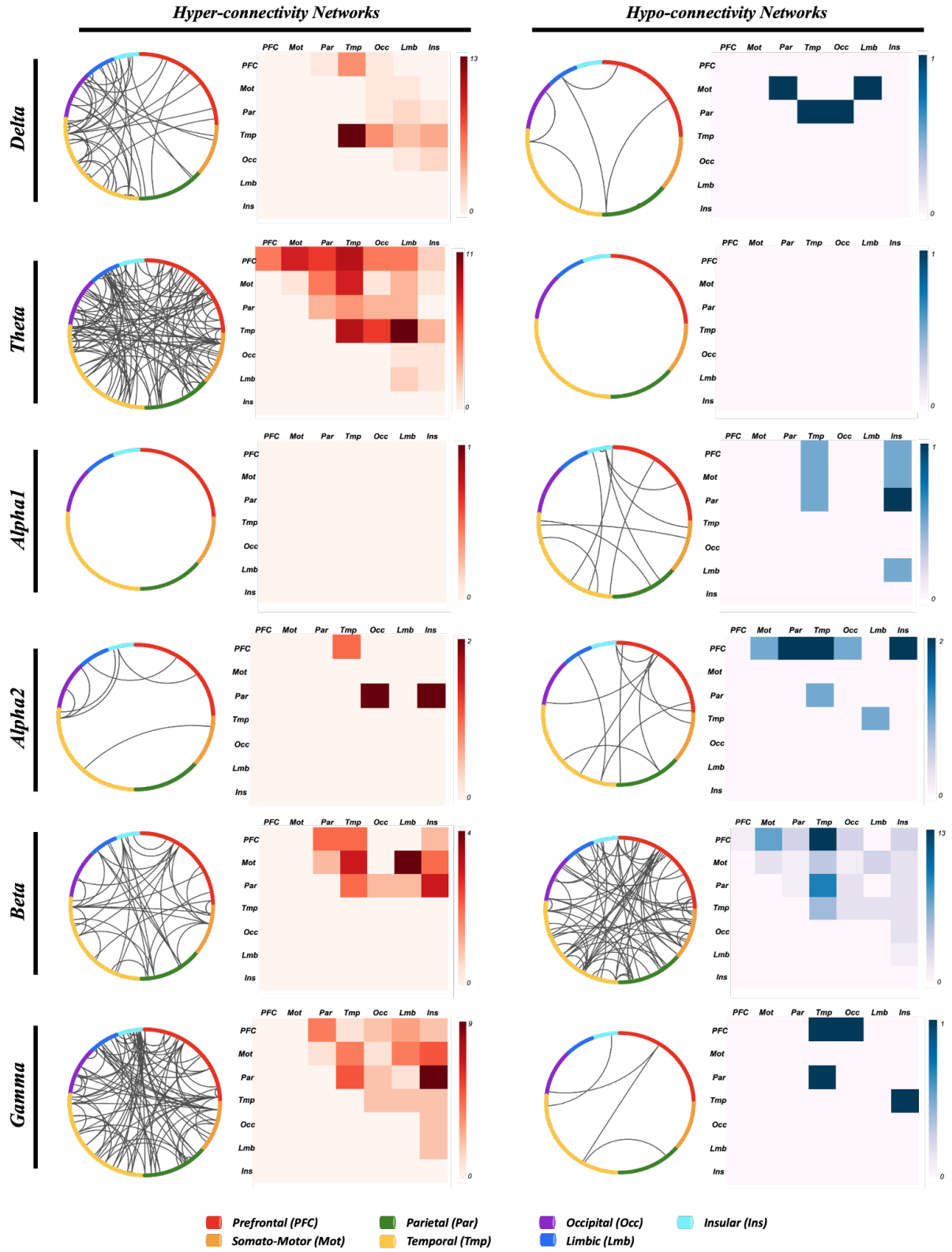

Figure 4- Representation of the network signature of anxiety in patients with PD. *Circular plots (left) and matrix plot (right) of the significant networks Delta, Theta, Alpha1, Alpha2, Beta and Gamma frequency bands. Red and blue shades represent the number of connections in the hyper-connectivity networks and hypo-connectivity networks respectively.*

Upon examining the interactions between the cortical lobes within these networks, we observed that the hyper-connectivity networks displayed dense functional connections primarily between the temporal, limbic and insular lobes. Specifically, the most prominent connections were temporo-temporal in delta, temporo-limbic in theta, motor-limbic in beta and insular-parietal in gamma bands. Regarding the hypo-connectivity networks, the insular lobe exhibited denser connections in the alpha band, with insular-parietal connections being the most dominant in alpha1 and insular-frontal connections prevailing in alpha2. Additionally, fronto-temporal hypo-connections were prevalent in beta bands. To illustrate these findings, circular and matrix plots displaying the interaction between the lobes of interest in the hypo/hyper connectivity networks across all bands are illustrated in Figure 4.

Network signature score

Following the analysis of the spectral signature, we also investigated the association between the network signature score (NSS) and the clinical evaluation of anxiety. This score represents the ratio between the average connectivity of the hyper-connectivity edges and that of the hypo-connectivity edges in all frequency bands. Results showed that this NSS was significantly higher in the PD-A group compared to both PD-NA and HC groups ($p<0.001$, Bonferroni corrected, Figure 5-A). The NSS at BL showed a strong correlation with the BAI score not only at BL ($R=0.61$, $p<10^{-10}$, Figure 5-B) but also at 3Y ($R=0.77$, $p<10^{-7}$, Figure 5-C). A positive trend toward significance was also shown after 5Y ($R=0.33$, $p=0.07$, Figure 5-D) demonstrating notable predictive ability.

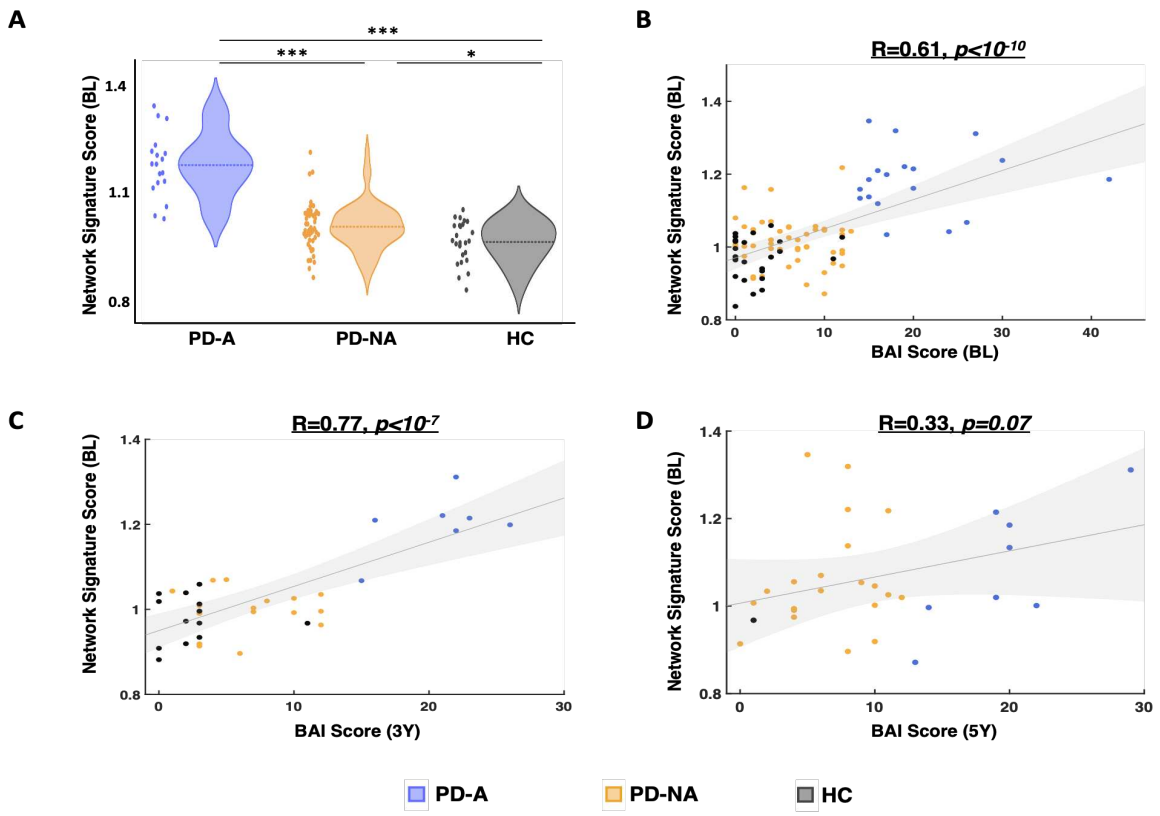

Figure 5- Network signature score (NSS) of anxiety in PD and its relationship with the BAI score. ***A)*** *Distribution of the NSS between the three groups: PD patients with anxiety (PD-A), without anxiety (PD-NA) and healthy controls (HC). Relationship between the NSS at BL and BAI score:* ***B)*** *at BL,* ***C)*** *at 3Y,* ***D)*** *at 5Y. *** p<0.001, ** p<0.01, * p<0.05 (p-values are corrected using Bonferroni for multiple comparisons).*

General mixed signature score

The general mixed signature score, which combines both spectral and network signatures of anxiety in PD, demonstrated significant differences between the PD-A group and both PD-NA and HC groups ($p<0.001$, Bonferroni corrected, Figure 6-A). When examining its correlation with the clinical score of anxiety, the results showed that the MSS was strongly correlated with the BAI score not only at BL ($R=0.52$, $p<10^{-6}$, Figure 6-B) but also at both follow-up examinations after 3Y ($R=0.61$, $p<10^{-4}$, Figure 6-C) and 5Y ($R=0.37$, $p<0.05$, Figure 6-D).

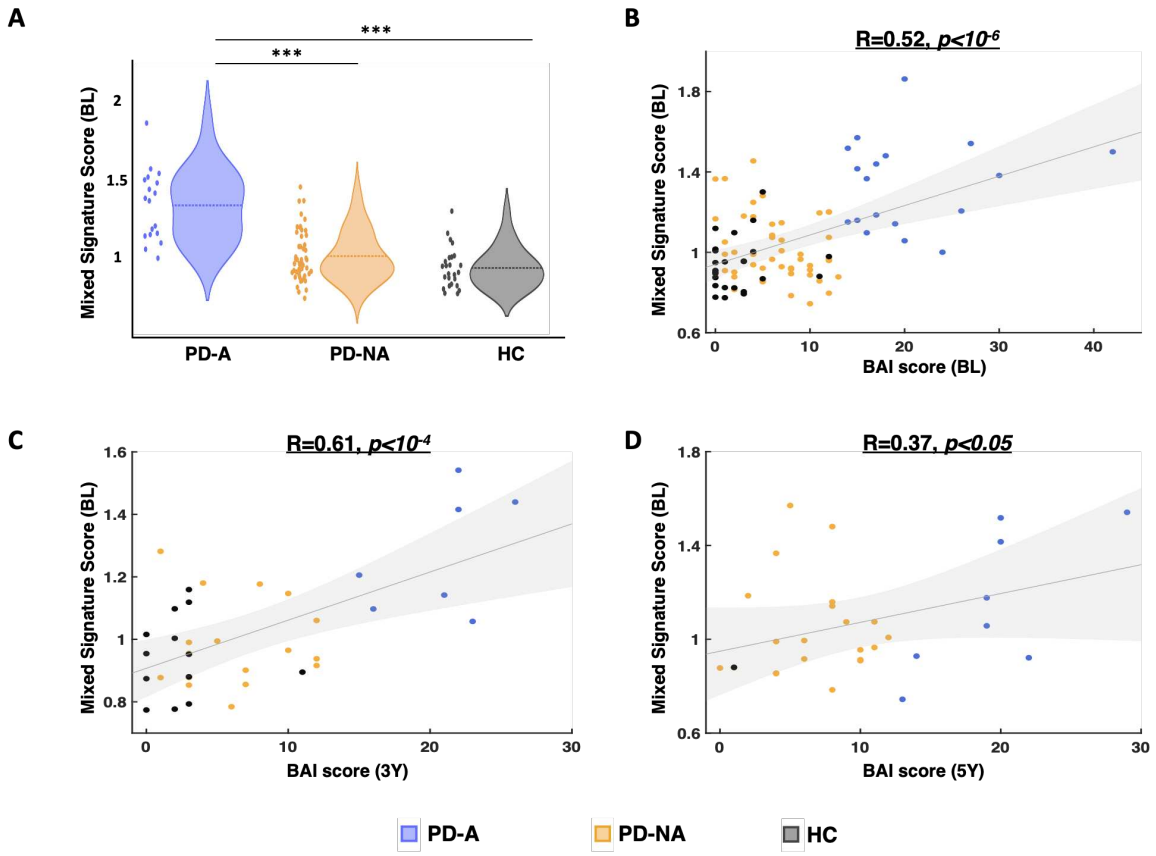

Figure 6- The general mixed signature score of anxiety in PD and its relationship with the BAI score. A) *Distribution of the mixed signature score between the three groups: PD patients with anxiety (PD-A), without anxiety (PD-NA) and healthy controls (HC). Relationship between the mixed signature score at BL and BAI score:* ***B)*** *at BL,* ***C)*** *at 3Y,* ***D)*** *at 5Y. *** $p<0.001$ (p-values are corrected using Bonferroni for multiple comparisons).*

Discussion

In the present study, we aimed to identify the electrophysiological signatures of PD-related anxiety using resting state HD-EEG. While controlling the presence of other neuropsychiatric symptoms (depression and apathy), we showed that anxiety in PD is characterized by increased delta power -at the scalp level- in the frontal and parietal lobes as well as reduced beta power in the frontal lobe. Our functional connectivity analysis revealed that hyper-connectivity networks dominate in delta, theta and gamma bands while hypo-connectivity networks are more present in alpha and beta bands, with the frontal, temporal, limbic and insular lobes exhibiting the majority of significant connections. Electrophysiological scores (SSS/ NSS/ MSS) computed from the spectral/network signatures distinguish the PD-A group from both PD-NA and HC groups and are correlated with the clinical scores of anxiety at BL as well as at 3Y and 5Y, demonstrating predictive capacity.

Our spectral analysis at the channel-frequency level allowed for an accurate spatial-spectral mapping of the power features that characterize the PD-A group compared to both the PD-NA and HC groups. The increased power in delta and decreased power in low beta (13-20 Hz) are consistent with the global spectral patterns observed in the single previous EEG study that compared PD-A and PD-NA patients[31]. Our findings were also consistent with spectral patterns observed in anxious non-parkinsonian subjects. Increased delta power in frontal and parietal lobes was reported to characterize induced anxiety in obsessive compulsive-disorder patients[49]. Negative correlation between the powers of delta and beta bands in frontal regions was also shown in highly anxious healthy females performing a social task[50]. In addition, decreases in absolute and relative powers of slow and fast beta were observed in anxious adolescents[51] and in patients with social phobia[52]. Nonetheless, positive delta-beta correlations and decreases in delta power have been also reported in social anxiety disorders but in studies with low-density EEG systems [52,53]. Spatially, the frontal lobe was the most featured in our PD-anxiety spectral signature. Of interest, disruptions in the prefrontal cortex were consistently reported in neuroimaging studies, characterizing anxiety disorders not only in PD patients [22,23,25,26,31] but also in non-PD individuals [50,52,54].

Regarding the network signature of PD-related anxiety, we have demonstrated that hyper-connectivity networks were mostly dominant in delta, theta and gamma bands. Previous functional connectivity studies have associated increased severity of anxiety in PD patients with increased functional connectivity between cortical regions of the orbito-frontal cortex and both the inferior-middle temporal and parahippocampal gyri[28] as well as between the insular lobe and both the prefrontal, and cingulate cortices[31]. These findings support the manifestation of the insula, the caudodorsal region of the cingulate gyrus, and the regions within the temporal and frontal lobes as well as their interactions as the most implicated in the hyper-connectivity networks of our results. Indeed, the insula along with the dorsal anterior cingulate (limbic) cortex and the medial prefrontal cortex are all parts of the fear/anxiety circuitry[55] and activations and abnormalities in those regions have been consistently reported in different types of anxiety disorders in the general population [56–59] and in PD subjects[21,25,31]. This can be interpreted by the pivotal role of these core regions in processing fear, negative affect, worrisome thoughts and emotions [60–62]. Additionally, hyperconnectivity between subcortical regions, mainly the amygdala and the putamen, and cortical regions of the fear/anxiety circuitry were also persistently associated with anxiety in PD[21,28,63]. While our analysis included only cortical regions, the dominance of the hyperconnectivity networks suggests a positive cortical-subcortical correlation between oscillations that stem from these regions.

Furthermore, we observed hypo-connectivity networks in alpha and beta bands, predominantly in the frontal and insular lobes. Consistent with our findings, previous research has shown that patterns of decreased connectivity within the frontal lobe are indicative of anxiety in PD patients [25,28]. Moreover, functional dysconnectivity within and between the salience network, which involves mainly the insular lobe, has also been reported to reflect anxiety disorders in non-PD individuals[57,64–66].

Importantly, our hypo/hyper-connectivity networks were also shown to be associated with the clinical traits of anxiety in all participants not only at baseline but also longitudinally after 3 years and 5 years. This association, validated also when combining both spectral and network signatures, can highlight the predictive capacity of our EEG-based markers of anxiety. However, despite this internal/longitudinal validation of our anxiety signature, external validation on an independent cohort is necessary for further endorsement.

Finally, some patients in both PD-A and PD-NA groups were under antidepressant and anxiolytic medications during EEG and neuropsychological assessments sessions. Here, we controlled for this issue by demonstrating that the anxiety and depression medication statuses did not differ significantly between PD groups. Besides, topographic EEG changes reported in generalized anxiety disorders during anxiety treatments[67,68] suggested decreased spectral power of delta and alpha bands along with increased power of beta band[69–71]. Antidepressant medication[72] has also been shown to reduce slow wave EEG activity and increase the power in alpha band[73,74]. Notably, these spectral patterns were not reported in our study to characterize the PD-A group, which included patients taking anxiolytics and antidepressants. Excluding these patients would have been an alternative solution in this study, however this would have reduced the sample size in the PD-A group by half and subsequently restricted our statistical analysis. Therefore, further research studying the neural correlates of anxiety in PD patients without anxiety/depression medications is still necessary for further validation.

Conclusion

To summarize, this is the first case-control resting-state HD-EEG study to investigate the neural correlates of anxiety in PD. Our findings suggest that increased fronto-parietal delta power, decreased frontal beta power, and prevailed hyperconnectivity in several frequency bands are all EEG-based signatures of the PD-related anxiety. These signatures have the longitudinal predictive capacity for clinical outcomes. Identifiying such non-invasive markers may provide new perceptions into the development of advanced biomarkers. Further research

could also establish resting-satte HD-EEG as a tool for more accurate prognosis and diagnosis of anxiety in PD and contribute in elevating the development of corresponding effective therapies.

References

1. Broen, M. P. G., Narayen, N. E., Kuijf, M. L., Dissanayaka, N. N. W. & Leentjens, A. F. G. Prevalence of anxiety in Parkinson's disease: A systematic review and meta-analysis. *Mov. Disord.* **31**, 1125–1133 (2016).
2. Reynolds, K., Pietrzak, R. H., El-Gabalawy, R., Mackenzie, C. S. & Sareen, J. Prevalence of psychiatric disorders in U.S. older adults: findings from a nationally representative survey. *World Psychiatry Off. J. World Psychiatr. Assoc. WPA* **14**, 74–81 (2015).
3. Shiba, M. *et al.* Anxiety disorders and depressive disorders preceding Parkinson's disease: A case-control study. *Mov. Disord.* **15**, 669–677 (2000).
4. Ishihara, L. & Brayne, C. A systematic review of depression and mental illness preceding Parkinson's disease. *Acta Neurol. Scand.* **113**, 211–220 (2006).
5. Dissanayaka, N. N. N. W. *et al.* The clinical spectrum of anxiety in Parkinson's disease. *Mov. Disord.* **29**, 967–975 (2014).
6. Aarsland, D., Marsh, L. & Schrag, A. Neuropsychiatric symptoms in Parkinson's disease. *Mov. Disord.* **24**, 2175–2186 (2009).
7. Siemers, E. R., Shekhar, A., Quaid, K. & Dickson, H. Anxiety and motor performance in parkinson's disease. *Mov. Disord.* **8**, 501–506 (1993).
8. Coakeley, S., Martens, K. E. & Almeida, Q. J. Management of anxiety and motor symptoms in Parkinson's disease. *Expert Rev. Neurother.* **14**, 937–946 (2014).
9. Pirogovsky-Turk, E. *et al.* Neuropsychiatric Predictors of Cognitive Decline in Parkinson Disease: A Longitudinal Study. *Am. J. Geriatr. Psychiatry* **25**, 279–289 (2017).
10. Dissanayaka, N. N. W. *et al.* Anxiety is associated with cognitive impairment in newly-diagnosed Parkinson's disease. *Parkinsonism Relat. Disord.* **36**, 63–68 (2017).
11. Reynolds, G. O., Hanna, K. K., Neargarder, S. & Cronin-Golomb, A. The relation of anxiety and cognition in Parkinson's disease. *Neuropsychology* **31**, 596–604 (2017).
12. Ehgoetz Martens, K. A., Silveira, C. R. A., Intzandt, B. N. & Almeida, Q. J. State anxiety predicts cognitive performance in patients with Parkinson's disease. *Neuropsychology* **32**, 950–957 (2018).
13. Toloraia, K. *et al.* Anxiety, Depression, and Apathy as Predictors of Cognitive Decline in Patients With Parkinson's Disease-A Three-Year Follow-Up Study. *Front. Neurol.* **13**, 792830 (2022).
14. Dissanayaka, N. N. W. *et al.* Anxiety disorders in Parkinson's disease: Prevalence and risk factors. *Mov. Disord.* **25**, 838–845 (2010).

15. Hanna, K. K. & Cronin-Golomb, A. Impact of Anxiety on Quality of Life in Parkinson's Disease. *Park. Dis.* **2012**, e640707 (2011).
16. Rutten, S. *et al.* Anxiety in Parkinson's disease: Symptom dimensions and overlap with depression and autonomic failure. *Parkinsonism Relat. Disord.* **21**, 189–193 (2015).
17. Wen, M.-C., Chan, L. L., Tan, L. C. S. & Tan, E. K. Depression, anxiety, and apathy in Parkinson's disease: insights from neuroimaging studies. *Eur. J. Neurol.* **23**, 1001–1019 (2016).
18. Broen, M. P. G. *et al.* Clinical Markers of Anxiety Subtypes in Parkinson Disease. *J. Geriatr. Psychiatry Neurol.* **31**, 55–62 (2018).
19. Abraham, D. S. *et al.* Sex Differences in Parkinson's Disease Presentation and Progression. *Parkinsonism Relat. Disord.* **69**, 48–54 (2019).
20. Pontone, G. M. *et al.* Report from a multidisciplinary meeting on anxiety as a non-motor manifestation of Parkinson's disease. *Npj Park. Dis.* **5**, 1–9 (2019).
21. Carey, G. *et al.* Anxiety in Parkinson's disease is associated with changes in the brain fear circuit. *Parkinsonism Relat. Disord.* **80**, 89–97 (2020).
22. Wang, X. *et al.* Cerebral metabolic change in Parkinson's disease patients with anxiety: A FDG-PET study. *Neurosci. Lett.* **653**, 202–207 (2017).
23. Wee, N. *et al.* Neural correlates of anxiety symptoms in mild Parkinson's disease: A prospective longitudinal voxel-based morphometry study. *J. Neurol. Sci.* **371**, 131–136 (2016).
24. Oosterwijk, C. S., Vriend, C., Berendse, H. W., van der Werf, Y. D. & van den Heuvel, O. A. Anxiety in Parkinson's disease is associated with reduced structural covariance of the striatum. *J. Affect. Disord.* **240**, 113–120 (2018).
25. Carey, G. *et al.* Neuroimaging of Anxiety in Parkinson's Disease: A Systematic Review. *Mov. Disord.* **36**, 327–339 (2021).
26. Criaud, M. *et al.* Anxiety in Parkinson's disease: Abnormal resting activity and connectivity. *Brain Res.* **1753**, 147235 (2021).
27. Wang, X. *et al.* Alterations of the amplitude of low-frequency fluctuations in anxiety in Parkinson's disease. *Neurosci. Lett.* **668**, 19–23 (2018).
28. Dan, R. *et al.* Separate neural representations of depression, anxiety and apathy in Parkinson's disease. *Sci. Rep.* **7**, 12164 (2017).
29. Newson, J. J. & Thiagarajan, T. C. EEG Frequency Bands in Psychiatric Disorders: A Review of Resting State Studies. *Front. Hum. Neurosci.* **12**, (2019).
30. Livint Popa, L., Dragos, H., Pantelemon, C., Verisezan Rosu, O. & Strilciuc, S. The

Role of Quantitative EEG in the Diagnosis of Neuropsychiatric Disorders. *J. Med. Life* **13**, 8–15 (2020).

31. Betrouni, N. *et al.* Anxiety in Parkinson's disease: A resting-state high density EEG study. *Neurophysiol. Clin.* **52**, 202–211 (2022).
32. Yassine, S. *et al.* Functional Brain Dysconnectivity in Parkinson's Disease: A 5-Year Longitudinal Study. *Mov. Disord. Off. J. Mov. Disord. Soc.* (2022) doi:10.1002/mds.29026.
33. Chaturvedi, M. *et al.* Phase lag index and spectral power as QEEG features for identification of patients with mild cognitive impairment in Parkinson's disease. *Clin. Neurophysiol.* **130**, 1937–1944 (2019).
34. Hughes, A. J., Daniel, S. E., Kilford, L. & Lees, A. J. Accuracy of clinical diagnosis of idiopathic Parkinson's disease: a clinico-pathological study of 100 cases. *J. Neurol. Neurosurg. Psychiatry* **55**, 181–184 (1992).
35. Nasreddine, Z. S. *et al.* The Montreal Cognitive Assessment, MoCA: A Brief Screening Tool For Mild Cognitive Impairment. *J. Am. Geriatr. Soc.* **53**, 695–699 (2005).
36. Litvan, I. *et al.* Diagnostic criteria for mild cognitive impairment in Parkinson's disease: Movement Disorder Society Task Force guidelines. *Mov. Disord. Off. J. Mov. Disord. Soc.* **27**, 349–356 (2012).
37. Beck, A. T., Ward, C. H., Mendelson, M., Mock, J. & Erbaugh, J. An inventory for measuring depression. *Arch. Gen. Psychiatry* **4**, 561–571 (1961).
38. Lueken, U. *et al.* [Psychometric properties of a German version of the Apathy Evaluation Scale]. *Fortschr. Neurol. Psychiatr.* **74**, 714–722 (2006).
39. Beck, A. T., Epstein, N., Brown, G. & Steer, R. A. An inventory for measuring clinical anxiety: Psychometric properties. *J. Consult. Clin. Psychol.* **56**, 893–897 (1988).
40. Leentjens, A. F. G. *et al.* Anxiety rating scales in Parkinson's disease: a validation study of the Hamilton anxiety rating scale, the Beck anxiety inventory, and the hospital anxiety and depression scale. *Mov. Disord. Off. J. Mov. Disord. Soc.* **26**, 407–415 (2011).
41. Pedroni, A., Bahreini, A. & Langer, N. Automagic: Standardized preprocessing of big EEG data. *NeuroImage* **200**, 460–473 (2019).
42. Welch, P. The use of fast Fourier transform for the estimation of power spectra: A method based on time averaging over short, modified periodograms. *IEEE Trans. Audio Electroacoustics* **15**, 70–73 (1967).
43. Hassan, M. & Wendling, F. Electroencephalography Source Connectivity: Aiming for High Resolution of Brain Networks in Time and Space. *IEEE Signal Process. Mag.* **35**,

81–96 (2018).

44. Gramfort, A., Papadopoulo, T., Olivi, E. & Clerc, M. OpenMEEG: opensource software for quasistatic bioelectromagnetics. *Biomed. Eng. OnLine* **9**, 45 (2010).

45. Hämäläinen, M. S. & Ilmoniemi, R. J. Interpreting magnetic fields of the brain: minimum norm estimates. *Med. Biol. Eng. Comput.* **32**, 35–42 (1994).

46. Fan, L. *et al.* The Human Brainnetome Atlas: A New Brain Atlas Based on Connectional Architecture. *Cereb. Cortex* **26**, 3508–3526 (2016).

47. Lachaux, J.-P., Rodriguez, E., Martinerie, J. & Varela, F. J. Measuring phase synchrony in brain signals. *Hum. Brain Mapp.* **8**, 194–208 (1999).

48. Tomlinson, C. L. *et al.* Systematic review of levodopa dose equivalency reporting in Parkinson's disease. *Mov. Disord. Off. J. Mov. Disord. Soc.* **25**, 2649–2653 (2010).

49. Kamaradova, D. *et al.* EEG correlates of induced anxiety in obsessive–compulsive patients: comparison of autobiographical and general anxiety scenarios. *Neuropsychiatr. Dis. Treat.* **14**, 2165–2174 (2018).

50. Harrewijn, A., Van der Molen, M. J. W. & Westenberg, P. M. Putative EEG measures of social anxiety: Comparing frontal alpha asymmetry and delta–beta cross-frequency correlation. *Cogn. Affect. Behav. Neurosci.* **16**, 1086–1098 (2016).

51. Éismont, E., Aliyeva, T., Lutsyuk, N. & Pavlenko, V. EEG Correlates of Different Types of Anxiety in 14- to 15YearOld Teenagers. *Neurophysiology* **40**, 377–384 (2008).

52. Sachs, G., Anderer, P., Dantendorfer, K. & Saletu, B. EEG mapping in patients with social phobia. *Psychiatry Res. Neuroimaging* **131**, 237–247 (2004).

53. Miskovic, V. *et al.* Frontal brain oscillations and social anxiety: A cross-frequency spectral analysis during baseline and speech anticipation. *Biol. Psychol.* **83**, 125–132 (2010).

54. Engel, K., Bandelow, B., Gruber, O. & Wedekind, D. Neuroimaging in anxiety disorders. *J. Neural Transm.* **116**, 703–716 (2009).

55. Shin, L. M. & Liberzon, I. The Neurocircuitry of Fear, Stress, and Anxiety Disorders. *Neuropsychopharmacology* **35**, 169–191 (2010).

56. Northoff, G. Anxiety Disorders and the Brain's Resting State Networks: From Altered Spatiotemporal Synchronization to Psychopathological Symptoms. *Adv. Exp. Med. Biol.* **1191**, 71–90 (2020).

57. MacNamara, A., DiGangi, J. & Phan, K. L. Aberrant Spontaneous and Task-Dependent Functional Connections in the Anxious Brain. *Biol. Psychiatry Cogn. Neurosci. Neuroimaging* **1**, 278–287 (2016).

58. Kim, Y.-K. & Yoon, H.-K. Common and distinct brain networks underlying panic and social anxiety disorders. *Prog. Neuropsychopharmacol. Biol. Psychiatry* **80**, 115–122 (2018).
59. Sylvester, C. M. *et al.* Functional network dysfunction in anxiety and anxiety disorders. *Trends Neurosci.* **35**, 527–535 (2012).
60. Shackman, A. J. *et al.* The integration of negative affect, pain and cognitive control in the cingulate cortex. *Nat. Rev. Neurosci.* **12**, 154–167 (2011).
61. Paulus, M. P. & Stein, M. B. An Insular View of Anxiety. *Biol. Psychiatry* **60**, 383–387 (2006).
62. Stein, M. B., Simmons, A. N., Feinstein, J. S. & Paulus, M. P. Increased Amygdala and Insula Activation During Emotion Processing in Anxiety-Prone Subjects. *Am. J. Psychiatry* **164**, 318–327 (2007).
63. Wang, X. *et al.* Altered putamen functional connectivity is associated with anxiety disorder in Parkinson's disease. *Oncotarget* **8**, 81377–81386 (2017).
64. Massullo, C. *et al.* Dysregulated brain salience within a triple network model in high trait anxiety individuals: A pilot EEG functional connectivity study. *Int. J. Psychophysiol.* **157**, 61–69 (2020).
65. Li, R. *et al.* Dissociable salience and default mode network modulation in generalized anxiety disorder: a connectome-wide association study. *Cereb. Cortex* bhac509 (2023) doi:10.1093/cercor/bhac509.
66. Geng, H., Li, X., Chen, J., Li, X. & Gu, R. Decreased Intra- and Inter-Salience Network Functional Connectivity is Related to Trait Anxiety in Adolescents. *Front. Behav. Neurosci.* **9**, 350 (2016).
67. Sawada, H. *et al.* Pharmacological interventions for anxiety in Parkinson's disease sufferers. *Expert Opin. Pharmacother.* **19**, 1071–1076 (2018).
68. Garakani, A. *et al.* Pharmacotherapy of Anxiety Disorders: Current and Emerging Treatment Options. *Front. Psychiatry* **11**, (2020).
69. Buchsbaum, M. S. *et al.* Topographic EEG changes with benzodiazepine administration in generalized anxiety disorder. *Biol. Psychiatry* **20**, 832–842 (1985).
70. Michail, E., Chouvarda, I. & Maglaveras, N. Benzodiazepine administration effect on EEG Fractal Dimension: results and causalities. in *2010 Annual International Conference of the IEEE Engineering in Medicine and Biology* 2350–2353 (2010). doi:10.1109/IEMBS.2010.5627851.
71. Hardmeier, M. *et al.* Intranasal Midazolam: Pharmacokinetics and Pharmacodynamics

Assessed by Quantitative EEG in Healthy Volunteers. *Clin. Pharmacol. Ther.* **91**, 856–862 (2012).

72. Gabriel, F. C. *et al.* Pharmacological treatment of depression: A systematic review comparing clinical practice guideline recommendations. *PLOS ONE* **15**, e0231700 (2020).

73. Bruder, G. E. *et al.* Electroencephalographic Alpha Measures Predict Therapeutic Response to a Selective Serotonin Reuptake Inhibitor Antidepressant: Pre- and Post-Treatment Findings. *Biol. Psychiatry* **63**, 1171–1177 (2008).

74. Schenk, G. K., Filler, W., Ranft, W. & Zerbin, D. Double-blind comparisons of a selective serotonin reuptake inhibitor, zimelidine, and placebo on quantified EEG parameters and psychological variables. *Acta Psychiatr. Scand.* **63**, 303–313 (1981).

Supplementary Materials

Electrophysiological signatures of anxiety in Parkinson's disease

Sahar Yassine[1,2,3,*] MSc, Sourour Almarouk[1,3,9,*] MSc, Ute Gschwandtner[4] MD, Manon Auffret[1,3,6,7,] PharmD, PhD, Mahmoud Hassan[3,8,10†] PhD, Marc Verin[1,3,5,6,†] MD, PhD, Peter Fuhr[4,†] MD

[1] Univ Rennes 1, LTSI - U1099, F-35000 Rennes, France

[2] NeuroKyma, F-35000 Rennes, France

[3] Behavior & Basal Ganglia, CIC1414, CIC-IT, CHU Rennes, Rennes, France

[4] Dept. of Neurology, Hospitals of the University of Basel, Basel, Switzerland

[5] Movement Disorders Unit, Neurology Department, Pontchaillou University Hospital, Rennes, France

[6] Institut des Neurosciences Cliniques de Rennes (INCR), Rennes, France

[7] France Développement Electronique, Monswiller, France

[8] School of Science and Engineering, Reykjavik University, Reykjavik, Iceland

[9] Neuroscience Research Centre, Lebanese University, Faculty of Medicine, Beirut, Lebanon

[10] MINDIG, F-35000, Rennes, France

[*,†] **These authors contributed equally to this work.**

Table S1- Demographic, clinical and main neuropsychiatric characteristics of the main cohort longitudinally expressed as: mean (standard deviation). y: years, M/F: Male/Female, MoCA: Montreal Cognitive Assessment, MCI (Y/N): Mild Cognitive Impairment (yes/no), UPDRS-III: Unified Parkinson's Disease Rating Scale-motor examination, LEDD: Levodopa Equivalent Daily Dose, BAI: Beck Anxiety Inventory score, BDI-II: Beck Depression Inventory, second edition score, AES: Apathy Evaluation Scale.

	Baseline		**3 years**		**5 years**	
	PD (N=77)	**HC (N=32)**	**PD (N=45)**	**HC (N=21)**	**PD (N=44)**	**HC (N=3)**
Demographic						
Age (y)	66.2 (8.2)	65.3 (5.6)	70.9 (7.9)	68.7 (4.9)	71.7 (7.8)	65.6 (4.1)
Sex (M/F)	51/26	18/14	31/14	9/12	28/14	2/1
Education (y)	14.6 (3.2)	13.8 (2.9)	14.8 (3.1)	13.6 (3.1)	15.1 (3.1)	11 (2)
Clinical						
Disease duration (y)	5.4 (5.2)	-	8 (5.2)	-	10.4 (4.9)	-
MoCA (/30)	26 (2.4)	26.8 (2.5)	25.2 (3.5)	27.4 (2.2)	25.1 (5.1)	
MCI (Y/N)	25/52	-	16/29	-	16/28	-
MMSE (/30)	28.7 (1.2)	29.4 (1)	28.2 (2.3)	29 (1.5)	28.3 (1.9)	
UPDRS-II	6.6 (4.7)	-	10.8 (5.7)	-	9.6 (6.6)	-
UPDRS-III	15.5 (11)	-	20.5 (12.1)	-	19.5 (13.1)	-
Medication						
LEDD (mg/day)	676 (466)	-	707 (445)	-	633 (386)	-
Neuropsychiatric tests						
BAI (/63)	9.7 (8)	2.9 (4)	11.5 (7.5)	2.3 (2.6)	9.6 (6.9)	3.3 (4.9)
BDI-II (/63)	7.9 (4.9)	2.6 (2.4)	7.8 (4.7)	1.8 (1.7)	6.7 (6.1)	4 (3.6)
AES (/63)	32.9 (8.4)	24.1 (5.1)	31.2 (7.1)	25.1 (5.7)	31.7 (8.6)	27.7 (9)

Table S2- Demographic, clinical and main neuropsychiatric characteristics of the study cohort longitudinally expressed as: mean (standard deviation). y: years, M/F: Male/Female, MoCA: Montreal Cognitive Assessment, MCI (Y/N): Mild Cognitive Impairment (yes/no), UPDRS-III: Unified Parkinson's Disease Rating Scale-motor examination, LEDD: Levodopa Equivalent Daily Dose, BAI: Beck Anxiety Inventory score, BDI-II: Beck Depression Inventory, second edition score, AES: Apathy Evaluation Scale.

	Baseline		**3 years**		**5 years**	
	PD (N=68)	**HC (N=25)**	**PD (N=42)**	**HC (N=17)**	**PD (N=29)**	**HC (N=1)**
Demographic						
Age (y)	66.4 (8.3)	66.6 (4)	70.5 (7.9)	68.9 (6.1)	71 (7)	69
Sex (M/F)	46/22	15/10	28/14	8/9	17/12	1/0
Education (y)	14.8 (3.1)	14.2 (2.9)	14.8 (3.1)	13.4 (3.2)	14.1 (3.1)	13
Clinical						
Disease duration (y)	5.2 (5.2)	-	7.5 (4.7)	-	9.4 (3.8)	-
MoCA (/30)	26 (2.4)	26.6 (2.7)	25.2 (3.6)	27.2 (2.3)	25.7 (3.6)	
MCI (Y/N)	22/46	-	15/27	-	7/22	-
UPDRS-III	14.8 (11.2)	-	20.1 (12)	-	17.6 (12.8)	-
Medication						
LEDD (mg/day)	652 (465)	-	667 (436)	-	558 (343)	-
Neuropsychiatric tests						
BAI (/63)	9.9 (7.9)	2.4 (3.2)	11.5 (7.4)	2.2 (2.6)	10.2 (7)	1
BDI-II (/63)	7.7 (4.9)	2.6 (2.5)	7.8 (4.8)	1.9 (1.7)	7.1 (6.6)	5
AES (/63)	33(8.6)	24.1 (5.1)	31.4 (7.1)	25.1 (5.7)	30.9 (7.6)	37

Table S3- Affiliation of the EEG channels to the four lobes of interest

Lobes	EEG channels
Frontal lobe	E2, E3, E4, E5, E6, E7, E8, E11, E12, E13, E14, E15, E16, E17, E19, E20, E21, E22, E23, E24, E26, E27, E28, E29, E30, E33, E34, E35, E36, E38, E39, E40, E41, E42, E43, E47, E48, E49, E50, E51, E55, E56, E57, E58, E61, E62, E63, E64, E68, E69, E194, E195, E196, E197, E198, E202, E203, E204, E205, E206, E207, E210, E211, E212, E213, E214, E215, E220, E221, E222, E223, E224.
Parietal lobe	E9, E44, E45, E52, E53, E59, E60, E65, E66, E70, E71, E72, E74, E75, E76, E77, E78, E79, E80, E81, E84, E85, E86, E87, E88, E89, E90, E96, E97, E98, E99, E100, E101, E109, E110, E119, E128, E129, E130, E131, E132, E140, E141, E142, E143, E144, E152, E153, E154, E155, E161, E162, E163, E164, E170, E171, E172, E173, E179, E180, E181, E182, E183, E184, E185, E186, E192, E193.
Temporal lobe	E67, E73, E82, E83, E91, E92, E93, E94, E95, E102, E103, E104, E105, E111, E112, E177, E178, E188, E189, E190, E191, E199, E200, E201, E208, E209, E216, E217, E218, E219, E225, E227, E228, E229, E231, E232, E233, E235, E236, E237, E239, E240, E242, E243, E245, E246, E247, E249, E250, E251, E253, E254, E255, E256.
Occipital lobe	E106, E107, E108, E113, E114, E115, E116, E117, E118, E120, E121, E122, E123, E124, E125, E126, E127, E133, E134, E135, E136, E137, E138, E139, E145, E146, E147, E148, E149, E150, E151, E156, E157, E158, E159, E160, E165, E166, E167, E168, E169, E174, E175, E176, E187.

Table S4- Affiliation of brain regions to the seven lobes of interest

Lobes of Interest	Brain regions
Prefrontal cortex (PFC)	Middle frontal gyrus (L/R)
	Orbito-frontal cortex (L/R)
	Superior frontal gyrus (L/R)
	Inferior frontal gyrus (L/R)
Motorstrip (Mot)	Precentral gyrus (L/R)
	Paracentral lobule (L/R)
	Postcentral gyrus (L/R)
Parietal lobe (Par)	Inferior parietal lobule (L/R)
	Superior parietal lobule (L/R)
	Precuneus (L/R)
Temporal network (Tmp)	Inferior temporal gyrus (L/R)
	Middle temporal gyrus (L/R)
	Superior temporal gyrus (L/R)
	Parahippocampal gyrus (L/R)
	Fusiform gyrus (L/R)
	Posterior superior temporal sulcus (L/R)
Occipital lobe (Occ)	Lateral occipital cortex (L/R)
	MedioVentral occipital cortex (L/R)
Limbic lobe (Lmb)	Caudal cingulate gyrus (L/R)
	Ventral cingulate gyrus (L/R)
	Dorsal cingulate gyrus (L/R)
Insular lobe (Ins)	Insular gyrus (L/R)

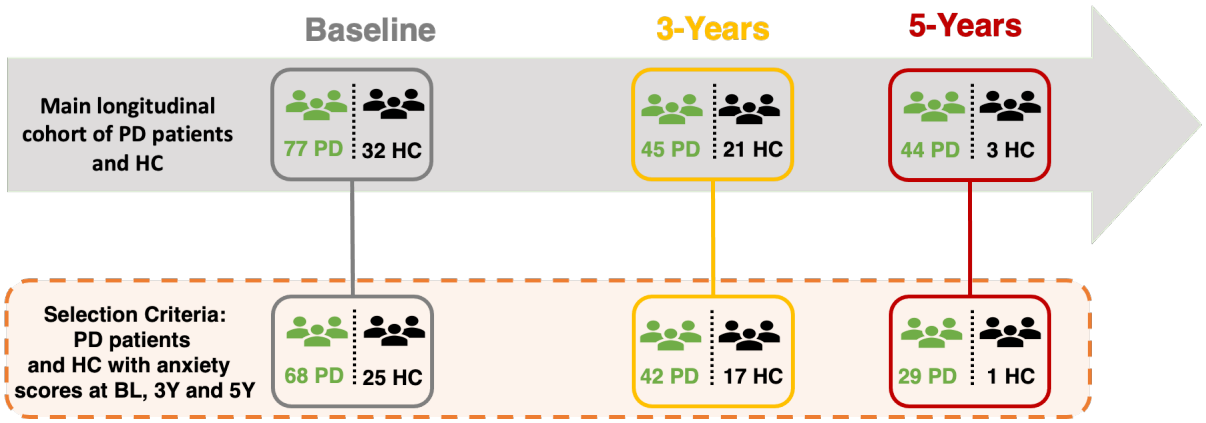

Figure S1- Flowchart of the main study cohort and the subcohort of participants included in this study.

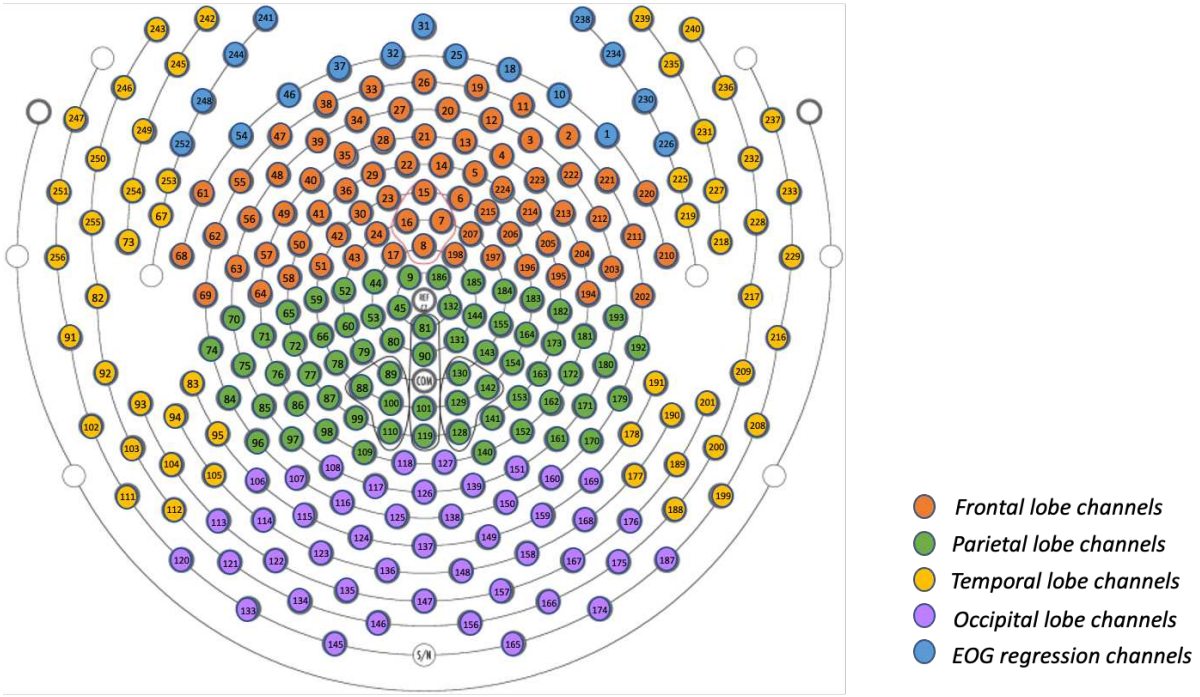

Figure S2- EGI 256-channels sensor layout and the affiliation of the channels to the four lobes of interest: Frontal lobe (orange), Parietal lobe (green), temporal lobe (yellow) and occipital lobe (purple). The 17 channels used for EOG regression are marked in blue.

CHAPTER 5: GENERAL DISCUSSION

5.1. Overview of the thesis aims and results

One of the key challenges in clinical neuroscience is understanding how neurological disorders, such as PD, affect brain function from disease onset and throughout their progression. PD is one of the most prevalent neurological conditions that contributes significantly to the global burden of disability due to its variability in symptoms and progression (Bloem et al., 2021; Kalia & Lang, 2015; Poewe et al., 2017). This highlights the critical clinical need to develop novel biomarkers that can accurately and reliably characterize the pathological mechanisms underlying these prominent aspects in PD and track their longitudinal evolution, to ultimately monitor the efficacy of disease-modifying and therapeutic interventions. In recent years, EEG has emerged as a promising tool for this purpose. It is a direct, non-invasive, inexpensive, and easy-to-use neuroimaging technique that has been recognized to enable the extraction of relevant information about brain activity alterations in several pathological conditions (Müller-Putz, 2020; Shirahige et al., 2020; Geraedts et al., 2018; Cozac, Gschwandtner, et al., 2016; Q. Wang et al., 2020). Despite extensive literature and important strides in biomarker research for disease symptoms and progression via various neuroimaging techniques, the use of EEG in longitudinal studies has been rarely explored. Therefore, in this thesis, we used longitudinal resting-state high-density EEG to track the progression of brain activity in PD patients, deconstruct their heterogeneity, assess their subgroups' disease trajectories, and identify the neural correlates of their PD-related anxiety. The main results of this thesis are summarized as follows:

1. The longitudinal tracking of functional brain networks in PD patients using resting state EEG over a period of 5 years revealed patterns of progressively decreased connectivity, primarily between the fronto-temporal lobes of the right hemisphere, in alpha2 and beta bands. These large-scale dysconnectivity networks are unique to PD patients and are not observed in healthy controls and are correlated with the global cognitive profile of the patients.

2. When investigating the longitudinal progression in subgroups of patients based on the lateralization of motor symptoms, we discovered that patterns of decreased

connectivity, mainly in the right hemisphere, characterize the evolution of the disease in PD patients with left-sided symptoms (LPD). In contrast, patterns of functional dysconnectivity, mostly dominant in the left hemisphere, delineate the progression of the disease in PD patients with right-sided symptoms (RPD).

3. Resting state EEG can identify three distinct subtypes of PD patients, characterized by different levels of disruptions in the somatomotor network (delta and beta bands), frontotemporal network (alpha2 band), and default mode network (alpha1 band). These subtypes are associated with different clinical profiles and can be classified into either moderate-only-motor or diffuse-malignant at 5 years.
4. EEG-based features characterizing the moderate-only-motor subtypes from the diffuse-malignant subtype at 5 years are relevant throughout the disease trajectory and can predict the cognitive decline in the patients from baseline, when the cognitive clinical scores were in extensive overlap.

5. Through an investigation of the electrophysiological fingerprints of PD-related anxiety, we observed frequency-dependent patterns of altered spectral power, as well as functional hyper- and hypo-connectivity networks, distinguishing the anxious PD group from both non-anxious PD patients and healthy controls. We also found that the corresponding quantifiable electrophysiological scores correlated with the clinical outcome of anxiety throughout the disease progression.

5.2. Reliable biomarkers in PD: key elements and pitfalls

The accurate prediction of the onset and progression of complex heterogeneous diseases, such as PD, is a vital challenge in providing optimal patient counseling, symptom-specific care and effective treatments. Meeting this challenge is dependent on the development of reliable biomarkers that not only characterize the disease but also accurately track and predict its evolution. Cross-sectional studies are shown to be prevalent in neuroimaging research targeting biomarkers of PD, offering insights about the underlying pathophysiology of different motor and non-motor symptoms (McGhee et al., 2013; Mitchell et al., 2021; Parnetti et al., 2019; Surguchov, 2022). However, when it comes to disease progression and predicting disease outcome, longitudinal studies are more relevant. In fact, longitudinal studies offer the opportunity to extract biomarkers with regards to the influence of time. They provide a causal link between the changes in the brain patterns and later outcomes of the disease at the clinical

and neurophysiological level. This constitutes a fundamental step toward prediction/prognosis assessments not only at the group average level but also at the individual scale. One of the major examples in this premise is the Parkinson Progression Marker Initiative (PPMI) cohort which provided a longitudinal dataset of clinical, biological and neuroimaging data conceptualized mainly to improve and validate biomarkers development strategies (Marek et al., 2011). Multiple studies have used this cohort to derive biomarkers of progression, disease heterogeneity, cognitive decline and specific symptoms (Dadu et al., 2022; Fereshtehnejad et al., 2017; Fiorenzato et al., 2018; Kang et al., 2016; Markello et al., 2021; J. H. Park et al., 2020; Schrag et al., 2017; Simuni, Caspell-Garcia, et al., 2018; Zeighami et al., 2019). Unfortunately, this cohort does not include any electrophysiological data (EEG/MEG), and to date, very few longitudinal studies have used such neuroimaging techniques to investigate such biomarkers (Arnaldi et al., 2017; Caviness et al., 2015; Chaturvedi et al., 2019; Cozac, Chaturvedi, et al., 2016; Olde Dubbelink, Stoffers, Deijen, Twisk, Stam, & Berendse, 2013; Olde Dubbelink, Stoffers, Deijen, Twisk, Stam, Hillebrand, et al., 2013). Direct, non-invasive, easy-to-use and potential mobile neuroimaging technologies such as EEG could be considered as an advantageous tool for biomarkers frameworks in clinical settings (Müller-Putz, 2020). This emphasizes the importance of the longitudinal EEG dataset used in this thesis to characterize multiple aspects-of-interest in PD and to subsequently derive EEG-based markers and assess their evolution over time and their predictive capacity. Despite the significant advantage of longitudinal studies in general and this dataset particularly, one of their main limitations is the decreasing sample size over time, mainly at the follow-up timepoints. This is due to the difficulty in upholding longitudinal studies as participants tend to drop off after a relatively long period (5 years) for several reasons, including losing interest in participating, travelling, moving from the area, illness or even death...

Another factor that has emerged recently as a key element in biomarker discovery efforts is the prior definition of disease subtypes based on their shared patterns of biological abnormalities, rather than their common clinical features (A. Espay et al., 2017; A. J. Espay et al., 2017, 2020). In fact, the debate whether PD should be viewed as a single, cohesive entity or a complex multisystem disorder with distinct etiologic and pathophysiologic entities is relatively new (A. J. Espay et al., 2020; Farrow et al., 2022; Weiner, 2008). The traditional hypothesis that considers PD as a whole and partitions patients based on their clinical similarities has proven useful in comprehending the underlying mechanisms of the symptoms and developing effective treatments that alleviate them (Paolini Paoletti et al., 2019). However, when it comes to

targeting disease-modifying and neuroprotective interventions, multiple phase-three clinical trials have failed (A. Espay & Stecher, 2020). This has led to an increased recognition of PD as a complex-heterogeneous interaction of intrinsic and extrinsic factors, suggesting the need to reevaluate biomarker discovery efforts by targeting smaller, well-defined subsets of PD patients that share subsequent biological aberrations (A. J. Espay et al., 2017).

Indeed, the concept of discrete clusters with mutual underlying abnormalities could offer a valuable approach to retrieve biomarkers that can predict, at early stages of the disease, which individuals are likely to experience a benign disease course versus those who will have a more aggressive slope of declines toward a malignant disease course (A. J. Espay & Marras, 2019). In fact, this was one of our main motivations to conduct the disease subtyping study of this thesis. We wanted to examine to which extent can EEG-based features bring relevant information about disease trajectories in subgroups of patients. In other words, we aimed to identify subgroup-specific biomarkers and investigate whether they can predict the only-motor versus the diffuse malignant trajectories at earlier stages of the disease when the clinical scores were not sufficient for making accurate judgment. Evidently, insights gained from such research would be of utmost interest not only for novel disease modifying therapies, but also for the existing surgical interventions, such as deep brain stimulation, as early identification of patients at risk for cognitive impairment could prevent future side-effects of the procedure (Limousin & Foltynie, 2019; Witt et al., 2013). Convergent biomarkers of neurophysiological-based subtypes would ultimately enhance the emerging stratified medicine model toward better neuroprotection interventions and clinical trials.

Finally, it is worth mentioning that reliable biomarkers of PD, or any other neurodegenerative disorders, need to be validated and replicated on external cohorts. Although our results were consistent with several other studies using different or similar neuroimaging techniques, it is essential to replicate the findings in new longitudinal cohorts to validate them. Unfortunately, this was not possible in this thesis due to the absence of publicly available longitudinal EEG cohorts of PD patients.

5.3. Clinical and methodological considerations

One of the main clinical considerations that should be pointed out in this thesis is that the EEG data of PD patients were obtained during their "ON" medication state, when patients self-administered their daily dopaminergic medication. Despite the advantage of the medication in

reducing the magnitude of motor symptoms in patients and subsequently decreasing movement artifacts in their EEG data and improving the quality of their recordings, the effect of dopaminergic medication may still be present in the measures of brian oscillations and functional connectivity, as demonstrated by several studies (Esposito et al., 2013; Silberstein et al., 2005). However, we attempted to reduce the effect of this issue by accounting for the levodopa equivalent daily dose (LEDD) as a confounding factor in all our statistical analyses. Further validation of our results independently from the medication state of the patients is highly recommended in this context.

Regarding the methodological considerations, while we carefully selected the most appropriate and previously validated EEG processing methods for our analysis pipeline to obtain the EEG-based features used in our three studies, the large number of methodological choices in this pipeline raises concerns about analytical variability. Starting from the preprocessing of the EEG signals, we applied a "quasi automatic" preprocessing pipeline using the Automagic toolbox, with minimum subjective intervention to ensure the quality of the data. Currently there is no standardized preprocessing pipeline for EEG data and a recent comparative study has shown considerable variability in results when using different software tools to preprocess EEG signals (Kabbara et al., 2022). Despite the robust preprocessing steps implemented in the chosen toolbox Automagic, we believe that further validation of our results using other preprocessing toolboxes is necessary in the future.

Furthermore, another methodological consideration that presents a challenge in the processing pipeline is the selection of the most accurate combination of inverse solution and functional connectivity method for the "EEG source connectivity" approach, which aims to reconstruct the dynamics of brain regions at the source level. Extensive investigations were recently carried out in the team by (Allouch et al., 2022, 2023) to study the effect of the choice of inverse solution and connectivity method on studies outcomes in both real and simulated EEG data. While they found that no single combination of methods outperforms all others, they did identify wMNE as one of the most effective methods for accurately resolving the inverse problem, consistent with previous findings (Hassan et al., 2014; Hassan, Merlet, et al., 2017). Furthermore, concerning the choice of connectivity method, the debate regarding whether to consider or ignore spurious connections between reconstructed adjacent sources is still ongoing. While some studies have suggested disregarding zero-lag interactions among signals at the cortical level to reduce the effect of source leakage (Brookes et al., 2012; Colclough et al., 2015), others have shown that such approaches may overlook genuine connectivity

occurring at zero-lag or between closely situated brain sources (Brookes et al., 2014; Finger et al., 2016; Schoffelen & Gross, 2009). In their studies, Allouch and colleagues have shown that PLV performed well as a connectivity method without source leakage correction, and orthogonalized AEC was a robust choice for connectivity method with source leakage correction. Based on these findings, we chose these methods for our analysis. However, it is important to acknowledge the potential influence of these choices on our results.

Finally, regarding our methodological choice for the clustering analysis in the disease subtyping study, we opted for a robust approach that combined the SNF method and spectral clustering. This approach has been previously validated as effective in partitioning PD patients into meaningful subgroups (Markello et al., 2021). However, other disease subtyping studies have utilized machine learning or deep learning models in this context (Dadu et al., 2022; Salmanpour et al., 2021; X. Zhang et al., 2019). While these techniques have shown promise in disease subtyping, their main limitations are the lack of interpretability, particularly in deep learning models, and the need for large datasets for model construction and validation. In our case, the limited sample size precluded the use of such techniques.

5.4. Conclusion and perspectives

In this thesis, our primary objective was to investigate the extent to which longitudinal resting-state EEG can accurately characterize the abnormal brain functions related to PD such as disease progression, disease subtypes and PD-related anxiety. We also sought to identify corresponding EEG-based markers that correlate with and predict the clinical outcomes of the patients. Overall, our results were promising in this context, yet they can be definitely further extended in light of the aforementioned limitations, in order to obtain more reliable markers validated and replicated on larger datasets.

In a currently undergoing study, we are aiming to adopt the opposite approach of our disease subtyping study by performing a clustering analysis on the clinical features to identify clinically relevant subtypes at later stages of the disease and subsequently investigate their retrospective markers of severity and progression.

In future work, we believe that along with EEG, integrating additional data modalities into the biomarker identification models for PD in the context of longitudinal studies would be of great interest. Such approaches would offer a simultaneous multi-view of the neuropathological

processes and add extra dimensions that may be relevant for the biomarker measures. An example of such frameworks would be the use of simultaneously recorded scalp-EEG data with lead field potential data at the subcortical level from implemented electrodes after surgical interventions. Such data modalities could provide complementary information about both cortical and subcortical altered brain mechanisms occurring in the patients.

Another possible aspect that could be investigated using such longitudinal EEG datasets in PD is the longitudinal effect of the PD-related medications in patients. By considering the "On" medication state of the patients and the evolution of their doses in time, one could be interested in investigating the related changes in the brain networks with the medication's intake and the evolution of both motor and cognitive clinical scores of the patients. This could ultimately illustrate the long-term effect of the medications in PD patients and potentially derive adequate biomarkers of treatments responsiveness at the individual level.

In addition, and inspired from our first study of disease progression, one future interest could be predicting the evolution of the clinical trajectories of the patients based on the hemisphere of the disease onset. Several studies have shown a direct relationship between the laterality of the disease and the deterioration of motor and non-motor symptoms. By investigating these aspects using longitudinal EEG, we could provide potential progression markers that may aid in predicting disease trajectories.

Finally, in light of our second study, we showed that the integration of static EEG-based spectral power and functional connectivity features into data-driven models can be useful in resolving complex problems such as disease subtyping and may lead to meaningful outcomes. However, an extension of this work could be integrating additional EEG-based features derived from dynamic characteristics, network topology features and modular network organizations. These features could be obtained not only from resting-state data but also from specific-task paradigms.

REFERENCES

Aarsland, D., Batzu, L., Halliday, G. M., Geurtsen, G. J., Ballard, C., Ray Chaudhuri, K., & Weintraub, D. (2021). Parkinson disease-associated cognitive impairment. *Nature Reviews Disease Primers*, *7*(1), Article 1. https://doi.org/10.1038/s41572-021-00280-3

Aarsland, D., Marsh, L., & Schrag, A. (2009). Neuropsychiatric symptoms in Parkinson's disease. *Movement Disorders*, *24*(15), 2175–2186. https://doi.org/10.1002/mds.22589

Acharya, U. R., Vinitha Sree, S., Swapna, G., Martis, R. J., & Suri, J. S. (2013). Automated EEG analysis of epilepsy: A review. *Knowledge-Based Systems*, *45*, 147–165. https://doi.org/10.1016/j.knosys.2013.02.014

Ahirwal, M. K., Kumar, A., Londhe, N. D., & Bikrol, H. (2016). Scalp connectivity networks for analysis of EEG signal during emotional stimulation. *2016 International Conference on Communication and Signal Processing (ICCSP)*, 0592–0596. https://doi.org/10.1109/ICCSP.2016.7754208

Al-Ezzi, A., Kamel, N., Faye, I., & Gunaseli, E. (2020). Review of EEG, ERP, and Brain Connectivity Estimators as Predictive Biomarkers of Social Anxiety Disorder. *Frontiers in Psychology*, *11*. https://www.frontiersin.org/articles/10.3389/fpsyg.2020.00730

Allouch, S., Duprez, J., Khalil, M., Hassan, M., Modolo, J., & Kabbara, A. (2022). Methods Used to Estimate EEG Source-Space Networks: A Comparative Simulation-Based Study. *2022 44th Annual International Conference of the IEEE Engineering in Medicine & Biology Society (EMBC)*, 3590–3593. https://doi.org/10.1109/EMBC48229.2022.9871047

Allouch, S., Kabbara, A., Duprez, J., Khalil, M., Modolo, J., & Hassan, M. (2023). Effect of channel density, inverse solutions and connectivity measures on EEG resting-state networks reconstruction: A simulation study. *NeuroImage*, *271*, 120006. https://doi.org/10.1016/j.neuroimage.2023.120006

Amboni, M., Tessitore, A., Esposito, F., Santangelo, G., Picillo, M., Vitale, C., Giordano, A., Erro, R., de Micco, R., Corbo, D., Tedeschi, G., & Barone, P. (2015). Resting-state functional connectivity associated with mild cognitive impairment in Parkinson's disease. *Journal of Neurology*, *262*(2), 425–434. https://doi.org/10.1007/s00415-014-7591-5

Anzolin, A., Presti, P., Van De Steen, F., Astolfi, L., Haufe, S., & Marinazzo, D. (2019). Quantifying the Effect of Demixing Approaches on Directed Connectivity Estimated Between Reconstructed EEG Sources. *Brain Topography*, *32*(4), 655–674. https://doi.org/10.1007/s10548-019-00705-z

Aquino, C. C., Duffley, G., Hedges, D. M., Vorwerk, J., House, P. A., Ferraz, H. B., Rolston, J. D., Butson, C. R., & Schrock, L. E. (2019). Interleaved deep brain stimulation for dyskinesia management in Parkinson's disease. *Movement Disorders*, *34*(11), 1722–1727. https://doi.org/10.1002/mds.27839

Arnaldi, D., De Carli, F., Famà, F., Brugnolo, A., Girtler, N., Picco, A., Pardini, M., Accardo,

J., Proietti, L., Massa, F., Bauckneht, M., Morbelli, S., Sambuceti, G., & Nobili, F. (2017). Prediction of cognitive worsening in de novo Parkinson's disease: Clinical use of biomarkers: Prediction of Cognitive Worsening in PD. *Movement Disorders*, *32*(12), 1738–1747. https://doi.org/10.1002/mds.27190

Arns, M., Conners, C. K., & Kraemer, H. C. (2013). A Decade of EEG Theta/Beta Ratio Research in ADHD: A Meta-Analysis. *Journal of Attention Disorders*, *17*(5), 374–383. https://doi.org/10.1177/1087054712460087

Ascherio, A., & Schwarzschild, M. A. (2016). The epidemiology of Parkinson's disease: Risk factors and prevention. *The Lancet. Neurology*, *15*(12), 1257–1272. https://doi.org/10.1016/S1474-4422(16)30230-7

Baggio, H.-C., Segura, B., Sala-Llonch, R., Marti, M.-J., Valldeoriola, F., Compta, Y., Tolosa, E., & Junqué, C. (2015). Cognitive impairment and resting-state network connectivity in Parkinson's disease. *Human Brain Mapping*, *36*(1), 199–212. https://doi.org/10.1002/hbm.22622

Baiano, C., Barone, P., Trojano, L., & Santangelo, G. (2020). Prevalence and clinical aspects of mild cognitive impairment in Parkinson's disease: A meta-analysis. *Movement Disorders*, *35*(1), 45–54.

Baillet, S., Mosher, J. C., & Leahy, R. M. (2001). Electromagnetic brain mapping. *IEEE Signal Processing Magazine*, *18*(6), 14–30. https://doi.org/10.1109/79.962275

Balestrino, R., & Martinez-Martin, P. (2017). Neuropsychiatric symptoms, behavioural disorders, and quality of life in Parkinson's disease. *Journal of the Neurological Sciences*, *373*, 173–178. https://doi.org/10.1016/j.jns.2016.12.060

Ballarini, T., Mueller, K., Albrecht, F., Růžička, F., Bezdicek, O., Růžička, E., Roth, J., Vymazal, J., Jech, R., & Schroeter, M. L. (2019). Regional gray matter changes and age predict individual treatment response in Parkinson's disease. *NeuroImage: Clinical*, *21*, 101636. https://doi.org/10.1016/j.nicl.2018.101636

Barber, T. R., Klein, J. C., Mackay, C. E., & Hu, M. T. M. (2017). Neuroimaging in pre-motor Parkinson's disease. *NeuroImage: Clinical*, *15*, 215–227. https://doi.org/10.1016/j.nicl.2017.04.011

Bassett, D. S., Nelson, B. G., Mueller, B. A., Camchong, J., & Lim, K. O. (2012). Altered resting state complexity in schizophrenia. *NeuroImage*, *59*(3), Article 3. https://doi.org/10.1016/j.neuroimage.2011.10.002

Baumann, C. R., Held, U., Valko, P. O., Wienecke, M., & Waldvogel, D. (2014). Body side and predominant motor features at the onset of Parkinson's disease are linked to motor and nonmotor progression. *Movement Disorders*, *29*(2), 207–213. https://doi.org/10.1002/mds.25650

Bayram, E., Kaplan, N., Shan, G., & Caldwell, J. Z. K. (2020). The longitudinal associations between cognition, mood and striatal dopaminergic binding in Parkinson's Disease. *Neuropsychology, Development, and Cognition. Section B, Aging, Neuropsychology and Cognition*, *27*(4), 581–594. https://doi.org/10.1080/13825585.2019.1653445

Bear, M., Connors, B., & Paradiso, M. A. (2020). *Neuroscience: Exploring the Brain, Enhanced Edition: Exploring the Brain, Enhanced Edition*. Jones & Bartlett Learning.

Beavan, M. S., & Schapira, A. H. V. (2013). Glucocerebrosidase mutations and the pathogenesis of Parkinson disease. *Annals of Medicine*, *45*(8), 511–521.

https://doi.org/10.3109/07853890.2013.849003
Benabid, A. L., Chabardes, S., Mitrofanis, J., & Pollak, P. (2009). Deep brain stimulation of the subthalamic nucleus for the treatment of Parkinson's disease. *The Lancet Neurology*, *8*(1), 67–81. https://doi.org/10.1016/S1474-4422(08)70291-6
Betrouni, N., Alazard, E., Bayot, M., Carey, G., Derambure, P., Defebvre, L., Leentjens, A. F., Delval, A., & Dujardin, K. (2022). Anxiety in Parkinson's disease: A resting-state high density EEG study. *Neurophysiologie Clinique*, *52*(3), 202–211. https://doi.org/10.1016/j.neucli.2022.01.001
Biasiucci, A., Franceschiello, B., & Murray, M. M. (2019). Electroencephalography. *Current Biology*, *29*(3), R80–R85. https://doi.org/10.1016/j.cub.2018.11.052
Binnie, C. D., & Prior, P. F. (1994). Electroencephalography. *Journal of Neurology, Neurosurgery & Psychiatry*, *57*(11), 1308–1319. https://doi.org/10.1136/jnnp.57.11.1308
Bloem, B. R., Okun, M. S., & Klein, C. (2021). Parkinson's disease. *The Lancet*, *397*(10291), 2284–2303. https://doi.org/10.1016/S0140-6736(21)00218-X
Blondel, V. D., Guillaume, J.-L., Lambiotte, R., & Lefebvre, E. (2008). Fast unfolding of communities in large networks. *Journal of Statistical Mechanics: Theory and Experiment*, *2008*(10), P10008. https://doi.org/10.1088/1742-5468/2008/10/P10008
Boeve, B. F. (2013). Idiopathic REM sleep behaviour disorder in the development of Parkinson's disease. *The Lancet Neurology*, *12*(5), 469–482. https://doi.org/10.1016/S1474-4422(13)70054-1
Boon, L. I., Geraedts, V. J., Hillebrand, A., Tannemaat, M. R., Contarino, M. F., Stam, C. J., & Berendse, H. W. (2019). A systematic review of MEG-based studies in Parkinson's disease: The motor system and beyond. *Human Brain Mapping*, *40*(9), 2827–2848. https://doi.org/10.1002/hbm.24562
Boonstra, J. T., Michielse, S., Temel, Y., Hoogland, G., & Jahanshahi, A. (2021). Neuroimaging Detectable Differences between Parkinson's Disease Motor Subtypes: A Systematic Review. *Movement Disorders Clinical Practice*, *8*(2), 175–192. https://doi.org/10.1002/mdc3.13107
Borck, C. (2018). *Brainwaves: A Cultural History of Electroencephalography*. Taylor & Francis. https://doi.org/10.4324/9781315569840
Borroni, B., Premi, E., Formenti, A., Turrone, R., Alberici, A., Cottini, E., Rizzetti, C., Gasparotti, R., & Padovani, A. (2015). Structural and functional imaging study in dementia with Lewy bodies and Parkinson's disease dementia. *Parkinsonism & Related Disorders*, *21*(9), 1049–1055. https://doi.org/10.1016/j.parkreldis.2015.06.013
Bosboom, J. L. W., Stoffers, D., Wolters, E. Ch., Stam, C. J., & Berendse, H. W. (2008). MEG resting state functional connectivity in Parkinson's disease related dementia. *Journal of Neural Transmission*, *116*(2), 193. https://doi.org/10.1007/s00702-008-0132-6
Bove, C., & Travagli, R. A. (2019). Neurophysiology of the brain stem in Parkinson's disease. *Journal of Neurophysiology*, *121*(5), 1856–1864. https://doi.org/10.1152/jn.00056.2019
Braak, H., Ghebremedhin, E., Rüb, U., Bratzke, H., & Del Tredici, K. (2004). Stages in the

development of Parkinson's disease-related pathology. *Cell and Tissue Research*, *318*(1), 121–134. https://doi.org/10.1007/s00441-004-0956-9

Braak, H., Rüb, U., Jansen Steur, E. N. H., Del Tredici, K., & de Vos, R. a. I. (2005). Cognitive status correlates with neuropathologic stage in Parkinson disease. *Neurology*, *64*(8), 1404–1410. https://doi.org/10.1212/01.WNL.0000158422.41380.82

Braak, H., Tredici, K. D., Rüb, U., de Vos, R. A. I., Jansen Steur, E. N. H., & Braak, E. (2003). Staging of brain pathology related to sporadic Parkinson's disease. *Neurobiology of Aging*, *24*(2), 197–211. https://doi.org/10.1016/S0197-4580(02)00065-9

Brás, I. C., & Outeiro, T. F. (2021). Alpha-Synuclein: Mechanisms of Release and Pathology Progression in Synucleinopathies. *Cells*, *10*(2), Article 2. https://doi.org/10.3390/cells10020375

Bridi, J. C., & Hirth, F. (2018). Mechanisms of α-Synuclein Induced Synaptopathy in Parkinson's Disease. *Frontiers in Neuroscience*, *12*. https://www.frontiersin.org/articles/10.3389/fnins.2018.00080

Broen, M. P. G., Narayen, N. E., Kuijf, M. L., Dissanayaka, N. N. W., & Leentjens, A. F. G. (2016). Prevalence of anxiety in Parkinson's disease: A systematic review and meta-analysis. *Movement Disorders*, *31*(8), 1125–1133. https://doi.org/10.1002/mds.26643

Bronstein, J. M., Tagliati, M., Alterman, R. L., Lozano, A. M., Volkmann, J., Stefani, A., Horak, F. B., Okun, M. S., Foote, K. D., Krack, P., Pahwa, R., Henderson, J. M., Hariz, M. I., Bakay, R. A., Rezai, A., Marks, W. J., Jr, Moro, E., Vitek, J. L., Weaver, F. M., … DeLong, M. R. (2011). Deep Brain Stimulation for Parkinson Disease: An Expert Consensus and Review of Key Issues. *Archives of Neurology*, *68*(2), 165. https://doi.org/10.1001/archneurol.2010.260

Brookes, M. J., Hale, J. R., Zumer, J. M., Stevenson, C. M., Francis, S. T., Barnes, G. R., Owen, J. P., Morris, P. G., & Nagarajan, S. S. (2011). Measuring functional connectivity using MEG: Methodology and comparison with fcMRI. *NeuroImage*, *56*(3), 1082–1104. https://doi.org/10.1016/j.neuroimage.2011.02.054

Brookes, M. J., O'Neill, G. C., Hall, E. L., Woolrich, M. W., Baker, A., Palazzo Corner, S., Robson, S. E., Morris, P. G., & Barnes, G. R. (2014). Measuring temporal, spectral and spatial changes in electrophysiological brain network connectivity. *NeuroImage*, *91*, 282–299. https://doi.org/10.1016/j.neuroimage.2013.12.066

Brookes, M. J., Woolrich, M. W., & Barnes, G. R. (2012). Measuring functional connectivity in MEG: A multivariate approach insensitive to linear source leakage. *NeuroImage*, *63*(2), 910–920. https://doi.org/10.1016/j.neuroimage.2012.03.048

Brück, A., Aalto, S., Rauhala, E., Bergman, J., Marttila, R., & Rinne, J. O. (2009). A follow-up study on 6-[18F]fluoro-L-dopa uptake in early Parkinson's disease shows nonlinear progression in the putamen. *Movement Disorders: Official Journal of the Movement Disorder Society*, *24*(7), 1009–1015. https://doi.org/10.1002/mds.22484

Brunner, C., Billinger, M., Seeber, M., Mullen, T. R., & Makeig, S. (2016). Volume Conduction Influences Scalp-Based Connectivity Estimates. *Frontiers in Computational Neuroscience*, *10*, 121. https://doi.org/10.3389/fncom.2016.00121

Burciu, R. G., Chung, J. W., Shukla, P., Ofori, E., Li, H., McFarland, N. R., Okun, M. S., & Vaillancourt, D. E. (2016). Functional MRI of disease progression in Parkinson

disease and atypical parkinsonian syndromes. *Neurology*, *87*(7), 709–717. https://doi.org/10.1212/WNL.0000000000002985

Buzsáki, G., Anastassiou, C. A., & Koch, C. (2012). The origin of extracellular fields and currents—EEG, ECoG, LFP and spikes. *Nature Reviews Neuroscience*, *13*(6), Article 6. https://doi.org/10.1038/nrn3241

Byeon, J., Choi, T. Y., Won, G. H., Lee, J., & Kim, J. W. (2020). A novel quantitative electroencephalography subtype with high alpha power in ADHD: ADHD or misdiagnosed ADHD? *PLOS ONE*, *15*(11), e0242566. https://doi.org/10.1371/journal.pone.0242566

Calabresi, P., Picconi, B., Tozzi, A., Ghiglieri, V., & Di Filippo, M. (2014). Direct and indirect pathways of basal ganglia: A critical reappraisal. *Nature Neuroscience*, *17*(8), Article 8. https://doi.org/10.1038/nn.3743

Cao, J., Zhao, Y., Shan, X., Wei, H.-L., Guo, Y., Chen, L., Erkoyuncu, J. A., & Sarrigiannis, P. G. (2022). Brain functional and effective connectivity based on electroencephalography recordings: A review. *Human Brain Mapping*, *43*(2), 860–879. https://doi.org/10.1002/hbm.25683

Carey, G., Görmezoğlu, M., de Jong, J. J. A., Hofman, P. A. M., Backes, W. H., Dujardin, K., & Leentjens, A. F. G. (2021). Neuroimaging of Anxiety in Parkinson's Disease: A Systematic Review. *Movement Disorders*, *36*(2), 327–339. https://doi.org/10.1002/mds.28404

Carey, G., Lopes, R., Viard, R., Betrouni, N., Kuchcinski, G., Devignes, Q., Defebvre, L., Leentjens, A. F. G., & Dujardin, K. (2020). Anxiety in Parkinson's disease is associated with changes in the brain fear circuit. *Parkinsonism & Related Disorders*, *80*, 89–97. https://doi.org/10.1016/j.parkreldis.2020.09.020

Carmona Arroyave, J. A., Tobón Quintero, C. A., Suárez Revelo, J. J., Ochoa Gómez, J. F., García, Y. B., Gómez, L. M., & Pineda Salazar, D. A. (2019). Resting functional connectivity and mild cognitive impairment in Parkinson's disease. An electroencephalogram study. *Future Neurology*, *14*(2), FNL18. https://doi.org/10.2217/fnl-2018-0048

Cassani, R., Estarellas, M., San-Martin, R., Fraga, F. J., & Falk, T. H. (2018). Systematic Review on Resting-State EEG for Alzheimer's Disease Diagnosis and Progression Assessment. *Disease Markers*, *2018*, 5174815. https://doi.org/10.1155/2018/5174815

Catani, M., & ffytche, D. H. (2005). The rises and falls of disconnection syndromes. *Brain: A Journal of Neurology*, *128*(Pt 10), 2224–2239. https://doi.org/10.1093/brain/awh622

Caviness, J. N., Hentz, J. G., Belden, C. M., Shill, H. A., Driver-Dunckley, E. D., Sabbagh, M. N., Powell, J. J., & Adler, C. H. (2015). Longitudinal EEG Changes Correlate with Cognitive Measure Deterioration in Parkinson's Disease. *Journal of Parkinson's Disease*, *5*(1), 117–124. https://doi.org/10.3233/JPD-140480

Caviness, J. N., Hentz, J. G., Evidente, V. G., Driver-Dunckley, E., Samanta, J., Mahant, P., Connor, D. J., Sabbagh, M. N., Shill, H. A., & Adler, C. H. (2007). Both early and late cognitive dysfunction affects the electroencephalogram in Parkinson's disease. *Parkinsonism & Related Disorders*, *13*(6), 348–354. https://doi.org/10.1016/j.parkreldis.2007.01.003

Caviness, J. N., Utianski, R. L., Hentz, J. G., Beach, T. G., Dugger, B. N., Shill, H. A.,

Driver-Dunckley, E. D., Sabbagh, M. N., Mehta, S., & Adler, C. H. (2016). Differential spectral quantitative electroencephalography patterns between control and Parkinson's disease cohorts. *European Journal of Neurology*, *23*(2), 387–392. https://doi.org/10.1111/ene.12878

Cenci, M. A. (2014). Presynaptic Mechanisms of l-DOPA-Induced Dyskinesia: The Findings, the Debate, and the Therapeutic Implications. *Frontiers in Neurology*, *5*, 242. https://doi.org/10.3389/fneur.2014.00242

Chaturvedi, M., Bogaarts, J. G., Kozak (Cozac), V. V., Hatz, F., Gschwandtner, U., Meyer, A., Fuhr, P., & Roth, V. (2019). Phase lag index and spectral power as QEEG features for identification of patients with mild cognitive impairment in Parkinson's disease. *Clinical Neurophysiology*, *130*(10), 1937–1944. https://doi.org/10.1016/j.clinph.2019.07.017

Chaudhuri, K. R., Healy, D. G., & Schapira, A. H. (2006). Non-motor symptoms of Parkinson's disease: Diagnosis and management. *The Lancet Neurology*, *5*(3), 235–245. https://doi.org/10.1016/S1474-4422(06)70373-8

Chaudhuri, K. R., & Schapira, A. H. V. (2009). Non-motor symptoms of Parkinson's disease: Dopaminergic pathophysiology and treatment. *The Lancet. Neurology*, *8*(5), 464–474. https://doi.org/10.1016/S1474-4422(09)70068-7

Christopher, L., Duff-Canning, S., Koshimori, Y., Segura, B., Boileau, I., Chen, R., Lang, A. E., Houle, S., Rusjan, P., & Strafella, A. P. (2015). Salience network and parahippocampal dopamine dysfunction in memory-impaired Parkinson disease. *Annals of Neurology*, *77*(2), 269–280. https://doi.org/10.1002/ana.24323

Coakeley, S., Martens, K. E., & Almeida, Q. J. (2014). Management of anxiety and motor symptoms in Parkinson's disease. *Expert Review of Neurotherapeutics*, *14*(8), 937–946. https://doi.org/10.1586/14737175.2014.936388

Cohen, D. (1972). Magnetoencephalography: Detection of the Brain's Electrical Activity with a Superconducting Magnetometer. *Science*, *175*(4022), 664–666. https://doi.org/10.1126/science.175.4022.664

Colclough, G. L., Brookes, M. J., Smith, S. M., & Woolrich, M. W. (2015). A symmetric multivariate leakage correction for MEG connectomes. *Neuroimage*, *117*, 439–448. https://doi.org/10.1016/j.neuroimage.2015.03.071

Colclough, G. L., Woolrich, M. W., Tewarie, P. K., Brookes, M. J., Quinn, A. J., & Smith, S. M. (2016). How reliable are MEG resting-state connectivity metrics? *NeuroImage*, *138*, 284–293. https://doi.org/10.1016/j.neuroimage.2016.05.070

Connolly, B., & Fox, S. H. (2014). Treatment of cognitive, psychiatric, and affective disorders associated with Parkinson's disease. *Neurotherapeutics*, *11*(1), 78–91. https://doi.org/10.1007/s13311-013-0238-x

Corti, O., Lesage, S., & Brice, A. (2011). What Genetics Tells us About the Causes and Mechanisms of Parkinson's Disease. *Physiological Reviews*, *91*(4), 1161–1218. https://doi.org/10.1152/physrev.00022.2010

Cozac, V. V., Chaturvedi, M., Hatz, F., Meyer, A., Fuhr, P., & Gschwandtner, U. (2016). Increase of EEG Spectral Theta Power Indicates Higher Risk of the Development of Severe Cognitive Decline in Parkinson's Disease after 3 Years. *Frontiers in Aging Neuroscience*, *8*. https://doi.org/10.3389/fnagi.2016.00284

Cozac, V. V., Gschwandtner, U., Hatz, F., Hardmeier, M., Rüegg, S., & Fuhr, P. (2016). Quantitative EEG and Cognitive Decline in Parkinson's Disease. *Parkinson's Disease*, *2016*, 9060649. https://doi.org/10.1155/2016/9060649

Dadu, A., Satone, V., Kaur, R., Hashemi, S. H., Leonard, H., Iwaki, H., Makarious, M. B., Billingsley, K. J., Bandres-Ciga, S., Sargent, L. J., Noyce, A. J., Daneshmand, A., Blauwendraat, C., Marek, K., Scholz, S. W., Singleton, A. B., Nalls, M. A., Campbell, R. H., & Faghri, F. (2022). Identification and prediction of Parkinson's disease subtypes and progression using machine learning in two cohorts. *Npj Parkinson's Disease*, *8*(1), Article 1. https://doi.org/10.1038/s41531-022-00439-z

Daffre, C., Oliver, K. I., & Pace-Schott, E. F. (2020). Neurocircuitry of Anxiety Disorders. In E. Bui, M. E. Charney, & A. W. Baker (Eds.), *Clinical Handbook of Anxiety Disorders: From Theory to Practice* (pp. 15–41). Springer International Publishing. https://doi.org/10.1007/978-3-030-30687-8_2

Dale, A. M., & Sereno, M. I. (1993). Improved Localizadon of Cortical Activity by Combining EEG and MEG with MRI Cortical Surface Reconstruction: A Linear Approach. *Journal of Cognitive Neuroscience*, *5*(2), 162–176. https://doi.org/10.1162/jocn.1993.5.2.162

Dan, R., Růžička, F., Bezdicek, O., Růžička, E., Roth, J., Vymazal, J., Goelman, G., & Jech, R. (2017). Separate neural representations of depression, anxiety and apathy in Parkinson's disease. *Scientific Reports*, *7*(1), Article 1. https://doi.org/10.1038/s41598-017-12457-6

Dayan, E., & Browner, N. (2017). Alterations in striato-thalamo-pallidal intrinsic functional connectivity as a prodrome of Parkinson's disease. *NeuroImage: Clinical*, *16*, 313–318. https://doi.org/10.1016/j.nicl.2017.08.003

de Aguiar Neto, F. S., & Rosa, J. L. G. (2019). Depression biomarkers using non-invasive EEG: A review. *Neuroscience & Biobehavioral Reviews*, *105*, 83–93. https://doi.org/10.1016/j.neubiorev.2019.07.021

Delgado-Alvarado, M., Gago, B., Navalpotro-Gomez, I., Jiménez-Urbieta, H., & Rodriguez-Oroz, M. C. (2016). Biomarkers for dementia and mild cognitive impairment in Parkinson's disease: Biomarkers and Cognition in Parkinson's Disease. *Movement Disorders*, *31*(6), 861–881. https://doi.org/10.1002/mds.26662

Desikan, R. S., Ségonne, F., Fischl, B., Quinn, B. T., Dickerson, B. C., Blacker, D., Buckner, R. L., Dale, A. M., Maguire, R. P., Hyman, B. T., Albert, M. S., & Killiany, R. J. (2006). An automated labeling system for subdividing the human cerebral cortex on MRI scans into gyral based regions of interest. *NeuroImage*, *31*(3), Article 3. https://doi.org/10.1016/j.neuroimage.2006.01.021

Destrieux, C., Fischl, B., Dale, A., & Halgren, E. (2010). Automatic parcellation of human cortical gyri and sulci using standard anatomical nomenclature. *NeuroImage*, *53*(1), 1–15. https://doi.org/10.1016/j.neuroimage.2010.06.010

Deuschl, G., & Agid, Y. (2013). Subthalamic neurostimulation for Parkinson's disease with early fluctuations: Balancing the risks and benefits. *The Lancet. Neurology*, *12*(10), 1025–1034. https://doi.org/10.1016/S1474-4422(13)70151-0

Devignes, Q., Lopes, R., & Dujardin, K. (2022). Neuroimaging outcomes associated with mild cognitive impairment subtypes in Parkinson's disease: A systematic review.

Parkinsonism & Related Disorders, *95*, 122–137. https://doi.org/10.1016/j.parkreldis.2022.02.006

Dickson, D. W. (2018). Neuropathology of Parkinson disease. *Parkinsonism & Related Disorders*, *46 Suppl 1*(Suppl 1), S30–S33. https://doi.org/10.1016/j.parkreldis.2017.07.033

Dickson, D. W., Braak, H., Duda, J. E., Duyckaerts, C., Gasser, T., Halliday, G. M., Hardy, J., Leverenz, J. B., Del Tredici, K., Wszolek, Z. K., & Litvan, I. (2009). Neuropathological assessment of Parkinson's disease: Refining the diagnostic criteria. *The Lancet Neurology*, *8*(12), 1150–1157. https://doi.org/10.1016/S1474-4422(09)70238-8

Díez-Cirarda, M., Strafella, A. P., Kim, J., Peña, J., Ojeda, N., Cabrera-Zubizarreta, A., & Ibarretxe-Bilbao, N. (2018). Dynamic functional connectivity in Parkinson's disease patients with mild cognitive impairment and normal cognition. *NeuroImage. Clinical*, *17*, 847–855. https://doi.org/10.1016/j.nicl.2017.12.013

Dijkstra, A. A., Voorn, P., Berendse, H. W., Groenewegen, H. J., Netherlands Brain Bank, Rozemuller, A. J. M., & van de Berg, W. D. J. (2014). Stage-dependent nigral neuronal loss in incidental Lewy body and Parkinson's disease. *Movement Disorders: Official Journal of the Movement Disorder Society*, *29*(10), 1244–1251. https://doi.org/10.1002/mds.25952

Dissanayaka, N. N. N. W., White, E., O'Sullivan, J. D., Marsh, R., Pachana, N. A., & Byrne, G. J. (2014). The clinical spectrum of anxiety in Parkinson's disease. *Movement Disorders*, *29*(8), 967–975. https://doi.org/10.1002/mds.25937

Dissanayaka, N. N. W., Lawson, R. A., Yarnall, A. J., Duncan, G. W., Breen, D. P., Khoo, T. K., Barker, R. A., & Burn, D. J. (2017). Anxiety is associated with cognitive impairment in newly-diagnosed Parkinson's disease. *Parkinsonism & Related Disorders*, *36*, 63–68. https://doi.org/10.1016/j.parkreldis.2017.01.001

Dissanayaka, N. N. W., Sellbach, A., Matheson, S., O'Sullivan, J. D., Silburn, P. A., Byrne, G. J., Marsh, R., & Mellick, G. D. (2010). Anxiety disorders in Parkinson's disease: Prevalence and risk factors. *Movement Disorders*, *25*(7), 838–845. https://doi.org/10.1002/mds.22833

Djaldetti, R., Ziv, I., & Melamed, E. (2006). The mystery of motor asymmetry in Parkinson's disease. *The Lancet Neurology*, *5*(9), 796–802. https://doi.org/10.1016/S1474-4422(06)70549-X

Dorsey, E. R., Sherer, T., Okun, M. S., & Bloem, B. R. (2018). The Emerging Evidence of the Parkinson Pandemic. *Journal of Parkinson's Disease*, *8*(s1), S3–S8. https://doi.org/10.3233/JPD-181474

Dovzhenok, A., & Rubchinsky, L. L. (2012). On the Origin of Tremor in Parkinson's Disease. *PLOS ONE*, *7*(7), e41598. https://doi.org/10.1371/journal.pone.0041598

Dubbelink, K. T. E. O., Hillebrand, A., Twisk, J. W. R., Deijen, J. B., Stoffers, D., Schmand, B. A., Stam, C. J., & Berendse, H. W. (2014). Predicting dementia in Parkinson disease by combining neurophysiologic and cognitive markers. *Neurology*, *82*(3), 263–270. https://doi.org/10.1212/WNL.0000000000000034

Dugger, B. N., & Dickson, D. W. (2017). Pathology of Neurodegenerative Diseases. *Cold Spring Harbor Perspectives in Biology*, *9*(7), a028035.

https://doi.org/10.1101/cshperspect.a028035
Dukic, S., McMackin, R., Costello, E., Metzger, M., Buxo, T., Fasano, A., Chipika, R., Pinto-Grau, M., Schuster, C., Hammond, M., Heverin, M., Coffey, A., Broderick, M., Iyer, P. M., Mohr, K., Gavin, B., McLaughlin, R., Pender, N., Bede, P., … Nasseroleslami, B. (2021). Resting-state EEG reveals four subphenotypes of amyotrophic lateral sclerosis. *Brain*, awab322. https://doi.org/10.1093/brain/awab322
Ehgoetz Martens, K. A., Silveira, C. R. A., Intzandt, B. N., & Almeida, Q. J. (2018). State anxiety predicts cognitive performance in patients with Parkinson's disease. *Neuropsychology*, *32*, 950–957. https://doi.org/10.1037/neu0000478
Eichel, H. von, Heine, J., Wegner, F., Rogozinski, S., Stiel, S., Groh, A., Krey, L., Höglinger, G. U., & Klietz, M. (2022). Neuropsychiatric Symptoms in Parkinson's Disease Patients Are Associated with Reduced Health-Related Quality of Life and Increased Caregiver Burden. *Brain Sciences*, *12*(1), Article 1. https://doi.org/10.3390/brainsci12010089
Ellmore, T. M., Castriotta, R. J., Hendley, K. L., Aalbers, B. M., Furr-Stimming, E., Hood, A. J., Suescun, J., Beurlot, M. R., Hendley, R. T., & Schiess, M. C. (2013). Altered Nigrostriatal and Nigrocortical Functional Connectivity in Rapid Eye Movement Sleep Behavior Disorder. *Sleep*, *36*(12), 1885–1892. https://doi.org/10.5665/sleep.3222
Emre, M., Aarsland, D., Brown, R., Burn, D. J., Duyckaerts, C., Mizuno, Y., Broe, G. A., Cummings, J., Dickson, D. W., Gauthier, S., Goldman, J., Goetz, C., Korczyn, A., Lees, A., Levy, R., Litvan, I., McKeith, I., Olanow, W., Poewe, W., … Dubois, B. (2007). Clinical diagnostic criteria for dementia associated with Parkinson's disease. *Movement Disorders: Official Journal of the Movement Disorder Society*, *22*(12), 1689–1707; quiz 1837. https://doi.org/10.1002/mds.21507
Erro, R., Vitale, C., Amboni, M., Picillo, M., Moccia, M., Longo, K., Santangelo, G., De Rosa, A., Allocca, R., Giordano, F., Orefice, G., De Michele, G., Santoro, L., Pellecchia, M. T., & Barone, P. (2013). The Heterogeneity of Early Parkinson's Disease: A Cluster Analysis on Newly Diagnosed Untreated Patients. *PLoS ONE*, *8*(8), e70244. https://doi.org/10.1371/journal.pone.0070244
Espay, A., Brundin, P., & Lang, A. (2017). Precision medicine for disease modification in Parkinson disease. *Nature Reviews. Neurology*, *13*. https://doi.org/10.1038/nrneurol.2016.196
Espay, A. J., Kalia, L. V., Gan-Or, Z., Williams-Gray, C. H., Bedard, P. L., Rowe, S. M., Morgante, F., Fasano, A., Stecher, B., Kauffman, M. A., Farrer, M. J., Coffey, C. S., Schwarzschild, M. A., Sherer, T., Postuma, R. B., Strafella, A. P., Singleton, A. B., Barker, R. A., Kieburtz, K., … Lang, A. E. (2020). Disease modification and biomarker development in Parkinson disease: Revision or reconstruction? *Neurology*, *94*(11), 481–494. https://doi.org/10.1212/WNL.0000000000009107
Espay, A. J., & Marras, C. (2019). Clinical Parkinson disease subtyping does not predict pathology. *Nature Reviews Neurology*, *15*(4), Article 4. https://doi.org/10.1038/s41582-019-0153-9
Espay, A. J., Schwarzschild, M. A., Tanner, C. M., Fernandez, H. H., Simon, D. K., Leverenz, J. B., Merola, A., Chen-Plotkin, A., Brundin, P., Kauffman, M. A., Erro,

R., Kieburtz, K., Woo, D., Macklin, E. A., Standaert, D. G., & Lang, A. E. (2017). Biomarker-driven phenotyping in Parkinson disease: A translational missing link in disease-modifying clinical trials. *Movement Disorders : Official Journal of the Movement Disorder Society*, *32*(3), 319–324. https://doi.org/10.1002/mds.26913

Espay, A., & Stecher, B. (2020). *Brain Fables: The Hidden History of Neurodegenerative Diseases and a Blueprint to Conquer Them*. Cambridge University Press.

Esposito, F., Tessitore, A., Giordano, A., De Micco, R., Paccone, A., Conforti, R., Pignataro, G., Annunziato, L., & Tedeschi, G. (2013). Rhythm-specific modulation of the sensorimotor network in drug-naive patients with Parkinson's disease by levodopa. *Brain: A Journal of Neurology*, *136*(Pt 3), 710–725. https://doi.org/10.1093/brain/awt007

Fan, L., Li, H., Zhuo, J., Zhang, Y., Wang, J., Chen, L., Yang, Z., Chu, C., Xie, S., Laird, A. R., Fox, P. T., Eickhoff, S. B., Yu, C., & Jiang, T. (2016). The Human Brainnetome Atlas: A New Brain Atlas Based on Connectional Architecture. *Cerebral Cortex (New York, NY)*, *26*(8), 3508–3526. https://doi.org/10.1093/cercor/bhw157

Farrow, S. L., Cooper, A. A., & O'Sullivan, J. M. (2022). Redefining the hypotheses driving Parkinson's diseases research. *Npj Parkinson's Disease*, *8*(1), Article 1. https://doi.org/10.1038/s41531-022-00307-w

Feigin, V. L., Abajobir, A. A., Abate, K. H., Abd-Allah, F., Abdulle, A. M., Abera, S. F., Abyu, G. Y., Ahmed, M. B., Aichour, A. N., Aichour, I., Aichour, M. T. E., Akinyemi, R. O., Alabed, S., Al-Raddadi, R., Alvis-Guzman, N., Amare, A. T., Ansari, H., Anwari, P., Ärnlöv, J., … Vos, T. (2017). Global, regional, and national burden of neurological disorders during 1990–2015: A systematic analysis for the Global Burden of Disease Study 2015. *The Lancet Neurology*, *16*(11), 877–897. https://doi.org/10.1016/S1474-4422(17)30299-5

Fereshtehnejad, S.-M., Romenets, S. R., Anang, J. B. M., Latreille, V., Gagnon, J.-F., & Postuma, R. B. (2015). New Clinical Subtypes of Parkinson Disease and Their Longitudinal Progression: A Prospective Cohort Comparison With Other Phenotypes. *JAMA Neurology*, *72*(8), 863–873. https://doi.org/10.1001/jamaneurol.2015.0703

Fereshtehnejad, S.-M., Zeighami, Y., Dagher, A., & Postuma, R. B. (2017). Clinical criteria for subtyping Parkinson's disease: Biomarkers and longitudinal progression. *Brain*, *140*(7), 1959–1976. https://doi.org/10.1093/brain/awx118

Filippi, M., Basaia, S., Sarasso, E., Stojkovic, T., Stankovic, I., Fontana, A., Tomic, A., Piramide, N., Stefanova, E., Markovic, V., Kostic, V. S., & Agosta, F. (2020). Longitudinal brain connectivity changes and clinical evolution in Parkinson's disease. *Molecular Psychiatry*. https://doi.org/10.1038/s41380-020-0770-0

Finger, H., Bönstrup, M., Cheng, B., Messé, A., Hilgetag, C., Thomalla, G., Gerloff, C., & König, P. (2016). Modeling of Large-Scale Functional Brain Networks Based on Structural Connectivity from DTI: Comparison with EEG Derived Phase Coupling Networks and Evaluation of Alternative Methods along the Modeling Path. *PLOS Computational Biology*, *12*(8), e1005025. https://doi.org/10.1371/journal.pcbi.1005025

Fiorenzato, E., Biundo, R., Cecchin, D., Frigo, A. C., Kim, J., Weis, L., Strafella, A. P., & Antonini, A. (2018). Brain Amyloid Contribution to Cognitive Dysfunction in Early-

Stage Parkinson's Disease: The PPMI Dataset. *Journal of Alzheimer's Disease*, *66*(1), 229–237. https://doi.org/10.3233/JAD-180390

Follett, K. A., Weaver, F. M., Stern, M., Hur, K., Harris, C. L., Luo, P., Marks, W. J., Rothlind, J., Sagher, O., Moy, C., Pahwa, R., Burchiel, K., Hogarth, P., Lai, E. C., Duda, J. E., Holloway, K., Samii, A., Horn, S., Bronstein, J. M., … CSP 468 Study Group. (2010). Pallidal versus subthalamic deep-brain stimulation for Parkinson's disease. *The New England Journal of Medicine*, *362*(22), 2077–2091. https://doi.org/10.1056/NEJMoa0907083

Foltynie, T., & Hariz, M. I. (2010). Surgical management of Parkinson's disease. *Expert Review of Neurotherapeutics*, *10*(6), 903–914. https://doi.org/10.1586/ern.10.68

Fonseca, L. C., Tedrus, G. M. a. S., Letro, G. H., & Bossoni, A. S. (2009). Dementia, mild cognitive impairment and quantitative EEG in patients with Parkinson's disease. *Clinical EEG and Neuroscience*, *40*(3), 168–172. https://doi.org/10.1177/155005940904000309

Fornito, A., & Bullmore, E. T. (2015). Connectomics: A new paradigm for understanding brain disease. *European Neuropsychopharmacology*, *25*(5), 733–748. https://doi.org/10.1016/j.euroneuro.2014.02.011

Fornito, A., Zalesky, A., & Breakspear, M. (2015). The connectomics of brain disorders. *Nature Reviews Neuroscience*, *16*(3), 159–172. https://doi.org/10.1038/nrn3901

Fornito, A., Zalesky, A., & Bullmore, E. T. (Eds.). (2016). Fundamentals of Brain Network Analysis. In *Fundamentals of Brain Network Analysis* (pp. i–ii). Academic Press. https://doi.org/10.1016/B978-0-12-407908-3.09996-9

Fox, M. D., & Raichle, M. E. (2007). Spontaneous fluctuations in brain activity observed with functional magnetic resonance imaging. *Nature Reviews Neuroscience*, *8*(9), Article 9. https://doi.org/10.1038/nrn2201

Fox, S. H., Katzenschlager, R., Lim, S.-Y., Ravina, B., Seppi, K., Coelho, M., Poewe, W., Rascol, O., Goetz, C. G., & Sampaio, C. (2011). The Movement Disorder Society Evidence-Based Medicine Review Update: Treatments for the motor symptoms of Parkinson's disease. *Movement Disorders: Official Journal of the Movement Disorder Society*, *26 Suppl 3*, S2-41. https://doi.org/10.1002/mds.23829

Fraga González, G., Van der Molen, M. J. W., Žarić, G., Bonte, M., Tijms, J., Blomert, L., Stam, C. J., & Van der Molen, M. W. (2016). Graph analysis of EEG resting state functional networks in dyslexic readers. *Clinical Neurophysiology*, *127*(9), 3165–3175. https://doi.org/10.1016/j.clinph.2016.06.023

Frankemolle, A. M. M., Wu, J., Noecker, A. M., Voelcker-Rehage, C., Ho, J. C., Vitek, J. L., McIntyre, C. C., & Alberts, J. L. (2010). Reversing cognitive–motor impairments in Parkinson's disease patients using a computational modelling approach to deep brain stimulation programming. *Brain*, *133*(3), 746–761. https://doi.org/10.1093/brain/awp315

Friston, K. J. (2011). Functional and effective connectivity: A review. *Brain Connectivity*, *1*(1), 13–36. https://doi.org/10.1089/brain.2011.0008

Fuchs, M., Wagner, M., Köhler, T., & Wischmann, H. A. (1999). Linear and nonlinear current density reconstructions. *Journal of Clinical Neurophysiology: Official Publication of the American Electroencephalographic Society*, *16*(3), 267–295.

https://doi.org/10.1097/00004691-199905000-00006
Garcia-Ruiz, P. J., Chaudhuri, K. R., & Martinez-Martin, P. (2014). Non-motor symptoms of Parkinson's disease A review…from the past. *Journal of the Neurological Sciences*, *338*(1), 30–33. https://doi.org/10.1016/j.jns.2014.01.002
Gasca-Salas, C., García-Lorenzo, D., Garcia-Garcia, D., Clavero, P., Obeso, J. A., Lehericy, S., & Rodríguez-Oroz, M. C. (2019). Parkinson's disease with mild cognitive impairment: Severe cortical thinning antedates dementia. *Brain Imaging and Behavior*, *13*(1), 180–188. https://doi.org/10.1007/s11682-017-9751-6
Geraedts, V. J., Boon, L. I., Marinus, J., Gouw, A. A., van Hilten, J. J., Stam, C. J., Tannemaat, M. R., & Contarino, M. F. (2018). Clinical correlates of quantitative EEG in Parkinson disease: A systematic review. *Neurology*, *91*(19), 871–883. https://doi.org/10.1212/WNL.0000000000006473
Goedert, M., Spillantini, M. G., Del Tredici, K., & Braak, H. (2013). 100 years of Lewy pathology. *Nature Reviews. Neurology*, *9*(1), 13–24. https://doi.org/10.1038/nrneurol.2012.242
Goetz, C. G. (2011). The History of Parkinson's Disease: Early Clinical Descriptions and Neurological Therapies. *Cold Spring Harbor Perspectives in Medicine*, *1*(1), a008862. https://doi.org/10.1101/cshperspect.a008862
Goldenberg, M. M. (2008). Medical Management of Parkinson's Disease. *Pharmacy and Therapeutics*, *33*(10), 590–606.
Goldman, J., & Litvan, I. (2011). Mild Cognitive Impairment in Parkinson's Disease. *Minerva Medica*, *102*, 441–459.
Goldman, S. M. (2014). Environmental Toxins and Parkinson's Disease. *Annual Review of Pharmacology and Toxicology*, *54*(1), 141–164. https://doi.org/10.1146/annurev-pharmtox-011613-135937
Goldman, S. M., Marek, K., Ottman, R., Meng, C., Comyns, K., Chan, P., Ma, J., Marras, C., Langston, J. W., Ross, G. W., & Tanner, C. M. (2019). Concordance for Parkinson's disease in twins: A 20-year update. *Annals of Neurology*, *85*(4), 600–605. https://doi.org/10.1002/ana.25441
Gomes, M. da M., & Engelhardt, E. (2013). Jean-Martin Charcot, father of modern neurology: An homage 120 years after his death. *Arquivos de Neuro-Psiquiatria*, *71*, 815–817. https://doi.org/10.1590/0004-282X20130128
Gonzalez-Latapi, P., Bayram, E., Litvan, I., & Marras, C. (2021). Cognitive Impairment in Parkinson's Disease: Epidemiology, Clinical Profile, Protective and Risk Factors. *Behavioral Sciences*, *11*(5), Article 5. https://doi.org/10.3390/bs11050074
González-Redondo, R., García-García, D., Clavero, P., Gasca-Salas, C., García-Eulate, R., Zubieta, J. L., Arbizu, J., Obeso, J. A., & Rodríguez-Oroz, M. C. (2014). Grey matter hypometabolism and atrophy in Parkinson's disease with cognitive impairment: A two-step process. *Brain*, *137*(8), 2356–2367. https://doi.org/10.1093/brain/awu159
Gowers William R. (1899). Paralysis agitans. *Macmillan*.
Gramfort, A., Papadopoulo, T., Olivi, E., & Clerc, M. (2010). OpenMEEG: Opensource software for quasistatic bioelectromagnetics. *BioMedical Engineering OnLine*, *9*(1), Article 1. https://doi.org/10.1186/1475-925X-9-45
Grech, R., Cassar, T., Muscat, J., Camilleri, K. P., Fabri, S. G., Zervakis, M., Xanthopoulos,

P., Sakkalis, V., & Vanrumste, B. (2008). Review on solving the inverse problem in EEG source analysis. *Journal of NeuroEngineering and Rehabilitation*, *5*(1), 25. https://doi.org/10.1186/1743-0003-5-25

Greenfield, J. G., & Bosanquet, F. D. (1953). THE BRAIN-STEM LESIONS IN PARKINSONISM. *Journal of Neurology, Neurosurgery & Psychiatry*, *16*(4), 213–226. https://doi.org/10.1136/jnnp.16.4.213

Halder, T., Talwar, S., Jaiswal, A. K., & Banerjee, A. (2019). Quantitative Evaluation in Estimating Sources Underlying Brain Oscillations Using Current Source Density Methods and Beamformer Approaches. *ENeuro*, *6*(4), ENEURO.0170-19.2019. https://doi.org/10.1523/ENEURO.0170-19.2019

Hall, C. N., Howarth, C., Kurth-Nelson, Z., & Mishra, A. (2016). Interpreting BOLD: Towards a dialogue between cognitive and cellular neuroscience. *Philosophical Transactions of the Royal Society of London. Series B, Biological Sciences*, *371*(1705), 20150348. https://doi.org/10.1098/rstb.2015.0348

Hämäläinen, M. S., & Ilmoniemi, R. J. (1994). Interpreting magnetic fields of the brain: Minimum norm estimates. *Medical & Biological Engineering & Computing*, *32*(1), Article 1. https://doi.org/10.1007/BF02512476

Han, C.-X., Wang, J., Yi, G.-S., & Che, Y.-Q. (2013). Investigation of EEG abnormalities in the early stage of Parkinson's disease. *Cognitive Neurodynamics*, *7*(4), 351–359. https://doi.org/10.1007/s11571-013-9247-z

Hartley, C. A., & Phelps, E. A. (2010). Changing fear: The neurocircuitry of emotion regulation. *Neuropsychopharmacology: Official Publication of the American College of Neuropsychopharmacology*, *35*(1), 136–146. https://doi.org/10.1038/npp.2009.121

Hartmann, C. J., Fliegen, S., Groiss, S. J., Wojtecki, L., & Schnitzler, A. (2019). An update on best practice of deep brain stimulation in Parkinson's disease. *Therapeutic Advances in Neurological Disorders*, *12*, 1756286419838096. https://doi.org/10.1177/1756286419838096

Hassan, M., Chaton, L., Benquet, P., Delval, A., Leroy, C., Plomhause, L., Moonen, A. J. H., Duits, A. A., Leentjens, A. F. G., van Kranen-Mastenbroek, V., Defebvre, L., Derambure, P., Wendling, F., & Dujardin, K. (2017). Functional connectivity disruptions correlate with cognitive phenotypes in Parkinson's disease. *NeuroImage: Clinical*, *14*, 591–601. https://doi.org/10.1016/j.nicl.2017.03.002

Hassan, M., Dufor, O., Merlet, I., Berrou, C., & Wendling, F. (2014). EEG source connectivity analysis: From dense array recordings to brain networks. *PloS One*, *9*(8), e105041.

Hassan, M., Merlet, I., Mheich, A., Kabbara, A., Biraben, A., Nica, A., & Wendling, F. (2017). Identification of interictal epileptic networks from dense-EEG. *Brain Topography*, *30*(1), 60–76.

Hassan, M., & Wendling, F. (2018). Electroencephalography Source Connectivity: Aiming for High Resolution of Brain Networks in Time and Space. *IEEE Signal Processing Magazine*, *35*(3), 81–96. https://doi.org/10.1109/MSP.2017.2777518

He, B., Sohrabpour, A., Brown, E., & Liu, Z. (2018). Electrophysiological Source Imaging: A Noninvasive Window to Brain Dynamics. *Annual Review of Biomedical Engineering*, *20*, 171–196. https://doi.org/10.1146/annurev-bioeng-062117-120853

Hedrich, T., Pellegrino, G., Kobayashi, E., Lina, J. M., & Grova, C. (2017). Comparison of the spatial resolution of source imaging techniques in high-density EEG and MEG. *NeuroImage*, *157*, 531–544. https://doi.org/10.1016/j.neuroimage.2017.06.022

Heinrichs-Graham, E., Santamaria, P. M., Gendelman, H. E., & Wilson, T. W. (2017). The cortical signature of symptom laterality in Parkinson's disease. *NeuroImage: Clinical*, *14*, 433–440. https://doi.org/10.1016/j.nicl.2017.02.010

Heisz, J. J., & McIntosh, A. R. (2013). Applications of EEG Neuroimaging Data: Event-related Potentials, Spectral Power, and Multiscale Entropy. *Journal of Visualized Experiments : JoVE*, *76*, 50131. https://doi.org/10.3791/50131

Heller, J., Brcina, N., Dogan, I., Holtbernd, F., Romanzetti, S., Schulz, J. B., Schiefer, J., & Reetz, K. (2017). Brain imaging findings in idiopathic REM sleep behavior disorder (RBD) – A systematic review on potential biomarkers for neurodegeneration. *Sleep Medicine Reviews*, *34*, 23–33. https://doi.org/10.1016/j.smrv.2016.06.006

Helmich, R. C., Thaler, A., van Nuenen, B. F. L., Gurevich, T., Mirelman, A., Marder, K. S., Bressman, S., Orr-Urtreger, A., Giladi, N., Bloem, B. R., Toni, I., & LRRK2 Ashkenazi Jewish Consortium. (2015). Reorganization of corticostriatal circuits in healthy G2019S LRRK2 carriers. *Neurology*, *84*(4), 399–406. https://doi.org/10.1212/WNL.0000000000001189

Hiseman, J. P., & Fackrell, R. (2017). Chapter Fourteen—Caregiver Burden and the Nonmotor Symptoms of Parkinson's Disease. In K. R. Chaudhuri & N. Titova (Eds.), *International Review of Neurobiology* (Vol. 133, pp. 479–497). Academic Press. https://doi.org/10.1016/bs.irn.2017.05.035

Hoehn M.M., & Yahr M.D. (1976). Parkinsonism: Onset, progression, and mortality. *Neurology*, *17; 427*.

Howell, M. J., & Schenck, C. H. (2015). Rapid Eye Movement Sleep Behavior Disorder and Neurodegenerative Disease. *JAMA Neurology*, *72*(6), 707–712. https://doi.org/10.1001/jamaneurol.2014.4563

Huang, Y., Zhang, J., Cui, Y., Yang, G., Liu, Q., & Yin, G. (2018). Sensor Level Functional Connectivity Topography Comparison Between Different References Based EEG and MEG. *Frontiers in Behavioral Neuroscience*, *12*. https://www.frontiersin.org/articles/10.3389/fnbeh.2018.00096

Hubert, L., & Arabie, P. (1985). Comparing partitions. *Journal of Classification*, *2*(1), 193–218. https://doi.org/10.1007/BF01908075

Ibarretxe-Bilbao, N., Junque, C., Segura, B., Baggio, H. C., Marti, M. J., Valldeoriola, F., Bargallo, N., & Tolosa, E. (2012). Progression of cortical thinning in early Parkinson's disease: Cortical Thinning in Early PD. *Movement Disorders*, *27*(14), 1746–1753. https://doi.org/10.1002/mds.25240

Iranzo, A., Fernández-Arcos, A., Tolosa, E., Serradell, M., Molinuevo, J. L., Valldeoriola, F., Gelpi, E., Vilaseca, I., Sánchez-Valle, R., Lladó, A., Gaig, C., & Santamaría, J. (2014). Neurodegenerative Disorder Risk in Idiopathic REM Sleep Behavior Disorder: Study in 174 Patients. *PLOS ONE*, *9*(2), e89741. https://doi.org/10.1371/journal.pone.0089741

Iranzo, A., Valldeoriola, F., Lomeña, F., Molinuevo, J. L., Serradell, M., Salamero, M., Cot, A., Ros, D., Pavía, J., Santamaria, J., & Tolosa, E. (2011). Serial dopamine

transporter imaging of nigrostriatal function in patients with idiopathic rapid-eye-movement sleep behaviour disorder: A prospective study. *The Lancet. Neurology*, *10*(9), 797–805. https://doi.org/10.1016/S1474-4422(11)70152-1

Ishihara, L., & Brayne, C. (2006). A systematic review of depression and mental illness preceding Parkinson's disease. *Acta Neurologica Scandinavica*, *113*(4), 211–220. https://doi.org/10.1111/j.1600-0404.2006.00579.x

Jacobs, G. R., Voineskos, A. N., Hawco, C., Stefanik, L., Forde, N. J., Dickie, E. W., Lai, M.-C., Szatmari, P., Schachar, R., Crosbie, J., Arnold, P. D., Goldenberg, A., Erdman, L., & Ameis, S. H. (2021). Integration of brain and behavior measures for identification of data-driven groups cutting across children with ASD, ADHD, or OCD. *Neuropsychopharmacology*, *46*(3), Article 3. https://doi.org/10.1038/s41386-020-00902-6

Jankovic, J. (2008). Parkinson's disease: Clinical features and diagnosis. *Journal of Neurology, Neurosurgery, and Psychiatry*, *79*(4), 368–376. https://doi.org/10.1136/jnnp.2007.131045

Jeong, J. (2004). EEG dynamics in patients with Alzheimer's disease. *Clinical Neurophysiology*, *115*(7), Article 7. https://doi.org/10.1016/j.clinph.2004.01.001

Jm Charcot, C. (1861). De la paralysie agitante. *Gaz Hebdomadaire Med Chir*, *8*, 765–767.

Joling, M., van den Heuvel, O. A., Berendse, H. W., Booij, J., & Vriend, C. (2018). Serotonin transporter binding and anxiety symptoms in Parkinson's disease. *Journal of Neurology, Neurosurgery, and Psychiatry*, *89*(1), 89–94. https://doi.org/10.1136/jnnp-2017-316193

Jones, S., Torsney, K. M., Scourfield, L., Berryman, K., & Henderson, E. J. (2020). Neuropsychiatric symptoms in Parkinson's disease: Aetiology, diagnosis and treatment. *BJPsych Advances*, *26*(6), 333–342. https://doi.org/10.1192/bja.2019.79

Kabbara, A., Forde, N., Maumet, C., & Hassan, M. (2022). *Successful reproduction of a large EEG study across software packages* (p. 2022.08.03.502683). bioRxiv. https://doi.org/10.1101/2022.08.03.502683

Kalia, L. V., & Lang, A. E. (2015). Parkinson's disease. *Lancet (London, England)*, *386*(9996), 896–912. https://doi.org/10.1016/S0140-6736(14)61393-3

Kang, J.-H., Irwin, D. J., Chen-Plotkin, A. S., Siderowf, A., Caspell, C., Coffey, C. S., Waligórska, T., Taylor, P., Pan, S., Frasier, M., Marek, K., Kieburtz, K., Jennings, D., Simuni, T., Tanner, C. M., Singleton, A., Toga, A. W., Chowdhury, S., Mollenhauer, B., … Shaw, L. M. (2013). Association of Cerebrospinal Fluid β-Amyloid 1-42, T-tau, P-tau181, and α-Synuclein Levels With Clinical Features of Drug-Naive Patients With Early Parkinson Disease. *JAMA Neurology*, *70*(10), 1277–1287. https://doi.org/10.1001/jamaneurol.2013.3861

Kang, J.-H., Mollenhauer, B., Coffey, C. S., Toledo, J. B., Weintraub, D., Galasko, D. R., Irwin, D. J., Van Deerlin, V., Chen-Plotkin, A. S., Caspell-Garcia, C., Waligórska, T., Taylor, P., Shah, N., Pan, S., Zero, P., Frasier, M., Marek, K., Kieburtz, K., Jennings, D., … The Parkinson's Progression Marker Initiative. (2016). CSF biomarkers associated with disease heterogeneity in early Parkinson's disease: The Parkinson's Progression Markers Initiative study. *Acta Neuropathologica*, *131*(6), 935–949. https://doi.org/10.1007/s00401-016-1552-2

Kenborg, L., Rugbjerg, K., Lee, P.-C., Ravnskjær, L., Christensen, J., Ritz, B., & Lassen, C. F. (2015). Head injury and risk for Parkinson disease: Results from a Danish case-control study. *Neurology*, *84*(11), 1098–1103. https://doi.org/10.1212/WNL.0000000000001362

Kim, D.-W., & Im, C.-H. (2018). EEG Spectral Analysis. In C.-H. Im (Ed.), *Computational EEG Analysis: Methods and Applications* (pp. 35–53). Springer. https://doi.org/10.1007/978-981-13-0908-3_3

Klassen, B. T., Hentz, J. G., Shill, H. A., Driver-Dunckley, E., Evidente, V. G. H., Sabbagh, M. N., Adler, C. H., & Caviness, J. N. (2011). Quantitative EEG as a predictive biomarker for Parkinson disease dementia. *Neurology*, *77*(2), 118–124. https://doi.org/10.1212/WNL.0b013e318224af8d

Kordower, J. H., Olanow, C. W., Dodiya, H. B., Chu, Y., Beach, T. G., Adler, C. H., Halliday, G. M., & Bartus, R. T. (2013). Disease duration and the integrity of the nigrostriatal system in Parkinson's disease. *Brain*, *136*(8), 2419–2431. https://doi.org/10.1093/brain/awt192

Lachaux, J.-P., Rodriguez, E., Martinerie, J., & Varela, F. J. (1999). Measuring phase synchrony in brain signals. *Human Brain Mapping*, *8*(4), 194–208. https://doi.org/10.1002/(SICI)1097-0193(1999)8:4<194::AID-HBM4>3.0.CO;2-C

Lai, M., Demuru, M., Hillebrand, A., & Fraschini, M. (2018). A comparison between scalp- and source-reconstructed EEG networks. *Scientific Reports*, *8*(1), Article 1. https://doi.org/10.1038/s41598-018-30869-w

Lancichinetti, A., & Fortunato, S. (2012). Consensus clustering in complex networks. *Scientific Reports*, *2*(1), Article 1. https://doi.org/10.1038/srep00336

Landau, S., Harris, V., Burn, D. J., Hindle, J. V., Hurt, C. S., Samuel, M., Wilson, K. C., & Brown, R. G. (2016). Anxiety and anxious-depression in Parkinson's disease over a 4-year period: A latent transition analysis. *Psychological Medicine*, *46*(3), 657–667. https://doi.org/10.1017/S0033291715002196

Latreille, V., Carrier, J., Gaudet-Fex, B., Rodrigues-Brazète, J., Panisset, M., Chouinard, S., Postuma, R. B., & Gagnon, J.-F. (2016). Electroencephalographic prodromal markers of dementia across conscious states in Parkinson's disease. *Brain: A Journal of Neurology*, *139*(Pt 4), 1189–1199. https://doi.org/10.1093/brain/aww018

Lawton, M., Ben-Shlomo, Y., May, M. T., Baig, F., Barber, T. R., Klein, J. C., Swallow, D. M. A., Malek, N., Grosset, K. A., Bajaj, N., Barker, R. A., Williams, N., Burn, D. J., Foltynie, T., Morris, H. R., Wood, N. W., Grosset, D. G., & Hu, M. T. M. (2018). Developing and validating Parkinson's disease subtypes and their motor and cognitive progression. *Journal of Neurology, Neurosurgery & Psychiatry*, *89*(12), 1279–1287. https://doi.org/10.1136/jnnp-2018-318337

Leaver, K., & Poston, K. L. (2015). Do CSF Biomarkers Predict Progression to Cognitive Impairment in Parkinson's disease patients? A Systematic Review. *Neuropsychology Review*, *25*(4), 411–423. https://doi.org/10.1007/s11065-015-9307-8

Leentjens, A. F. G., Dujardin, K., Marsh, L., Richard, I. H., Starkstein, S. E., & Martinez-Martin, P. (2011). Anxiety rating scales in Parkinson's disease: A validation study of the Hamilton anxiety rating scale, the Beck anxiety inventory, and the hospital anxiety and depression scale. *Movement Disorders: Official Journal of the Movement*

Disorder Society, *26*(3), 407–415. https://doi.org/10.1002/mds.23184

Lees, A. J. (2007). Unresolved issues relating to the Shaking Palsy on the celebration of James Parkinson's 250th birthday. *Movement Disorders*, *22*(S17), S327–S334. https://doi.org/10.1002/mds.21684

Lees, A. J., Hardy, J., & Revesz, T. (2009). Parkinson's disease. *Lancet (London, England)*, *373*(9680), 2055–2066. https://doi.org/10.1016/S0140-6736(09)60492-X

LeWitt, P. A., & Fahn, S. (2016). Levodopa therapy for Parkinson disease: A look backward and forward. *Neurology*, *86*(14 Suppl 1), S3-12. https://doi.org/10.1212/WNL.0000000000002509

Limousin, P., & Foltynie, T. (2019). Long-term outcomes of deep brain stimulation in Parkinson disease. *Nature Reviews Neurology*, *15*(4), Article 4. https://doi.org/10.1038/s41582-019-0145-9

Limousin, P., Pollak, P., Benazzouz, A., Hoffmann, D., Le Bas, J. F., Broussolle, E., Perret, J. E., & Benabid, A. L. (1995). Effect of parkinsonian signs and symptoms of bilateral subthalamic nucleus stimulation. *Lancet (London, England)*, *345*(8942), 91–95. https://doi.org/10.1016/s0140-6736(95)90062-4

Lin, F.-H., Witzel, T., Ahlfors, S. P., Stufflebeam, S. M., Belliveau, J. W., & Hämäläinen, M. S. (2006). Assessing and improving the spatial accuracy in MEG source localization by depth-weighted minimum-norm estimates. *NeuroImage*, *31*(1), 160–171. https://doi.org/10.1016/j.neuroimage.2005.11.054

Litvan, I., Goldman, J. G., Tröster, A. I., Schmand, B. A., Weintraub, D., Petersen, R. C., Mollenhauer, B., Adler, C. H., Marder, K., Williams-Gray, C. H., Aarsland, D., Kulisevsky, J., Rodriguez-Oroz, M. C., Burn, D. J., Barker, R. A., & Emre, M. (2012). Diagnostic criteria for mild cognitive impairment in Parkinson's disease: Movement Disorder Society Task Force guidelines. *Movement Disorders: Official Journal of the Movement Disorder Society*, *27*(3), 349–356. https://doi.org/10.1002/mds.24893

Liu, G., Peng, J., Liao, Z., Locascio, J. J., Corvol, J.-C., Zhu, F., Dong, X., Maple-Grødem, J., Campbell, M. C., Elbaz, A., Lesage, S., Brice, A., Mangone, G., Growdon, J. H., Hung, A. Y., Schwarzschild, M. A., Hayes, M. T., Wills, A.-M., Herrington, T. M., … Scherzer, C. R. (2021). Genome-wide survival study identifies a novel synaptic locus and polygenic score for cognitive progression in Parkinson's disease. *Nature Genetics*, *53*(6), Article 6. https://doi.org/10.1038/s41588-021-00847-6

Liu, Q., Farahibozorg, S., Porcaro, C., Wenderoth, N., & Mantini, D. (2017). Detecting large-scale networks in the human brain using high-density electroencephalography. *Human Brain Mapping*, *38*(9), 4631–4643. https://doi.org/10.1002/hbm.23688

Livint Popa, L., Dragos, H., Pantelemon, C., Verisezan Rosu, O., & Strilciuc, S. (2020). The Role of Quantitative EEG in the Diagnosis of Neuropsychiatric Disorders. *Journal of Medicine and Life*, *13*(1), 8–15. https://doi.org/10.25122/jml-2019-0085

Luu, P., Jiang, Z., Poulsen, C., Mattson, C., Smith, A., & Tucker, D. M. (2011). Learning and the Development of Contexts for Action. *Frontiers in Human Neuroscience*, *5*, 159. https://doi.org/10.3389/fnhum.2011.00159

Ma, X., Su, W., Li, S., Li, C., Wang, R., Chen, M., & Chen, H. (2018). Cerebellar atrophy in different subtypes of Parkinson's disease. *Journal of the Neurological Sciences*, *392*,

105–112. https://doi.org/10.1016/j.jns.2018.06.027

Mahlknecht, P., Foltynie, T., Limousin, P., & Poewe, W. (2022). How Does Deep Brain Stimulation Change the Course of Parkinson's Disease? *Movement Disorders*, *37*(8), 1581–1592. https://doi.org/10.1002/mds.29052

Majbour, N. K., Abdi, I. Y., Dakna, M., Wicke, T., Lang, E., Ali Moussa, H. Y., Thomas, M. A., Trenkwalder, C., Safieh-Garabedian, B., Tokuda, T., Mollenhauer, B., & El-Agnaf, O. (2021). Cerebrospinal α-Synuclein Oligomers Reflect Disease Motor Severity in DeNoPa Longitudinal Cohort. *Movement Disorders: Official Journal of the Movement Disorder Society*, *36*(9), 2048–2056. https://doi.org/10.1002/mds.28611

Majbour, N. K., Vaikath, N. N., Eusebi, P., Chiasserini, D., Ardah, M., Varghese, S., Haque, M. E., Tokuda, T., Auinger, P., Calabresi, P., Parnetti, L., & El-Agnaf, O. M. A. (2016). Longitudinal changes in CSF alpha-synuclein species reflect Parkinson's disease progression. *Movement Disorders*, *31*(10), 1535–1542. https://doi.org/10.1002/mds.26754

Mak, E., Su, L., Williams, G. B., Firbank, M. J., Lawson, R. A., Yarnall, A. J., Duncan, G. W., Owen, A. M., Khoo, T. K., Brooks, D. J., Rowe, J. B., Barker, R. A., Burn, D. J., & O'Brien, J. T. (2015). Baseline and longitudinal grey matter changes in newly diagnosed Parkinson's disease: ICICLE-PD study. *Brain*, *138*(10), 2974–2986. https://doi.org/10.1093/brain/awv211

Mak, E., Zhou, J., Tan, L. C. S., Au, W. L., Sitoh, Y. Y., & Kandiah, N. (2014). Cognitive deficits in mild Parkinson's disease are associated with distinct areas of grey matter atrophy. *Journal of Neurology, Neurosurgery & Psychiatry*, *85*(5), 576–580. https://doi.org/10.1136/jnnp-2013-305805

Marek, K., Jennings, D., Lasch, S., Siderowf, A., Tanner, C., Simuni, T., Coffey, C., Kieburtz, K., Flagg, E., Chowdhury, S., Poewe, W., Mollenhauer, B., Klinik, P.-E., Sherer, T., Frasier, M., Meunier, C., Rudolph, A., Casaceli, C., Seibyl, J., … Taylor, P. (2011). The Parkinson Progression Marker Initiative (PPMI). *Progress in Neurobiology*, *95*(4), 629–635. https://doi.org/10.1016/j.pneurobio.2011.09.005

Markello, R. D., Shafiei, G., Tremblay, C., Postuma, R. B., Dagher, A., & Misic, B. (2021). Multimodal phenotypic axes of Parkinson's disease. *Npj Parkinson's Disease*, *7*(1), 1–12. https://doi.org/10.1038/s41531-020-00144-9

McGhee, D. J., Royle, P. L., Thompson, P. A., Wright, D. E., Zajicek, J. P., & Counsell, C. E. (2013). A systematic review of biomarkers for disease progression in Parkinson's disease. *BMC Neurology*, *13*(1), 35. https://doi.org/10.1186/1471-2377-13-35

McMackin, R., Bede, P., Pender, N., Hardiman, O., & Nasseroleslami, B. (2019). Neurophysiological markers of network dysfunction in neurodegenerative diseases. *NeuroImage: Clinical*, *22*, 101706. https://doi.org/10.1016/j.nicl.2019.101706

Mehrkanoon, S., Breakspear, M., Britz, J., & Boonstra, T. W. (2014). Intrinsic Coupling Modes in Source-Reconstructed Electroencephalography. *Brain Connectivity*, *4*(10), 812–825. https://doi.org/10.1089/brain.2014.0280

Meles, S. K., Oertel, W. H., & Leenders, K. L. (2021). Circuit imaging biomarkers in preclinical and prodromal Parkinson's disease. *Molecular Medicine*, *27*(1), 111. https://doi.org/10.1186/s10020-021-00327-x

Mestre, T. A., Fereshtehnejad, S.-M., Berg, D., Bohnen, N. I., Dujardin, K., Erro, R., Espay, A. J., Halliday, G., van Hilten, J. J., Hu, M. T., Jeon, B., Klein, C., Leentjens, A. F. G., Marinus, J., Mollenhauer, B., Postuma, R., Rajalingam, R., Rodríguez-Violante, M., Simuni, T., … Marras, C. (2021). Parkinson's Disease Subtypes: Critical Appraisal and Recommendations. *Journal of Parkinson's Disease*, *11*(2), 395–404. https://doi.org/10.3233/JPD-202472

Michel, C. M., & Brunet, D. (2019). EEG Source Imaging: A Practical Review of the Analysis Steps. *Frontiers in Neurology*, *10*. https://doi.org/10.3389/fneur.2019.00325

Michel, C. M., Murray, M. M., Lantz, G., Gonzalez, S., Spinelli, L., & de Peralta, R. G. (2004). EEG source imaging. *Clinical Neurophysiology*, *115*(10), 2195–2222.

Michely, J., Volz, L. J., Barbe, M. T., Hoffstaedter, F., Viswanathan, S., Timmermann, L., Eickhoff, S. B., Fink, G. R., & Grefkes, C. (2015). Dopaminergic modulation of motor network dynamics in Parkinson's disease. *Brain*, *138*(3), 664–678. https://doi.org/10.1093/brain/awu381

Mitchell, T., Lehéricy, S., Chiu, S. Y., Strafella, A. P., Stoessl, A. J., & Vaillancourt, D. E. (2021). Emerging Neuroimaging Biomarkers Across Disease Stage in Parkinson Disease: A Review. *JAMA Neurology*, *78*(10), 1262–1272. https://doi.org/10.1001/jamaneurol.2021.1312

Montine, T. J., Shi, M., Quinn, J. F., Peskind, E. R., Craft, S., Ginghina, C., Chung, K. A., Kim, H., Galasko, D. R., Jankovic, J., Zabetian, C. P., Leverenz, J. B., & Zhang, J. (2010). CSF Aβ42 and tau in Parkinson's disease with cognitive impairment. *Movement Disorders*, *25*(15), 2682–2685. https://doi.org/10.1002/mds.23287

Moustafa, A. A., Chakravarthy, S., Phillips, J. R., Gupta, A., Keri, S., Polner, B., Frank, M. J., & Jahanshahi, M. (2016). Motor symptoms in Parkinson's disease: A unified framework. *Neuroscience & Biobehavioral Reviews*, *68*, 727–740. https://doi.org/10.1016/j.neubiorev.2016.07.010

Movement Disorder Society Task Force on Rating Scales for Parkinson's Disease. (2003). The Unified Parkinson's Disease Rating Scale (UPDRS): Status and recommendations. *Movement Disorders: Official Journal of the Movement Disorder Society*, *18*(7), 738–750. https://doi.org/10.1002/mds.10473

Mu, J., Chaudhuri, K. R., Bielza, C., de Pedro-Cuesta, J., Larrañaga, P., & Martinez-Martin, P. (2017). Parkinson's Disease Subtypes Identified from Cluster Analysis of Motor and Non-motor Symptoms. *Frontiers in Aging Neuroscience*, *9*. https://www.frontiersin.org/articles/10.3389/fnagi.2017.00301

Müller-Putz, G. R. (2020). Chapter 18—Electroencephalography. In N. F. Ramsey & J. del R. Millán (Eds.), *Handbook of Clinical Neurology* (Vol. 168, pp. 249–262). Elsevier. https://doi.org/10.1016/B978-0-444-63934-9.00018-4

Munhoz, R. P., Espay, A. J., Morgante, F., Li, J.-Y., Teive, H. A., Dunn, E., Gallin, E., & Litvan, I. (2013). Long-duration Parkinson's disease: Role of lateralization of motor features. *Parkinsonism & Related Disorders*, *19*(1), 77–80. https://doi.org/10.1016/j.parkreldis.2012.07.008

Nalls, M. A., Blauwendraat, C., Vallerga, C. L., Heilbron, K., Bandres-Ciga, S., Chang, D., Tan, M., Kia, D. A., Noyce, A. J., Xue, A., Bras, J., Young, E., von Coelln, R., Simón-Sánchez, J., Schulte, C., Sharma, M., Krohn, L., Pihlstrøm, L., Siitonen, A., …

Zhang, F. (2019). Identification of novel risk loci, causal insights, and heritable risk for Parkinson's disease: A meta-analysis of genome-wide association studies. *The Lancet Neurology*, *18*(12), 1091–1102. https://doi.org/10.1016/S1474-4422(19)30320-5

Nandhagopal, R., Kuramoto, L., Schulzer, M., Mak, E., Cragg, J., McKenzie, J., McCormick, S., Ruth, T. J., Sossi, V., de la Fuente-Fernandez, R., & Stoessl, A. J. (2011). Longitudinal evolution of compensatory changes in striatal dopamine processing in Parkinson's disease. *Brain*, *134*(11), 3290–3298. https://doi.org/10.1093/brain/awr233

Nasreddine, Z. S., Phillips, N. A., Bédirian, V., Charbonneau, S., Whitehead, V., Collin, I., Cummings, J. L., & Chertkow, H. (2005). The Montreal Cognitive Assessment, MoCA: A Brief Screening Tool For Mild Cognitive Impairment. *Journal of the American Geriatrics Society*, *53*(4), 695–699. https://doi.org/10.1111/j.1532-5415.2005.53221.x

National Collaborating Centre for Chronic Conditions (UK). (2006). *Parkinson's Disease: National Clinical Guideline for Diagnosis and Management in Primary and Secondary Care*. Royal College of Physicians (UK). http://www.ncbi.nlm.nih.gov/books/NBK48513/

Nemade, D., Subramanian, T., & Shivkumar, V. (2021). An Update on Medical and Surgical Treatments of Parkinson's Disease. *Aging and Disease*, *12*(4), 1021–1035. https://doi.org/10.14336/AD.2020.1225

Olde Dubbelink, K. T. E., Schoonheim, M. M., Deijen, J. B., Twisk, J. W. R., Barkhof, F., & Berendse, H. W. (2014). Functional connectivity and cognitive decline over 3 years in Parkinson disease. *Neurology*, *83*(22), 2046–2053. https://doi.org/10.1212/WNL.0000000000001020

Olde Dubbelink, K. T. E., Stoffers, D., Deijen, J. B., Twisk, J. W. R., Stam, C. J., & Berendse, H. W. (2013). Cognitive decline in Parkinson's disease is associated with slowing of resting-state brain activity: A longitudinal study. *Neurobiology of Aging*, *34*(2), 408–418. https://doi.org/10.1016/j.neurobiolaging.2012.02.029

Olde Dubbelink, K. T. E., Stoffers, D., Deijen, J. B., Twisk, J. W. R., Stam, C. J., Hillebrand, A., & Berendse, H. W. (2013). Resting-state functional connectivity as a marker of disease progression in Parkinson's disease: A longitudinal MEG study. *NeuroImage: Clinical*, *2*, 612–619. https://doi.org/10.1016/j.nicl.2013.04.003

Olsen, L. K., Dowd, E., & McKernan, D. P. (2018). A role for viral infections in Parkinson's etiology? *Neuronal Signaling*, *2*(2), NS20170166. https://doi.org/10.1042/NS20170166

Oostenveld, R., & Praamstra, P. (2001). The five percent electrode system for high-resolution EEG and ERP measurements. *Clinical Neurophysiology*, *112*(4), 713–719. https://doi.org/10.1016/S1388-2457(00)00527-7

Oppenheim, H. (1905). Zur Diagnose, Prognose und Therapie der Paralysis agitans. *DMW - Deutsche Medizinische Wochenschrift*, *31*(43), 1705–1710. https://doi.org/10.1055/s-0029-1188410

Paolini Paoletti, F., Tambasco, N., & Parnetti, L. (2019). Levodopa treatment in Parkinson's disease: Earlier or later? *Annals of Translational Medicine*, *7*(Suppl 6), S189. https://doi.org/10.21037/atm.2019.07.36

Pappatà, S., Santangelo, G., Aarsland, D., Vicidomini, C., Longo, K., Bronnick, K., Amboni, M., Erro, R., Vitale, C., Caprio, M. G., Pellecchia, M. T., Brunetti, A., Michele, G. D., Salvatore, M., & Barone, P. (2011). Mild cognitive impairment in drug-naive patients with PD is associated with cerebral hypometabolism. *Neurology*, *77*(14), 1357–1362. https://doi.org/10.1212/WNL.0b013e3182315259

Park, A., & Stacy, M. (2009). Non-motor symptoms in Parkinson's disease. *Journal of Neurology*, *256*(3), 293–298. https://doi.org/10.1007/s00415-009-5240-1

Park, J. H., Lee, S. H., Kim, Y., Park, S.-W., Byeon, G. H., Jang, J.-W., & Initiative, the P. P. M. (2020). Depressive symptoms are associated with worse cognitive prognosis in patients with newly diagnosed idiopathic Parkinson disease. *Psychogeriatrics*, *20*(6), 880–890. https://doi.org/10.1111/psyg.12601

Parkinson, J. (2002). An Essay on the Shaking Palsy. *J Neuropsychiatry Clin Neurosci*.

Parnetti, L., Gaetani, L., Eusebi, P., Paciotti, S., Hansson, O., El-Agnaf, O., Mollenhauer, B., Blennow, K., & Calabresi, P. (2019). CSF and blood biomarkers for Parkinson's disease. *The Lancet Neurology*, *18*(6), 573–586. https://doi.org/10.1016/S1474-4422(19)30024-9

Pascual-Marqui, R. D., Lehmann, D., Koenig, T., Kochi, K., Merlo, M. C., Hell, D., & Koukkou, M. (1999). Low resolution brain electromagnetic tomography (LORETA) functional imaging in acute, neuroleptic-naive, first-episode, productive schizophrenia. *Psychiatry Research*, *90*(3), 169–179. https://doi.org/10.1016/s0925-4927(99)00013-x

Pearl, J. (1988). *Probabilistic Reasoning in Intelligent Systems: Networks of Plausible Inference*. Morgan Kaufmann Publishers Inc.

Pedroni, A., Bahreini, A., & Langer, N. (2019). Automagic: Standardized preprocessing of big EEG data. *NeuroImage*, *200*, 460–473. https://doi.org/10.1016/j.neuroimage.2019.06.046

Peláez Suárez, A. A., Berrillo Batista, S., Pedroso Ibáñez, I., Casabona Fernández, E., Fuentes Campos, M., & Chacón, L. M. (2021). EEG-Derived Functional Connectivity Patterns Associated with Mild Cognitive Impairment in Parkinson's Disease. *Behavioral Sciences*, *11*(3), Article 3. https://doi.org/10.3390/bs11030040

Pereda, E., Quiroga, R. Q., & Bhattacharya, J. (2005). Nonlinear multivariate analysis of neurophysiological signals. *Progress in Neurobiology*, *77*(1–2), 1–37. https://doi.org/10.1016/j.pneurobio.2005.10.003

Pereira, J. B., Svenningsson, P., Weintraub, D., Brønnick, K., Lebedev, A., Westman, E., & Aarsland, D. (2014). Initial cognitive decline is associated with cortical thinning in early Parkinson disease. *Neurology*, *82*(22), 2017–2025. https://doi.org/10.1212/WNL.0000000000000483

Perepezko, K., Naaz, F., Wagandt, C., Dissanayaka, N. N., Mari, Z., Nanavati, J., Bakker, A., & Pontone, G. M. (2021). Anxiety in Parkinson's Disease: A Systematic Review of Neuroimaging Studies. *The Journal of Neuropsychiatry and Clinical Neurosciences*, *33*(4), 280–294. https://doi.org/10.1176/appi.neuropsych.20110272

Pfeiffer, R. F. (2016). Non-motor symptoms in Parkinson's disease. *Parkinsonism & Related Disorders*, *22 Suppl 1*, S119-122. https://doi.org/10.1016/j.parkreldis.2015.09.004

Pfister, H., Kaynig, V., Botha, C. P., Bruckner, S., Dercksen, V. J., Hege, H.-C., & Roerdink,

J. B. T. M. (2014). Visualization in Connectomics. In C. D. Hansen, M. Chen, C. R. Johnson, A. E. Kaufman, & H. Hagen (Eds.), *Scientific Visualization: Uncertainty, Multifield, Biomedical, and Scalable Visualization* (pp. 221–245). Springer. https://doi.org/10.1007/978-1-4471-6497-5_21

Picillo, M., Santangelo, G., Erro, R., Cozzolino, A., Amboni, M., Vitale, C., Barone, P., & Pellecchia, M. T. (2017). Association between dopaminergic dysfunction and anxiety in de novo Parkinson's disease. *Parkinsonism & Related Disorders*, *37*, 106–110. https://doi.org/10.1016/j.parkreldis.2017.02.010

Pinter, B., Diem-Zangerl, A., Wenning, G. K., Scherfler, C., Oberaigner, W., Seppi, K., & Poewe, W. (2015). Mortality in Parkinson's disease: A 38-year follow-up study. *Movement Disorders: Official Journal of the Movement Disorder Society*, *30*(2), 266–269. https://doi.org/10.1002/mds.26060

Pirogovsky-Turk, E., Moore, R. C., Filoteo, J. V., Litvan, I., Song, D. D., Lessig, S. L., & Schiehser, D. M. (2017). Neuropsychiatric Predictors of Cognitive Decline in Parkinson Disease: A Longitudinal Study. *The American Journal of Geriatric Psychiatry*, *25*(3), 279–289. https://doi.org/10.1016/j.jagp.2016.10.004

Poewe, W. (2008). Non-motor symptoms in Parkinson's disease. *European Journal of Neurology*, *15*(s1), 14–20. https://doi.org/10.1111/j.1468-1331.2008.02056.x

Poewe, W., & Antonini, A. (2015). Novel formulations and modes of delivery of levodopa. *Movement Disorders: Official Journal of the Movement Disorder Society*, *30*(1), 114–120. https://doi.org/10.1002/mds.26078

Poewe, W., & Mahlknecht, P. (2009). The clinical progression of Parkinson's disease. *Parkinsonism & Related Disorders*, *15*, S28–S32. https://doi.org/10.1016/S1353-8020(09)70831-4

Poewe, W., Seppi, K., Tanner, C. M., Halliday, G. M., Brundin, P., Volkmann, J., Schrag, A.-E., & Lang, A. E. (2017). Parkinson disease. *Nature Reviews. Disease Primers*, *3*, 17013. https://doi.org/10.1038/nrdp.2017.13

Ponsen, M. M., Stam, C. J., Bosboom, J. L. W., Berendse, H. W., & Hillebrand, A. (2013). A three dimensional anatomical view of oscillatory resting-state activity and functional connectivity in Parkinson's disease related dementia: An MEG study using atlas-based beamforming. *NeuroImage: Clinical*, *2*, 95–102. https://doi.org/10.1016/j.nicl.2012.11.007

Pontone, G. M., Williams, J. R., Anderson, K. E., Chase, G., Goldstein, S. R., Grill, S., Hirsch, E. S., Lehmann, S., Little, J. T., Margolis, R. L., Rabins, P. V., Weiss, H. D., & Marsh, L. (2011). Anxiety and self-perceived health status in Parkinson's disease. *Parkinsonism & Related Disorders*, *17*(4), 249–254. https://doi.org/10.1016/j.parkreldis.2011.01.005

Pourzinal, D., Yang, J., Lawson, R. A., McMahon, K. L., Byrne, G. J., & Dissanayaka, N. N. (2022). Systematic review of data-driven cognitive subtypes in Parkinson disease. *European Journal of Neurology*, *29*(11), 3395–3417. https://doi.org/10.1111/ene.15481

Prodoehl, J., Burciu, R. G., & Vaillancourt, D. E. (2014). Resting State Functional Magnetic Resonance Imaging in Parkinson's Disease. *Current Neurology and Neuroscience Reports*, *14*(6), 448. https://doi.org/10.1007/s11910-014-0448-6

Rahayel, S., Postuma, R. B., Montplaisir, J., Génier Marchand, D., Escudier, F., Gaubert, M., Bourgouin, P.-A., Carrier, J., Monchi, O., Joubert, S., Blanc, F., & Gagnon, J.-F. (2018). Cortical and subcortical gray matter bases of cognitive deficits in REM sleep behavior disorder. *Neurology*, *90*(20), e1759–e1770. https://doi.org/10.1212/WNL.0000000000005523

Recasens, A., & Dehay, B. (2014). Alpha-synuclein spreading in Parkinson's disease. *Frontiers in Neuroanatomy*, *8*. https://www.frontiersin.org/articles/10.3389/fnana.2014.00159

Reynolds, G. O., Hanna, K. K., Neargarder, S., & Cronin-Golomb, A. (2017). The relation of anxiety and cognition in Parkinson's disease. *Neuropsychology*, *31*, 596–604. https://doi.org/10.1037/neu0000353

Riederer, P., & Sian-Hülsmann, J. (2012). The significance of neuronal lateralisation in Parkinson's disease. *Journal of Neural Transmission*, *119*(8), 953–962. https://doi.org/10.1007/s00702-012-0775-1

Ritz, B., Ascherio, A., Checkoway, H., Marder, K. S., Nelson, L. M., Rocca, W. A., Ross, G. W., Strickland, D., Van Den Eeden, S. K., & Gorell, J. (2007). Pooled analysis of tobacco use and risk of Parkinson disease. *Archives of Neurology*, *64*(7), 990–997. https://doi.org/10.1001/archneur.64.7.990

Rodriguez-Sanchez, F., Rodriguez-Blazquez, C., Bielza, C., Larrañaga, P., Weintraub, D., Martinez-Martin, P., Rizos, A., Schrag, A., & Chaudhuri, K. R. (2021). Identifying Parkinson's disease subtypes with motor and non-motor symptoms via model-based multi-partition clustering. *Scientific Reports*, *11*(1), Article 1. https://doi.org/10.1038/s41598-021-03118-w

Rolinski, M., Griffanti, L., Piccini, P., Roussakis, A. A., Szewczyk-Krolikowski, K., Menke, R. A., Quinnell, T., Zaiwalla, Z., Klein, J. C., Mackay, C. E., & Hu, M. T. M. (2016). Basal ganglia dysfunction in idiopathic REM sleep behaviour disorder parallels that in early Parkinson's disease. *Brain*, *139*(8), 2224–2234. https://doi.org/10.1093/brain/aww124

Rutten, S., Ghielen, I., Vriend, C., Hoogendoorn, A. W., Berendse, H. W., Leentjens, A. F. G., van der Werf, Y. D., Smit, J. H., & van den Heuvel, O. A. (2015). Anxiety in Parkinson's disease: Symptom dimensions and overlap with depression and autonomic failure. *Parkinsonism & Related Disorders*, *21*(3), 189–193. https://doi.org/10.1016/j.parkreldis.2014.11.019

Sagna, A., Gallo, J. J., & Pontone, G. M. (2014). Systematic review of factors associated with depression and anxiety disorders among older adults with Parkinson's disease. *Parkinsonism & Related Disorders*, *20*(7), 708–715. https://doi.org/10.1016/j.parkreldis.2014.03.020

Salmanpour, M. R., Shamsaei, M., Saberi, A., Hajianfar, G., Soltanian-Zadeh, H., & Rahmim, A. (2021). Robust identification of Parkinson's disease subtypes using radiomics and hybrid machine learning. *Computers in Biology and Medicine*, *129*, 104142. https://doi.org/10.1016/j.compbiomed.2020.104142

Sánchez-Reyes, L.-M., Rodríguez-Reséndiz, J., Avecilla-Ramírez, G. N., García-Gomar, M.-L., & Robles-Ocampo, J.-B. (2021). Impact of EEG Parameters Detecting Dementia Diseases: A Systematic Review. *IEEE Access*, *9*, 78060–78074.

https://doi.org/10.1109/ACCESS.2021.3083519
Sargolzaei, S., Cabrerizo, M., Goryawala, M., Eddin, A. S., & Adjouadi, M. (2015). Scalp EEG brain functional connectivity networks in pediatric epilepsy. *Computers in Biology and Medicine*, *56*, 158–166. https://doi.org/10.1016/j.compbiomed.2014.10.018
Sasikumar, S., & Strafella, A. P. (2020). Imaging Mild Cognitive Impairment and Dementia in Parkinson's Disease. *Frontiers in Neurology*, *11*. https://www.frontiersin.org/articles/10.3389/fneur.2020.00047
Savica, R., Grossardt, B. R., Bower, J. H., Ahlskog, J. E., & Rocca, W. A. (2013). Incidence and pathology of synucleinopathies and tauopathies related to parkinsonism. *JAMA Neurology*, *70*(7), 859–866. https://doi.org/10.1001/jamaneurol.2013.114
Scherfler, C., Frauscher, B., Schocke, M., Iranzo, A., Gschliesser, V., Seppi, K., Santamaria, J., Tolosa, E., Högl, B., Poewe, W., & SINBAR (Sleep Innsbruck Barcelona) Group. (2011). White and gray matter abnormalities in idiopathic rapid eye movement sleep behavior disorder: A diffusion-tensor imaging and voxel-based morphometry study. *Annals of Neurology*, *69*(2), 400–407. https://doi.org/10.1002/ana.22245
Schoffelen, J.-M., & Gross, J. (2009). Source connectivity analysis with MEG and EEG. *Human Brain Mapping*, *30*(6), 1857–1865.
Schrag, A., Siddiqui, U. F., Anastasiou, Z., Weintraub, D., & Schott, J. M. (2017). Clinical variables and biomarkers in prediction of cognitive impairment in patients with newly diagnosed Parkinson's disease: A cohort study. *The Lancet Neurology*, *16*(1), 66–75. https://doi.org/10.1016/S1474-4422(16)30328-3
Schuepbach, W. M. M., Rau, J., Knudsen, K., Volkmann, J., Krack, P., Timmermann, L., Hälbig, T. D., Hesekamp, H., Navarro, S. M., Meier, N., Falk, D., Mehdorn, M., Paschen, S., Maarouf, M., Barbe, M. T., Fink, G. R., Kupsch, A., Gruber, D., Schneider, G.-H., … Deuschl, G. (2013). Neurostimulation for Parkinson's Disease with Early Motor Complications. *New England Journal of Medicine*, *368*(7), 610–622. https://doi.org/10.1056/NEJMoa1205158
Seeley, W. W., Crawford, R. K., Zhou, J., Miller, B. L., & Greicius, M. D. (2009). Neurodegenerative diseases target large-scale human brain networks. *Neuron*, *62*(1), 42–52. https://doi.org/10.1016/j.neuron.2009.03.024
Segura, B., Baggio, H. C., Marti, M. J., Valldeoriola, F., Compta, Y., Garcia-Diaz, A. I., Vendrell, P., Bargallo, N., Tolosa, E., & Junque, C. (2014). Cortical thinning associated with mild cognitive impairment in Parkinson's disease. *Movement Disorders: Official Journal of the Movement Disorder Society*, *29*(12), 1495–1503. https://doi.org/10.1002/mds.25982
Seppi, K., Ray Chaudhuri, K., Coelho, M., Fox, S. H., Katzenschlager, R., Perez Lloret, S., Weintraub, D., Sampaio, C., & the collaborators of the Parkinson's Disease Update on Non-Motor Symptoms Study Group on behalf of the Movement Disorders Society Evidence-Based Medicine Committee. (2019). Update on treatments for nonmotor symptoms of Parkinson's disease-an evidence-based medicine review. *Movement Disorders: Official Journal of the Movement Disorder Society*, *34*(2), 180–198. https://doi.org/10.1002/mds.27602
Seppi, K., Weintraub, D., Coelho, M., Perez-Lloret, S., Fox, S. H., Katzenschlager, R.,

Hametner, E.-M., Poewe, W., Rascol, O., Goetz, C. G., & Sampaio, C. (2011). The Movement Disorder Society Evidence-Based Medicine Review Update: Treatments for the non-motor symptoms of Parkinson's disease. *Movement Disorders: Official Journal of the Movement Disorder Society*, *26 Suppl 3*(0 3), S42-80. https://doi.org/10.1002/mds.23884

Shen, L.-H., Liao, M.-H., & Tseng, Y.-C. (2012). Recent Advances in Imaging of Dopaminergic Neurons for Evaluation of Neuropsychiatric Disorders. *BioMed Research International*, *2012*, e259349. https://doi.org/10.1155/2012/259349

Shiba, M., Bower, J. H., Maraganore, D. M., McDonnell, S. K., Peterson, B. J., Ahlskog, J. E., Schaid, D. J., & Rocca, W. A. (2000). Anxiety disorders and depressive disorders preceding Parkinson's disease: A case-control study. *Movement Disorders*, *15*(4), 669–677. https://doi.org/10.1002/1531-8257(200007)15:4<669::AID-MDS1011>3.0.CO;2-5

Shin, L. M., & Liberzon, I. (2010). The Neurocircuitry of Fear, Stress, and Anxiety Disorders. *Neuropsychopharmacology*, *35*(1), Article 1. https://doi.org/10.1038/npp.2009.83

Shirahige, L., Berenguer-Rocha, M., Mendonça, S., Rocha, S., Rodrigues, M. C., & Monte-Silva, K. (2020). Quantitative Electroencephalography Characteristics for Parkinson's Disease: A Systematic Review. *Journal of Parkinson's Disease*, *10*(2), 455–470. https://doi.org/10.3233/JPD-191840

Siemers, E. R., Shekhar, A., Quaid, K., & Dickson, H. (1993). Anxiety and motor performance in parkinson's disease. *Movement Disorders*, *8*(4), 501–506. https://doi.org/10.1002/mds.870080415

Silberstein, P., Pogosyan, A., Kühn, A. A., Hotton, G., Tisch, S., Kupsch, A., Dowsey-Limousin, P., Hariz, M. I., & Brown, P. (2005). Cortico-cortical coupling in Parkinson's disease and its modulation by therapy. *Brain: A Journal of Neurology*, *128*(Pt 6), 1277–1291. https://doi.org/10.1093/brain/awh480

Simon, D. K., Tanner, C. M., & Brundin, P. (2020). Parkinson Disease Epidemiology, Pathology, Genetics and Pathophysiology. *Clinics in Geriatric Medicine*, *36*(1), 1–12. https://doi.org/10.1016/j.cger.2019.08.002

Simuni, T., Caspell-Garcia, C., Coffey, C. S., Weintraub, D., Mollenhauer, B., Lasch, S., Tanner, C. M., Jennings, D., Kieburtz, K., Chahine, L. M., & Marek, K. (2018). Baseline prevalence and longitudinal evolution of non-motor symptoms in early Parkinson's disease: The PPMI cohort. *Journal of Neurology, Neurosurgery & Psychiatry*, *89*(1), 78–88. https://doi.org/10.1136/jnnp-2017-316213

Simuni, T., Siderowf, A., Lasch, S., Coffey, C. S., Caspell-Garcia, C., Jennings, D., Tanner, C. M., Trojanowski, J. Q., Shaw, L. M., Seibyl, J., Schuff, N., Singleton, A., Kieburtz, K., Toga, A. W., Mollenhauer, B., Galasko, D., Chahine, L. M., Weintraub, D., Foroud, T., … Initiative*, the P. P. M. (2018). Longitudinal Change of Clinical and Biological Measures in Early Parkinson's Disease: Parkinson's Progression Markers Initiative Cohort. *Movement Disorders*, *33*(5), 771–782. https://doi.org/10.1002/mds.27361

Sohrabpour, A., Lu, Y., Kankirawatana, P., Blount, J., Kim, H., & He, B. (2015). Effect of EEG electrode number on epileptic source localization in pediatric patients. *Clinical*

Neurophysiology, *126*(3), 472–480. https://doi.org/10.1016/j.clinph.2014.05.038

Song, J., Davey, C., Poulsen, C., Luu, P., Turovets, S., Anderson, E., Li, K., & Tucker, D. (2015). EEG source localization: Sensor density and head surface coverage. *Journal of Neuroscience Methods*, *256*, 9–21. https://doi.org/10.1016/j.jneumeth.2015.08.015

Song, W., Raza, H. K., Lu, L., Zhang, Z., Zu, J., Zhang, W., Dong, L., Xu, C., Gong, X., Lv, B., & Cui, G. (2021). Functional MRI in Parkinson's disease with freezing of gait: A systematic review of the literature. *Neurological Sciences*, *42*(5), 1759–1771. https://doi.org/10.1007/s10072-021-05121-5

Sporns, O., Chialvo, D. R., Kaiser, M., & Hilgetag, C. C. (2004). Organization, development and function of complex brain networks. *Trends in Cognitive Sciences*, *8*(9), 418–425. https://doi.org/10.1016/j.tics.2004.07.008

Stam, C. J. (2014). Modern network science of neurological disorders. *Nature Reviews Neuroscience*, *15*(10), Article 10. https://doi.org/10.1038/nrn3801

Stefanik, L., Erdman, L., Ameis, S. H., Foussias, G., Mulsant, B. H., Behdinan, T., Goldenberg, A., O'Donnell, L. J., & Voineskos, A. N. (2018). Brain-Behavior Participant Similarity Networks Among Youth and Emerging Adults with Schizophrenia Spectrum, Autism Spectrum, or Bipolar Disorder and Matched Controls. *Neuropsychopharmacology*, *43*(5), Article 5. https://doi.org/10.1038/npp.2017.274

Stoffers, D., Bosboom, J. L. W., Deijen, J. B., Wolters, E. C., Berendse, H. W., & Stam, C. J. (2007). Slowing of oscillatory brain activity is a stable characteristic of Parkinson's disease without dementia. *Brain*, *130*(7), 1847–1860. https://doi.org/10.1093/brain/awm034

Stoffers, D., Bosboom, J. L. W., Deijen, J. B., Wolters, E. Ch., Stam, C. J., & Berendse, H. W. (2008). Increased cortico-cortical functional connectivity in early-stage Parkinson's disease: An MEG study. *NeuroImage*, *41*(2), 212–222. https://doi.org/10.1016/j.neuroimage.2008.02.027

Storch, A., Schneider, C. B., Wolz, M., Stürwald, Y., Nebe, A., Odin, P., Mahler, A., Fuchs, G., Jost, W. H., Chaudhuri, K. R., Koch, R., Reichmann, H., & Ebersbach, G. (2013). Nonmotor fluctuations in Parkinson disease: Severity and correlation with motor complications. *Neurology*, *80*(9), 800–809. https://doi.org/10.1212/WNL.0b013e318285c0ed

Strafella, A. P., Bohnen, N. I., Pavese, N., Vaillancourt, D. E., van Eimeren, T., Politis, M., Tessitore, A., Ghadery, C., Lewis, S., & Group, on behalf of I.-N. S. (2018). Imaging Markers of Progression in Parkinson's Disease. *Movement Disorders Clinical Practice*, *5*(6), 586–596. https://doi.org/10.1002/mdc3.12673

Surguchov, A. (2022). Biomarkers in Parkinson's Disease. In P. V. Peplow, B. Martinez, & T. A. Gennarelli (Eds.), *Neurodegenerative Diseases Biomarkers: Towards Translating Research to Clinical Practice* (pp. 155–180). Springer US. https://doi.org/10.1007/978-1-0716-1712-0_7

Szwedo, A. A., Dalen, I., Pedersen, K. F., Camacho, M., Bäckström, D., Forsgren, L., Tzoulis, C., Winder-Rhodes, S., Hudson, G., Liu, G., Scherzer, C. R., Lawson, R. A., Yarnall, A. J., Williams-Gray, C. H., Macleod, A. D., Counsell, C. E., Tysnes, O.-B., Alves, G., Maple-Grødem, J., & Collaboration, P. I. C. (2022). GBA and APOE

Impact Cognitive Decline in Parkinson's Disease: A 10-Year Population-Based Study. *Movement Disorders*, *37*(5), 1016–1027. https://doi.org/10.1002/mds.28932

Tadel, F., Baillet, S., Mosher, J. C., Pantazis, D., & Leahy, R. M. (2011). Brainstorm: A user-friendly application for MEG/EEG analysis. *Computational Intelligence and Neuroscience*, *2011*, 879716. https://doi.org/10.1155/2011/879716

Tait, L., Özkan, A., Szul, M. J., & Zhang, J. (2021). A systematic evaluation of source reconstruction of resting MEG of the human brain with a new high-resolution atlas: Performance, precision, and parcellation. *Human Brain Mapping*, *42*(14), 4685–4707. https://doi.org/10.1002/hbm.25578

Tan, M. M. X., Lawton, M. A., Jabbari, E., Reynolds, R. H., Iwaki, H., Blauwendraat, C., Kanavou, S., Pollard, M. I., Hubbard, L., Malek, N., Grosset, K. A., Marrinan, S. L., Bajaj, N., Barker, R. A., Burn, D. J., Bresner, C., Foltynie, T., Wood, N. W., Williams-Gray, C. H., … Morris, H. R. (2021). Genome-Wide Association Studies of Cognitive and Motor Progression in Parkinson's Disease. *Movement Disorders*, *36*(2), 424–433. https://doi.org/10.1002/mds.28342

Tanner, C. M., Goldman, S. M., Ross, G. W., & Grate, S. J. (2014). The disease intersection of susceptibility and exposure: Chemical exposures and neurodegenerative disease risk. *Alzheimer's & Dementia: The Journal of the Alzheimer's Association*, *10*(3 Suppl), S213-225. https://doi.org/10.1016/j.jalz.2014.04.014

Tessitore, A., Cirillo, M., & De Micco, R. (2019). Functional Connectivity Signatures of Parkinson's Disease. *Journal of Parkinson's Disease*, *9*(4), 637–652. https://doi.org/10.3233/JPD-191592

Tessitore, A., Giordano, A., De Micco, R., Russo, A., & Tedeschi, G. (2014). Sensorimotor Connectivity in Parkinson's Disease: The Role of Functional Neuroimaging. *Frontiers in Neurology*, *5*, 180. https://doi.org/10.3389/fneur.2014.00180

Thobois, S., Guillouet, S., & Broussolle, E. (2001). Contributions of PET and SPECT to the understanding of the pathophysiology of Parkinson's disease. *Neurophysiologie Clinique/Clinical Neurophysiology*, *31*(5), 321–340. https://doi.org/10.1016/S0987-7053(01)00273-8

Thobois, S., Prange, S., Sgambato-Faure, V., Tremblay, L., & Broussolle, E. (2017). Imaging the Etiology of Apathy, Anxiety, and Depression in Parkinson's Disease: Implication for Treatment. *Current Neurology and Neuroscience Reports*, *17*(10), 76. https://doi.org/10.1007/s11910-017-0788-0

Toloraia, K., Meyer, A., Beltrani, S., Fuhr, P., Lieb, R., & Gschwandtner, U. (2022). Anxiety, Depression, and Apathy as Predictors of Cognitive Decline in Patients With Parkinson's Disease—A Three-Year Follow-Up Study. *Frontiers in Neurology*, *13*. https://doi.org/10.3389/fneur.2022.792830

Traud, A., Kelsic, E., Mucha, P., & Porter, M. (2016). Comparing Community Structure to Characteristics in Online Collegiate Social Networks. *SIAM REVIEW*, *53*(3). https://ora.ox.ac.uk/objects/uuid:c6a822c3-589a-4b39-9f95-2543ae979104

Trinh, J., Zeldenrust, F. M. J., Huang, J., Kasten, M., Schaake, S., Petkovic, S., Madoev, H., Grünewald, A., Almuammar, S., König, I. R., Lill, C. M., Lohmann, K., Klein, C., & Marras, C. (2018). Genotype-phenotype relations for the Parkinson's disease genes SNCA, LRRK2, VPS35: MDSGene systematic review. *Movement Disorders*, *33*(12),

1857–1870. https://doi.org/10.1002/mds.27527
Tuovinen, N., Seppi, K., de Pasquale, F., Müller, C., Nocker, M., Schocke, M., Gizewski, E. R., Kremser, C., Wenning, G. K., Poewe, W., Djamshidian, A., Scherfler, C., & Seki, M. (2018). The reorganization of functional architecture in the early-stages of Parkinson's disease. *Parkinsonism & Related Disorders*, *50*, 61–68. https://doi.org/10.1016/j.parkreldis.2018.02.013
Twelves, D., Perkins, K. S. M., & Counsell, C. (2003). Systematic review of incidence studies of Parkinson's disease. *Movement Disorders: Official Journal of the Movement Disorder Society*, *18*(1), 19–31. https://doi.org/10.1002/mds.10305
Van de Steen, F., Faes, L., Karahan, E., Songsiri, J., Valdes-Sosa, P. A., & Marinazzo, D. (2019). Critical comments on EEG sensor space dynamical connectivity analysis. *Brain Topography*, *32*(4), Article 4.
van Rooden, S. M., Colas, F., Martínez-Martín, P., Visser, M., Verbaan, D., Marinus, J., Chaudhuri, R. K., Kok, J. N., & van Hilten, J. J. (2011). Clinical subtypes of Parkinson's disease. *Movement Disorders*, *26*(1), 51–58. https://doi.org/10.1002/mds.23346
van Rooden, S. M., Heiser, W. J., Kok, J. N., Verbaan, D., van Hilten, J. J., & Marinus, J. (2010). The identification of Parkinson's disease subtypes using cluster analysis: A systematic review. *Movement Disorders*, *25*(8), 969–978. https://doi.org/10.1002/mds.23116
Van Veen, B. D., van Drongelen, W., Yuchtman, M., & Suzuki, A. (1997). Localization of brain electrical activity via linearly constrained minimum variance spatial filtering. *IEEE Transactions on Bio-Medical Engineering*, *44*(9), 867–880. https://doi.org/10.1109/10.623056
Vilas, D., Segura, B., Baggio, H. C., Pont-Sunyer, C., Compta, Y., Valldeoriola, F., José Martí, M., Quintana, M., Bayés, A., Hernández-Vara, J., Calopa, M., Aguilar, M., Junqué, C., Tolosa, E., & the Barcelona LRRK2 Study Group. (2016). Nigral and striatal connectivity alterations in asymptomatic LRRK2 mutation carriers: A magnetic resonance imaging study. *Movement Disorders: Official Journal of the Movement Disorder Society*, *31*(12), 1820–1828. https://doi.org/10.1002/mds.26799
Voges, J., Hilker, R., Bötzel, K., Kiening, K. L., Kloss, M., Kupsch, A., Schnitzler, A., Schneider, G.-H., Steude, U., Deuschl, G., & Pinsker, M. O. (2007). Thirty days complication rate following surgery performed for deep-brain-stimulation. *Movement Disorders: Official Journal of the Movement Disorder Society*, *22*(10), 1486–1489. https://doi.org/10.1002/mds.21481
Volkmann, J., Daniels, C., & Witt, K. (2010). Neuropsychiatric effects of subthalamic neurostimulation in Parkinson disease. *Nature Reviews. Neurology*, *6*(9), 487–498. https://doi.org/10.1038/nrneurol.2010.111
Vriend, C., Boedhoe, P. S. W., Rutten, S., Berendse, H. W., van der Werf, Y. D., & van den Heuvel, O. A. (2016). A smaller amygdala is associated with anxiety in Parkinson's disease: A combined FreeSurfer-VBM study. *Journal of Neurology, Neurosurgery, and Psychiatry*, *87*(5), 493–500. https://doi.org/10.1136/jnnp-2015-310383
Wang, B., Mezlini, A. M., Demir, F., Fiume, M., Tu, Z., Brudno, M., Haibe-Kains, B., & Goldenberg, A. (2014). Similarity network fusion for aggregating data types on a

genomic scale. *Nature Methods*, *11*(3), 333–337. https://doi.org/10.1038/nmeth.2810
Wang, H. E., Bénar, C. G., Quilichini, P. P., Friston, K. J., Jirsa, V. K., & Bernard, C. (2014). A systematic framework for functional connectivity measures. *Frontiers in Neuroscience*, *8*. https://www.frontiersin.org/articles/10.3389/fnins.2014.00405
Wang, J., Barstein, J., Ethridge, L. E., Mosconi, M. W., Takarae, Y., & Sweeney, J. A. (2013). Resting state EEG abnormalities in autism spectrum disorders. *Journal of Neurodevelopmental Disorders*, *5*(1), 24. https://doi.org/10.1186/1866-1955-5-24
Wang, Q., Meng, L., Pang, J., Zhu, X., & Ming, D. (2020). Characterization of EEG Data Revealing Relationships With Cognitive and Motor Symptoms in Parkinson's Disease: A Systematic Review. *Frontiers in Aging Neuroscience*, *12*. https://www.frontiersin.org/articles/10.3389/fnagi.2020.587396
Wang, X., Li, J., Wang, M., Yuan, Y., Zhu, L., Shen, Y., Zhang, H., & Zhang, K. (2018). Alterations of the amplitude of low-frequency fluctuations in anxiety in Parkinson's disease. *Neuroscience Letters*, *668*, 19–23. https://doi.org/10.1016/j.neulet.2018.01.010
Wang, X., Li, J., Yuan, Y., Wang, M., Ding, J., Zhang, J., Zhu, L., Shen, Y., Zhang, H., & Zhang, K. (2017). Altered putamen functional connectivity is associated with anxiety disorder in Parkinson's disease. *Oncotarget*, *8*(46), 81377–81386. https://doi.org/10.18632/oncotarget.18996
Wang, X., Zhang, J., Yuan, Y., Li, T., Zhang, L., Ding, J., Jiang, S., Li, J., Zhu, L., & Zhang, K. (2017). Cerebral metabolic change in Parkinson's disease patients with anxiety: A FDG-PET study. *Neuroscience Letters*, *653*, 202–207. https://doi.org/10.1016/j.neulet.2017.05.062
Wee, N., Wen, M.-C., Kandiah, N., Chander, R. J., Ng, A., Au, W. L., & Tan, L. C. S. (2016). Neural correlates of anxiety symptoms in mild Parkinson's disease: A prospective longitudinal voxel-based morphometry study. *Journal of the Neurological Sciences*, *371*, 131–136. https://doi.org/10.1016/j.jns.2016.10.021
Wein, S., Deco, G., Tomé, A. M., Goldhacker, M., Malloni, W. M., Greenlee, M. W., & Lang, E. W. (2021). Brain Connectivity Studies on Structure-Function Relationships: A Short Survey with an Emphasis on Machine Learning. *Computational Intelligence and Neuroscience*, *2021*, e5573740. https://doi.org/10.1155/2021/5573740
Weiner, W. J. (2008). There Is No Parkinson Disease. *Archives of Neurology*, *65*(6), 705–708. https://doi.org/10.1001/archneur.65.6.705
Welch, P. (1967). The use of fast Fourier transform for the estimation of power spectra: A method based on time averaging over short, modified periodograms. *IEEE Transactions on Audio and Electroacoustics*, *15*(2), 70–73. https://doi.org/10.1109/TAU.1967.1161901
Wen, M.-C., Chan, L. L., Tan, L. C. S., & Tan, E. K. (2016). Depression, anxiety, and apathy in Parkinson's disease: Insights from neuroimaging studies. *European Journal of Neurology*, *23*(6), 1001–1019. https://doi.org/10.1111/ene.13002
Wendling, F., Ansari-Asl, K., Bartolomei, F., & Senhadji, L. (2009). From EEG signals to brain connectivity: A model-based evaluation of interdependence measures. *Journal of Neuroscience Methods*, *183*(1), 9–18. https://doi.org/10.1016/j.jneumeth.2009.04.021

Witt, K., Granert, O., Daniels, C., Volkmann, J., Falk, D., van Eimeren, T., & Deuschl, G. (2013). Relation of lead trajectory and electrode position to neuropsychological outcomes of subthalamic neurostimulation in Parkinson's disease: Results from a randomized trial. *Brain*, *136*(7), 2109–2119. https://doi.org/10.1093/brain/awt151

Wolters, A. F., van de Weijer, S. C. F., Leentjens, A. F. G., Duits, A. A., Jacobs, H. I. L., & Kuijf, M. L. (2019). Resting-state fMRI in Parkinson's disease patients with cognitive impairment: A meta-analysis. *Parkinsonism & Related Disorders*, *62*, 16–27. https://doi.org/10.1016/j.parkreldis.2018.12.016

Wooten, G. F., Currie, L. J., Bovbjerg, V. E., Lee, J. K., & Patrie, J. (2004). Are men at greater risk for Parkinson's disease than women? *Journal of Neurology, Neurosurgery, and Psychiatry*, *75*(4), 637–639. https://doi.org/10.1136/jnnp.2003.020982

Xia, R., & Mao, Z.-H. (2012). Progression of motor symptoms in Parkinson's disease. *Neuroscience Bulletin*, *28*(1), 39–48. https://doi.org/10.1007/s12264-012-1050-z

Xu, Y., Yang, J., Hu, X., & Shang, H. (2016). Voxel-based meta-analysis of gray matter volume reductions associated with cognitive impairment in Parkinson's disease. *Journal of Neurology*, *263*(6), 1178–1187. https://doi.org/10.1007/s00415-016-8122-3

Yang, B., Wang, X., Mo, J., Li, Z., Gao, D., Bai, Y., Zou, L., Zhang, X., Zhao, X., Wang, Y., Liu, C., Zhao, B., Guo, Z., Zhang, C., Hu, W., Zhang, J., & Zhang, K. (2021). The amplitude of low-frequency fluctuation predicts levodopa treatment response in patients with Parkinson's disease. *Parkinsonism & Related Disorders*, *92*, 26–32. https://doi.org/10.1016/j.parkreldis.2021.10.003

Yassine, S., Gschwandtner, U., Auffret, M., Achard, S., Verin, M., Fuhr, P., & Hassan, M. (2022). Functional Brain Dysconnectivity in Parkinson's Disease: A 5-Year Longitudinal Study. *Movement Disorders: Official Journal of the Movement Disorder Society*. https://doi.org/10.1002/mds.29026

You, H., Mariani, L.-L., Mangone, G., Le Febvre de Nailly, D., Charbonnier-Beaupel, F., & Corvol, J.-C. (2018). Molecular basis of dopamine replacement therapy and its side effects in Parkinson's disease. *Cell and Tissue Research*, *373*(1), 111–135. https://doi.org/10.1007/s00441-018-2813-2

Yu, C., Zhou, Y., Liu, Y., Jiang, T., Dong, H., Zhang, Y., & Walter, M. (2011). Functional segregation of the human cingulate cortex is confirmed by functional connectivity based neuroanatomical parcellation. *NeuroImage*, *54*(4), 2571–2581. https://doi.org/10.1016/j.neuroimage.2010.11.018

Yu & Shi. (2003). Multiclass spectral clustering. *Proceedings Ninth IEEE International Conference on Computer Vision*, 313–319 vol.1. https://doi.org/10.1109/ICCV.2003.1238361

Zahoor, I., Shafi, A., & Haq, E. (2018). Pharmacological Treatment of Parkinson's Disease. In T. B. Stoker & J. C. Greenland (Eds.), *Parkinson's Disease: Pathogenesis and Clinical Aspects*. Codon Publications. http://www.ncbi.nlm.nih.gov/books/NBK536726/

Zalesky, A., Fornito, A., & Bullmore, E. T. (2010). Network-based statistic: Identifying differences in brain networks. *NeuroImage*, *53*(4), 1197–1207. https://doi.org/10.1016/j.neuroimage.2010.06.041

Zarei, M., Ibarretxe-Bilbao, N., Compta, Y., Hough, M., Junque, C., Bargallo, N., Tolosa, E., & Martí, M. J. (2013). Cortical thinning is associated with disease stages and dementia in Parkinson's disease. *Journal of Neurology, Neurosurgery, and Psychiatry*, *84*(8), 875–881. https://doi.org/10.1136/jnnp-2012-304126

Zeighami, Y., Fereshtehnejad, S.-M., Dadar, M., Collins, D. L., Postuma, R. B., & Dagher, A. (2019). Assessment of a prognostic MRI biomarker in early de novo Parkinson's disease. *NeuroImage: Clinical*, *24*, 101986. https://doi.org/10.1016/j.nicl.2019.101986

Zeighami, Y., Ulla, M., Iturria-Medina, Y., Dadar, M., Zhang, Y., Larcher, K. M.-H., Fonov, V., Evans, A. C., Collins, D. L., & Dagher, A. (2015). Network structure of brain atrophy in de novo Parkinson's disease. *ELife*, *4*, e08440. https://doi.org/10.7554/eLife.08440

Zhan, Z.-W., Lin, L.-Z., Yu, E.-H., Xin, J.-W., Lin, L., Lin, H.-L., Ye, Q.-Y., Chen, X.-C., & Pan, X.-D. (2018). Abnormal resting-state functional connectivity in posterior cingulate cortex of Parkinson's disease with mild cognitive impairment and dementia. *CNS Neuroscience & Therapeutics*, *24*(10), 897–905. https://doi.org/10.1111/cns.12838

Zhang, H., Qiu, Y., Luo, Y., Xu, P., Li, Z., Zhu, W., Wu, Q., Tao, W., Guan, Q., & Chen, F. (2019). The relationship of anxious and depressive symptoms in Parkinson's disease with voxel-based neuroanatomical and functional connectivity measures. *Journal of Affective Disorders*, *245*, 580–588. https://doi.org/10.1016/j.jad.2018.10.364

Zhang, X., Chou, J., Liang, J., Xiao, C., Zhao, Y., Sarva, H., Henchcliffe, C., & Wang, F. (2019). Data-Driven Subtyping of Parkinson's Disease Using Longitudinal Clinical Records: A Cohort Study. *Scientific Reports*, *9*(1), Article 1. https://doi.org/10.1038/s41598-018-37545-z

Zhang, Y., Wu, W., Toll, R. T., Naparstek, S., Maron-Katz, A., Watts, M., Gordon, J., Jeong, J., Astolfi, L., Shpigel, E., Longwell, P., Sarhadi, K., El-Said, D., Li, Y., Cooper, C., Chin-Fatt, C., Arns, M., Goodkind, M. S., Trivedi, M. H., … Etkin, A. (2021). Identification of psychiatric disorder subtypes from functional connectivity patterns in resting-state electroencephalography. *Nature Biomedical Engineering*, *5*(4), 309–323. https://doi.org/10.1038/s41551-020-00614-8

Zimmermann, R., Gschwandtner, U., Hatz, F., Schindler, C., Bousleiman, H., Ahmed, S., Hardmeier, M., Meyer, A., Calabrese, P., & Fuhr, P. (2015). Correlation of EEG slowing with cognitive domains in nondemented patients with Parkinson's disease. *Dementia and Geriatric Cognitive Disorders*, *39*(3–4), 207–214. https://doi.org/10.1159/000370110

COLLEGE SCIENCES
DOCTORAL DE LA VIE
BRETAGNE ET DE LA SANTE

Université de Rennes

Titre : L' EEG dans la maladie de Parkinson : suivi longitudinal et phénotypage de la maladie

Mots clés : EEG, Maladie de Parkinson, état de repos, progression, phénotypage, anxiété

Résumé : La maladie de Parkinson (MP) est le trouble du mouvement le plus courant et une affection neurologique complexe qui a un impact significatif sur le fardeau mondial de l'incapacité en raison de sa variabilité de symptômes et de progression. Des biomarqueurs fiables capables de prédire la gravité et la progression de la MP sont essentiels pour des soins optimaux des patients et des traitements efficaces. l'électroencéphalographie (EEG) a montré qu'il est un outil utile à cette fin dans la pratique clinique. Cette thèse vise à étudier le potentiel de l'EEG pour caractériser les fonctions cérébrales anormales associées à différents aspects de la MP et identifier des mesures basées sur l'EEG qui peuvent prédire les résultats de la maladie. La première étude examine le changement longitudinal des réseaux fonctionnels cérébraux des patients atteints de MP sur une période de 5 ans, tandis que la deuxième étude vise à identifier les sous-types de MP en déconstruisant l'hétérogénéité de la maladie basée sur des caractéristiques dérivées de l'EEG. La troisième étude exploite les empreintes électrophysiologiques qui caractérisent l'anxiété chez les patients atteints de MP. Dans l'ensemble, les résultats montrent différents schémas d'anomalies qui caractérisent les aspects distincts d'intérêt, et les mesures basées sur l'EEG se corréle et prédit l'évolution clinique de la maladie. Cette thèse montre le potentiel de l'EEG dans le développement de biomarqueurs fiables des symptômes et de la progression de la MP.

Title : EEG in Parkinson's disease: longitudinal tracking and disease phenotyping

Keywords : EEG, Parkinson's disease, resting-state, progression, phenotyping, anxiety

Abstract : Parkinson's disease (PD) is the most common movement disorder and a complex neurological condition that significantly impacts the global burden of disability due to its variability in symptoms and progression. Reliable biomarkers that can predict PD severity and progression are essential for optimal patient care and effective treatments. In recent years, electroencephalography has emerged as a useful tool for this purpose in clinical practice.This dissertation aims to investigate the potential of longitudinal resting-state HD-EEG to characterize abnormal brain functions associated with different aspects of PD and identify EEG-based measures that can predict disease outcomes. The first study examines the longitudinal change in brain functional networks of PD patients over 5 years, while the second study aims to identify PD subtypes by deconstructing disease heterogeneity based on EEG-derived features. The third study exploits the electrophysiological fingerprints that characterize anxiety in PD patients and correlate with clinical disease outcomes related to anxiety throughout disease progression. Overall, the results show different patterns of abnormalities that characterize the distinct aspects of interest, and EEG-based measures can correlate with the clinical outcomes of the disease and predict its evolutions. The study demonstrates the potential of resting-state HD-EEG in developing reliable biomarkers of PD symptoms and progression, leading to more accurate prognosis, diagnosis, and better therapeutics strategies.